ZooKeys 1115: 1–71 (2022)
doi: 10.3897/zookeys.1115.83266
https://zookeys.pensoft.net

RESEARCH ARTICLE

A peer-reviewed open-access journal
ZooKeys
Launched to accelerate biodiversity research

Symbiotic copepods (Cyclopoida and Siphonostomatoida) collected by light trap from Korea

Jimin Lee[1], Cheon Young Chang[2], Il-Hoi Kim[3]

1 *Marine Ecosystem and Biological Research Center, Korea Institute of Ocean Science & Technology, Busan 49111, Republic of Korea* **2** *Department of Biological Science, Daegu University, Gyeongsan 38453, Republic of Korea* **3** *Korea Institute of Coastal Ecology, 302-802, Seokcheon-ro 397, Bucheon 14449, Republic of Korea*

Corresponding author: Il-Hoi Kim (ihkim@gwnu.ac.kr)

Academic editor: Danielle Defaye | Received 10 March 2022 | Accepted 22 June 2022 | Published 28 July 2022

https://zoobank.org/C3E233F1-0EF7-4D2D-BD4A-A32AE7C4DF5E

Citation: Lee J, Chang CY, Kim I-H (2022) Symbiotic copepods (Cyclopoida and Siphonostomatoida) collected by light trap from Korea. ZooKeys 1115: 1–71. https://doi.org/10.3897/zookeys.1115.83266

Abstract

Thirty-nine species of symbiotic copepods, comprising 24 species of poecilostome Cyclopoida and 15 species of Siphonostomatoida, are reported from Korean waters, which were collected using underwater light traps at 33 collection sites around the South Korean coast. Ten new species are described: *Hemicyclops rapax* **sp. nov.** in the family Clausidiidae; *Pontoclausia cochleata* **sp. nov.** and *P. pristina* **sp. nov.** in the family Clausiidae; *Heteranthessius unisetatus* **sp. nov.** in the family Lichomolgidae; *Pusanomyicola sensitivus* **gen. nov., sp. nov.** in the family Myicolidae; *Polyankylis bogilensis* **sp. nov.** in the family Polyankyliidae; *Pseudanthessius linguifer* **sp. nov.** in the Pseudanthessiidae; *Eupolymniphilus foliatus* **sp. nov.** in the family Sabelliphilidae; and *Acontiophorus estivalis* **sp. nov.** and *Thermocheres pacificus* **sp. nov**. in the family Asterocheridae. Supplementary descriptions or notes for other species are provided as appropriate.

Keywords

Copepoda, Crustacea, new genus, new species, taxonomy

Introduction

Light traps are useful tools for collecting marine animals. According to McLeod and Costello (2017), at least 12 phyla of benthic and planktonic animals have been collected in light traps from the world. Animals collected by light traps are unsuitable for strict quantitative research; however, they are often in good condition and well suited for morphological and taxonomic study (Øresland 2007). In some cases, animals seldom taken by other methods can be caught by the light trap (Hernandez Jr. and Shaw 2003; Øresland 2007; Porter et al. 2008).

Crustaceans are the most abundant marine animals that are caught in light traps (Chan et al. 2016). McLeod and Costello (2017) counted 129 marine crustacean species collected in light traps to the date of their study in the world, including 44 copepod species consisting of 29 calanoid species and 15 other species. Holmes (1985) described the fish-parasitic copepod *Anchistrotos lucipetus* as a new species that was collected using a light trap in Irish waters, indicating that strict parasitic animals can be caught in light traps.

Recently copepods caught in light traps have been recorded frequently in Korea (Chang and Song 1995; Chang 2012, 2014; Lee and Chang 2016; Lee et al. 2016; Cho et al. 2018; Jeon et al. 2018, 2019). These copepod species were benthic and planktonic, but not genuinely symbiotic. During the past decade we have collected marine copepods from Korean coasts using a light trap, and the symbiotic copepods (poecilostome Cyclopoida and Siphonostomatoida) are recorded in the present paper.

Materials and methods

Copepod specimens in this study were collected using underwater light traps at 33 collection sites (Fig. 1, Table 1) around the South Korean coast during the period from March 2013 to September 2021. Most of these collection sites are fishing ports with water depths less than 10 m. The light traps were made of PVC pipe of ~ 12 cm in diameter and 40 cm long, with a transparent funnel entrance and white-colored LED flashlight inside, as in Sigurdsson et al. (2014). At each collection site, the light trap was deployed on the sea bottom for one or two hours in the early night usually an hour after sunset mainly around the end of the month. Collected material consisting of various invertebrates and fish larvae was fixed with 5% formalin for ~ 1 h and then transferred to 70% ethanol for preservation. The symbiotic copepods were sorted out from the collected material for the present taxonomic study. Before microscopic observation, selected specimens were soaked in lactic acid for ~ ten min. Drawings were made with a drawing apparatus on the microscope. Type specimens have been deposited in the Marine Biodiversity Institute of Korea (**MABIK**), Seocheon, Korea. Scientific names were checked against those in WoRMS (WoRMS Editorial Board 2021).

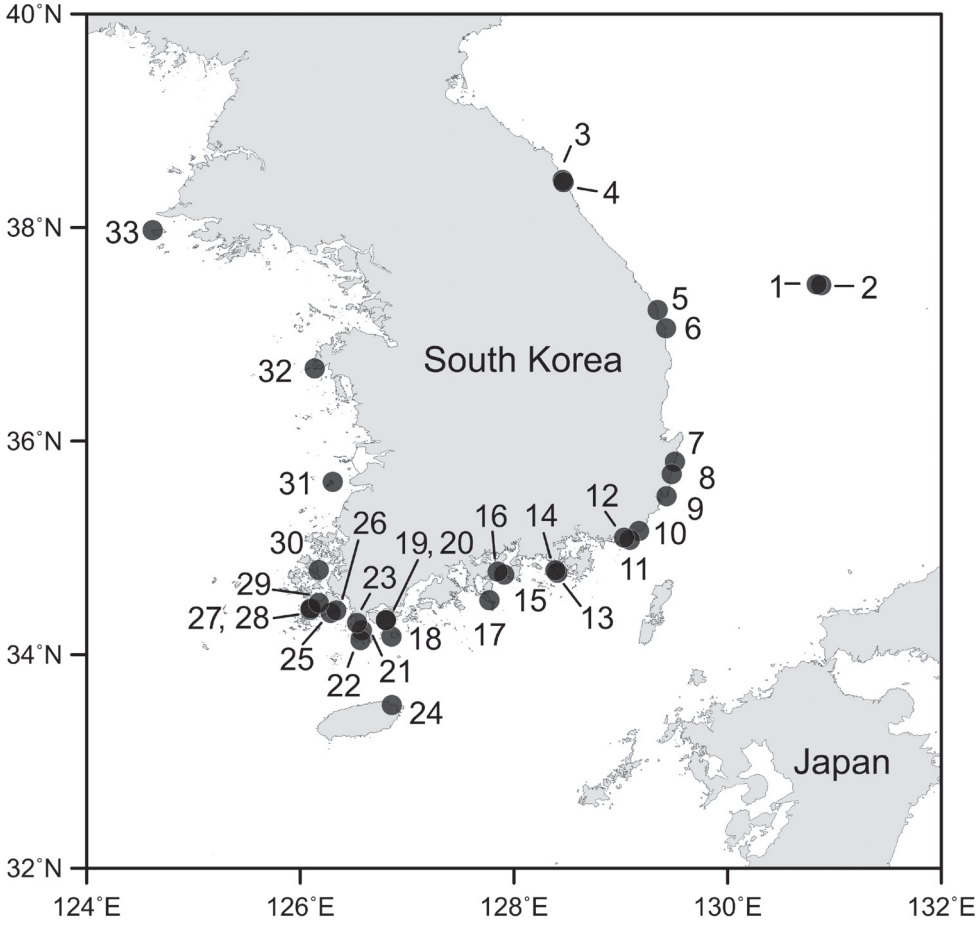

Figure 1. Map showing the collection sites in South Korea.

Taxonomic account

Order Cyclopoida Burmeister, 1834
Family Anthessiidae Humes, 1986
Genus *Anthessius* Della Valle, 1880

***Anthessius atrinae* Suh & Choi, 1991**

Material examined. One ♀, Site 12, 16 Mar. 2013.

Remarks. This copepod has been known only from the bivalve *Atrina pectinata* (Linnaeus, 1767). The copepod is presumed to have escaped from its bivalve host in a fish market aquarium into the adjacent waters of the collection site, where the host cannot dwell due to the water pollution.

Table 1. Collection sites.

Sites	Localities	Coordinates
1	Sadong, Ulleung I.	37°27'35.7"N, 130°52'34.6"E
2	Namyang, Ulleung I.	37°28'01.3"N, 130°50'01.4"E
3	Geojin, Goseong	38°26'38"N, 128°27'27"E
4	Ban-am, Goseong	38°25'30"N, 128°27'47"E
5	Imwon, Samcheok	37°13'44"N, 129°20'45"E
6	Jukbyeon, Uljin	37°03'22"N, 129°25'22"E
7	Gampo, Gyeongju	35°48'29"N, 129°30'19"E
8	Eupcheon, Gyeongju	35°41'32.6"N, 129°28'30.4"E
9	Bangeojin, Ulsan	35°29'03.9"N, 129°25'44.5"E
10	Haeundae, Pusan	35°09'30"N, 129°10'14"E
11	Yeongdo, Pusan	35°04'31.0"N, 129°05'08.7"E
12	Near Pusan Fish Market	35°05'46"N, 129°01'51"E
13	Minam-ri, Tongyeong	34°46'02.9"N, 128°24'21.1"E
14	Junghwa-ri, Tongyeong	34°47'25.1"N, 128°23'17.9"E
15	Honghyeon-ri, Namhae I.	34°45'00.5"N, 127°54'33.9"E
16	Deogweol, Namhae I	34°46'35.3"N, 127°50'57"E
17	Geum-oh I.	34°30'33.1"N, 127°46'10.1"E
18	Doryak-ri, Cheongsan I.	34°10'12"N, 126°51'13"E
19	Ul-mool, Sinji I.	34°19'25.4"N, 126°48'06.7"E
20	Myeongsa, Sinji I.	34°19'25.48"N, 126°48'05.04"E
21	Nohwa I.	34°13'28"N, 126°53'47"E
22	Yesong, Bogil I.	34°08'11"N, 126°33'49"E
23	Galdu, Haenam	34°17'57"N, 126°31'50"E
24	Saehwa, Jeju I.	33°31'45"N, 126°51'25"E
25	Geumgap-ri, Chindo I.	34°23'30.7"N, 126°17'01.1"E
26	Chopyeong, Chindo I.	34°24'46.3"N, 126°20'11.1"E
27	Saepo, Chindo I.	34°25'10.4"N, 126°05'39.0"E
28	Gahak, Chindo I.	34°25'52.7"N, 126°05'51.4"E
29	Bojeon, Chindo I.	34°29'08.5"N, 126°10'18.5"E
30	Gosan, Palgeum I.	34°47'38"N, 126°10'22"E
31	Wido I.	35°37'04"N, 126°18'15"E
32	Sinjin, Taean	36°40'50"N, 126°08'05"E
33	Dumoojin, Baekryeongdo I.	37°58'31"N, 124°37'10"E

Anthessius graciliunguis Do & Kajihara, 1984

Fig. 2

Material examined. Twenty ♀♀, 9 ♂♂, Site 4, 19 Jul. 2016; 2 ♀♀, Site 5, 21 Jul. 2016; 37 ♀♀, 2 ♂♂, Site 7, 21 Jun. 2019; 7 ♀♀, 3 ♂♂, Site 8, 18 May 2015; 17♀♀, 2 ♂♂, Site 9, 17 May 2015; 8 ♀♀, 2 ♂♂, Site 11, 03 Jun. 2019; 1♀, 1 ♂, Site 11, 07 Jul. 2020; 9 ♀♀, Site 11, 16 Apr. 2014; 10 ♀♀, Site 11, 20 Aug. 2020; 11 ♀♀, Site 12, 16 Mar. 2013; 1♀, 1 ♂, Site 13, 03 Jul. 2020; 9 ♀♀, 1 ♂, Site 14, 03 Jul. 2020; 1 ♀, Site 15, 04 Jul. 2020; 6 ♀♀, Site 16, 04 Jul. 2020; 5 ♀♀, Site 17, 13 May 2015; 24 ♀♀, 4 ♂♂, Site 18, 27 Apr. 2017; 2 ♀♀, Site 19, 05 Jun. 2020; 6 ♀♀, 2 ♂♂, Site 21, 26 May 2017; 62 ♀♀, 13 ♂♂, Site 22, 26 Apr. 2021; 30 ♀♀, 10 ♂♂, Site 22, 31 May 2021; 11 ♀♀, 3 ♂♂, Site 23, 24 Apr. 2021; 3 ♀♀, 1 ♂, Site 26, 06 Jul. 2016; 10 ♀♀, 1 ♂, Site 32, 24 May 2020; 4 ♀♀, 2 ♂♂, Site 33, 11 Aug. 2020.

Supplementary description of female. Body (Fig. 2A) narrow. Body length of figured specimen 1.72 mm. Prosome 1.8 × longer than wide (1.06 × 0.59 mm), ~ 60%

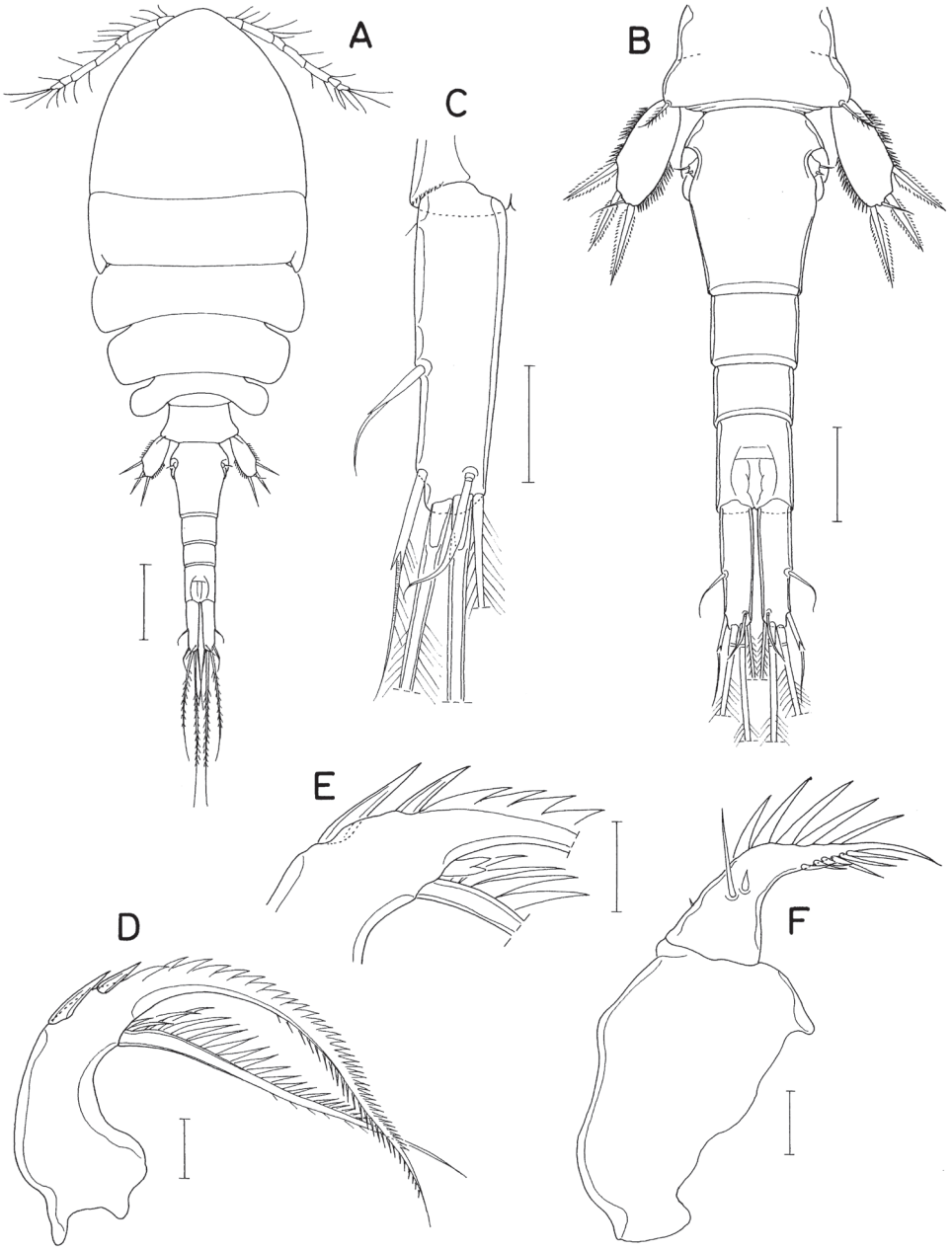

Figure 2. *Anthessius graciliunguis* Do & Kajihara, female **A** habitus **B** urosome **C** left caudal ramus, dorsal **D** mandible, dorsal **E** area between inner seta and distal lash of mandible, ventral **F** maxilla. Scale bars: 0.2 mm (**A**); 0.1 mm (**B**); 0.05 mm (**C**); 0.02 mm (**D–F**).

as long as body length. Cephalothorax with dorsal suture line between cephalosome and first pedigerous somite; posterolateral corners conically produced. Genital double-somite (Fig. 2B) ~ 1.25 × longer than wide (198 × 160 μm), widest at proximal 30%

region followed by gradually narrowed distal 70% of double-somite. Caudal ramus (Fig. 2C) 3.49 × longer than wide (136 × 39 μm), gradually narrowed distally, armed with six setae; seta II (outer lateral seta) positioned at 55% of ramus length, with stiff, spiniform proximal half and setiform distal half; seta III (outer distal seta) consisting of distally bifurcate, spiniform proximal part and thin, setiform distal part; seta VII (dorsal seta) annulated proximally, with slightly broadened middle region.

Mandible (Fig. 2D, E) with bifurcate, rudimentary element on ventral side between bases of distal lash and inner seta; inner seta as long as distal lash. Maxilla (Fig. 2F) consisting of syncoxa and basis; basis terminated in spiniform distal lash, armed with three setae (setae I–III); seta I (inner seta) small, rudimentary, positioned close to seta II; seta II simple; seta III minute, almost invisible; distal lash armed with five spines along convex outer margin and six spinules along inner margin.

Leg 4 with three spines and five setae on third exopodal segment. Leg 5 exopod 2.1 × longer than wide.

Description. Male. Body form as in female. Body length of measured specimen 1.20 mm.

Remarks. *Anthessius graciliunguis* Do & Kajihara, 1984 was described originally as an associate of the mussel *Mytilus galloprovincialis* Lamarck, 1819 from Japan (Do and Kajihara 1984). Kim (1998, 2010a) recorded four additional bivalve host species in Korea: *Mizuhopecten yessoensis* (Jay, 1857), *Pecten albicans* (Schröter, 1802), *Scaeochlamys squamata* (Gmelin, 1791), and *Solecurtus divaricatus* (Lischke, 1869) in Korea. Ueda et al. (2006) found this copepod species in plankton samples in Japan. In the present study, this copepod occurred most frequently from 19 of 33 collection sites around the coasts of South Korea. Although we have not examined the Korean population of *M. galloprovincialis* for copepods, this mussel seems to be the major host of *A. graciliunguis*, considering that only this mussel inhabits all of those 19 collection sites.

The diagnostic morphological features of the female of *A. graciliunguis* are as follows: (1) the caudal ramus is ~ 3.5 × longer than wide, (2) the terminal segment of antenna is 3.0 × longer than wide; (3) the convex outer margin of the distal lash of maxilla is ornamented with five spines; (4) the third exopodal segment of leg 4 is armed with three spines and five setae; and (5) the exopod of leg 5 is 2.1 × longer than wide. The first (1) and last (5) may be the simple combination of features sufficient to differentiate *A. graciliunguis* from its congeners.

Family Clausidiidae Embleton, 1901
Genus *Conchyliurus* Bocquet & Stock, 1957

Conchyliurus quintus Tanaka, 1961

Material examined. One ♂, Site 4, 19 Jul. 2016; 1 ♀, Site 12, 16 Mar. 2013; 1 ♀, Site 33, 11 Aug. 2020.

Remarks. In Korea, *Conchyliurus quintus* is widely distributed along the entire coast. It has a low host specificity, inhabiting 12 species of bivalves in Korea (Kim 2004).

Genus *Hemicyclops* Boeck, 1872

***Hemicyclops japonicus* Itoh & Nishida, 1993**

Material examined. Two ♀♀, Site 11, 16 Apr. 2014; 20 ♀♀, 17 ♂♂, Site 22, 31 May 2021; 1 ♀, Site 24, 16 May 2019.

Remarks. This species is easily identifiable due to the characteristic genital double-somite of the female, which has a deep lateral constriction between the anterior third and posterior two-thirds and a pointed process on each lateral margin. The host of this copepod is still unknown.

***Hemicyclops nasutus* Moon & Kim, 2010**

Material examined. One ♀, Site 11, 16 Apr. 2014; 1 ♂, Site 20, 05 Jun. 2020; 1 ♀, 7 ♂♂, Site 22, 31 May 2021; 1 ♀, Site 23, 24 Apr. 2021; 1 ♀, 2 ♂♂, Site 27, 09 Jul. 2016.

Brief description of male. Body form as in female. Body length 1.30 mm. Urosome six-segmented. Genital somite wider than long. Caudal ramus 3.03 × longer than wide (115 × 38 μm). Antennule with same armature formula as in female. Antenna, mandible, maxillule the same as those of female. Basis (distal segment) of maxilla terminating in stout claw. Maxilliped four-segmented; first segment (syncoxa) with single large spinulose seta subdistally on inner margin; second segment (basis) broadened proximally, markedly tapering distally, armed with two unequal setae (one spinulose and one minute), and ornamented with three longitudinal rows of denticles along inner margin; small third segment (first endopodal segment) unarmed; terminal segment forming long, curved claw bearing two setae proximally.

Leg 1 different from that of female in absence of inner distal spine on basis. Legs 2–4 as in female. Leg 5 consisting of single dorsolateral seta on fifth pedigerous somite and exopod; protopod completely fused with somite. Leg 6 represented by one spine on posterolateral corner of genital operculum.

Remarks. Moon and Kim (2010) described this species based on a single female found on an unidentified polychaete from the Yellow Sea, Korea. The male is recorded here for the first time.

***Hemicyclops rapax* sp. nov.**

https://zoobank.org/9FE3EF15-2C7B-4266-B619-190EAEE13FC8

Figs 3–6

Material examined. ***Holotype*** ♀ (MABIK CR00250118) and ***paratype*** ♀ (MABIK CR00250119) preserved in 90% alcohol, Site 22 (Yesong, Bogil Island, south coast, 34°08'11"N, 126°33'48"E), 31 May 2021, leg. J. Lee; paratype ♂ (MABIK CR00250123, figured) dissected and mounted on a slide, Site 22, 26 April 2021, leg.

J. Lee and C. Y. Chang; 1 ♀ preserved in 90% alcohol and 1 ♀ (figured) dissected and mounted on a slide, Site 11 (Yeongdo, Pusan, 35°04'31.0"N, 129°05'08.7"E), 07 Jul. 2020, leg. J. G. Kim.

Description. Female. Body (Fig. 3A) moderately stout, dorsoventrally flattened. Body length 1.10 mm in dissected and figured specimen (1.22 mm in holotype). Prosome 680 × 555 μm, ~ 56% as long as body length. Posterolateral corners of all prosomal somites pointed or angular. Urosome (Fig. 3B) five-segmented. Fifth pedigerous somite 234 μm wide, slightly wider than genital double-somite. Genital double-somite subcircular, flattened ventrally, thin laterally, slightly wider than long (220 × 227 μm) in dissected specimen or slightly longer than wide in smaller other specimens; lateral margin with small denticle (this denticle absent smaller specimens) as indicated by arrowhead in Fig. 3B; genital apertures positioned dorsolaterally at anterior part of double-somite. Three abdominal somites 84 × 136 μm, 61 × 127 μm, and 45 × 114 μm, respectively. Genital double-somite and first two free abdominal somites with membranous fringe along posterior margin. Anal somite with row of spinules along posteroventral margin. Caudal ramus (Fig. 3C) short, 1.15 × longer than wide (55 × 48 μm), slightly longer than anal somite, armed with six setae (setae II-VII), and ornamented with setules on distal half of inner margin and fine spinules along posteroventral margin; seta II (outer lateral seta) positioned at midlength of ramus, spiniform in proximal half but setiform in distal half; seta III (outer distal seta) also proximally spiniform and distally setiform; dorsal seta (seta VII) annulated proximally; setae II, III, and VII naked, but other three setae pinnate.

Rostrum small, with convex posterior margin. Antennule (Fig. 3D) 237 μm long, seven-segmented; armature formula 4, 14, 6, 3, 4+aesthetasc, 2+aesthetasc, and 7+aesthetasc; first segment ornamented with fines setules on anterior surface; setae and aesthetascs slender; most setae naked except single on each fourth and fifth segments and three on terminal segment. Antenna (Fig. 3E) consisting of coxa, basis and three-segmented endopod; armature formula 0, 1, 1, 4, and 7; basis ornamented with two patches of spinules on inner margin and several setules on outer margin; first endopodal segment with acutely pointed outer distal corner and patch of spinules on inner surface and patch of small spinules at inner distal corner; second endopodal segment with prominent inner distal prolongation (this prolongation distinctly longer than wide; its two apical setae strong, claw-like), ornamented with broad spinules along inner margin and row of small spinules near outer distal corner; third endopodal segment as long as wide, ornamented with two rows of minute setules on outer side; four of seven setae on third endopodal segment claw-like, wrinkled in middle.

Labrum (Fig. 4A) with denticles and spinules on posterior margin. Labium (Fig. 4B) denticulated along anterior margin, spinulose subapically. Mandible (Fig. 3F) distally armed with one stout, denticulate element, one spinulose, plate-like element and two pinnate setae. Paragnath (Fig. 3G) lobate, ornamented with fine setules on middle and subdistal regions and spinules on distal region, with trace of articulation subdistally. Maxillule (Fig. 3H) unequally bilobed distally; smaller inner lobe armed with three weakly pinnate setae; larger outer lobe with five pinnate setae. Maxilla

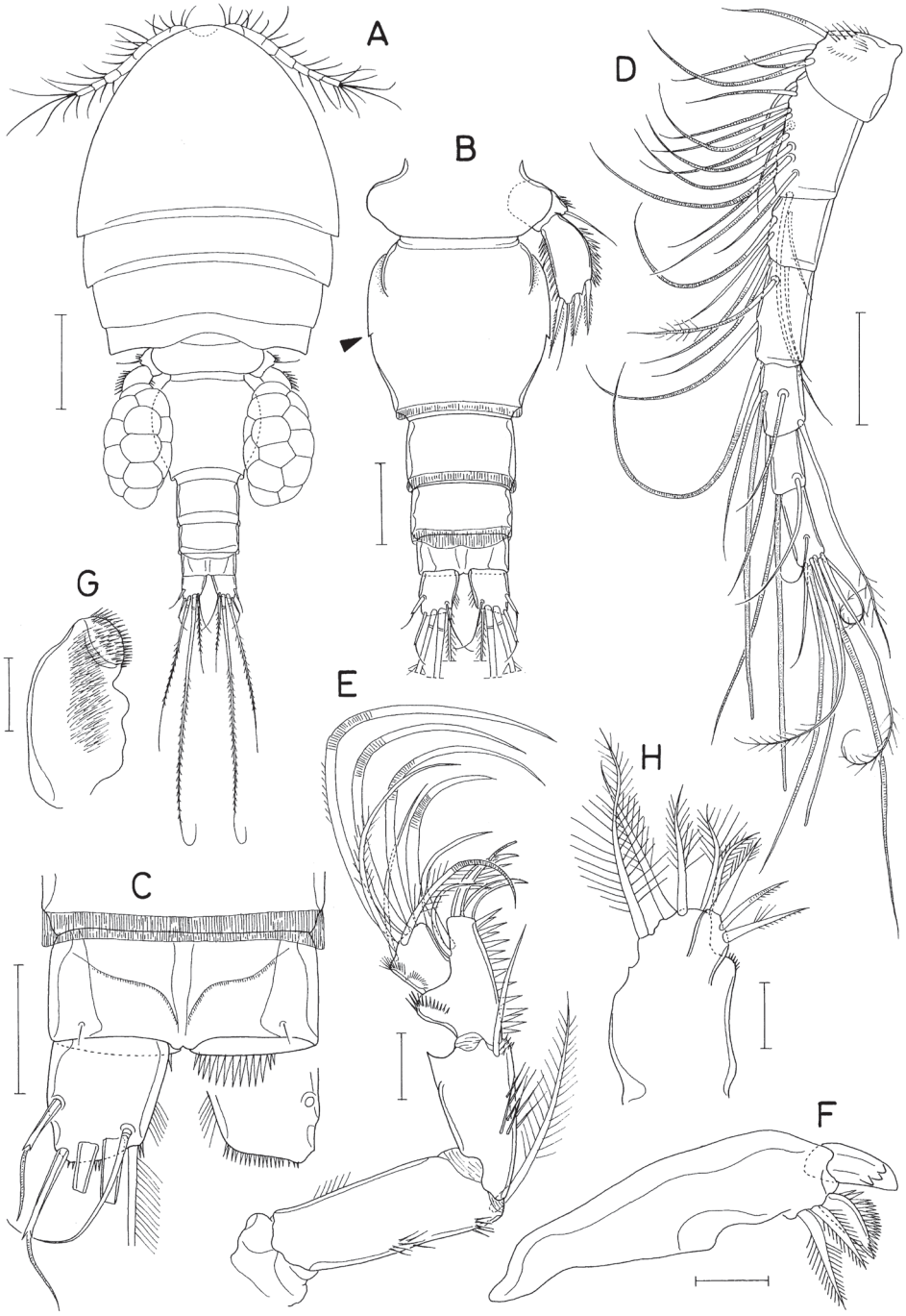

Figure 3. *Hemicyclops rapax* sp. nov., female **A** habitus, dorsal **B** urosome, dorsal (arrowhead indicates a small denticle on lateral margin of genital double-somite) **C** anal somite and caudal rami, dorsal **D** antennule **E** antenna **F** mandible **G** paragnath **H** maxillule. Scale bars: 0.2 mm (**A**); 0.1 mm (**B**); 0.05 mm (**C, D**); 0.02 mm (**E–H**).

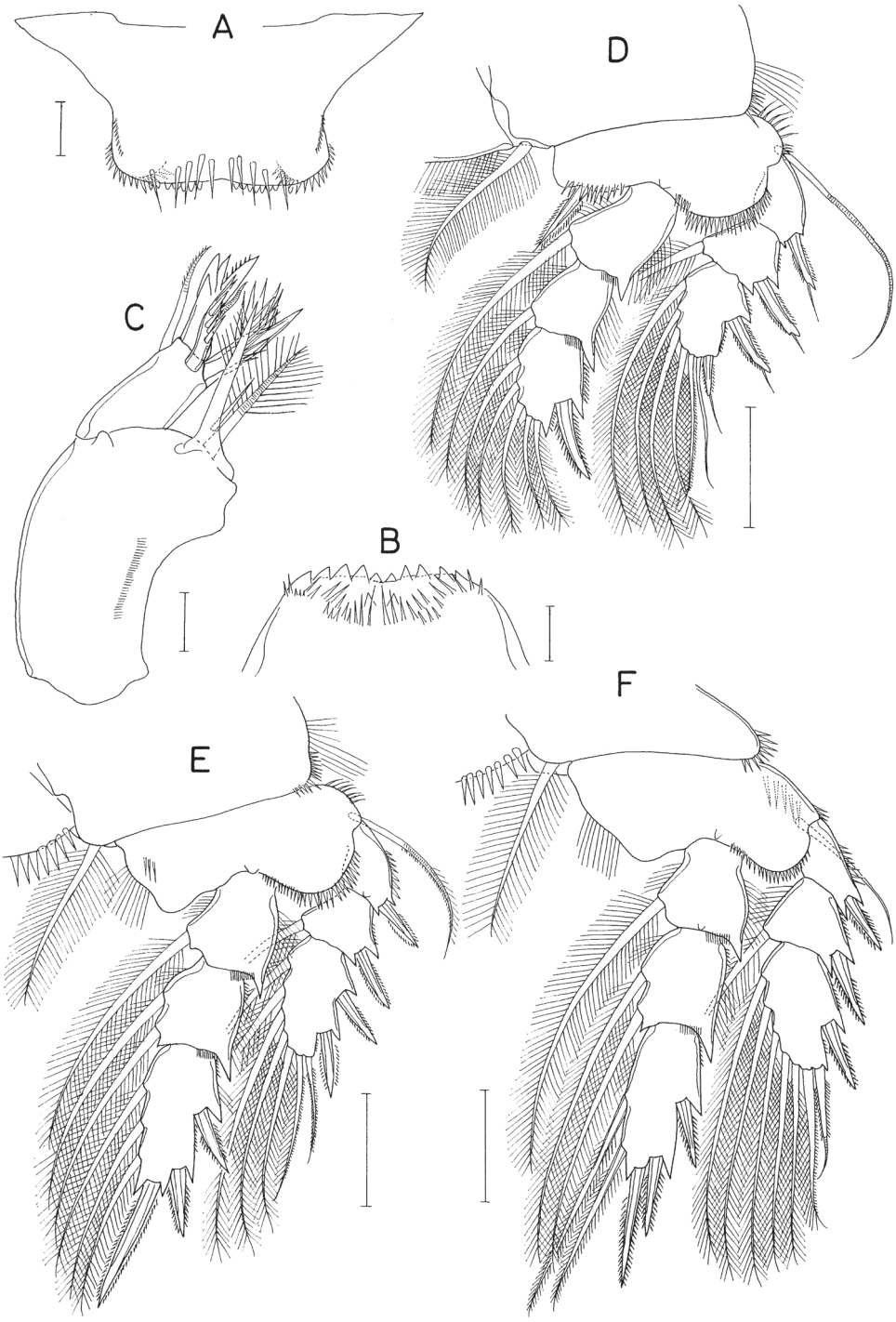

Figure 4. *Hemicyclops rapax* sp. nov., female **A** labrum **B** labium **C** maxilla **D** leg 1 **E** leg 2 **F** leg 4. Scale bars: 0.02 mm (**A–C**); 0.05 mm (**D–F**).

(Fig. 4C) two-segmented; proximal segment (syncoxa) armed with three setae, smallest one setule-like, inserted on proximal region of spiniform largest seta, and ornamented with row of minute spinules on proximal region; distal segment (basis) distally armed with three heavily spinulose or denticulate spines and single seta. Maxilliped (Fig. 5A) four-segmented; first segment (syncoxa) with two large setae on inner margin; second segment (basis) also with two large setae on inner margin; third segment (first endopodal segment) short, unarmed; terminal segment (second endopodal segment) forming large hook (this hook much longer than proximal three segments), proximally armed with one spine bearing seven spinules on outer margin and four small, naked setae (Fig. 5B).

Legs 1–4 biramous, with three-segmented rami (Fig. 4D–F); basis spinulose along outer margin and posterior margin between bases of rami. Intercoxal plate setulose in leg 1 (Fig. 4D) but spinulose in legs 2–4 (Fig. 4E, F). Outer spines on exopod of leg 1 tipped with setule. Leg 3 armed and shaped as leg 2. Two inner setae on third endopodal segment of leg 4 stiff, spiniform. Armature formula for legs 1–4 as follows:

	Coxa	Basis	Exopod	Endopod
Leg 1	0-1	1-I	I-0; I-1; II, 6	0-1; 0-1; I, 5
Legs 2 & 3	0-1	1-0	I-0; I-1; II, 7	0-1; 0-2; I, II, 3
Leg 4	0-1	1-0	I-0; I-1; II, 6	0-1; 0-2; I, II, 2

Leg 5 (Fig. 5C) two-segmented; proximal segment (protopod) with one slender outer seta and row of spinules at outer distal region; distal segment (exopod) 1.95 × longer than wide (86 × 44 μm) densely ornamented with spinules along outer and inner margins, armed with three spines and one weakly pinnate seta; lengths of three spines 54, 50, and 56 μm respectively from outer to inner. Leg 6 invisible.

Male. Body (Fig. 6A) slightly larger than that of female. Body length 1.28 mm. Cephalothorax distinctly broader than next somites. Posterolateral corners of all prosomal somites blunt or rounded. Urosome (Fig. 6B) six-segmented. Fifth pedigerous somite with membranous flap on each side of posterodorsal margin. Genital somite much wider than long (152 × 255 μm), with finely serrate posterodorsal corners and single spine on genital operculum. All urosomal somites lacking membranous fringe on posterior margin. Four abdominal somites gradually shorter from proximal to distal. Caudal ramus 1.04 × longer than wide (50 × 48 μm).

Rostrum as in female. Antennule different from that of female in having one additional seta at proximal anterior margin of fourth segment (thus with 4 setae on this segment). Antenna, labrum, mandible, paragnath, maxillule as in female. Maxilla different from that of female; basis armed with two spines and one seta and terminating in stout, claw-like process bearing spinules on outer margin and granule-like papillae on distal region (Fig. 6C). Maxilliped (Fig. 6D) four-segmented; first segment (syncoxa) with one large, distally pinnate seta; second segment (basis) strongly tapering distally, armed with one pinnate seta, ornamented with three rows of denticles along inner margin; small third segment (first endopodal segment) unarmed; terminal segment as hook bearing two unequal setae proximally.

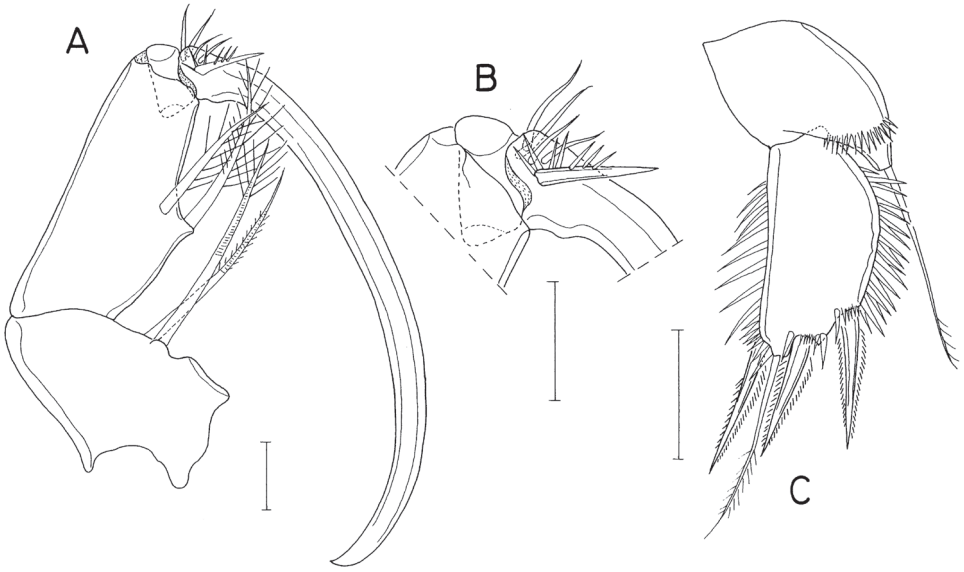

Figure 5. *Hemicyclops rapax* sp. nov., female **A** maxilliped **B** distal part of maxilliped **C** leg 5. Scale bars: 0.02 mm (**A, B**); 0.05 mm (**C**).

Leg 1 different from that of female in absence of inner distal element on basis (Fig. 6E). Legs 2–4 as in female. Leg 5 consisting of one naked dorsolateral seta on somite (protopod completely fused with somite) and exopod; exopod shaped and armed as in female. Leg 6 represented by single spine on genital operculum (Fig. 6B).

Etymology. The specific name *rapax* is derived from the Latin *rapa* (grasping), alluding to the grasping form of the female maxilliped.

Remarks. *Hemicyclops rapax* sp. nov. is characterized by its peculiar female maxilliped, in which the terminal segment is transformed to a large hook, as in the males of existing species. This form of female maxilliped is very unusual for the genus, since the terminal segment (second endopodal segment) of the female maxilliped in other species of the genus generally terminates in a spiniform process (or a spine). The only other example of this peculiar female maxilliped in *Hemicyclops* is that of *H. cylindraceus* (Pelseneer, 1929), as illustrated by Stock (1954), although the terminal hook is much less developed in the latter species. Otherwise, *H. cylindraceus* differs from *H. rapax* sp. nov. in having a narrow, almost cylindrical body, five setae on the first antennular segment, four setae (without spines) on the exopod of leg 5, and an inner distal element on the basis of leg 1 (Stock 1954).

Hemicyclops rapax sp. nov. may be differentiated from its congeners in other ways. In eight species in *Hemicyclops* the caudal ramus is short, less than 1.5 × longer than wide in the female, as in *H. rapax* sp. nov. In five of these eight species (*H. apiculus* Humes, 1995, *H. australis* Nicholls, 1944, *H. intermedius* Ummerkutty, 1962,

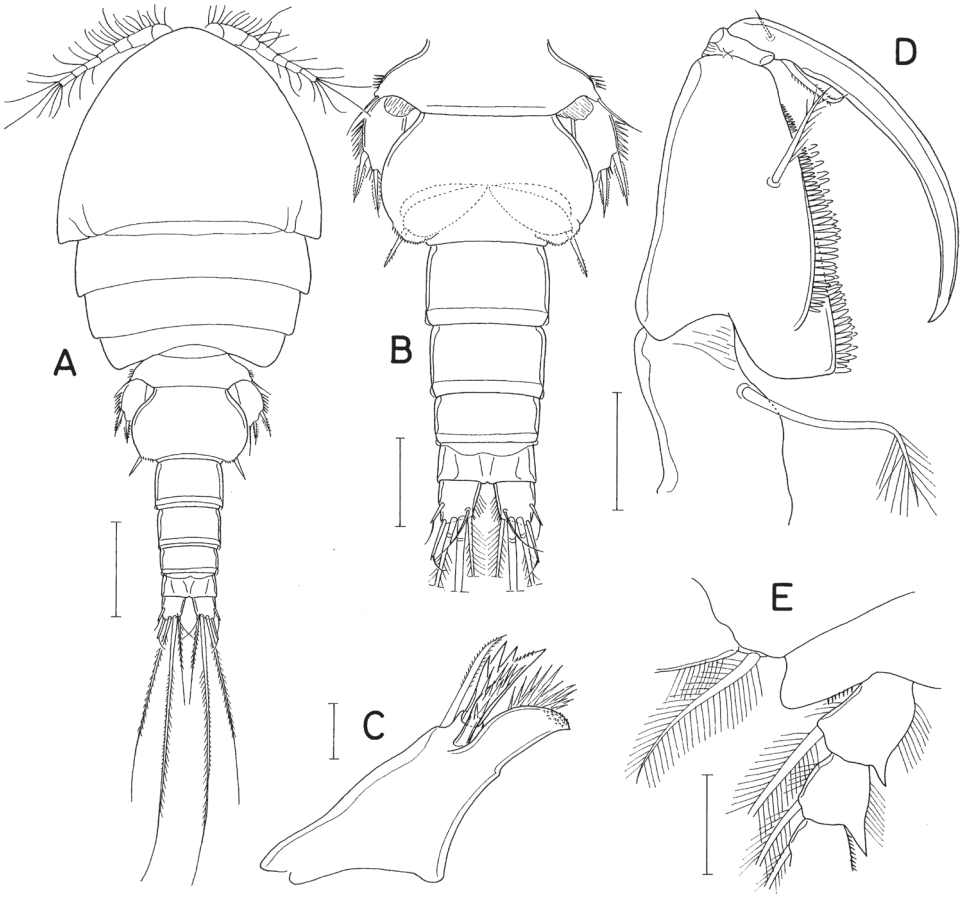

Figure 6. *Hemicyclops rapax* sp. nov., male **A** habitus, dorsal **B** urosome, dorsal **C** distal segment of maxilla **D** maxilliped **E** inner proximal region of leg 1. Scale bars: 0.2 mm (**A**); 0.1 mm (**B**); 0.02 mm (**C**); 0.05 mm (**D, E**).

H. parapiculus Kim & Hong, 2014, and *H. vicinalis* Humes, 1995), the genital double-somite of the female is distinctly longer than wide (more than 1.2 × longer than wide); in *H. tamilensis* (Thompson & T. Scott, 1903) the urosome of the female is six-segmented and the exopod of leg 5 is elongated; in *H. saxatilis* Ho & Kim, 1992 the basis of male leg 1 bears an inner distal spine, the first segment of the male maxilliped is armed with two (rather than one) setae, and the maxilla is not sexually dimorphic. In the remaining species, *H. leggii* (Thompson & T. Scott, 1903) described based on the male, the third endopodal segment is armed with five armature elements (I, 4, rather than I, 5), the basis of male leg 1 is armed with an inner distal spine, and the first segment of male maxilliped is armed with two setae. These differences are considered sufficient to distinguish the new species from these eight congeners.

Hemicyclops parilis Moon & Kim, 2010

Material examined. Two ♀♀, Site 11, 20 Aug. 2020; 1 ♀, Site 12, 16 Mar. 2013; 2 ♀♀, 1 ♂, Site 15, 04 Jul. 2020; 1 ♀, Site 20, 05 Jun. 2020; 2 ♀♀, 8 ♂♂, Site 26, 06 Jul. 2016; 1 ♂, Site 33, 11 Aug. 2020.

Remarks. Due to the close relatedness of this species to *H. gomsoensis* Ho & Kim, 1992, Moon and Kim (2010) compared it in detail with the latter species in the original description. Moon and Kim (2010) found *H. parilis* from burrows of unknown invertebrates on the south coast of Korea. The host of this copepod has turned out to be the decapod crustacean *Upogebia issaeffi* (Balss, 1913). We collected it at six collection sites in this study, which indicates that the decapod host is likely to occur at those sites.

Genus *Hersiliodes* Canu, 1888

Hersiliodes exiguus Kim & Stock, 1996

Material examined. One ♀, Site 1, 28 Jun. 2021; 1 ♀, Site 22, 31 May 2021.

Remarks. This is the second record of *Hersiliodes exiguus* which was originally recorded as an associate of the clam *Ruditapes philippinarum* (A. Adams & Reeve, 1850) inhabiting a brackish lagoon on the east coast of Korea (Kim and Stock 1996). The characteristic form of the female genital double-somite bearing a pair of lateral projections allows easy identification of this species without dissection.

Family Clausiidae Giesbrecht, 1895
Genus *Pontoclausia* Bacescu & Por, 1957

Pontoclausia cochleata sp. nov.

https://zoobank.org/0B9BBD7E-FB2C-42ED-B5BB-4DD3BF0927EA
Figs 7–9

Material examined. ***Holotype*** ♀ (MABIK CR00250124) dissected and mounted on a slide, Site 22 (Yesong, Bogil Island, south coast, 34°08'11"N, 126°33'49"E), 26 Apr. 2021, leg. J. Lee and C. Y. Chang; ***Paratype*** ♂ (MABIK CR00250125) dissected and mounted on a slide, Site 27 (Sepo, Chindo Island, southwest coast, 34°25'10.4"N, 126°05'39.0"E), 09 Jul. 2016, leg. J. Lee and C. Y. Chang.

Description. Female. Body (Fig. 7A) narrow, gradually narrowing from anterior to posterior. Body length 2.10 mm. Maximum width 523 μm across cephalothorax. Prosome 936 μm long, shorter than urosome, consisting of cephalothorax and second to fourth pedigerous somites. Cephalothorax wider than long, without dorsal suture line between cephalosome and first pedigerous somite. All prosomal somites with rounded lateral margins. Urosome six-segmented. Fifth pedigerous somite 340 μm wide. Genital somite ~ 1.8 × wider than long (170 × 304 μm), with convex lateral margins; genital aperture positioned dorsolaterally near middle of somite. Four abdominal somites

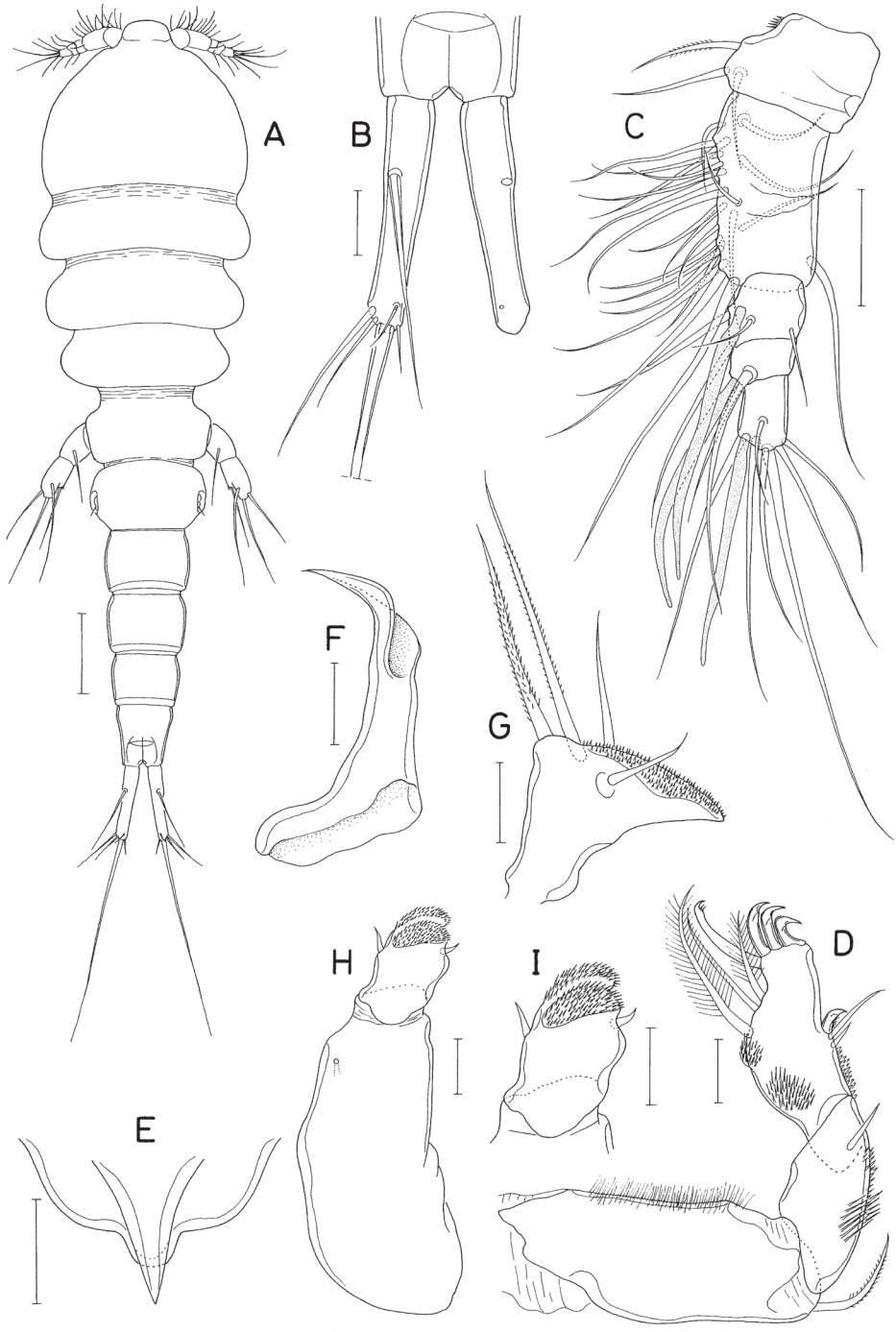

Figure 7. *Pontoclausia cochleata* sp. nov., female **A** habitus, dorsal **B** caudal rami, dorsal **C** antennule **D** antenna **E** labrum **F** mandible **G** maxillule **H** maxilla **I** distal segment of maxilla. Scale bars: 0.2 mm (**A**); 0.05 mm (**B, C**); 0.02 mm (**D–I**).

unornamented, 160 × 220 μm, 152 × 200 μm, 130 × 174 μm, and 148 × 144 μm, respectively. Anal somite tapering distally. Caudal rami (Fig. 7B) divergent; each ramus 4.9 × longer than wide (186 × 38 μm), gradually narrowed distally, armed with six stiff, naked setae (setae II–VII); seta II as long as ramus, positioned dorsolaterally at 34% region of ramus length; setae III to VII 136 μm, 83 μm, 532 μm, 38 μm, and 33 μm long, respectively; seta V much larger than other caudal setae, nearly 3.0 × longer than ramus.

Rostrum represented by spatulate anterior prominence of cephalothorax (Fig. 7A). Antennule (Fig. 7C) short, 190 μm long, five-segmented; armature formula 3, 24, 4+aesthetasc, 2+aesthetasc, and 7+aesthetasc; all setae naked; aesthetascs tapering in distal part; first segment with few minute spinules on proximal anterior margin. Antenna (Fig. 7D) three-segmented; first segment (coxobasis) longest, with one seta at inner distal corner and hair-like setules on outer margin; second segment (first endopodal segment) with one seta subdistally and two groups of spinules on inner surface; third segment (fused second and third endopodal segments) armed with one claw plus two setae on inner margin, four claws distally (outermost claw longest, bearing two minute spinules subdistally on inner margin), three setae on subdistal outer margin (middle one naked, but other two pinnate), and ornamented with three patches of spinules (two patches on outer side and one on proximal inner margin).

Labrum (Fig. 7E) small, not covering mouthparts, with protuberance in middle of posterior margin and large, tapering, beak-like process on dorsal surface. Mandible (Fig. 7F) unarmed but highly transformed; its distal part curved, tapering, scoop-like. Maxillule (Fig. 7G) as foot-like lobe, distally expanded medially, armed with four setae (two outer ones longer than other two); broadened distal surface covered with numerous spinules. Maxilla (Fig. 7H) two-segmented; proximal segment (syncoxa) unarmed, ~ twice longer than wide; distal segment (basis; Fig. 7I) blunt, with two spinulose pads apically, armed with two small subdistal setae each on inner and outer margins. Maxilliped (Fig. 8A) as unsegmented, tapering lobe tipped with one naked seta, ornamented with two subapical rows of setules (or spinules).

Legs 1–4 (Fig. 8B–E) biramous, with three-segmented rami; both rami of each leg slender, almost equal in length. Coxa lacking inner seta but ornamented with spinules on outer distal corner. Basis with spinules on distal margin between rami; outer seta long, naked. Terminal spine on third exopodal segment of legs 1–4 characteristically unequally bifurcate at tip. Armature formula for legs 1–4 as follows:

	Coxa	Basis	Exopod	Endopod
Leg 1	0-0	1-I	I-0; I-1; III, I, 4	0-1; 0-1; I, 2, 2
Leg 2	0-0	1-0	I-0; I-1; III, I, 5	0-1; 0-2; II, I, 3
Leg 3	0-0	1-0	I-0; I-1; II, I, 5	0-1; 0-2; II, I, 3
Leg 4	0-0	1-0	I-0; I-1; II, I, 5	0-1; 0-2; II, I, 2

Leg 5 (Fig. 8F) two-segmented; proximal segment (protopod) articulated from somite, armed with one dorsodistal seta of 180 μm long. Distal segment (exopod) 1.4 × longer than wide (114 × 82 μm), armed with four slender setae, single on inner margin and three on distal margin; inner margin seta 170 μm long; three distal setae 252, 180, and 261 μm

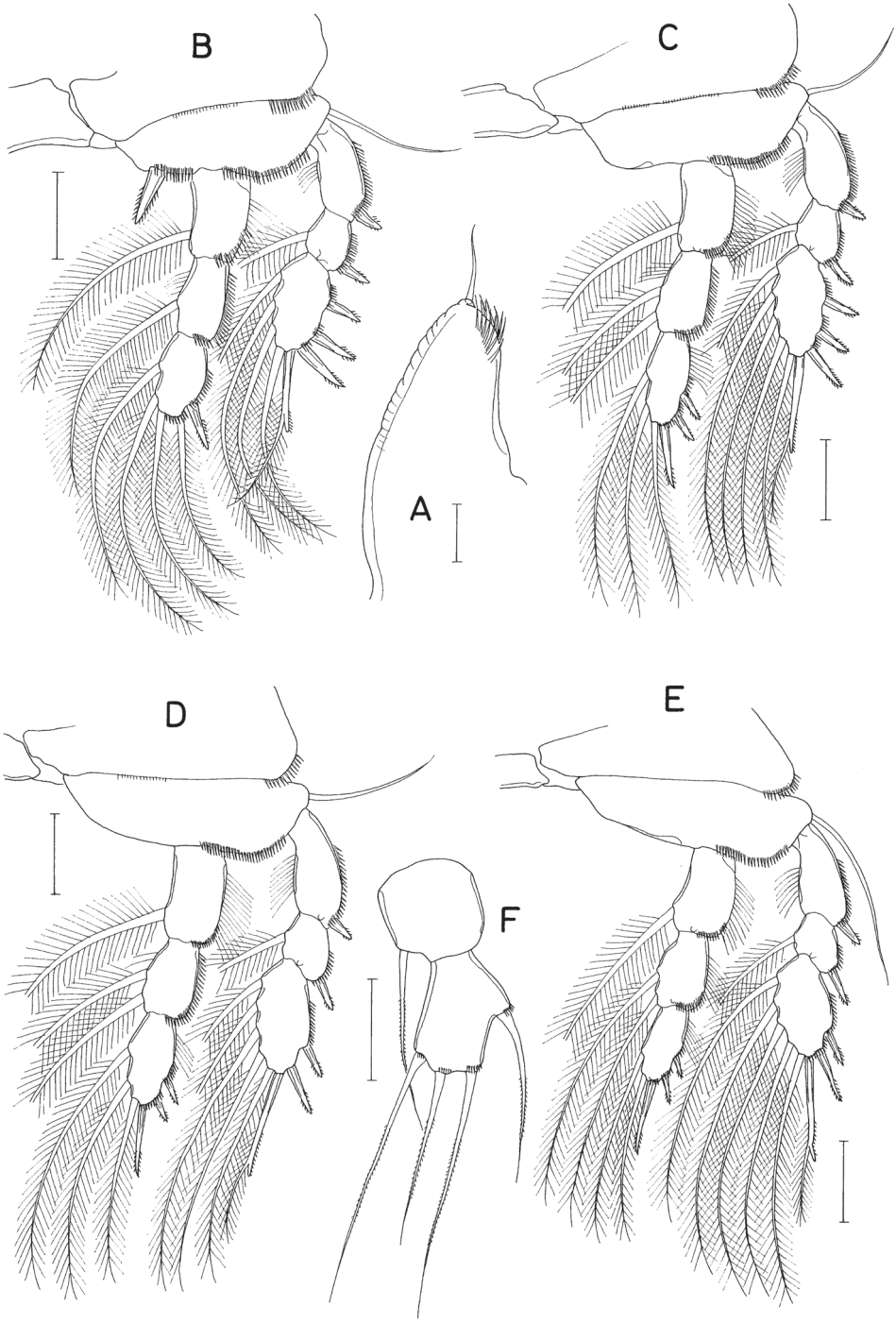

Figure 8. *Pontoclausia cochleata* sp. nov., female **A** maxilliped **B** leg 1 **C** leg 2 **D** leg 3 **E** leg 4 **F** leg 5. Scale bars: 0.02 mm (**A**); 0.05 mm (**B–E**); 0.1 mm (**F**).

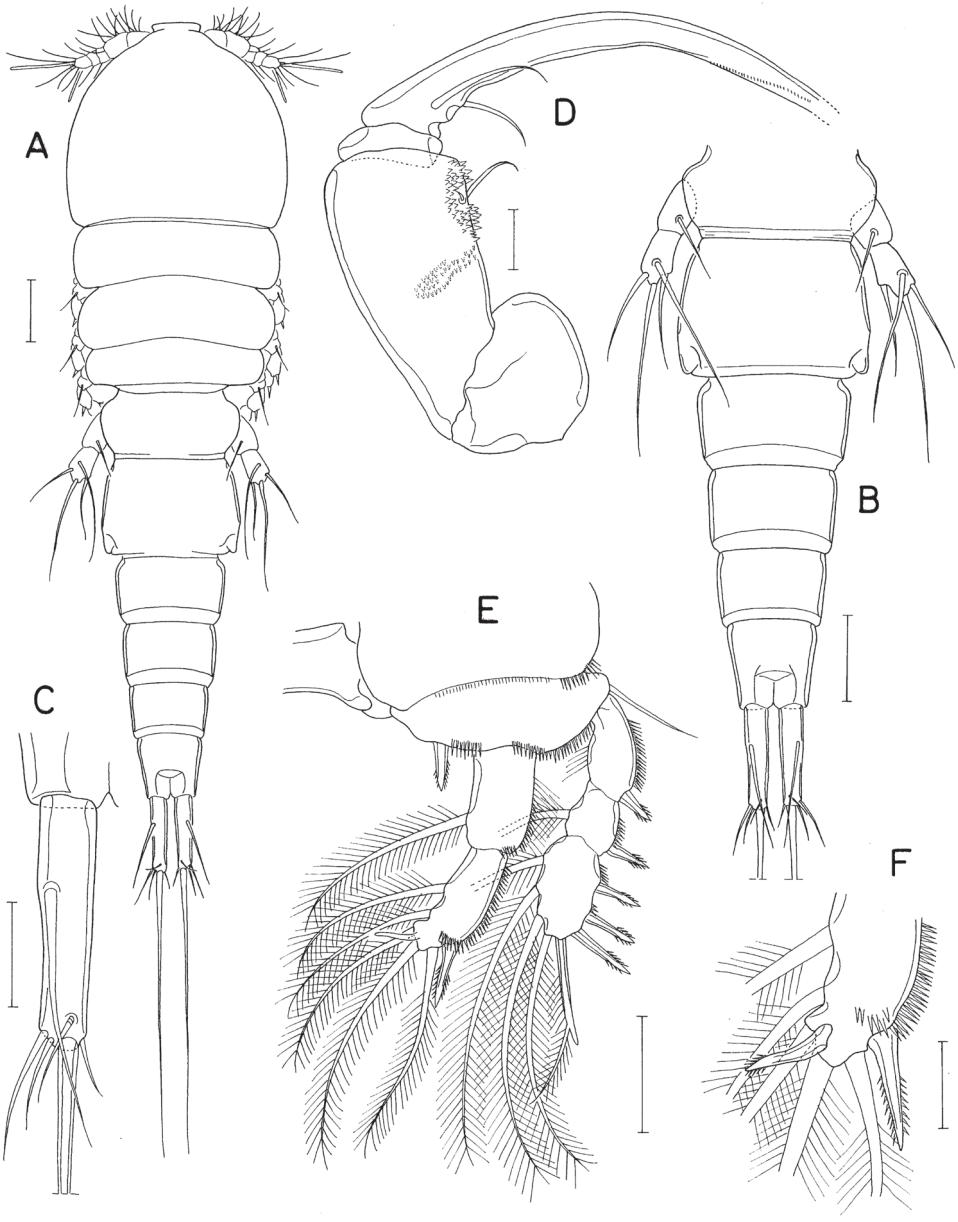

Figure 9. *Pontoclausia cochleata* sp. nov., male **A** habitus, dorsal **B** urosome, dorsal **C** left caudal ramus, dorsal **D** maxilliped **E** leg 1 **F** distal part of endopod of leg 1. Scale bars: 0.1 mm (**A**); 0.05 mm (**B, C**); 0.02 mm (**D, F**); 0.05 mm (**E**).

long respectively from inner to outer. All setae on leg 5 finely spinulose (or with minute setules). Leg 6 probably represented by single minute seta on genital operculum.

Male. Body form (Fig. 9A) as in female. Body length 1.36 mm. Urosome (Fig. 9B) six-segmented, as in female. Genital somite rectangular, wider than long

(158 × 224 μm), as wide as fifth pedigerous somite, gradually broadened distally; genital opercula indistinct, positioned at outer distal corners. Four abdominal somites 106 × 178 μm, 97 × 150 μm, 82 × 127 μm, 97 × 103 μm, respectively. Caudal ramus (Fig. 9C) 4.32 × longer than wide (121 × 28 μm), armed as in female.

Rostrum as in female. Antennule and antenna segmented and armed as in female. Labrum, mandible, maxillule, and maxilla also as in female. Maxilliped (Fig. 9D) four-segmented; first segment (syncoxa) wider than long, unarmed; second segment (basis) gradually broadened distally, armed with two unequal setae, one of them rudimentary, on subdistal inner margin, ornamented with two patches of scale-like spinules; short third segment (first endopodal segment) unarmed; terminal segment as long, arched hook bearing two simple setae proximally.

Leg 1 (Fig. 9E) with three-segmented exopod and two-segmented endopod; compound distal endopodal segment (Fig. 9F) armed with two spines plus five setae (formula I, 2, I, 3). Legs 2–4 as in female. Leg 5 also as in female; exopodal segment 1.5 × longer than wide (68 × 44 μm). Leg 6 not seen.

Etymology. The specific name *cochleata* is derived from the Latin *cochl* (a spoon), alluding to the spoon-like mandible of the new species.

Remarks. With the three-segmented rami of legs 1–4, the inner distal spine on the basis of leg 1, and the laterally positioned leg 5, the new species apparently belongs to the genus *Pontoclausia* which contains five known species (Ho and Kim 2003). Within the genus *Pontoclausia cochleata* sp. nov. may be clearly defined from other species by its three unique features: (1) the mandible is unarmed, with a scoop-like distal part, rather than armed with one or two armature elements as in congeners; (2) the maxilliped is unsegmented and tipped with one seta, rather than segmented and unarmed as in congeners; and (3) the third exopodal segment of leg 1 is armed with eight armature elements (formula III, I, 4), rather than six or seven elements as in congeners. It is remarkable that the form of the mandible of the new species is very unusual for the Clausiidae. Nevertheless, we have refrained from establishing a new genus, since other features of mouthparts and legs are as usual for the genera within Clausiidae.

***Pontoclausia pristina* sp. nov.**

https://zoobank.org/EBD91A7F-FD84-4B52-BD6A-590BAB4C21B8

Figs 10–12

Material examined. ***Holotype*** ♂ (MABIK CR00250126) dissected and mounted on a slide, Site 1 (Sadong, Ulleung Island, 37°27'35.7"N, 130°52'34.6"E), 28 Jun. 2021, leg. J. G. Kim.

Description. Male. Body (Fig. 10A) harpacticiform, slender, cylindrical. Body length 1.60 mm. Prosome ~ twice longer than wide (593 × 295 μm), much shorter than urosome, consisting of cephalothorax and second to fourth pedigerous somites. Cephalothorax 363 μm long, longer than wide, with roundly produced rostral apex. Fourth pedigerous somite with angular posterolateral corners. Urosome (Fig. 10B)

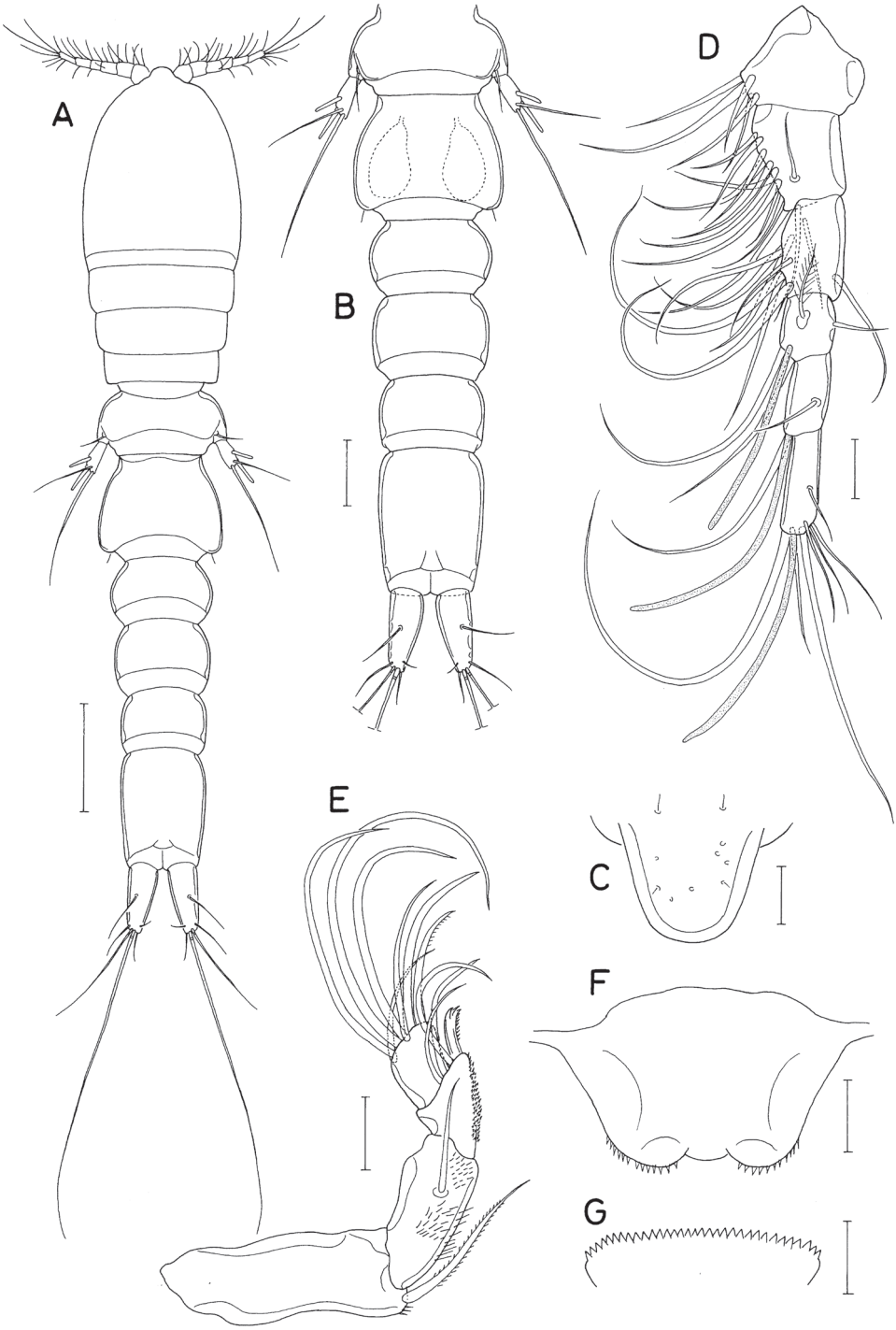

Figure 10. *Pontoclausia pristina* sp. nov., male **A** habitus, dorsal **B** urosome, dorsal **C** rostrum **D** antennule **E** antenna **F** labrum **G** labium. Scale bars: 0.2 mm (**A**); 0.1 mm (**B**); 0.02 mm (**C–G**).

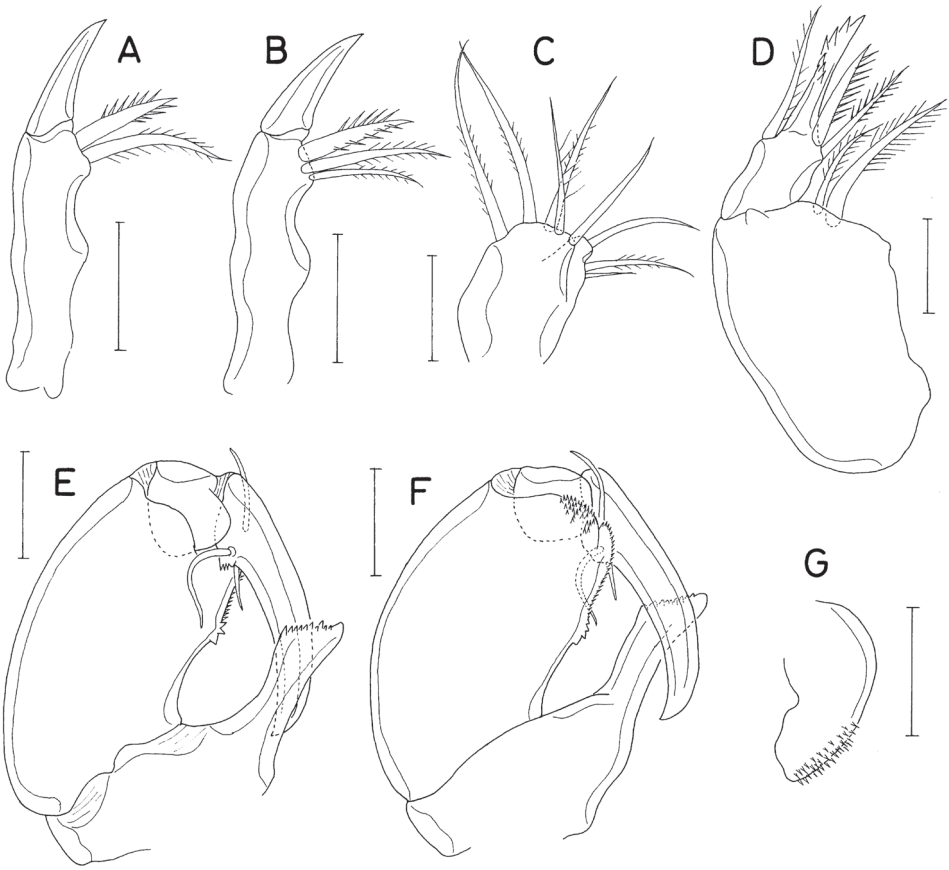

Figure 11. *Pontoclausia pristina* sp. nov., male **A, B** mandibles **C** maxillule **D** maxilla **E, F** maxillipeds **G** paragnath. Scale bars: 0.02 mm (**A–D, G**); 0.05 mm (**E, F**).

six-segmented. Fifth pedigerous somite 240 μm wide. Genital somite wider than long (194 × 230 μm), gradually broadened posteriorly. Four abdominal somites 115 × 188 μm, 127 × 179 μm, 109 × 160 μm, and 227 × 164 μm, respectively. Anal somite ~ twice longer than third abdominal somite. Caudal ramus (Fig. 10B) tapering, 2.46 × longer than wide (128 × 52 μm), armed with six thin, naked setae; distal longest seta (seta V) ~ 600 μm long, other setae short; seta II positioned dorsally at 48% region of ramus length.

Rostrum (Fig. 10C) well-sclerotized, gradually narrowed distally, with round apical margin. Antennule (Fig. 10D) 180 μm long, six-segmented; armature formula 5, 13, 9, 4+aesthetasc, 2+aesthetasc, and 7+aesthetasc; all setae naked except one on fourth segment; several of setae very long. Antenna (Fig. 10E) four-segmented; armature formula 1, 1, 3+claw, and 7; second segment (first endopodal segment) setulose on surfaces; third segment with densely arranged minute spinules on inner surface; claw of third segment distally trifurcate; terminal segment slightly longer than wide (17 × 15 μm); third outer seta on distal margin of terminal segment distinctly longer than other six setae.

Mouthparts small, except large maxilliped. Labrum (Fig. 10F) with very shallow posterior incision, roundly convex posterolateral lobes fringed with spinules along their posterior margin. Labium (Fig. 10G) denticulate, saw-like. Mandible (Fig. 11A, B) distally armed with one strong, claw-like spine plus two or three spinulose or pinnate setae. Paragnath (Fig. 11G) as spinulose lobe. Maxillule (Fig. 11C) distally bilobed; with three setae on smaller inner lobe (proximalmost small, hardly visible) and five setae on larger outer lobe. Maxilla (Fig. 11D) two-segmented; proximal segment (syncoxa) with two unequal setae medio-distally; distal segment (basis) with three setae and one spiniform process bearing six denticles. Maxilliped (Fig. 11E, F) massive, consisting of three segments and terminal claw; first segment with large medio-distal process bearing truncate, spinulose distal margin; second segment unarmed but ornamented with spinules along distal half of inner margin and patch of spinules at inner distal region; short third segment unarmed; terminal claw strong, with three setae proximally (two on one side and one on opposite side).

Legs 1–4 (Fig. 12A–E) biramous. Inner coxal seta absent in legs 1, 2, and 4, but present in leg 3. Leg 1 with three-segmented exopod and two-segmented endopod; first endopodal segment inflated; inner distal spine on basis large, spinulose. Legs 2–3 with three-segmented rami. First and second endopodal segment of legs 2–4 bearing one inner seta. Inner coxal seta of leg 3 short, thickened in proximal third but thin, weakly pinnate in distal two-thirds. Distal setae on third endopodal segment of legs 2 and 3 very long. Leg 4 with finely spinulose setae; inner setae on endopod stiff; spines on both rami elongated, setiform, hardly distinguishable from setae. Armature formula for legs 1–4 as follows:

	Coxa	Basis	Exopod	Endopod
Leg 1	0-0	1-I	I-0; I-1; III, I, 3	0-1; 0, II, 1
Leg 2	0-0	1-0	I-0; I-1; II, I, 4	0-1; 0-1; II, I, 3
Leg 3	0-1	1-0	I-0; I-1; II, I, 4	0-1; 0-1; II, I, 3
Leg 4	0-0	1-0	I-0; I-1; III, I, 2	0-1; 0-1; II, I, 2

Leg 5 (Fig. 10B) directed posterolaterally, clearly visible in dorsal view, consisting of one dorsolateral seta on fifth pedigerous somite and free exopod; exopodal segment 2.88 × longer than wide (72 × 25 μm), armed with two spines and two unequal setae; spines rod-shaped, spinulose in distal part, 60 and 52 μm long; setae spinulose, 245 and 136 μ long. Leg 6 (Fig. 12G) represented by one small, naked seta tipped on genital operculum.

Female. Unknown.

Etymology. The specific name of the new species is derived from the Latin *pristin* (primitive), referring to the primitive condition of its antenna and mouthparts.

Remarks. Although only a single male specimen is available for the description of *Pontoclausia pristina* sp. nov., it is distinctively characterized by its primitive antenna which is four-segmented with a full armature and by primitive, *Hemicyclops*-type mandible, maxillule and maxilla. The taxonomic position of the new species appears to be intermediate between the genera *Hemicyclops* and *Pontoclausia* of the Clausiidae. In the new species (1) the body is slender, harpacticiform (*Pontoclausia*-type feature); (2) the

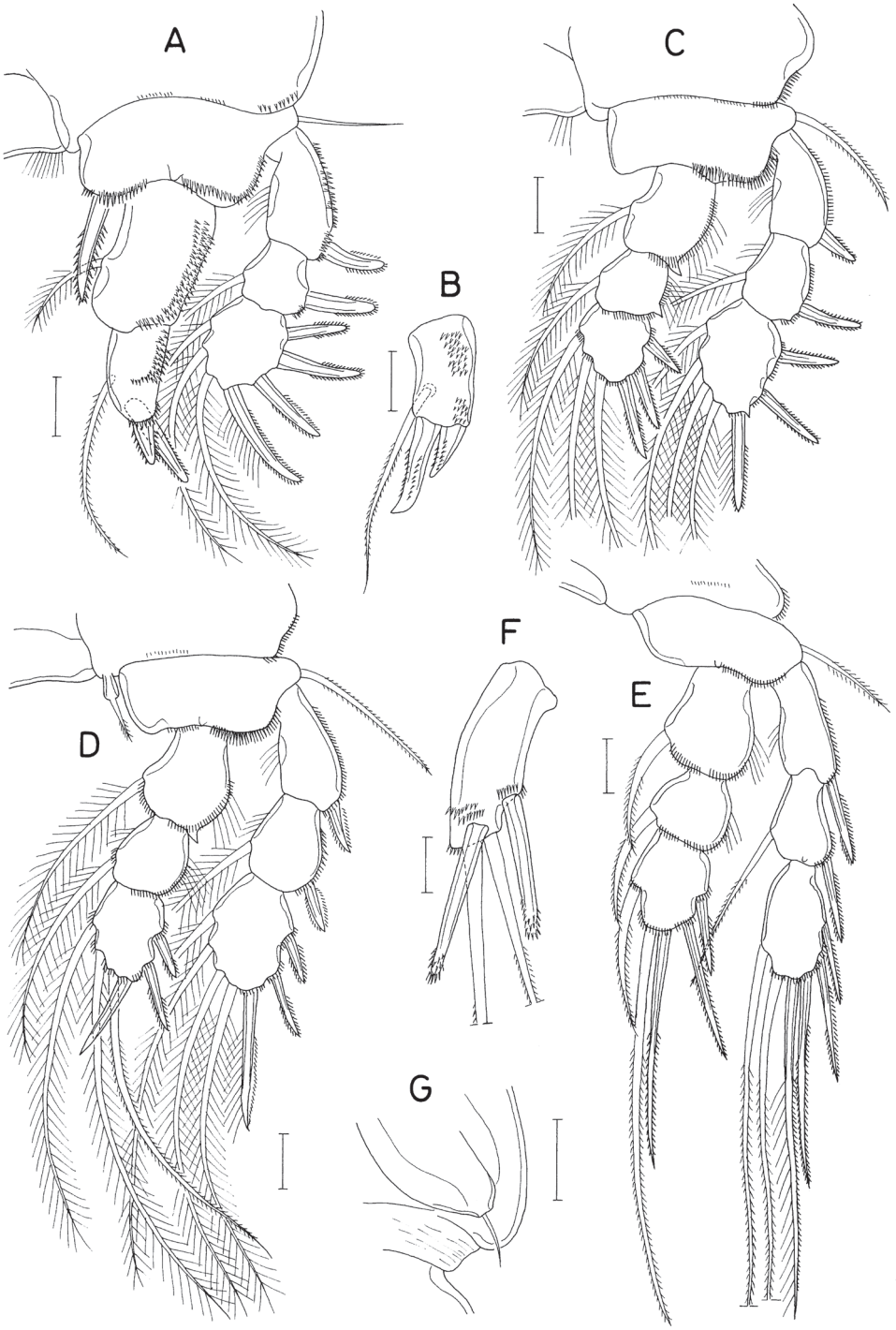

Figure 12. *Pontoclausia pristina* sp. nov., male **A** leg 1 **B** distal endopodal segment of leg 1 **C** leg 2 **D** leg 3 **E** leg 4 **F** exopod of leg 5 **G** left side of genital somite and leg 6, ventral. Scale bars: 0.02 mm (**A–F**); 0.05 mm (**G**).

antennule is six-segmented (*Pontoclausia*-type); (3) the antenna is four-segmented, with 1, 1, 4, and 7 armature elements respectively on the first to fourth segments (*Hemicyclops*-type); (4) the mandible bears three or four distal armature elements (*Hemicyclops*-type); (5) the maxillule is distally bilobed with a total of eight setae (*Hemicyclops*-type); (6) the maxilla is two-segmented, with two distinct setae on the proximal segment and three armature elements plus one spiniform process on the distal segment (*Hemicyclops*-type); (7) the endopod of male leg 1 is two-segmented (*Pontoclausia*-type); (8) most of swimming legs lack the inner coxal seta (*Pontoclausia*-type); (9) the second endopodal segment of legs 2–4 bears only a single inner seta (*Pontoclausia*-type); and (10) the setation of the third exopodal and endopodal segments of most swimming legs is reduced (*Pontoclausia*-type). We consider that the two-segmented condition of the endopod of male leg 2 (above character state 7), which is a consistent, typical feature of *Pontoclausia*, is the most important taxonomic feature for determining the familial position of the new species; therefore, we place it within the Clausiidae. *Pontoclausia pristina* sp. nov. is distinguished from its congeners and other species in the family by the above *Hemicyclops*-type features.

Family Kelleriidae Humes & Boxshall, 1996
Genus *Kelleria* Gurney, 1927

Kelleria andamanensis Sewell, 1949

Material examined. One ♀, Site 15, 04 Jul. 2020.

Remarks. Hong and Kim (2021) synonymized *K. grandisetiger* Kim, 2006 with *K. andamanensis* Sewell and redescribed it.

Family Lichomolgidae Kossmann, 1877
Genus *Herrmannella* Canu, 1891

Herrmannella dentata Avdeev, 1987

Material examined. One ♀, Site 12, 16 Mar. 2013.

Remarks. *Herrmannella dentata* was originally described as an associate of the bivalves *Mya japonica* Jay, 1857 and *Gari kazusensis* (Yokoyama, 1922) in the Peter the Great Bay, Russia (Avdeev 1987). In Korea, this copepod species has been found only from *Mya arenaria* Linnaeus, 1758 (previously reported as *Mya arenaria oonogai* Makiyama, 1935) on the south coast.

Herrmannella hoonsooi Kim I.H., 1992

Material examined. One ♂, Site 11, 03 Jun. 2019; 1 ♀, 4 ♂♂, Site 12, 16 Mar. 2013; 1 ♂, Site 17, 13 May 2015.

Remarks. This copepod species had been found only in the bivalve *Saxidomus purpurata* (Sowerby, 1852).

***Herrmannella macomae* Kim I.H. & Sato, 2010**

Material examined. One ♀, 3 ♂♂, Site 33, 11 Aug. 2020.

Remarks. Kim and Sato (2010) described *Herrmannella macomae* from the clam *Limecola contabulata* (Deshayes, 1855) (recorded as *Macoma contabulata*) in Mutsu Bay, Japan. This copepod is new to the Yellow Sea, Korea and this is only the second record of the species.

Genus *Heteranthessius* Scott T., 1904

***Heteranthessius unisetatus* sp. nov.**
https://zoobank.org/E7E5EAEE-6742-4312-8467-11EA6CF572F3
Figs 13, 14

Material examined. ***Holotype*** ♂ (MABIK CR00250127) dissected and mounted on a slide, Site 6 (Jukbyeon Port, Uljin, 36°49'26.4"N, 129°26'52.2"E), 21 Sep. 2020, leg. J. Lee and J. G. Kim.

Description. Male. Body (Fig. 13A) moderately narrow. Body length 1.92 mm. Prosome 1.08 mm long, comprising cephalothorax and second to fourth pedigerous somites. Cephalothorax 690 × 596 μm, distinctly longer than wide. All prosomal somites with rounded posterolateral corners. Urosome (Fig. 13B) six-segmented. Fifth pedigerous somite 200 μm wide. Genital somite subquadrate, longer than wide (309 × 265 μm), with rounded corners. Four abdominal somites 116 × 153 μm, 91 × 131 μm, 58 × 136 μm, and 91 × 149 μm, respectively. All abdominal somites smooth, without ornamentation. Caudal ramus broad, 1.64 × longer than wide (120 × 73 μm), with six setae; outer seta (seta II) short, naked, positioned at 45% region of ramus length; dorsal seta (seta VII) small and naked; other four setae pinnate.

Rostrum (Fig. 13C) broad, with round posterior margin. Antennule (Fig. 13D) 335 μm long, seven-segmented; armature formula 3, 12+2 aesthetascs, 2, 2+aesthetasc, 4+aesthetasc, 2+aesthetasc, and 7+aesthetasc; all setae naked; aesthetascs on second, fourth, and fifth segments large, broad, longer than antennular segments; aesthetasc on sixth segment small; aesthetasc on terminal segment as long as those of proximal segments but slender. Antenna (Fig. 13E) four-segmented, with armature formula 1, 1, 3, and 4+2 claws; terminal segment (third endopodal segment) gradually narrowed distally, 2.0 × longer than wide (76 × 38 μm); two terminal claws unequal, outer longer and thicker than inner, ~ 0.9 × as long as terminal segment.

Labrum (Fig. 13F) wider than long, with shallow posteromedian incision, fringed with broad membrane along posterior margin, pair of weak, tapering lobes at posteromedial region. Mandible (Fig. 13G) simple, with curved, elongate gnathobase bearing serrate margins. Maxillule (Fig. 13H) as small, digitiform lobe tipped with one naked seta. Maxilla (Fig. 13I) as large lobe tipped with one naked seta. Maxilliped (Fig. 14A) large, consisting of three segments and terminal claw; first segment as long as wide, unarmed; large second segment with one rudiment of seta and one large

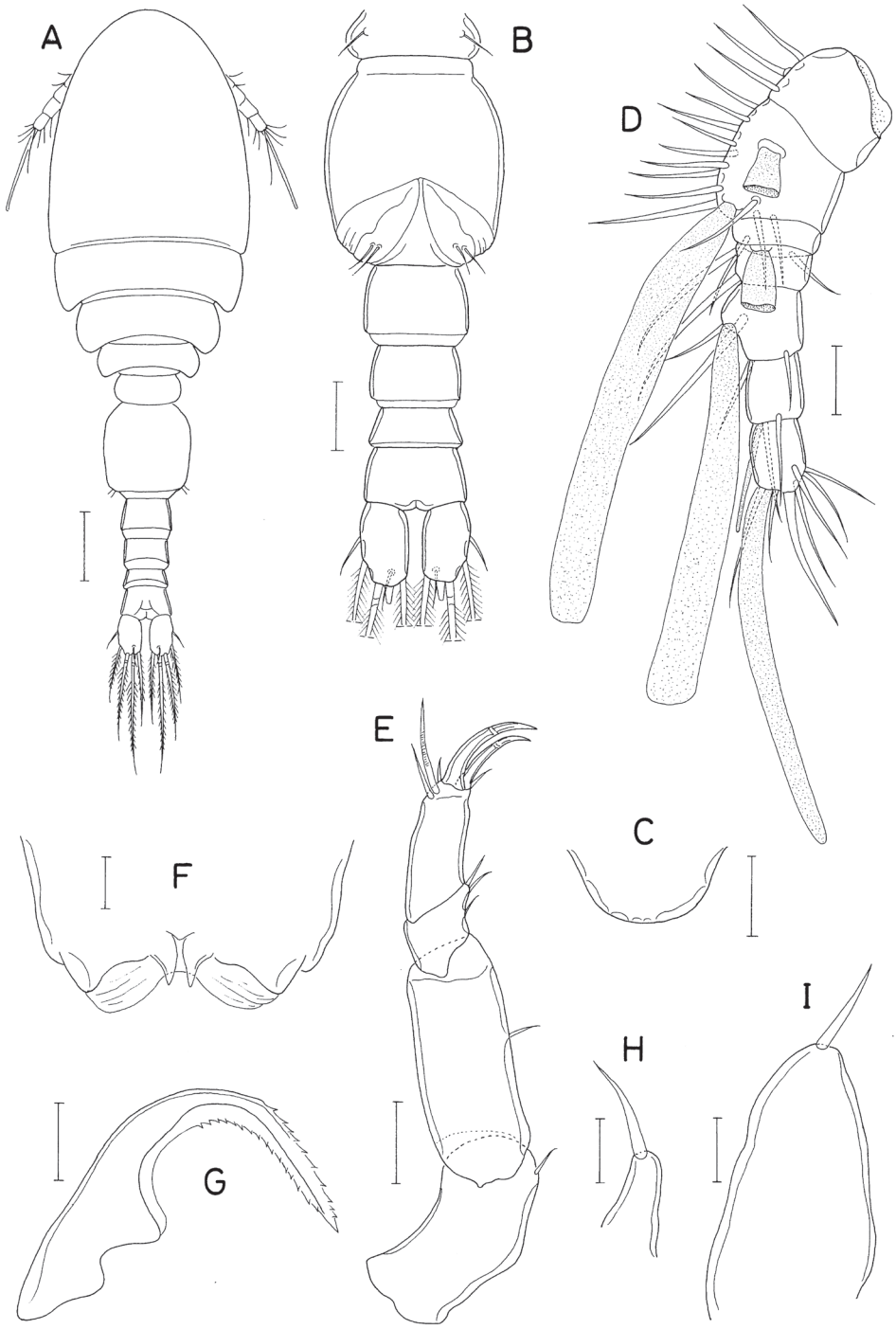

Figure 13. *Heteranthessius unisetatus* sp. nov., male **A** habitus, dorsal **B** urosome, ventral **C** rostrum **D** antennule **E** antenna **F** labrum **G** mandible **H** maxillule **I** maxilla. Scale bars: 0.2 mm (**A**); 0.1 mm (**B, C**); 0.05 mm (**D, E**); 0.02 mm(**F–I**).

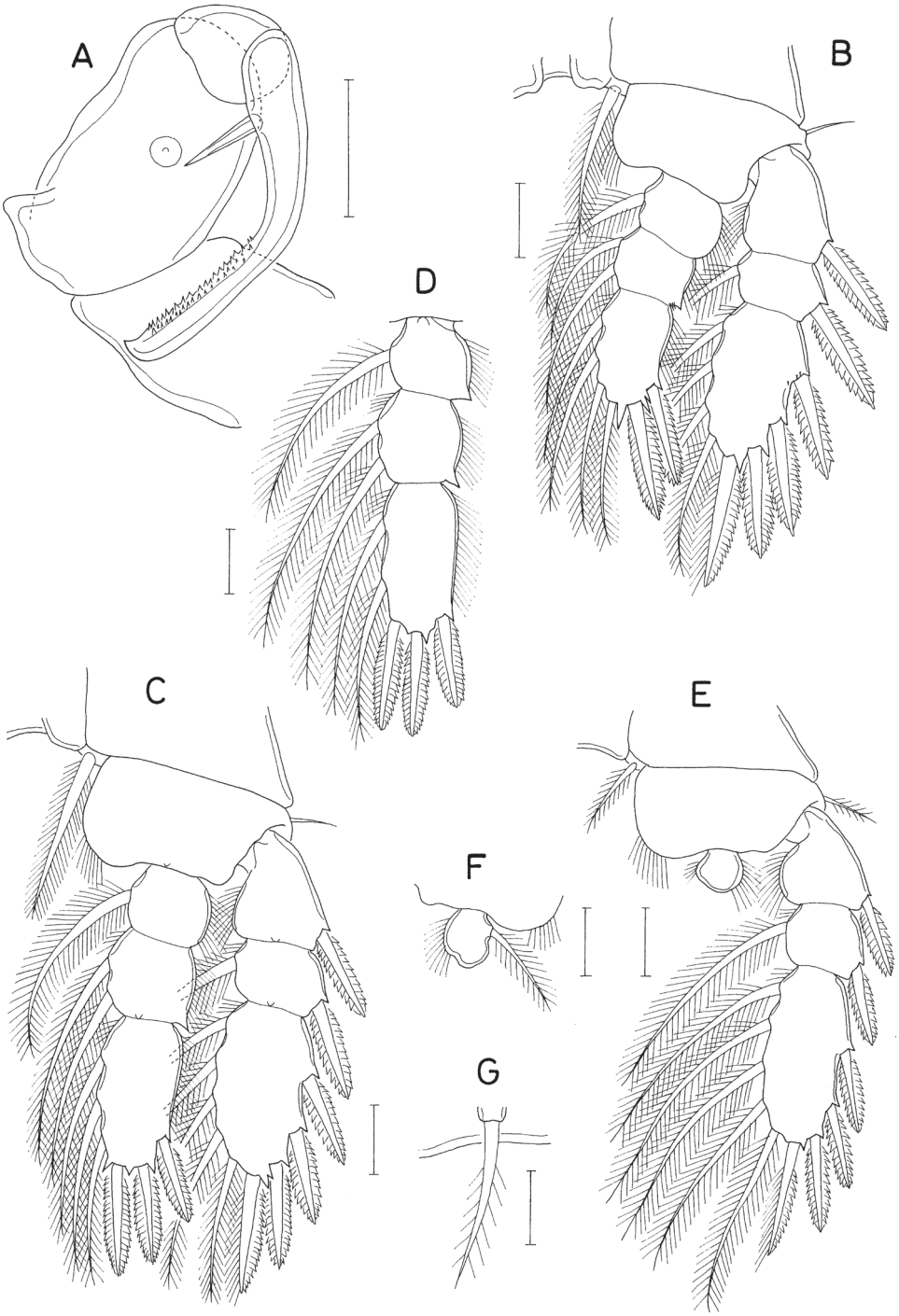

Figure 14. *Heteranthessius unisetatus* sp. nov., male **A** maxilliped **B** leg 1 **C** leg 2 **D** endopod of left leg 3 **E** leg 4 **F** endopod of right leg 4 **G** leg 5. Scale bars: 0.05 mm (**A–F**); 0.02 mm (**G**).

tubercle ventromedially; small third segment unarmed; terminal claw large, with one spine proximally and denticles on distal half of inner margin.

Legs 1–4 biramous; outer seta on basis small; spines on rami with densely serrate margins. Legs 1–3 (Fig. 14B–D) with three-segmented rami. Leg 4 (Fig. 14E) with three-segmented exopod and one-segmented endopod. Second endopodal segment of leg 1 characteristically with two inner setae. Endopod of leg 4 small, globular, with or without inner seta. Armature formula for legs 1–4 as follows:

	Coxa	Basis	Exopod	Endopod
Leg 1	0-1	1-0	I-0; I-1; III, I, 4	0-1; 0-2; I, I, 4
Leg 2	0-1	1-0	I-0; I-1; III, I, 5	0-1; 0-2; I, II, 3
Leg 3	0-1	1-0	I-0; I-1; III, I, 5	0-1; 0-2; I, II, 2
Leg 4	0-1	1-0	I-0; I-1; III, I, 5	0, 0, 1 (or 0, 0, 0)

Leg 5 (Fig. 14G) represented by small papilla tipped with one pinnate seta 47 μm long. Leg 6 (Fig. 13B) represented by two small setae on genital operculum.

Female. Unknown.

Etymology. The specific name of the new species is derived from Latin words, referring to the presence of a single seta on the maxillule and maxilla.

Remarks. The genus *Heteranthessius* consists of four known species: *H. dubius* (T. Scott, 1903) from an unknown host in Scotland (T. Scott 1903), *H. scotti* Bocquet, Stock & Bernard, 1959 from calcareous algae at Roscoff, France (Bocquet et al. 1959), *H. furcatus* Stock, 1971 from a tunicate in the Mediterranean Sea (Stock 1971), and *H. hoi* López-González & Conradi, 1995 from an actiniarian at Gibraltar (López-González and Conradi 1995). *Heteranthessius unisetatus* sp. nov. is easily distinguishable from the congeners by its unique morphological features: the maxillule bears only a single seta apically, against two setae in the four congeners, the maxilla is unsegmented, with a single seta apically, against two-segmented, with one spine or spiniform process and one seta on the distal segment in the congeners, and leg 5 is represented by a single seta, against two setae in the congeners. The most striking feature of the new species is the possession of two inner setae on the second endopodal segment of leg 1. Because the latter feature is very extraordinary and we have failed to find the same armature condition in other poecilostome copepods, it may be interpreted as an abnormality. However, it is remarkable that both left and right leg 1 display the same setation.

Genus *Modiolicola* Aurivillius, 1883

Modiolicola bifidus Tanaka, 1961

Material examined. Eight ♀♀, 2 ♂♂, Site 12, 16 Mar. 2013; 1 ♀, Site 23, 24 Apr. 2021.

Remarks. *Modiolicola bifidus* has a very low host specificity and is distributed all around the Korean. Kim (2004) recorded 12 bivalve species as hosts, including *Ruditapes philippinarum* (A. Adams & Reeve, 1850), the major host.

Family Myicolidae Yamaguti, 1936

***Pusanomyicola* gen. nov.**
https://zoobank.org/D280A953-BE0A-458B-A438-650794FC0354

Diagnosis. Male. Body narrow, cyclopiform, clearly segmented. Prosome consisting of cephalosome and four pedigerous somites. Urosome six-segmented. Caudal ramus with six setae, Antennule seven-segmented, heavily armed with setae and aesthetascs; first and second segments with multiple aesthetascs. Antenna three-segmented, consisting of coxobasis and two-segmented endopod, and terminated in single, strong claw. Labrum broader than long, with short posterolateral lobes. Mandible distally armed with three denticle-like elements, innermost one articulate at base. Maxillule as lobe tipped with two setae. Maxilla as lobe tipped with single seta. Maxilliped four-segmented; armature formula 0, 2, 0, and 1; terminal claw reduced, rudimentary. Legs 1–4 biramous, with three-segmented rami. Coxa of all swimming legs with small inner seta. Leg 1 lacking inner distal armature element on basis. Second endopodal segment of legs 2–4 armed with two inner setae. Third endopodal segment of legs 2 and 3 armed with three spines plus three setae (formula I, II, 3). Third exopodal segment of legs 3 and 4 armed with three spines plus five setae (formula II, I, 5). Leg 5 consisting of protopod and exopod; protopod well-defined from somite; exopod armed with three setae. Leg 6 represented by three setae on genital operculum.

Type species. *Pusanomyicola sensitivus* gen. nov., sp. nov. (original designation).

Etymology. The generic name is the combination of "Pusan", the type locality of the type species, and *Myicola*, the type genus of the family. Gender masculine.

Remarks. Boxshall and Halsey (2004) recognized eight genera in the family Myicolidae, including the highly transformed genus *Crucisoma* Kabata, 1981. While establishing the family Anthessiidae, Humes (1986) excluded *Conchocheres* Sars, 1918 from this family due to the lack of long elements on the mandible, the absence of the maxilliped in the female, and the presence of three setae only on the exopod of leg 5, but he did not determine the familial position of *Conchocheres*. Boxshall and Halsey (2004) tentatively placed *Conchocheres* in the Myicolidae on the basis of similarities in the armature of the antenna and in the form of the caudal rami, but they mentioned that the genus differed from all myicolids in the absence of the inner seta on the basis of leg 1, a characteristic found in the Anthessiidae.

It is notable that one typical feature of the Anthessiidae is in the antennule. In poecilostome cyclopods, the armature of three terminal segments of the antennule (4+aesthetasc, 2+aesthetasc, and 7+aesthetasc) is generally determined as early as the copepodid II stage, and this armature formula remains unchanged throughout subsequent developmental stages. However, the position of the aesthetasc on the antepenultimate segment (the segment of 4+aesthetasc) differs between the Anthessiidae and other poecilostome families, since the aesthetasc in the Anthessiidae is inserted at the distal corner, accompanied with anterodistal seta (Fig. 15B), whereas it is inserted near

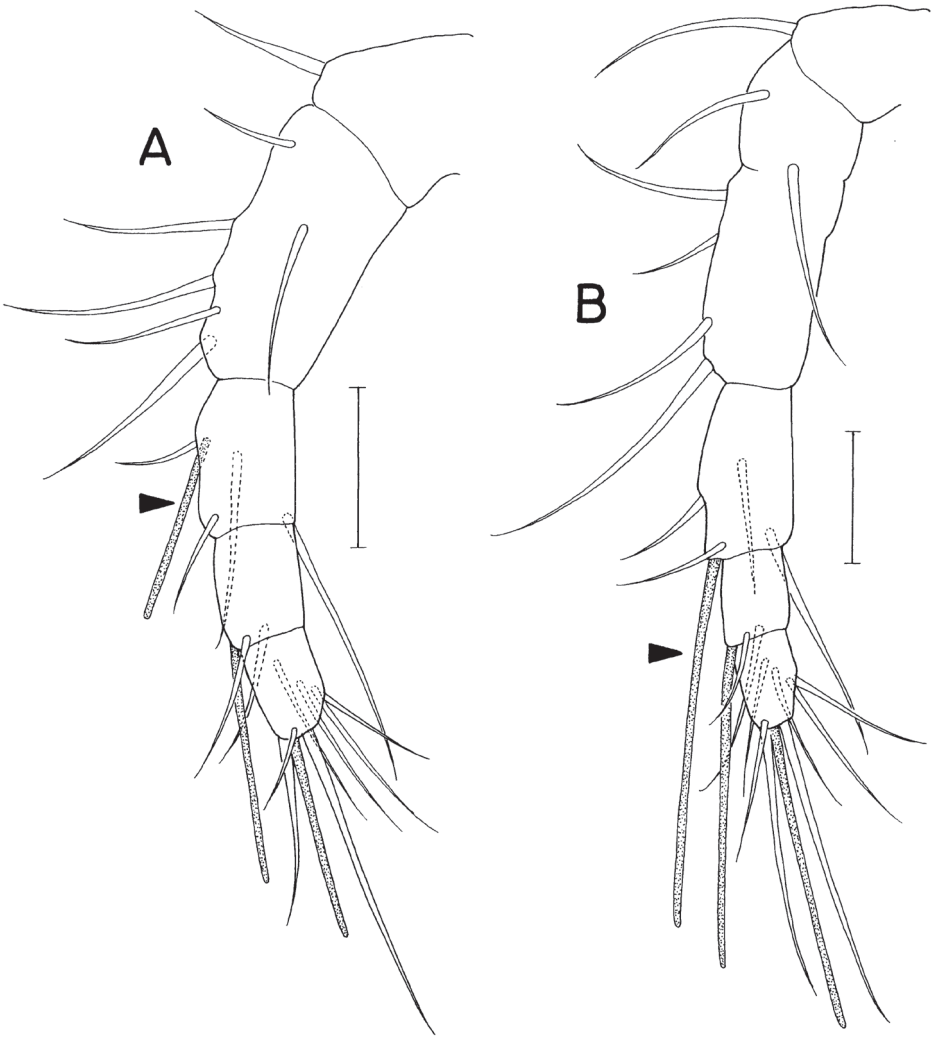

Figure 15. Antennule of copepodid II stage of *Critomolgus anthopleurus* Kim (**A**) and *Anthessius dolabellae* Humes & Ho,1965 (**B**). Scale bars: 0.02 mm. **A** redrawn from Kim (2003).

the proximal seta (Fig. 15A) in other poecilostome families, such as the Myicolidae, Clausidiidae, Ergasilidae, and lichomolgoid families. *Pusanomyicola* gen. nov. and *Conchocheres* share the armature pattern of the latter poecilostome families.

Pusanomyicola gen. nov. is more similar to *Conchocheres* than to any other known genera of the Myicolidae; their shared features are the unsegmented maxilla bearing a single distal element, the absence of the inner distal element on the basis of leg 1, and the possession of only three setae on the exopod of leg 5. Nevertheless, *Pusanomyicola* gen. nov. cannot be considered congeneric with *Conchocheres* due to their significant differences on the generic level, as follows: (1) the male urosome is five-segmented in

Conchocheres malleolatus Sars, 1918, the type and only species of *Conchocheres*, while it is six-segmented in *Pusanomyicola sensitivus* gen. nov., sp. nov.; (2) the male antennule of *C. malleolatus* bears five aesthetascs as illustrated by Sars (1918), but as many as 28 aesthetascs in *P. sensitivus* gen. nov., sp. nov.; (3) the male maxilliped of *C. malleolatus* bears a large terminal hook, while it is markedly reduced in *P. sensitivus* gen. nov., sp. nov.; (4) the third exopodal segment of leg 1 is armed with three spines plus four setae (II, I, 4) in *C. malleolatus*, but with four spines plus four setae (III, I, 4) in *P. sensitivus* gen. nov., sp. nov.; and (5) the third endopodal segment of leg 4 is armed with one spine plus three setae (I, 3) in *C. malleolatus*, but with three spines plus two setae (I, II, 2) in *P. sensitivus* gen. nov., sp. nov.

We place *Pusanomyicola* gen. nov. in the Myicolidae on the basis of its myicolid form of antenna bearing a single robust terminal claw and a truncate inner distal seta on the terminal segment, the presence of a group of spinules on the labrum, maxilla and genital operculum, and the myicolid form mandible. We confirm that *Conchocheres*, which shares important character states with *Pusanomyicola* gen. nov., is placed in the Myicolidae, as well.

***Pusanomyicola sensitivus* gen. nov., sp. nov.**

https://zoobank.org/5C31B845-08AB-455D-9249-29B7617CCA87

Figs 16, 17

Material examined. ***Holotype*** ♂ (MABIK CR00250128) dissected and mounted on a slide, Site 11 (Yeongdo, Pusan, 35°04'31.0"N, 129° 05'08.7"E), 07 Jul. 2020, leg. J. G. Kim.

Description. Male. Body (Fig. 16A) narrow, clearly segmented, gradually narrowed from anterior to posterior. Body length 2.06 mm. Maximum width 400 μm across cephalosome. Prosome 886 μm long, distinctly shorter than urosome, consisting of cephalosome and four pedigerous somites. All prosomal somites with rounded lateral margin. Urosome six-segmented. Fifth pedigerous somite short, narrower than genital somite. Genital somite nearly rectangular, 1.2 × longer than wide (273 × 227 μm); genital operculum (Fig. 17H) distinct, bearing three setae and row of scale-like spinules along inner distal margin. Four abdominal somites 177 × 159 μm, 150 × 127 μm, 100 × 109 μm, and 132 × 95 μm, respectively. Caudal ramus (Fig. 16B) slender, 7.9 × longer than wide (284 × 36 μm), armed with seven setae (seta I to VII), ornamented with many transverse rows of minute spinules; setae I and II positioned at same place at 23% length of ramus on outer margin; setae III–VI positioned on distal margin; seta VII positioned on dorsal surface at 38% length of ramus; all caudal setae naked, short, longest one (seta V) one-third as long as ramus.

Rostrum not developed. Antennule (Fig. 16C) 245 μm long, seven-segmented, densely armed with setae and aesthetascs; armature formula 4+7 aesthetascs, 15+15 aesthetascs, 4+2 aesthetascs, 4+aesthetasc, 2+aesthetasc, and 7+aesthetasc; all setae naked, mostly short; aesthetascs shorter than antennule. Antenna (Fig. 16D) three-

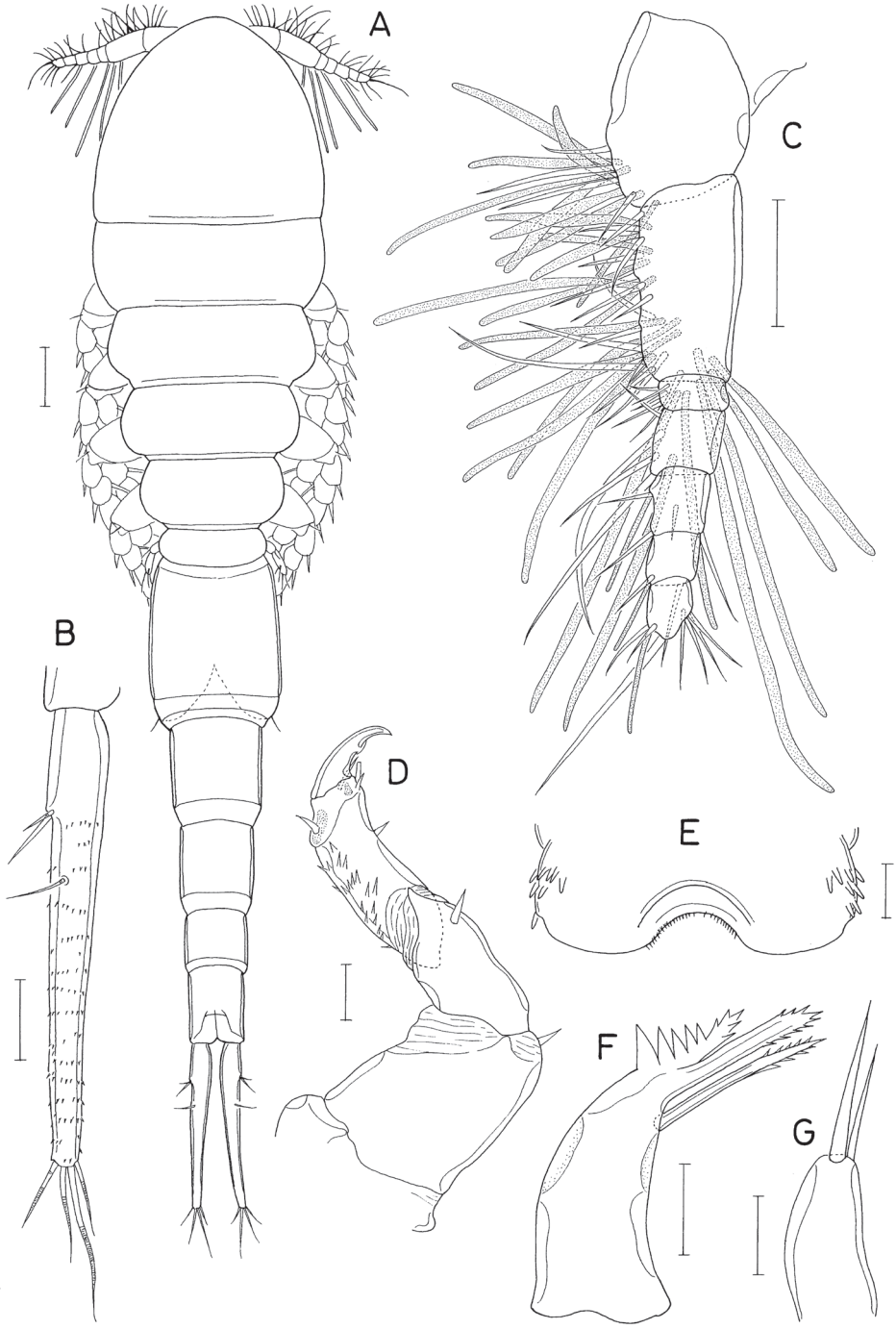

Figure 16. *Pusanomyicola sensitivus* gen. nov., sp. nov., male **A** habitus, dorsal **B** left caudal ramus, dorsal **C** antennule **D** antenna **E** labrum **F** mandible **G** maxillule. Scale bars: 0.1 mm (**A**); 0.05 mm (**B, C**); 0.02 mm (**D, E, G**); 0.01 mm(**F**).

segmented, consisting of coxobasis and two-segmented endopod; coxobasis as long as wide, with one short seta at inner distal corner; first endopodal segment ~ 1.5 × longer than wide, with one small seta at inner subdistal region; second endopodal segment twice longer than wide, terminated in strong claw, armed with five small setae (one on inner margin, one on subdistal outer margin, and three at inner distal corner, one of latter truncate), and ornamented with scattered scale-like spinules on outer surface; terminal claw half as long as second endopodal segment.

Labrum (Fig. 16E) much wider than long, with patch of several blunt spinules on each lateral surface; posteromedian incision shallow, semicircular, with finely spinulose margin. Mandible (Fig. 16F) narrowed distally, armed with three armature elements distally: short outer element not articulated at base, with five large teeth along outer margin and five denticles distally; longest middle element (stiff lash) straight, not articulated at base, with several denticles at distal part; slender inner element (spiniform seta) articulated at base, as long as middle element, denticulate distally. Maxillule (Fig. 16G) as digitiform lobe tipped with two unequal, naked setae. Maxilla (Fig. 17A) as tapering, unsegmented lobe bearing patch of spinules on posteroventral surface, tipped with one naked seta. Maxilliped (Fig. 17B) four-segmented; first segment (syncoxa) broader than long, unarmed; second segment (basis) rectangular, armed with one broad, leaf-like seta subdistally and one small seta distally; short third segment (first endopodal segment) unarmed; terminal segment (second endopodal segment) tapering, curved, trifurcate at tip, with one small seta on inner margin; claw or hook absent (or reduced to small middle process of distal tip).

Legs 1–4 (Fig. 17C–F) biramous, with three-segmented rami; inner coxal seta small, naked; outer seta on basis also small, naked; both rami of each leg almost equal in length; spines on exopods and endopods spinulose along both margins. Leg 1 lacking inner distal element of basis, but with three blunt dentiform spinules near base of endopod. Legs 3 and 4 with same armature on third exopodal segment. Armature formula for legs 1–4 as follows:

	Coxa	Basis	Exopod	Endopod
Leg 1	0-1	1-0	I-0; I-1; III, I, 4	0-1; 0-1; I, 2, 3
Leg 2	0-1	1-0	I-0; I-1; III, I, 5	0-1; 0-2; I, II, 3
Leg 3	0-1	1–0	I-0; I-1; II, I, 5	0-1; 0-2; I, II, 3
Leg 4	0-1	1-0	I-0; I-1; II, I, 5	0-1; 0-2; I, II, 2

Leg 5 (Fig. 17G) small, consisting of protopod and exopod; protopod articulated from somite, as long as wide, with one seta dorsodistally; exopod 3.0 × longer than wide (45 × 15 μm), armed with three naked setae (two on distal margin and one at 75% region of dorsal margin), ornamented with few spinules ventrodistally; setae on protopod and exopod shorter than exopodal segment. Leg 6 (Fig. 17H) represented by three naked setae on inner distal margin of genital operculum.

Female. Unknown.

Etymology. The specific name *sensitivus* refers to the presence of the multiple aesthetascs on the male antennule.

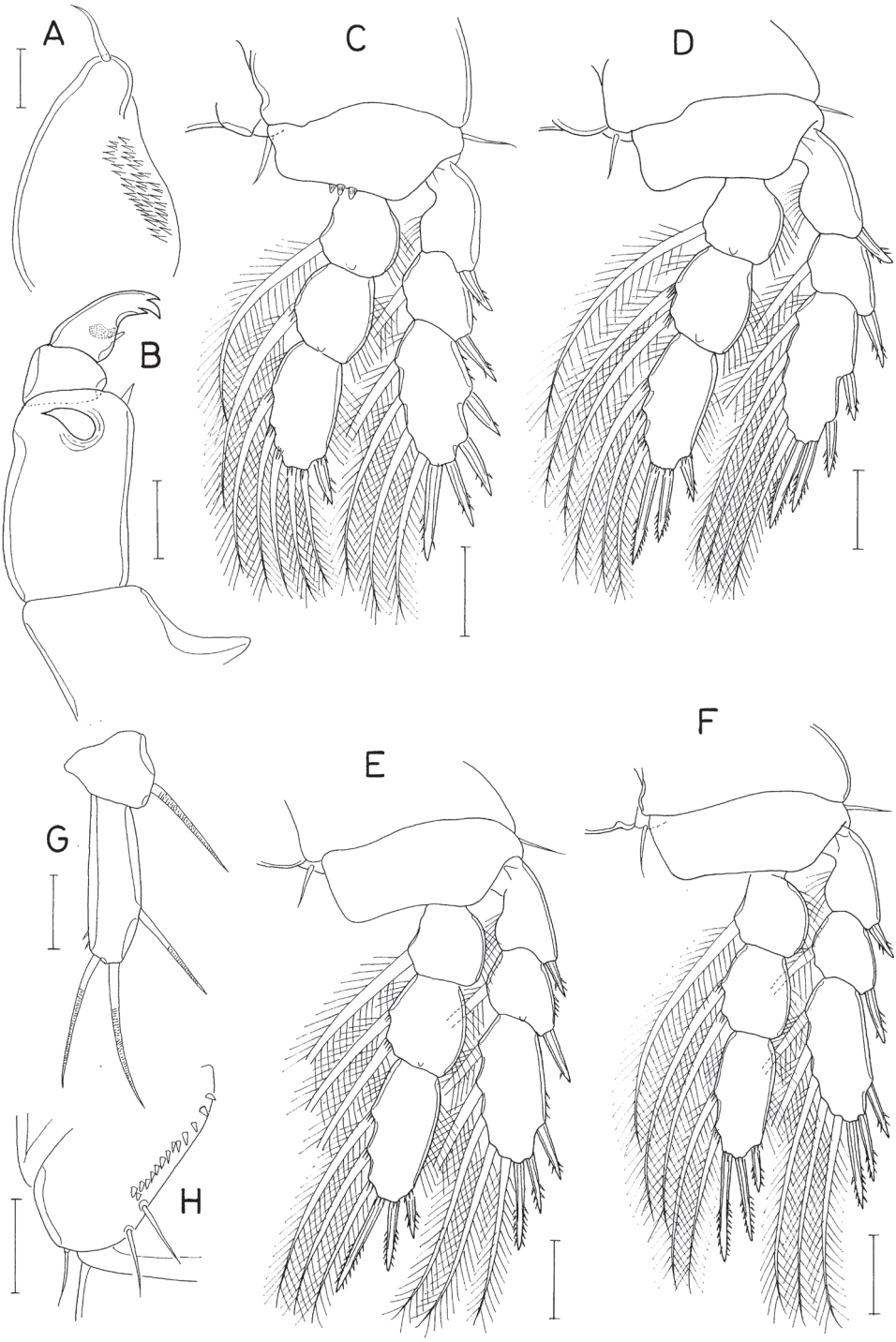

Figure 17. *Pusanomyicola sensitivus* gen. nov. sp. nov., male **A** maxilla **B** maxilliped **C** leg 1 **D** leg 2 **E** leg 3 **F** leg 4 **G** leg 5 **H** right genital operculum, ventral. Scale bars: 0.02 mm (**A, B, G**); 0.05 mm (**C–F, H**).

Family Polyankyliidae Ho & Kim I.H., 1997
Genus *Polyankylis* Ho & Kim I.H., 1997

***Polyankylis ovilaxa* Kim, 2014**

Material examined. One ♀, Site 27, 09 Jul. 2016.

Remarks. Kim (2014) described this copepod as an associate of the terebellid polychaete *Thelepus japonicus* Marenzeller, 1884 from the south coast of Korea.

***Polyankylis bogilensis* sp. nov.**
https://zoobank.org/DCF49374-198A-4824-910A-45D3C72A4C81
Figs 18, 19

Material examined. ***Holotype*** ♀ (MABIK CR00250129) dissected and mounted on a slide, Site 22 (Yesong, Bogil Island, south coast, 34°08'11"N, 126°33'49"E), 31 May 2021, leg. J. Lee.

Description. Female. Body (Fig. 18A) dorsoventrally flattened. Body length 1.10 mm. Prosome 1.54 × longer than wide (570 × 370 μm). Cephalothorax with faint dorsal suture line between cephalosome and first pedigerous somite, with rounded posterolateral corners. Second to fourth pedigerous somites with rounded anterolateral and posterolateral corners. Urosome (Fig. 18B) six-segmented. Fifth pedigerous somite 155 μm wide, slightly wider than genital double-somite. Genital double-somite 1.15 × longer than wide (170 × 148 μm), widest at proximal third of double-somite; posterior two-thirds gradually narrowing posteriorly; genital apertures positioned dorsolaterally at widest region of double-somite. Three free abdominal somites 70 × 93 μm, 56 × 86 μm, and 90 × 90 μm, respectively. All urosomal somites smooth, unornamented. Caudal rami straight backwards, rectangular, isolated from each other; each ramus (Fig. 18C) 2.96 × longer than wide (80 × 27 μm), armed with six setae (seta II-VII); seta II positioned dorsally at 45% region of ramus length; seta V much longer than other caudal setae; seta III feebly pinnate, other five setae naked.

Rostrum (Fig. 18A, D) as broad, spatulate anterior prominence of cephalothorax. Antennule (Fig. 18E) 295 μm long, six-segmented, gradually narrowed distally; armature formula 2, 7, 6 (or 2. 6, 7), 4+aesthetasc, 2+aesthetasc, and 7+aesthetasc; all setae naked. Antenna (Fig. 18F) four-segmented; first segment (coxobasis) with one seta at inner distal corner; second segment (first endopodal segment) longest, armed with one seta on inner margin and ornamented with setules on outer margin; short third segment with one small claw and two very unequal setae; terminal segment 1.28 × longer than wide (23 × 18 μm), distally armed with three claws of different lengths and three unequal setae, including minute outermost seta, and ornamented with minute spinules on subdistal outer margin.

Labrum (Fig. 18G) bilobed, with deep median incision and proximal sclerotization band; each lobe distinctly longer than wide (~ 41 × 25 μm), divided from proximal part

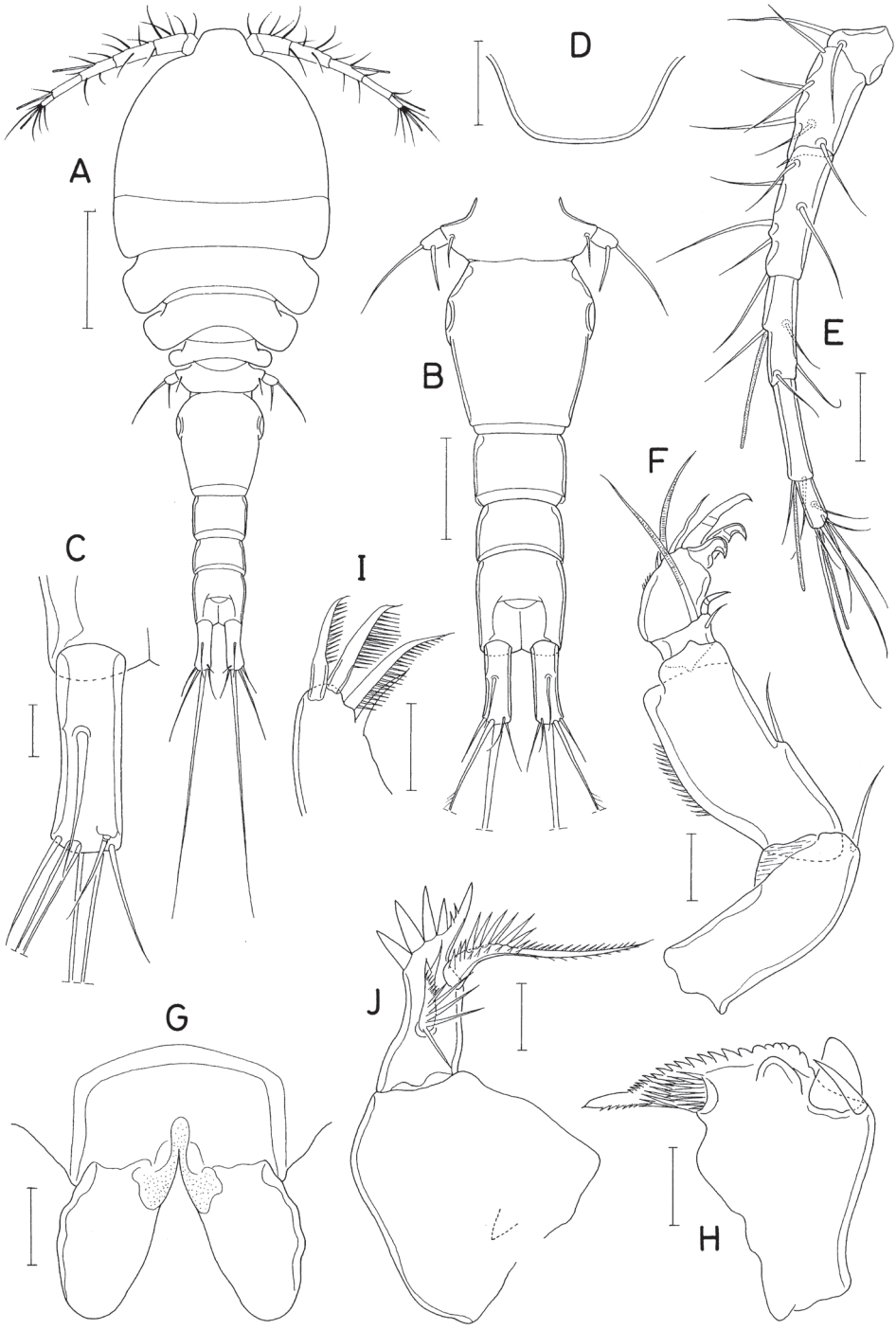

Figure 18. *Polyankylis bogilensis* sp. nov., female **A** habitus, dorsal **B** urosome, dorsal **C** left caudal ramus, dorsal **D** rostrum **E** antennule **F** antenna **G** labrum **H** mandible **I** maxillule **J** maxilla. Scale bars: 0.2 mm (**A**); 0.1 mm (**B**); 0.02 mm (**C, F–J**); 0.05 mm (**D, E**).

by weak suture line, with uneven outer margin. Mandible (Fig. 18H) with two very unequal outer scales (spiniform proximal one and large, plate-like distal one) followed by stout tubercle; inner margin short, with circular row of spinules at junction between distal lash and inner margin; distal lash short, denticulate along outer margin, with fine denticle along inner margin; terminal part of lash not flexible. Maxillule (Fig. 18I) lobate, armed with four setae; larger distal three setae pectinate along their inner margin; smaller inner margin seta naked, not articulated at base. Maxilla (Fig. 18J) two-segmented; proximal segment (syncoxa) broad, with one claw-like cusp on proximal part of posterior surface; distal segment (basis) armed with two spiniform setae (setae I and II), terminating in short, spiniform distal lash bearing four spines followed by one or two denticles along outer margin; seta I (inner seta) large, spinulose, proximal six spinules markedly larger than other spinules on seta; seta II (anterior seta) distally unequally bifurcate, with row of spinules, proximal four or five of these spinules much larger than distal spinules. Maxilliped (Fig. 19A) three-segmented; first segment (syncoxa) unarmed; second segment (basis) broadened, armed with two large setae distantly isolated from each other: proximal seta spiniform, curved, extending to distal tip of maxilliped, ornamented with three kinds of spinules, eight extremely long spinules on proximal part of inner margin followed distally by minute spinules and row of several small spinules along outer margin; distal seta straight, less than half as long as proximal seta, feebly spinulose along both margins; terminal segment (endopod) distally forming spinulose claw, proximally with one spine, one dentiform process and one small seta.

Leg 1–3 (Fig. 19B–D) biramous, each with three-segmented exopod and two-segmented endopod; coxa with minute spinules at outer distal corner and large, pinnate inner seta; outer seta on basis naked. Leg 3 dissimilar to leg 2 in having three inner setae (instead of four) on distal endopodal segment. Leg 4 (Fig. 19E) uniramous, with distinctly two-segmented exopod; endopod absent; coxa lacking inner seta; spines on exopod elongate. Armature formula for legs 1–4 as follows:

	Coxa	Basis	Exopod	Endopod
Leg 1	0-1	1-0	I-0; I-1; III, 4	0-1; I, 1, 5
Leg 2	0-1	1-0	I-0; I-1; III, 5	0-1; III, 4
Leg 3	0-1	1-0	I-0; I-1; III, 5	0-1; III, 3
Leg 4	0-0	1-0	I-0; II, I, 3	(lacking)

Leg 5 (Fig. 19F) consisting of one dorsolateral seta on fifth pedigerous somite and free exopod; exopodal segment 1.72 × longer than wide (31 × 18 μm) armed with one spine (45 μm long) one naked seta (91 μm long). Leg 6 unarmed (Fig. 19F).

Male. Unknown.

Etymology. The name of the new species is taken from the type locality, Bogil Island.

Remarks. The genus *Polyankylis* currently consists of three known species: *P. orientalis* Ho & Kim, 1997, *P. australis* Karanovic, 2008, and *P. ovilaxa*. *Polyankylis australis* is known from Australia (Karanovic 2008) and the other two from Korea (Ho and Kim 1997; Kim 2014). These three species are distinguished from *P. bogilensis* sp. nov. by different features, as follows: *P. orientalis* has a claw-like distal process on the

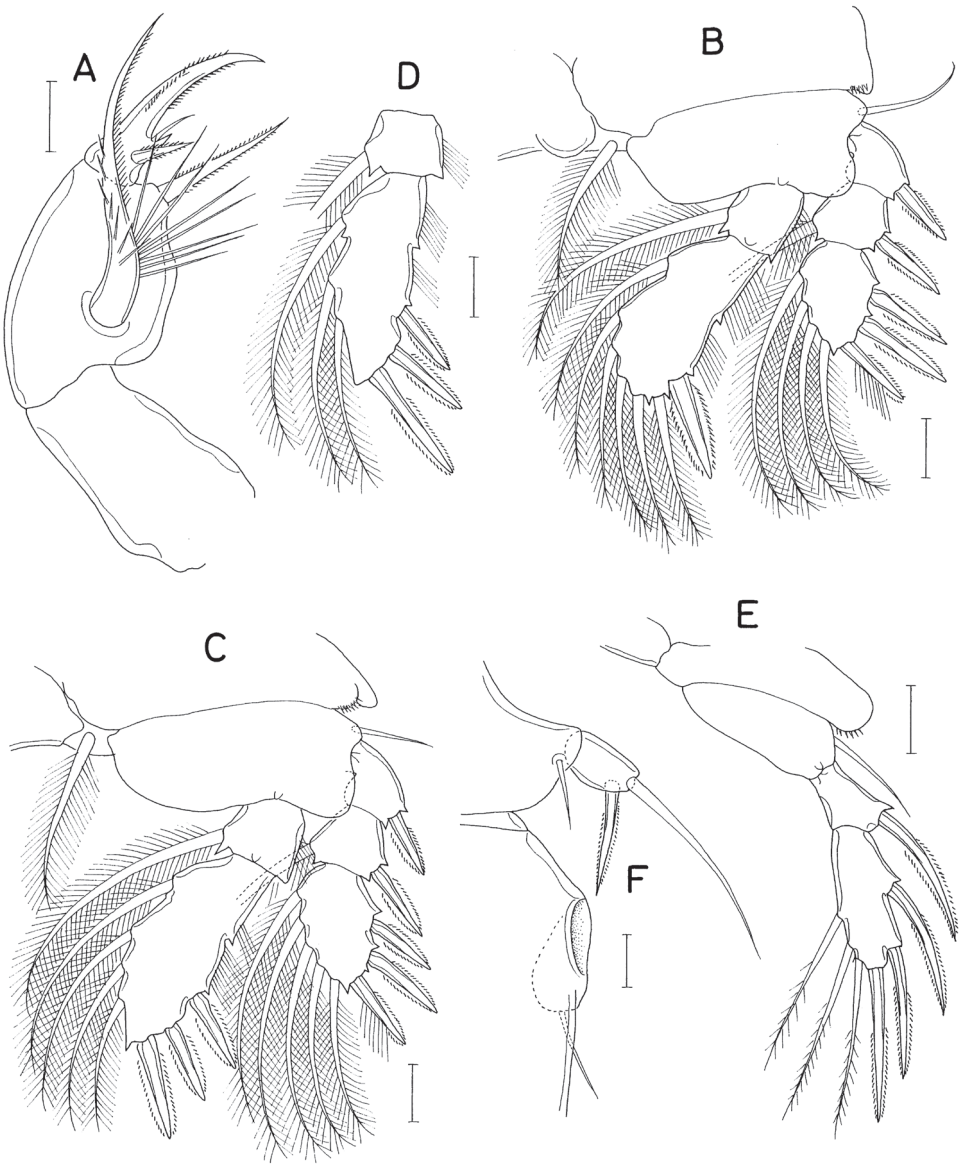

Figure 19. *Polyankylis bogilensis* sp. nov., female **A** maxilliped **B** leg 1 **C** leg 2 **D** endopod of leg 3 **E** leg 4 **F** leg 5 and genital aperture, dorsal. Scale bars: 0.02 mm.

coxobasis of the antenna (cf. this process absent in *P. bogilensis* sp. nov.) and a single-segmented exopod of leg 4 (cf. two-segmented in *P. bogilensis* sp. nov.); *P. australis* has an aesthetasc on the second endopodal segment of the antenna (cf. this aesthetasc absent in *P. bogilensis* sp. nov.), the terminal antennal segment is 3.5 × longer than wide (cf. 1.28 × longer than wide in *P. bogilensis* sp. nov.), and the maxillary syncoxa lacks a claw-like process (cf. this process present in *P. bogilensis* sp. nov.); and *P. ovilaxa* has

caudal rami which are 4.40 × longer than wide (cf. 2.96 × in *P. bogilensis* sp. nov.), the terminal antennal segment is 2.5 × longer than wide, and the maxillary syncoxa lacks the claw-like process.

Family Pseudanthessiidae Humes & Stock, 1972
Genus *Pseudanthessius* Claus, 1889

***Pseudanthessius linguifer* sp. nov.**
https://zoobank.org/99BB54CC-6289-4E0D-9B8C-8D4AE3EF5805
Figs 20, 21

Material examined. ***Holotype*** ♀ (MABIK CR00250120) and intact ***paratypes*** 3 ♀♀ (MABIK CR00250121) preserved in 90% alcohol, and paratype ♀ dissected and mounted on a slide, Site 22 (Yesong, Bogil Island, south coast, 34°08'11"N, 126°33'49"E), 31 May 2021, leg. J. Lee; ♀ dissected and mounted on a slide, Site 23 (Haenam, south coast, 34°17'57"N, 126°31'50"E), 24 Apr. 2021, leg. J. Lee and C. Y. Chang. Dissected specimens are retained in the collection of I.-H. Kim.

Description. Female. Body (Fig. 20A) narrow. Body length of dissected and figured paratype 1.23 mm (length range 1.17–1.32 mm, holotype 1.19 mm). Maximum width 385 μm across cephalothorax. Prosome 727 μm long. Cephalothorax 463 μm long, distinctly longer than wide, with weak dorsal suture line delimiting cephalosome and first pedigerous somite. Fourth pedigerous somite with point near posterolateral corners; other prosomal somites with rounded corners. Urosome (Fig. 20B) shorter than prosome, five-segmented. Fifth pedigerous somite 102 μm wide. Genital double-somite ~ 1.5 × longer than wide (182 × 123 μm), consisting of narrow anterior 17%, inflated middle 49%, and narrow posterior 34%; dorsally covered by brownish sticky material; genital apertures characteristically positioned ventrolaterally (Fig. 21G) at 45% region of double-somite length; broader middle region bearing linguiform process dorsolaterally, posterior to each genital aperture (Fig. 20C); narrow posterior region with four horizontal membranous flanges (Fig. 20C) on dorsal surface, anterior one short, curved. Three free abdominal somites 45 × 49 μm, 25 × 44 μm, and 56 × 42 μm, respectively. Anal somite with minute spinules along posteroventral margin. Caudal ramus (Fig. 20D) elongate, 10 × longer than wide (155 × 15.5 μm), 2.77 × longer than anal somite, armed with six setae (seta II–VII); seta II (outer lateral seta) positioned at 78% length of ramus; setae IV–VI pinnate, other three setae naked.

Rostrum (Fig. 20E) tapering, as long as wide, abruptly narrowed subdistally, with round apex. Antennule (Fig. 20F) 295 μm long, seven-segmented; armature formula 4, 13, 6, 3, 4+aesthetasc, 2+aesthetasc, and 7+aesthetasc; all setae thin, naked; aesthetascs also thin, setiform. Antenna (Fig. 20G) four-segmented; first segment (coxobasis) with one seta inner distally; second segment (first endopodal segment) with one seta on inner margin and fine spinules along outer margin; third segment short, armed with one slender claw and two setae; terminal segment 3.28 × long than wide (77 × 23 μm), armed with four slender claws (inner and outer claws longer than middle two) plus three setae, and ornamented with fine spinules along outer margin.

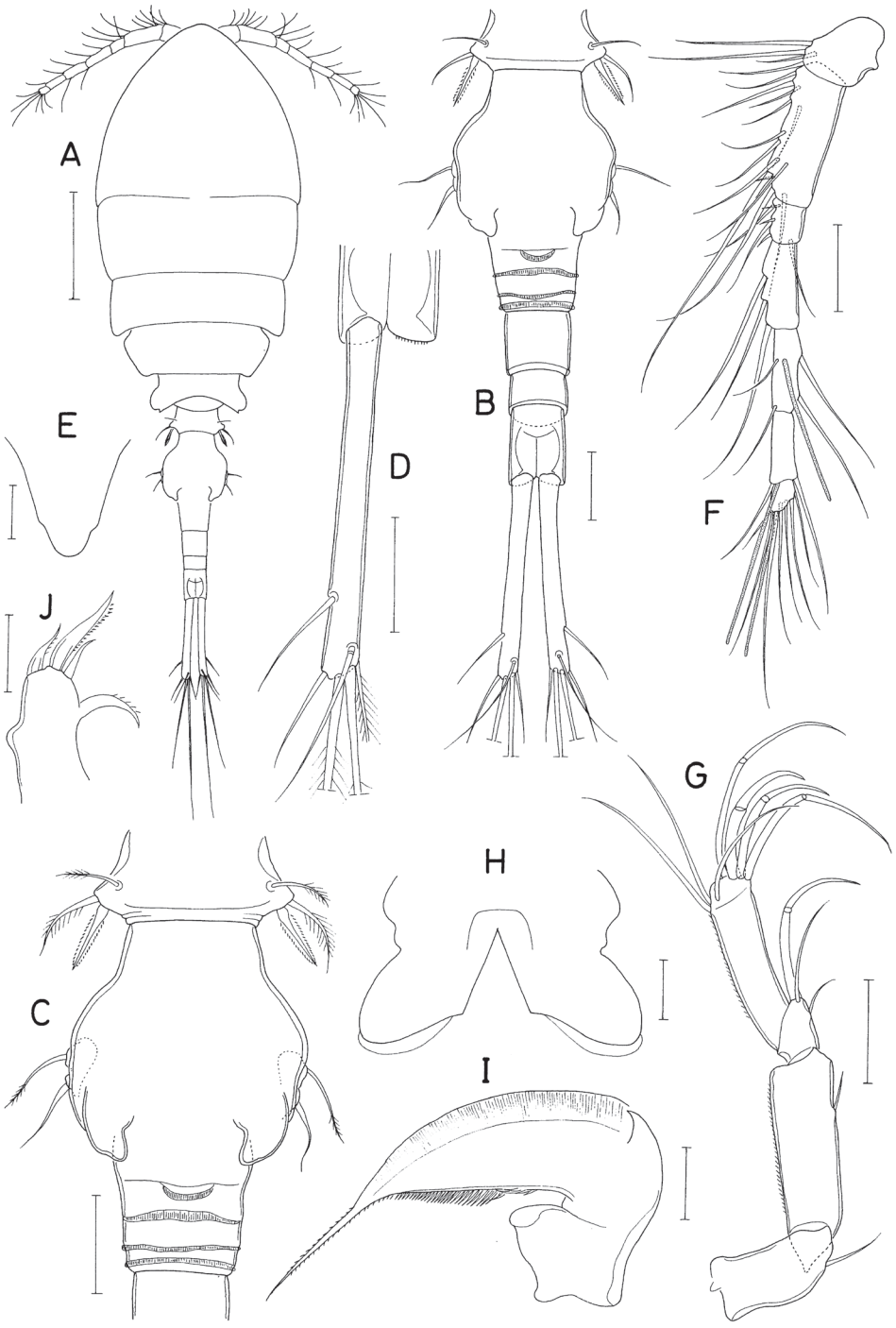

Figure 20. *Pseudanthessius linguifer* sp. nov., female **A** habitus, dorsal **B** urosome, dorsal **C** proximal somites of urosome, dorsal **D** left caudal ramus, dorsal **E** rostrum **F** antennule **G** antenna **H** labrum **I** mandible **J** maxillule. Scale bars: 0.2 mm (**A**); 0.05 mm (**B– D, F, G**); 0.02 mm (**E, H–J**).

Labrum (Fig. 20H) with long, divergent posterolateral lobes, with deep median incision; each lobe with angle on inner margin; posterior margin of lobes fringed with membrane. Mandible (Fig. 20I) with one large, tooth-like outer scale; gnathobase tapering, with row of minute spinules along inner margin, terminating in long, thin lash. Maxillule (Fig. 20J) with four unequal setae (three apical and one on inner margin) and one blunt tubercle on outer margin; middle of three distal setae larger than other two. Maxilla (Fig. 21A) two-segmented; proximal segment (syncoxa) unarmed; distal segment (basis) with extremely long distal lash and armed with two setae (setae I & II); distal lash longer than remaining part maxilla, bearing one large claw-like process proximally, spinulose along convex outer margin; seta I large, slightly longer than half length of distal lash, spinulose along both margins; seta II unequally bifurcate at tip, with setiform outer furca and spinule-like inner furca; seta III absent. Maxilliped (Fig. 21B) three-segmented; first segment (syncoxa) longest but unarmed; second segment (basis) armed with two very unequal setae (proximal seta large, spiniform, longer than width of segment, more than 4 × as long as small distal seta), and ornamented with several longitudinal rows of fine spinules on inner surface; small third segment (endopod) tapering, claw-like, proximally with one spine and one small seta.

Legs 1–4 (Fig. 21C–F) biramous. Legs 1–3 with three-segmented rami. Leg 4 with three-segmented exopod and one-segmented endopod. Inner coxal seta well-developed, pinnate in legs 1–4. Outer seta on basis thin, naked. Distal process between two distal spines on third endopodal segment of leg 2 blunt, slightly swollen. Three inner distal setae on third exopodal segment of legs 2 and 3 naked. Endopodal segment of leg 4 setulose on inner and outer margins, 2.6 × longer than wide (68 × 26 μm), bearing angle on outer margin; two distal spines 82 (inner) and 61 μm long (outer). Armature formula for legs 1–4 as follows:

	Coxa	Basis	Exopod	Endopod
Leg 1	0-1	1-0	I-0; I-1; III, I, 4	0-1; 0-1; I, 1, 4
Leg 2	0-1	1-0	I-0; I-1; III, I, 5	0-1; 0-2; I, II, 3
Leg 3	0-1	1-0	I-0; I-1; III, I, 5	0-1; 0-2; I, II, 2
Leg 4	0-1	1-0	I-0; I-1; II, I, 5	0, II, 0

Leg 5 (Fig. 21G) represented by one spine and two setae on lateral surface of fifth pedigerous somite. Leg 6 (Fig. 21G) represented on two setae on genital operculum; anterior seta thin, weakly pinnate; posterior seta naked, proximally broadened.

Male. Unknown.

Etymology. The specific name of the new species *linguifer* is derived from Latins *lingu* (the tongue) and *fer* (bear), referring to the presence of the tongue-like dorsolateral processes on the genital double-somite.

Remarks. The most conspicuous feature of *Pseudanthessius linguifer* sp. nov. is its elongate caudal rami, which are 10 × longer than wide. Such long caudal rami are exhibited by four congeners: *P. concinnus* Thompson & Scott, 1903, *P. dubius* Sars, 1918, *P. thorelli* (Brady & Robertson, 1875), and *P. stenosus* Kim & Hong, 2014. All of the other species in the genus have shorter caudal rami, at most 8.5 × longer than wide, as in *P. deficiens* Stock, Humes & Gooding, 1964 (Stock et al. 1964). *Pseudanthessius linguifer*

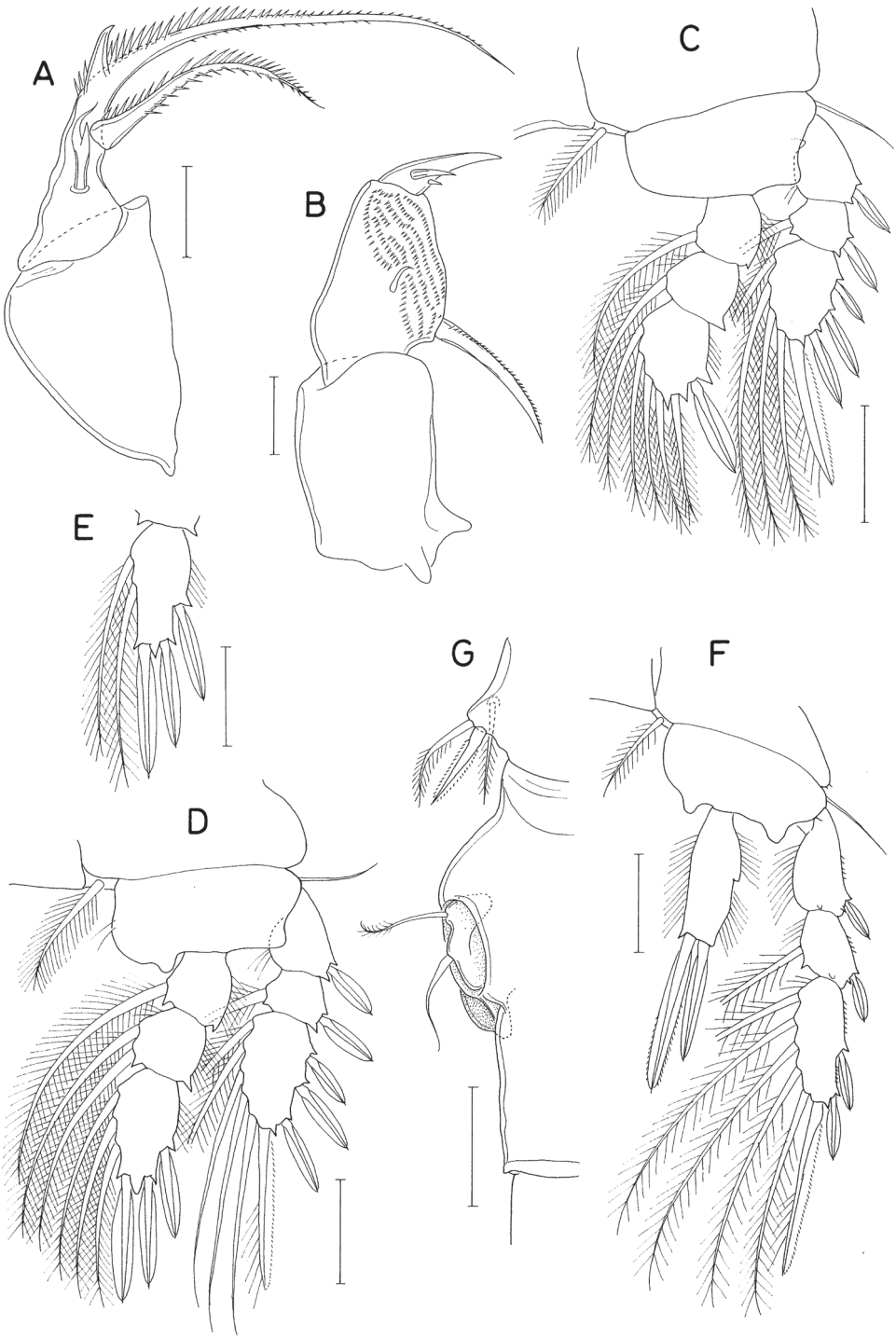

Figure 21. *Pseudanthessius linguifer* sp. nov., female **A** maxilla **B** maxilliped **C** leg 1 **D** leg 2 **E** third endopodal segment of leg 3 **F** leg 4 **G** leg 5 and genital aperture, dorsal. Scale bars: 0.02 mm (**A, B**); 0.05 mm (**C–G**).

sp. nov. differs from *P. concinnus* in having a large outer scale on the mandible (cf. the scale absent in *P. concinnus*) and two distal spines on the endopod of leg 4 (cf. one spine plus one seta in *P. concinnus*); from *P. dubius* in having the five-segmented urosome in the female (cf. four-segmented female urosome in *P. dubius*) and four distal claws on the antenna (cf. a single large claw in *P. dubius*); and from *P. thorelli* in having one spine plus one seta on the exopod of female leg 5 (cf. two setae in *P. thorelli*). *Pseudanthessius linguifer* sp. nov. resembles *P. stenosus* which is known from Thailand (Kim and Hong 2014) in many morphological aspects, in particular, the possession of the spinules-covered second segment (basis) of the female maxilliped and the bifurcate anterior seta (seta II) on the basis of the maxilla. However, the new species is distinguishable from *P. stenosus* and other congeners by its other outstanding features, such as the presence of the tongue-like dorsolateral processes on the genital double-somite, the extremely long distal lash of the maxilla, and the ventrolateral position of the genital apertures.

Family Rhynchomolgidae Humes & Stock, 1972
Genus *Critomolgus* Humes & Stock, 1983

***Critomolgus anthopleurus* Kim I.H., 1996**

Material examined. One ♀, Site 4, 19 Jul. 2016.

Remarks. The host of this copepod is the actiniarian *Anthopleura anjunae* Den Hartog & Vennam, 1993. The previously recorded host name *Anthopleura midori* Uchida & Muramatsu, 1958 is a junior synonym of *A. anjunae* (WoRMS Editorial Board 2021). It is remarkable that *C. anthopleurus* is an internal associate, living within the gastrovascular cavity of the actiniarian, but can be attracted to light.

Family Sabelliphilidae Gurney, 1927
Genus *Eupolymniphilus* Humes & Boxshall, 1996

***Eupolymniphilus orientalis* Kim, 2006**

Material examined. Five ♀♀, 2 ♂♂, Site 22, 26 Apr. 2021; 5 ♂♂, Site 27, 09 Apr. 2016.

Remarks. The host of this copepod is still unknown but is probably a polychaete.

***Eupolymniphilus foliatus* sp. nov.**
https://zoobank.org/BBF87DB7-F7BA-4642-8951-456E4885F148
Figs 22–24

Material examined. ***Holotype*** ♀ (MABIK CR00250130) and ***paratype*** ♂ dissected and mounted on a slide, and intact ***paratypes*** 2 ♂♂ (MABIK CR00250122) preserved in 90% alcohol, Site 2 (Namyang, Ulleung Island, Sea of Japan, 37°28'01.3"N, 130°50'01.4"E), 01 Jul. 2021, leg. J. G. Kim. Dissected paratype (♂) is retained in the collection of I.-H. Kim.

Description. Female. Body (Fig. 22A) moderately broad. Body length 1.44 mm. Prosome 840 × 586 μm, fusiform. Cephalothorax with dorsal suture line delimiting cephalosome and first pedigerous somite. Second to fourth pedigerous somites bearing angular posterolateral corners. Urosome (Fig. 22B) five-segmented. Fifth pedigerous somite expanded laterally, wider than genital double-somite, with sleeve-like, pronounced posterolateral corners. Genital double-somite longer than wide (210 × 184 μm), with convex lateral margins, widest at 45% region of double-somite. Three free abdominal somites 59 × 106 μm, 45 × 95 μm, and 80 × 91 μm, respectively. Anal somite unornamented, lacking any spinules. Caudal ramus (Fig. 22C) 3.33 × longer than wide (130 × 39 μm), ~ 1.6 × longer than anal somite, armed with six setae; seta II slightly expanded along proximal third, positioned dorsally at 56% region of ramus length.; setae IV–VI pinnate, other setae naked.

Rostrum (Fig. 22D) well-developed, slightly wider than long, with blunt apex. Antennule (Fig. 22E) 340 μm long, seven-segmented; first and second segments broader than distal segments; armature formula 4, 13, 6, 3, 4+aesthetasc, 2+aesthetasc, and 7+aesthetasc; all setae naked; third and terminal segments equally short. Antenna (Fig. 22F) four-segmented; armature formula 1, 1, 3+claw, and 4+3 claws; terminal segment (third endopodal segment) 2.65 × longer than wide (61 × 23 μm); claws on third and terminal segments slender, setiform; apical seta on terminal segment distinctly longer than other setae on same segment; innermost of three claws on terminal segment shorter than others.

Labrum (Fig. 22G) with distinctly defined, divergent posterolateral lobes and broad posteromedian incision. Mandible (Fig. 22H) with gnathobase bearing finely denticulate convex outer margin, ~ 15 unequal spinules along concave inner margin, and distal lash fringed with wrinkled membrane along outer margin and narrow membrane along inner margin; inner proximal region of gnathobase lacking notch; outer proximal region of blade with one small, indistinct scale. Maxillule (Fig. 22I) lobate, with one expanded, leaf-like, modified seta on inner margin and three (one longer and two shorter) apical setae. Maxilla (Fig. 22J) two-segmented; proximal segment (syncoxa) unarmed; distal segment (basis) distally with five spinules followed by three larger spinules and slender, spinulose lash, and armed with three setae (seta I-III); seta I (inner seta) large, spinulose along distal (outer) margin; seta II (anterior seta) slightly broadened, with acute distal tip; seta III (outer proximal seta) rudimentary. Maxilliped (Fig. 23A) three-segmented; first segment unarmed; second segment with two unequal setae subdistally; third segment narrow, pointed distally, with one small, subdistal seta.

Legs 1–4 (Fig. 23B–D) biramous with three-segmented rami; outer seta on basis small, naked. Inner coxal seta of all swimming legs well-developed, pinnate. Armature formula for legs 1–4 as follows:

	Coxa	Basis	Exopod	Endopod
Leg 1	0-1	1-0	I-0; I-1; III, I, 4	0-1; 0-1; I, 1, 4
Leg 2	0-1	1-0	I-0; I-1; III, I, 5	0-1; 0-2; I, II, 3
Leg 3	0-1	1-0	I-0; I-1; III, I, 5	0-1; 0-2; I, II, I+2
Leg 4	0-1	1-0	I-0; I-1; II, I, 5	0-1; 0-1; I, II, II

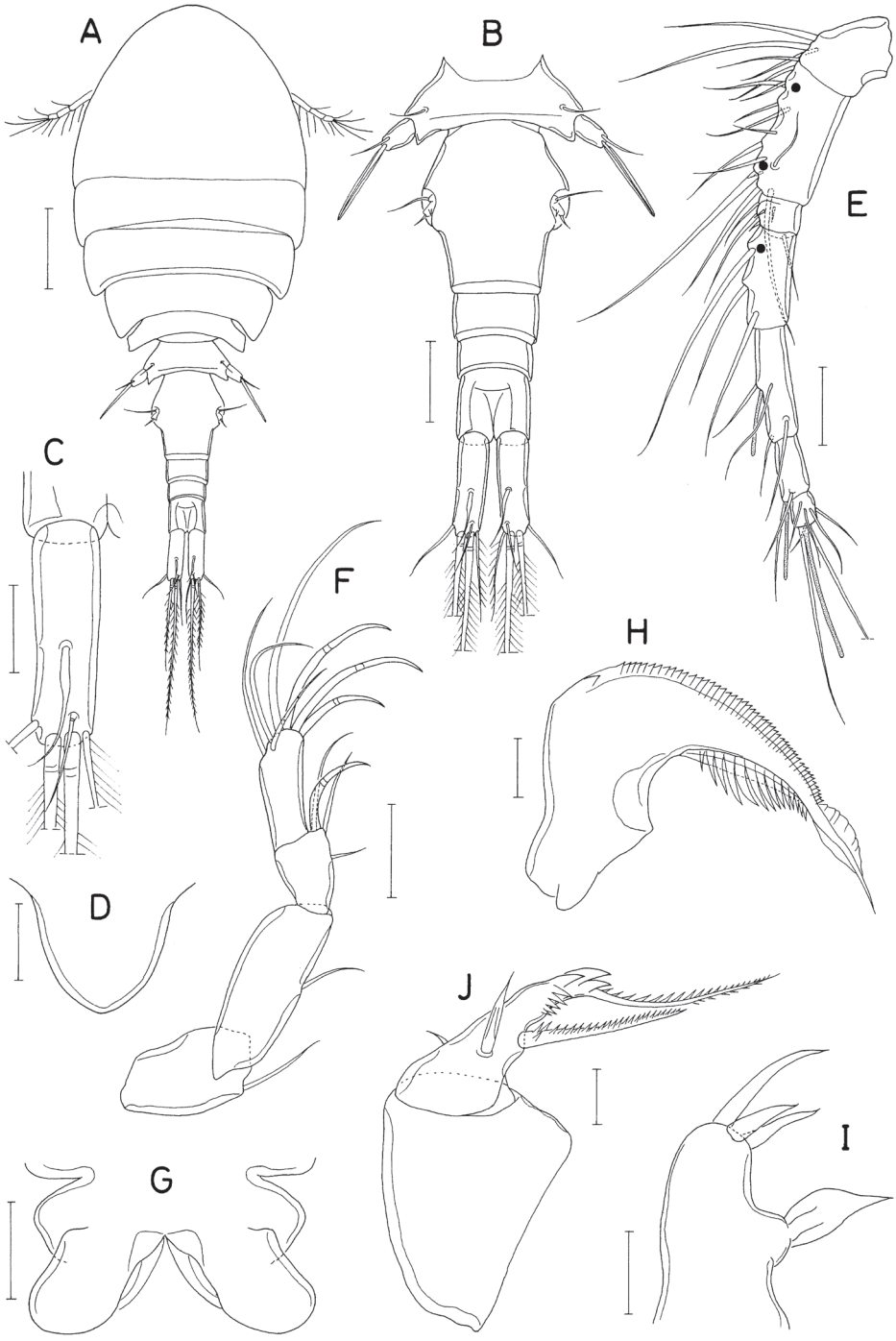

Figure 22. *Eupolymniphilus foliatus* sp. nov., female **A** habitus, dorsal **B** urosome, dorsal **C** left caudal ramus, dorsal **D** rostrum **E** antennule **F** antenna **G** labrum **H** mandible **I** maxillule **J** maxilla. Scale bars: 0.2 mm (**A**); 0.1 mm (**B**); 0.05 mm (**C–G**); 0.02 mm (**H–J**).

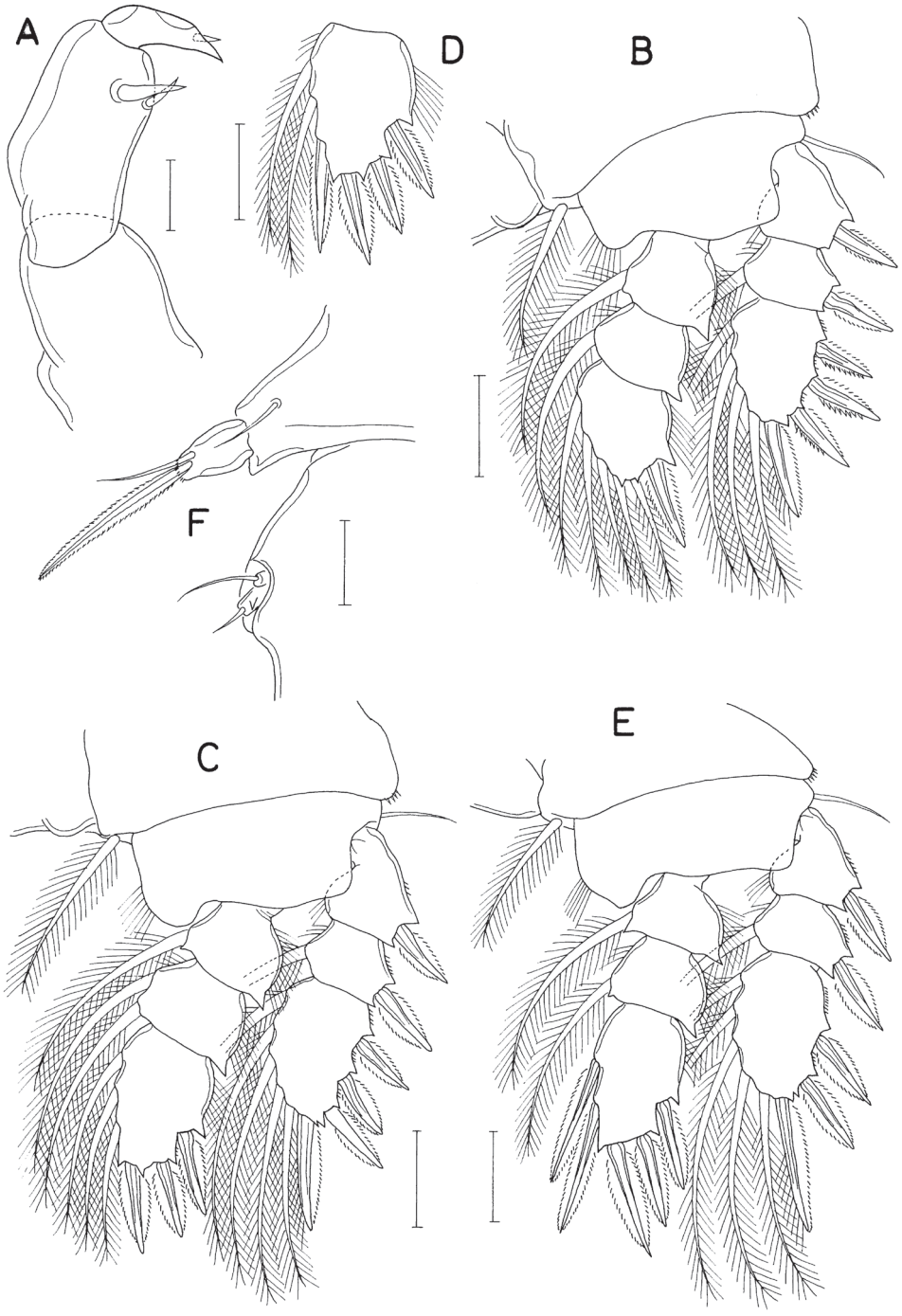

Figure 23. *Eupolymniphilus foliatus* sp. nov., female **A** maxilliped **B** leg 1 **C** leg 2 **D** third endopodal segment of leg 3 **E** leg 4 **F** left leg 5 and genital aperture. Scale bars: 0.02 mm (**A**); 0.05 mm (**B–F**).

Leg 5 (Fig. 23F) consisting of one small dorsolateral seta on fifth pedigerous somite and exopod; exopodal segment small, 1.59 × longer than wide (46 × 29 μm), widest at proximal third, narrowing distally, armed with one seta (60 μm long) and one elongate compound spine (117 μm long). Leg 6 (Fig. 23F) represented two small setae and single denticle on genital operculum

Male. Body (Fig. 24A) narrower and smaller than that of female. Body length 847 μm in dissected paratype (length range 782–847 μm). Prosome 495 × 287 μm. Urosome (Fig. 24B) six-segmented. Fifth pedigerous somite 109 μm wide, lacking posterolateral sleeve-like extension seen in female. Genital somite subquadrate, 127 × 124 μm, with rounded anterolateral corners and pointed posterolateral corners; genital operculum with pointed apex. Four abdominal somites 36 × 60 μm, 29 × 55 μm, 22 × 51 μm, and 36 × 56 μm, respectively. Caudal ramus 2.40 × longer than wide (60 × 25 μm), armed as in female.

Rostrum as in female. Antennule as in female, but with three additional aesthetascs at places of dark circles in Fig. 21E. Antenna, labrum, mandible as in female. Maxillule (Fig. 24C) with less expanded inner margin seta. Maxilla as in female. Maxilliped (Fig. 24D) consisting of three segments and terminal claw; first segment with one large tubercle at inner subdistal region; second segment with two unequal setae and one longitudinal row of spinules; small third segment unarmed; terminal claw elongate, as long as three segments, arched, bearing one setule and one large, slightly undulated seta proximally.

Legs 1–5 as in female. Leg 6 represented by two small setae on genital operculum (Fig. 24B).

Etymology. The specific name of the new species is from Latin *foli* (a leaf), alluding to the leaf-like inner seta of the maxillule.

Remarks. Differences between species of *Eupolymniphilus* are slight. However, *E. foliatus* sp. nov. can be differentiated from its congeners by the key character, the leaf-like modified inner seta of the maxillule. This seta in other species of the genus is known to be simple and slender. Another characteristic feature of the new species is the presence of thick membranes on the distal part of the mandibular lash.

The length-to-width ratio of the caudal ramus in *Eupolymniphilus* is somewhat variable among congeneric species. In the female, it is 3.5:1 in *E. finmarchicus* (Scott T., 1903) according to the illustration of G. O. Sars (1918), ~ 10:1 in *E. tenuicaudis* (G. O. Sars, 1918), 1.50:1 in *E. orientalis* Kim, 2006, 1.03:1 in *E. brevicaudatus* Kim, 2009, 2.69:1 in *E. occidentalis* Kim, 2009, and 3.05:1 in *E. mediterraneus* Costanzo, Brugnano & Zagami, 2013. Thus, *E. foliatus* sp. nov., in which the caudal ramus is 3.33 × longer than wide, is comparable to the three species, *E. finmarchicus*, *E. occidentalis*, and *E. mediterraneus*. Furthermore, they differ from the new species, as follows: *E. finmarchicus* has five setae on the first segment of the antennule (Bocquet et al. 1963), and the mandible lacks any outer scale; *E. occidentalis* has acutely pointed posterolateral corners on the second pedigerous somite (cf. with blunt posterolateral corners in *E. foliatus* sp. nov.), seven aesthetascs on the male antennule (cf. six aesthetascs in *E. foliatus* sp. nov.), and

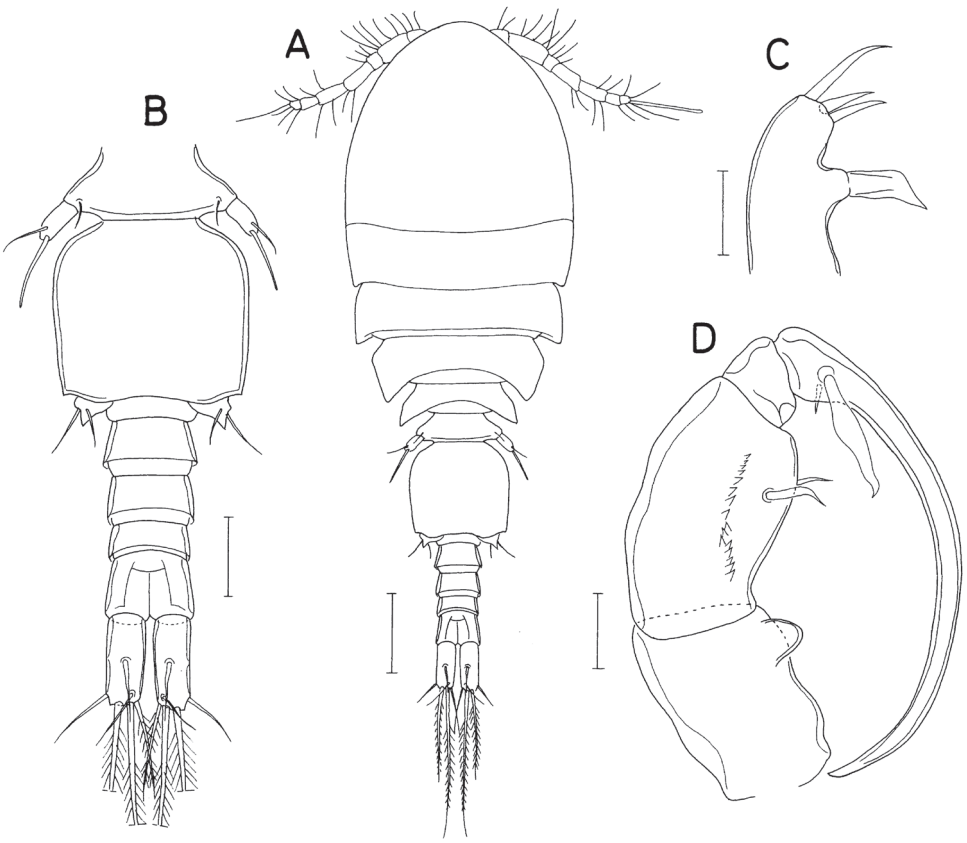

Figure 24. *Eupolymniphilus foliatus* sp. nov., male **A** habitus, dorsal **B** urosome, dorsal **C** maxillule **D** maxilliped. Scale bars: 0.1 mm (**A**); 0.05 mm (**B**); 0.02 mm (**C, D**).

a shorter terminal segment of the antenna which is 1.92 × longer than wide according to Kim (2009) (cf. 2.65 × longer than wide in *E. foliatus* sp. nov.); and *E. mediterraneus* has a small body size, 0.75 mm in the female, and the terminal segment of the antenna bears four claws (Costanzo et al. 2013) (cf. three claws in *E. foliatus* sp. nov.).

Family Taeniacanthidae Wilson C.B., 1911
Genus *Anchistrotos* Brian, 1906

***Anchistrotos kojimensis* Do & Ho, 1983**

Material examined. Two ♀♀, Site 31, 11 Nov. 2020.

Remarks. This is a fish-parasitic copepod, living in the gill cavity of the host. Known hosts of this copepod are the gobiid fishes *Acanthogobius flavimanus* (Temminck & Schlegel, 1845) and *A. hasta* (Temminck & Schlegel, 1845).

Order Siphonostomatoida Burmeister, 1835
Family Artotrogidae Brady, 1990
Genus *Artotrogus* Boeck, 1859

***Artotrogus acutus* Kim, 1996**

Material examined. One ♂, Site 4, 19 Jul. 2016; 1 ♀, 1 ♂, Site 11, 03 Jun. 2019; 2 ♂♂, Site 11, 10 Jun. 2020.

Genus *Ascidipontius* Kim I.H., 1996

***Ascidipontius rarus* Kim, 1996**

Material examined. One ♀, 1 ♂, Site 11, 10 Jun. 2020; 2 ♀♀, 1 ♂, Site 21, 26 Apr. 2021.

Genus *Bradypontius* Giesbrecht, 1895

***Bradypontius halocynthiae* Kim, 1996**

Material examined. One ♀, 1 ♂, Site 11, 10 Jun. 2020.

Genus *Cryptopontius* Giesbrecht, 1899

***Cryptopontius ascidius* Kim, 1996**

Material examined. One ♀, Site 11, 03 Jun. 2019; 5 ♀♀, Site 11, 10 Jun. 2019; 1 ♀, 10 ♂♂, Site 11, 10 Jun. 2020.

***Cryptopontius donghaensis* Kim, 1996**

Material examined. One ♀, 5 ♂♂, Site 1, 28 Jun. 2021; 1 ♀, 4 ♂♂, Site 2, 01 Jul. 2021; 1 ♀, Site 3, 17 Jul. 2016; 10 ♀♀, 41 ♂♂, Site 7, 19 Jul. 2016; 2 ♀♀, 5 ♂♂, Site 12, 16 Mar. 2013; 1 ♀, 4 ♂♂, Site 14, 04 Jul. 2020.

Remarks. This species is the most frequently found artotrogid copepod in Korean waters; living on sponges, among sea weeds, and on submerged fishing nets in ports (Kim 2010a).

Genus *Pteropontius* Giesbrecht, 1895

***Pteropontius trimerus* Kim, 1996**

Material examined. Five ♀♀, Site 33, 11 Aug. 2020.

Remarks. This copepod had been found only on the external surface of the tunicate *Halocynthia igaboja* Oka, 1906.

Family Asterocheridae Giesbrecht, 1899
Genus *Acontiophorus* Brady, 1880

***Acontiophorus estivalis* sp. nov.**
https://zoobank.org/5654B945-0217-4D32-A0EB-2BF6D204BD4E
Figs 25–27

Material examined. ***Holotype*** ♀ (MABIK CR00250115) and ***paratypes*** 3 ♀♀, 2 ♂♂ (MABIK CR00250116) preserved in 90% alcohol, and ***paratypes*** 1 ♀, 1 ♂ dissected and mounted on a slide, Site 11 (Yeongdo, Pusan, 35°04'31.0"N, 129°05'08.7"E), 07 Jul. 2020, leg. J. G. Kim. Dissected paratypes (1 ♀, 1 ♂) are retained in the collection of I.-H. Kim.

Description. Female. Body (Fig. 25A) stout, 938 μm long in dissected and figured paratype (length range 893–945 μm, holotype 945 μm). Prosome 625 × 425 μm, occupying 67% of body length, consisting of cephalothorax and second to fourth pedigerous somites. Cephalothorax 425 μm long, as long as wide, without any dorsal suture line delimiting cephalosome and first pedigerous somite. Cephalothorax and second to third pedigerous somites with membranous fringe along posterodorsal margin. Fourth pedigerous somite with deeply concave posterior margin. Urosome (Fig. 25B) four-segmented. Fifth pedigerous somite 133 μm wide, with round lateral margins. Genital double-somite wider than long (115 × 132 μm), consisting of laterally expanded anterior third and narrower posterior two-thirds, with pointed posterolateral corners; genital apertures positioned dorsolaterally at expanded anterior region. Two free abdominal somites 39 × 77 μm and 45 × 75 μm. Anal somite (Fig. 25C) ornamented on ventral surface with two groups of several large setules on medial region, scattered fine setules on lateral regions, and several spinules at medial posterior margin near bases of caudal rami. Caudal ramus (Fig. 25C) rectangular, 2.12 × longer than wide (70 × 33 μm), armed with six setae plus one aesthetasc-like element (indicated by arrowhead in Fig. 25C), and ornamented with fine setules on ventral surface and four transverse rows of minute spinules on inner margin; dorsal setae (setae VI and VII) naked, other setae pinnate; outer lateral seta (seta II) with long setules along outer margin but spinulose (or with short setules) along inner margin; seta VI inserted on prolongation of ramus.

Rostrum absent. Antennule (Fig. 25D) short, 147 μm long, 11-segmented; armature formula 2, 14, 4, 2, 2, 8, 2, 1+aesthetasc, 2, 4, and 7; aesthetasc on 8th segment large; setae densely arranged, difficult to distinguish from one another. Antenna (Fig. 25E) consisting of coxa, basis, one-segmented exopod, and two-segmented endopod; coxa short, unarmed; basis longest segment, narrowed in mid-region, with tuft of long setules at inner distal corner; exopod elongate, 6.0 × longer than wide (54 × 9 μm), extending to middle of second endopodal segment, armed with one small seta in middle, one minute seta subdistally, and one large, unilaterally pinnate seta (97 μm long) distally; first endopodal segment unarmed, 32 × 22 μm; second endopodal segment

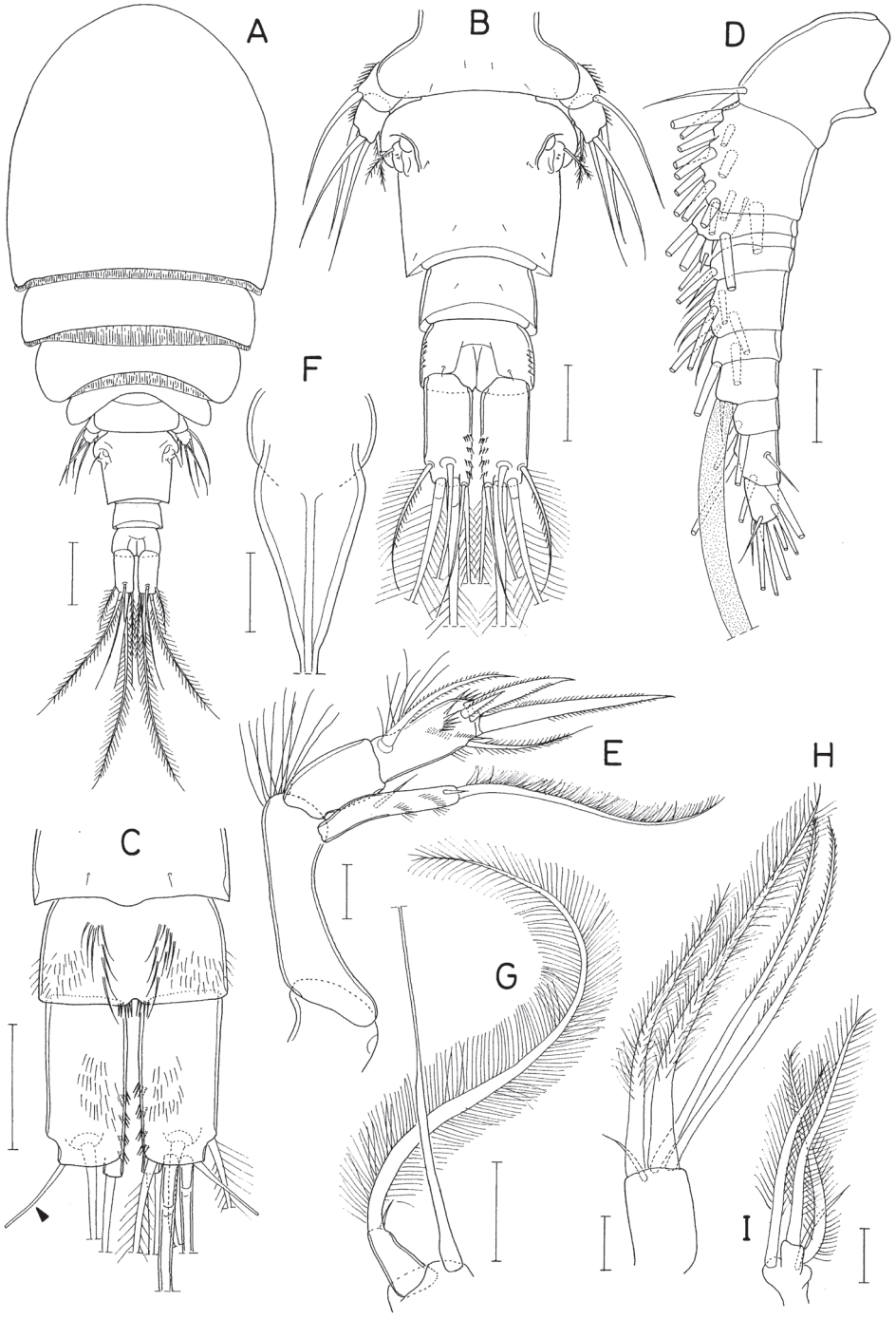

Figure 25. *Acontiophorus estivalis* sp. nov., female **A** habitus, dorsal **B** urosome, dorsal **C** anal somite and caudal rami, ventral **D** antennule **E** antenna **F** oral siphon **G** mandible **H** inner lobe of maxillule **I** outer lobe of maxillule. Scale bars: 0.1 mm (**A**); 0.05 mm (**B, C, F, G**); 0.02 mm (**D, E, H, I**).

2.2 × longer than wide (40 × 18 μm), armed with six setae consisting of one large proximal seta, three unequal subdistal setae (one minute, setule-like), and two broad apical setae 75 and 43 μm long, and ornamented with several rows of fine spinules or setules.

Oral siphon (Fig. 25F) consisting of conical proximal part (maximum width 67 μm) and thin distal part, extending to middle of genital double-somite. Mandible (Fig. 25G) consisting of thread-like stylet and palp; palp short, tapering, armed with one large, heavily pinnate seta and one minute, setule-like seta distally. Maxillule (Fig. 25H, I) bilobed; larger inner lobe armed with four large (two feebly pinnate and two plumose) and one small setae distally; smaller inner lobe armed with three pinnate and one small, naked setae. Maxilla (Fig. 26A) slender, two-segmented; proximal segment (syncoxa) unarmed, basally with short tube of maxillary gland; distal segment (basis) forming long claw, longer than proximal segment, ornamented with rows of small spinules and one tuft of few setules. Maxilliped (Fig. 26B) five-segmented, consisting of syncoxa, basis, three-segmented endopod, and terminal claw; syncoxa with trace of articulation delimiting praecoxal and coxal regions, coxal region with one seta on inner margin and row of spinules along outer margin; basis with one rudimentary seta at distal third of inner margin and row of spinules along outer margin; three endopodal segments armed with two, two, and one setae, respectively; terminal claw weakly curved, 66 μm long, more than twice longer than third endopodal segment (31 μm long).

Legs 1–4 (Fig. 26C–F) biramous, with three-segmented rami. Inner coxal seta well-developed in legs 1–4; outer seta on basis small in legs 1–3, but markedly large in leg 4. Inner distal spine on basis of leg 1 extending to middle of second endopodal segment. Second endopodal segment of legs 1–4 with bicuspid outer distal corner. Inner distal process of third endopodal segment of leg 1 acutely pointed. Armature formula for legs 1–4 as follows:

	Coxa	Basis	Exopod	Endopod
Leg 1	0-1	1–I	I-1; I-1; II, I, 5	0-1; 0-2; 1, 2, 3
Leg 2	0-1	1-0	I-1; I-1; III, I, 4	0-1; 0-2; 1, 1+I, 3
Leg 3	0-1	1-0	I-1; I-1; III, I, 3	0-1; 0-2; 1, I, 3
Leg 4	0-1	1-0	I-1; I-1; III, I, 3	0-1; 0-2; 1, I, 2

Leg 5 (Fig. 27A) two-segmented. First segment (protopod) broad, not articulated from somite, armed with large, naked outer distal seta and small, naked inner distal seta. Distal segment (exopod) 1.12 × longer than wide (28 × 25 μm), armed with five setae, and ornamented with fine setules on outer surface; two smaller setae on inner margin pinnate, terminal seta naked, two outer setae feebly pinnate. Leg 6 (Fig. 26G) represented by one pinnate seta and two minute setules on genital operculum.

Male. Body form (Fig. 27B) as in female. Body length 890 μm in dissected and figured paratype (length range 821–890 μm). Prosome 600 μm long. Cephalothorax slightly wider than long (374 × 407 μm). Urosome five-segmented, Genital somite much wider than long. First two free abdominal somites broadened distally, with pointed posterolateral corners. Caudal ramus 1.44 × longer than wide (46 × 32 μm), armed as in female.

Antennule (Fig. 27C) 168 μm long, 11-segmented; setae entangled, difficult to distinguish from one another; aesthetascs five on second segment, two on third, one on each 7th and 10th segment; aesthetasc on 10th segment large. Antenna as in female.

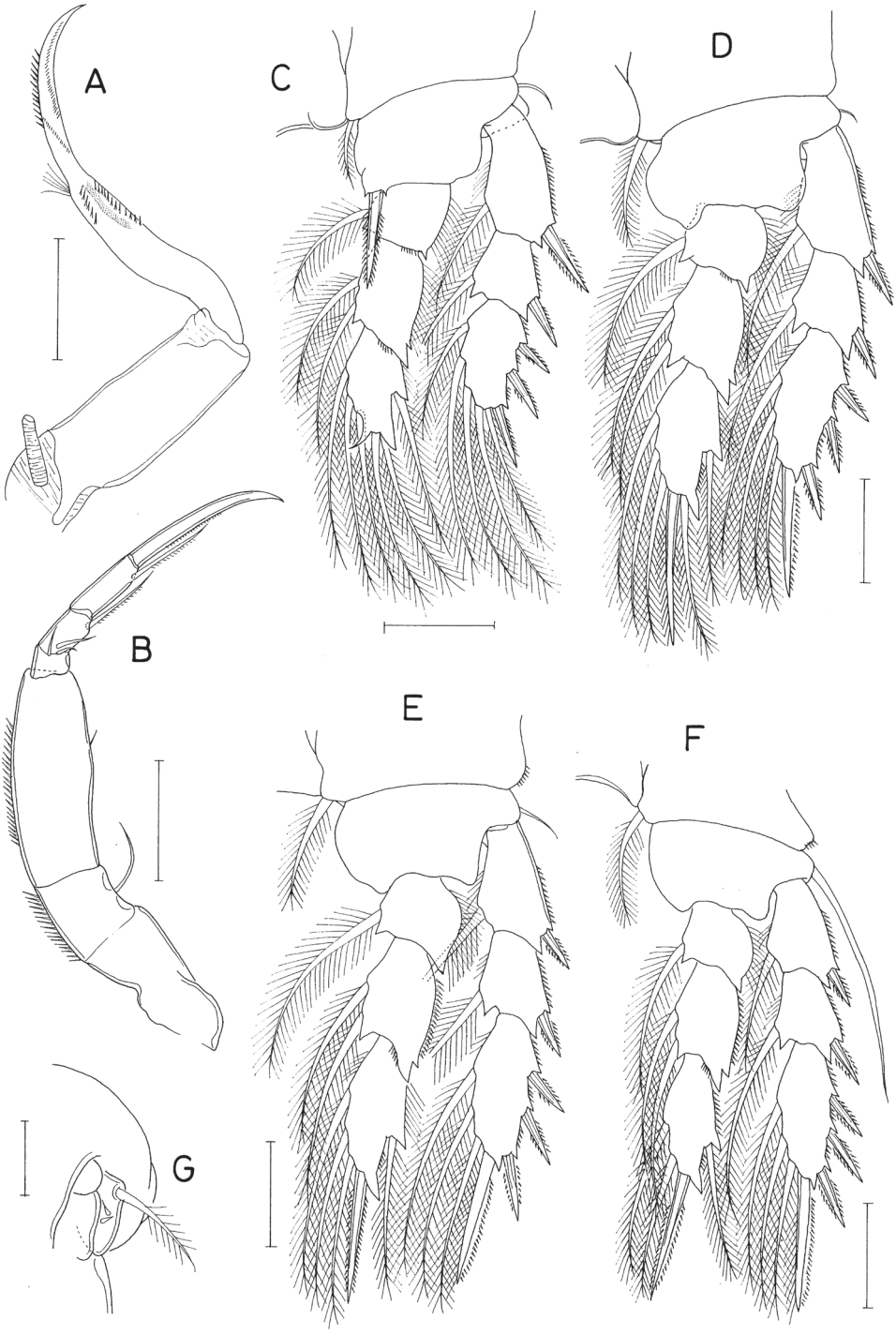

Figure 26. *Acontiophorus estivalis* sp. nov., female **A** maxilla **B** maxilliped **C** leg 1 **D** leg 2 **E** leg 3 **F** leg 4 **G** right genital aperture, dorsal. Scale bars: 0.05 mm (**A–F**); 0.02 mm (**G**).

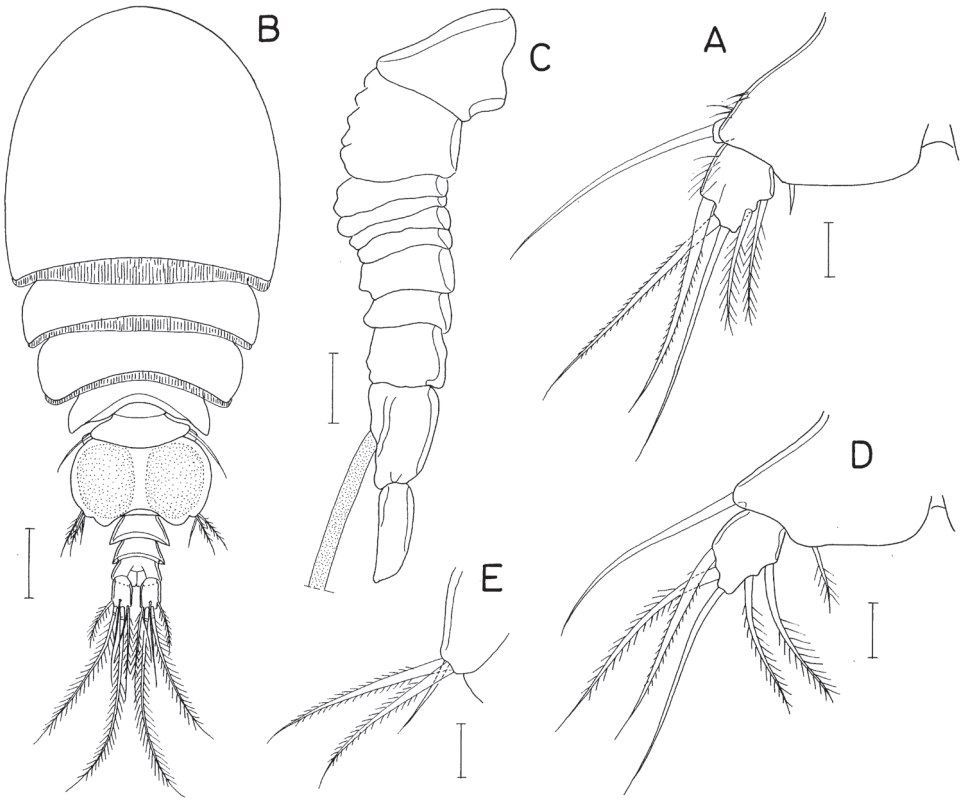

Figure 27. *Acontiophorus estivalis* sp. nov., female **A** leg 5, dorsal. Male **B** habitus, dorsal **C** antennule (setae omitted) **D** leg 5, dorsal **E** leg 6. Scale bars: 0.02 mm (**A, C–E**); 0.1 mm (**B**).

Oral siphon, mandible, maxillule, maxilla, maxilliped, and legs 1–4 same as those of female. Leg 5 (Fig. 27D) also shaped as in female; inner distal seta on protopod pinnate; exopodal segment 1.33 × longer than wide (32 × 24 μm), armed as in female. Leg 6 (Fig. 27E) represented by three setae (two larger, weakly pinnate and one smaller naked) on genital operculum.

Etymology. The specific name *estivalis* is derived from Latin *estival* (summer), indicating the discovery of the new species in the summer.

Remarks. The segmentation of the antennule appears to be a reliable character for the differentiation of *Acontiophorus* species. *Aconiophorus estivalis* sp. nov. has an 11-segmented antennule in the female; this feature is shared with three congeners, *A. antennatus* Hansen, 1923, *A. scutatus* (Brady & Robertson, 1873) and *A. zealandicus* Sewell, 1944. *Acontiphorus antennatus* was redescribed by Eiselt (1969) and according to his illustration and description, the caudal ramus of *A. antennatus* is ~ 4 × longer than wide in the female (cf. 2.12 × longer than wide in *A. estivalis* sp. nov.) and the third exopodal segment of leg 1 is armed with three spines and four setae (formula III, 4; against III, 5 in *A. estivalis* sp. nov.). In *A. zealandicus* the male antennule is ten-

segmented (cf. 11-segmented in *A. estivalis* sp. nov.) and the oral siphon is extremely long, extending beyond the caudal rami (Nicholls 1944) (cf. extending to middle of genital double-somite in A. *estivalis* sp. nov.). Therefore, *A. antennatus* and *A. zelandicus* can be distinguished from *A. estivalis* sp. nov. with confidence. *Acontiophorus estivalis* sp. nov. closely resembles *A. scutatus*. As noticeable differences between them, the caudal ramus of *A. scutatus* is 3 × longer than wide, and the oral siphon of the latter species extends to the caudal rami (Sars 1915) (cf. the siphon extends to the middle of the genital double-somite in *A. estivalis* sp. nov.). Additionally, the first segment of the male antennule of *A. scutatus* bears an aesthetasc, according to the illustration of Sars (1915), which is absent in *A. estivalis* sp. nov.

Genus *Dermatomyzon* Claus, 1889

***Dermatomyzon nigripes* (Brady & Robertson, 1880)**

Material examined. Two ♂♂, Site 1, 28 Jun. 2021; 1 ♀, Site 3, 17 July. 2016; 1 ♀, Site 4, 03 Jun. 2019; 2 ♀♀, Site 5, 21 Jun. 2016; 1 ♀, Site 6, 21 Sep. 2020; 1 ♀, 2 ♂♂, Site 11, 20 Aug. 2020; 2 ♀♀, 1 ♂, Site 13, 03 Jul. 2020; 6 ♀♀, 6 ♂♂, Site 16, 04 Jul. 2020.

Remarks. *Dermatomyzon nigripes* is a cosmopolitan species, and has frequently been collected in Korean coasts. The host of this copepod is still unknown.

Genus *Thermocheres* Kim I.H., 2010

***Thermocheres pacificus* sp. nov.**
https://zoobank.org/5F56B3F1-9731-49D8-A209-C6945F094AEA
Figs 28, 29

Material examined. ***Holotype*** ♂ (MABIK CR00250117) preserved in 90% alcohol, Site 22 (Yesong, Bogil Island, south coast, 34°08'11"N, 126°33'49"E), 26 Apr. 2021, leg. J. Lee and C. Y. Chang; ***Paratype*** ♂ dissected and mounted on a slide, Site 15 (Namhae Island, south coast, 34°45'00.5"N, 127°54'33.9"E), 04 Jul. 2020, leg. J. G. Kim. Dissected paratype is retained in the collection of I.-H. Kim.

Description. Male. Body (Fig. 28A) cyclopiform, moderately broad. Body length 1.14 mm in dissected and figured paratype (1.25 mm in holotype). Prosome 695 μm long, four-segmented, consisting of cephalothorax and three free pedigerous somites. All prosomal somites with acutely pointed posterolateral corners. Cephalothorax slightly wider than long (477 × 486 μm), consisting of completely fused cephalosome and first pedigerous somite, fringed with membrane along posterodorsal margin. Urosome (Fig. 28B) six-segmented. Fifth pedigerous somite narrower than genital somite, with tapered lateral apex. Genital somite quadrangular, wider than long (125 × 184 μm), with parallel lateral margins and pointed, tooth-like posterolateral corners; genital operculum well-developed, with one large cusp on distal margin and pair of unequal setae on tip of posterolateral apex. Four abdominal somites 57 × 140 μm, 45 × 125 μm,

36 × 116 μm, and 52 × 114 μm, respectively; first and second abdominal somites with acutely pointed, posteriorly extended posterolateral corners. Caudal ramus (Fig. 28B) 1.57 × longer than wide (83 × 53 μm), with six pinnate setae, ornamented with setules along inner margin; all setae positioned distally or subdistally.

Rostrum (Fig. 28C) slightly longer than wide, tapered, with angular apex. Antennule (Fig. 28D) 368 μm long, 17-segmented, geniculate between antepenultimate and penultimate segments; armature formula 1+aesthetasc, 2+aesthetasc, 2+aesthetasc, 2+aesthetasc, 2+aesthetasc, 2, 2+aesthetasc, 2, 7+3 aesthetascs, 2, 2+aesthetasc, 3+aesthetasc, 1, 2+aesthetasc, 1, 1+aesthetasc, and 11; setae naked, mostly short; aesthetascs thin but that of penultimate segment thicker. Antenna (Fig. 28E) consisting of coxa, basis, one-segmented exopod, and two-segmented endopod; coxa 35 × 17 μm, unarmed; basis 65 × 17 μm, with few spinules on outer margin; exopod 3 × longer than wide (18 × 6 μm), armed with two unequal setae distally and one seta near middle; first endopodal segment 38 × 15 μm, unarmed but with row of spinules on inner and outer margins; second endopodal segment 35 × 12 μm, terminated in long spiniform seta (107 μm long), armed with one seta on proximal inner margin, three (one minute) setae distally and subdistally, and ornamented with setules on inner and outer margin.

Oral siphon (Fig. 28F) 454 μm long, evenly tapering from proximal to distal, extending to insertions of leg 2. Mandible (Fig. 28G) consisting of short basal segment and elongate, slender stylet bearing 11 teeth distally. Maxillule (Fig. 28G) bilobed; small outer lobe 23 × 9 μm, distally with four setae, one naked, other three pinnate; elongate inner lobe based on segment-like extension, 127 × 15 μm, tipped with three thin, equally long, distally feebly pinnate setae. Maxilla (Fig. 28H) slender, consisting of syncoxa (189 μm long), basis (205 μm long) and terminal claw; basis with small seta at 70% region and small, tapering membrane distally; terminal claw (Fig. 28I) 64 μm long, curved, with row of spinules along proximal half of concave margin. Maxilliped (Fig. 29A, B) consisting of syncoxa, basis, four-segmented endopod, and terminal claw; syncoxa with one seta on inner distal corner; basis longest, with one blunt tubercle on inner margin bearing minute setule on distal margin of tubercle; endopodal segments with two, one, one, and one setae respectively; terminal claw slender, 103 μm long, weakly curved, ~ twice longer than terminal endopodal segment.

Legs 1–4 (Fig. 29C–F) biramous, with three-segmented rami. Outer seta on basis naked in leg 1 but pinnate in legs 2–4. Outer spine on first exopodal segment of leg 1 large, extending beyond base of first outer spine of third exopodal segment. Second endopodal segment of legs 1–4 with bicuspid outer distal corner. Inner distal seta on third exopodal segment of leg 4 distinctly smaller than proximal setae. Armature formula for legs 1–4 as follows:

	Coxa	Basis	Exopod	Endopod
Leg 1	0-1	1-1	I-1; I-1; III, 5	0-1; 0-2; 1, 2, 3
Leg 2	0-1	1-0	I-1; I-1; III, I, 5	0-1; 0-2; 1, 2, 3
Leg 3	0-1	1-0	I-1; I-1; III, I, 5	0-1; 0-2; 1, 1+I, 3
Leg 4	0-1	1-0	I-1; I-1; III, I, 5	0-1; 0-2; 1, I, 2

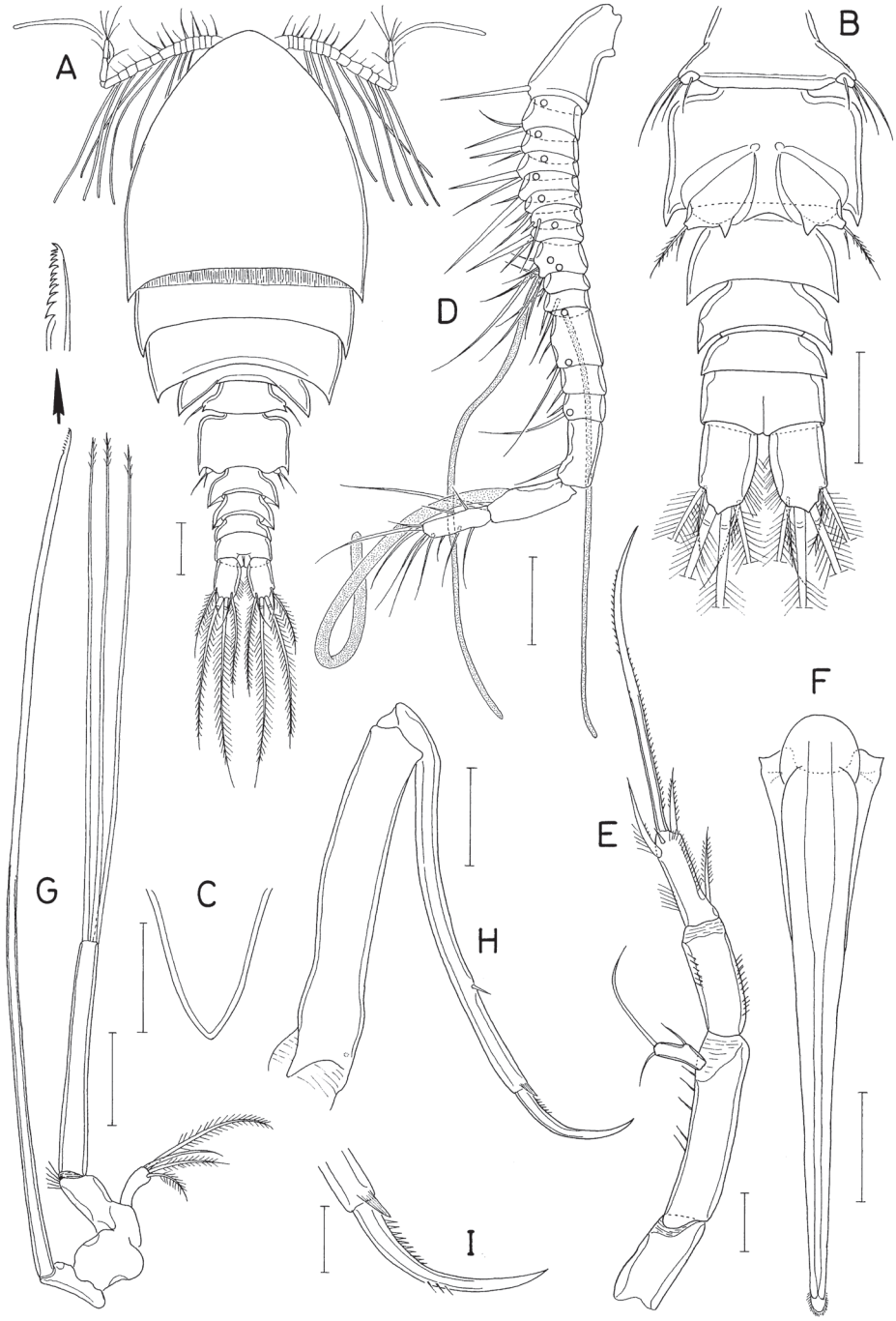

Figure 28. *Thermocheres pacificus* sp. nov., male **A** habitus, dorsal **B** urosome, ventral **C** rostrum **D** antennule (open circles indicate insertions of aesthetascs on opposite surface) **E** antenna **F** oral siphon **G** mandible and maxillule **H** maxilla **I** distal part of maxilla. Scale bars: 0.1 mm (**A, B, F**); 0.05 mm (**C, D, G, H**); 0.02 mm (**E, I**).

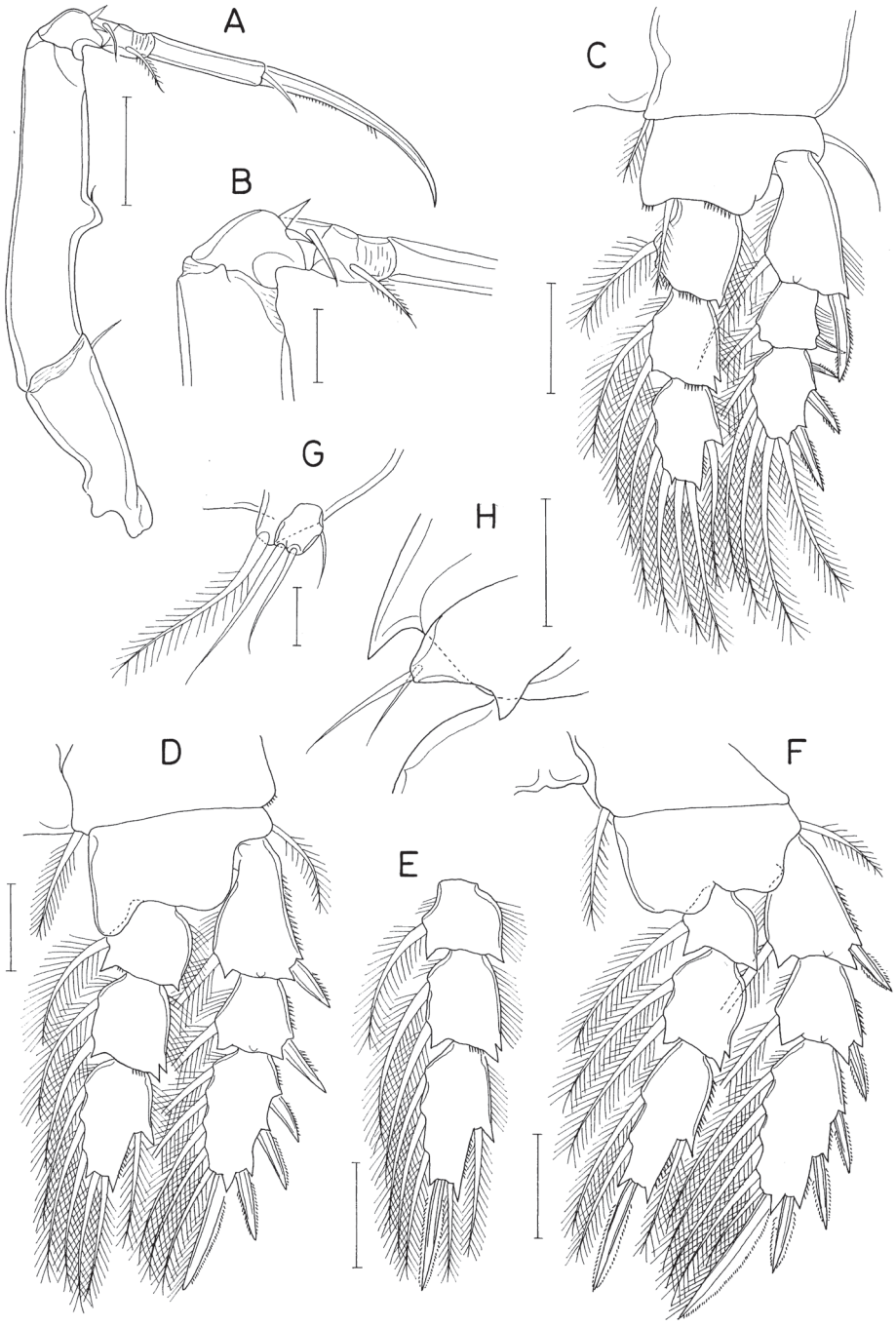

Figure 29. *Thermocheres pacificus* sp. nov., male **A** maxilliped **B** endopodal region of maxilliped **C** leg 1 **D** leg 2 **E** endopod of leg 3 **F** leg 4 **G** leg 5 **H** right genital operculum, ventral. Scale bars: 0.05 mm (**A, C–F, H**); 0.02 mm (**B, G**).

Leg 5 (Fig. 29G) consisting of pinnate lateral seta on fifth pedigerous somite and small exopod; exopodal segment 18 × 14 μm, articulated from somite, with three naked setae (two on distal margin and one on posterior margin). Leg 6 (Fig. 29H) represented by two naked setae on genital operculum.

Female. Unknown.

Etymology. The specific name of the new species refers to its discovery in the Pacific Ocean, in contrast with the Indian Ocean in which the type locality, Madagascar, of the type species is located.

Remarks. The discovery of this new species reinforces the taxonomic status of the genus *Thermocheres*. The type species of the genus, *T. validus* Kim, 2010, was described as an associate of a sponge in Madagascar (Kim 2010b). Although the new species is represented by only a single male, it exhibits diagnostic characters of the genus. In particular, the form of the maxillule in which the inner lobe is elongated and armed with three long, slender setae and the armature condition (formula III, I, 5) of the third exopodal segment of legs 2–4 are shared by the two species. Within the Asterocheridae, the latter character is shared only by *Australomyzon* Nicholls, 1944 and *Bythocheres* Humes, 1988. But *T. pacificus* sp. nov. and *T. validus* reveal two important differences, i.e., (1) one of four setae on the outer lobe of the maxillule is positioned in middle in *T. validus*, whereas all of the four setae are distally positioned in *T. pacificus* sp. nov.; and (2) the third endopodal segment of leg 4 is armed with one spine plus four setae (formula 1, 1+I, 2), but with one spine plus three setae (formula 1, I, 2) in *T. pacificus* sp. nov. These two differences are so significant that the Korean material should be separated from the type species as a new species. The proportional length of the caudal ramus and the developmental condition of the protopod of leg 5 also appear different between the two species, although these characters are subject to sexual dimorphism. *Thermocheres validus* was described on the basis of the female only.

Family Caligidae Burmeister, 1835
Genus *Caligus* Müller O.F., 1785

Caligus amblygenitalis Pillai, 1961
Figs 30–32

Caligus amblygenigtalis Pillai, 1961: 98, figs 8, 10; Ho and Lin, 2003: 56, figs 1, 2.
Caligus longipedis: Ho and Lin, 2001: 188, fig. 9 (male only).

Material examined. Two ♀♀, 5 ♂♂ (MABIK CR00250989–CR00250995), Site 7, 21 Nov. 2019; 1 ♂, Site 11, 10 Jun. 2019.

Description. Female. Body (Fig. 30A) 3.06 mm long. Cephalothoracic shield 1.66 × 1.52 mm. Lunules distinct. Thoracic zone of cephalothorax distinctly extending beyond posterior ends of lateral zones. Genital complex longer than wide (619 × 479 μm), nearly rectangular, not clearly articulated from fourth pedigerous somite.

Abdomen one-segmented, longer than wide (540 × 330 μm). Caudal ramus (Fig. 30B) 2.09 × longer than wide (167 × 80 μm), with three large and three small setae; one of small setae located on ventral surface of ramus.

Antennule (Fig. 30C) two-segmented; proximal segment 220 μm long, armed with 29 setae, two dorsal setae naked; distal segment 123 μm long, armed with 12 naked setae and two aesthetascs. Antenna (Fig. 30D) three-segmented; first segment with narrow, pointed process; second segment unarmed, with adhesion pad on anterior surface; third segment bearing curved distal claw and one small seta on convex margin. Postantennary process (Fig. 30D) bluntly tipped, with two papillae each bearing unbranched setule; another setule-bearing papilla on sternum posterior to process.

Mandible with 12 teeth on distal blade. Maxillule (Fig. 30D) comprising anterior papilla bearing three setae and bluntly tipped posterior process. Post-maxillular process (indicated by arrowhead in Fig. 30D) present postero-medial to maxillule. Maxilla (Fig. 30E) two-segmented; proximal segment unarmed; distal segment slender, bearing hyaline membrane at distal 38% region of segment and distally with short canna and long calamus; distal half of inner margin of distal segment with fine spinules. Maxilliped (Fig. 30F) slender, consisting of two segments and terminal claw; proximal segment proximally with sclerotized process; distal segment less than half length of proximal segment, unarmed; terminal claw short, proximally with one small seta. Sternal furca (Fig. 31A) with widely divergent, narrow tines.

Leg 1 (Fig. 30G) consisting of coxa, basis, two-segmented exopod and rudimentary endopod; basis with two setae (one outer and one medio-distal) and large patch of spinules on ventral surface; proximal exopodal segment with one small subdistal seta on outer margin; distal exopodal segment with three large, pinnate setae on medial margin, and four small, naked setal elements on distal margin, outer spines 1–3 each with accessory process. Leg 2 (Fig. 31B) as usual for the genus; armature formula I-1; I-1; II, I, 5 for exopod, 0-1; 0-2; 6 for endopod. Leg 3 as Fig. 31C, D. Leg 4 (Fig. 31E) consisting of protopod and two-segmented exopod; protopod with one small seta subdistally; proximal and distal segments of exopod armed with one and three spines, respectively. Leg 5 (Fig. 31F) represented by two papillae; outer and inner papillae tipped with one and two small setae, respectively.

Male. Body (Fig. 32A) 2.56 mm long. Urosome (Fig. 32B) indistinctly four-segmented. Fifth pedigerous somite (first urosomal somite) not clearly demarcated from genital complex. Genital complex rhomboidal, 424 × 323 μm. Abdomen indistinctly two-segmented; proximal somite 95 × 195 μm; distal somite 1.63 × longer than wide (273 × 168 μm). Caudal ramus (Fig. 32C) straight backwards, 2.39 × longer than wide (136 × 57 μm).

Antennule (Fig. 32D) armed as in female; proximal segment 172 μm long; distal segment elongated, 184 μm long, longer than proximal segment. Antenna (Fig. 32E) three-segmented; first segment with one corrugated pad; second segment with several corrugated pads; short third segment with one claw-like process, one leaf-like plate and one seta. Postantennary process acutely pointed, larger than that of female. Maxilliped (Fig. 32F) with blunt protrusion tipped with corrugated pad on inner margin. Sternal furca (Fig. 31G) with more slender tines than in female.

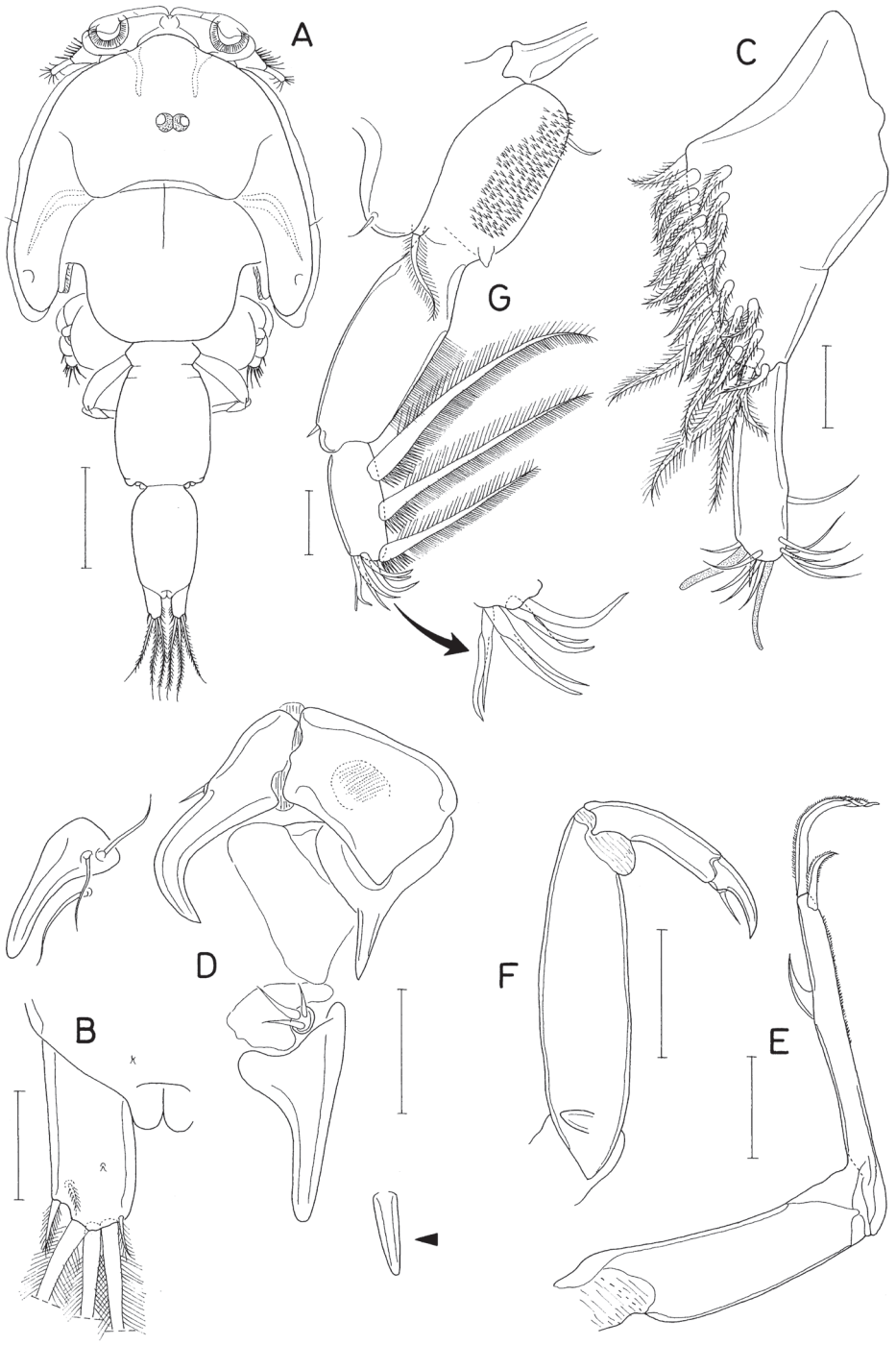

Figure 30. *Caligus amblygenitalis* Shiino, 1961, female **A** habitus, dorsal **B** caudal ramus, dorsal **C** antennule **D** antenna, postantennary process, maxillule, and post-maxillular process (indicated by arrowhead) **E** maxilla **F** maxilliped **G** leg 1. Scale bars: 0.5 mm (**A**); 0.1 mm (**B, D–F**); 0.05 mm (**C, G**).

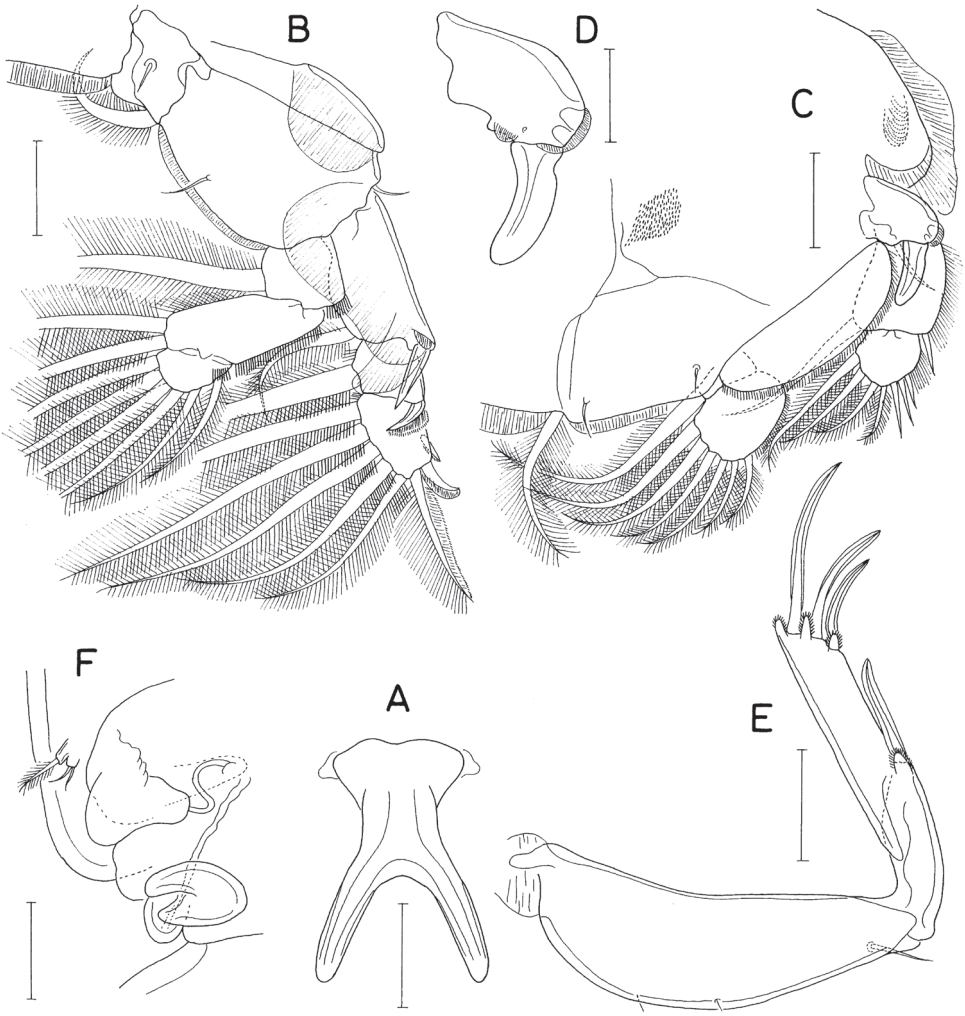

Figure 31. *Caligus amblygenitalis* Shiino, 1961, female **A** sternal furca **B** leg 2 **C** leg 3 **D** first exopodal segment of leg 3 **E** leg 4 **F** right genital area. Scale bars: 0.1 mm (**A–C, E**); 0.05 mm (**D, F**).

Leg 1 (Fig. 32H) different from that of female in absence of spinules on basis, elongate first exopodal segment, and the lack of an accessory process on outer distal spine 1 (Fig. 32I). Legs 2–4 as in female. Leg 5 (Fig. 32J) as in female. Leg 6 (Fig. 32J) represented by two small setae on genital operculum.

Remarks. *Caligus amblygenitalis* was originally described by Pillai (1961) on the basis of a single female specimen from India. Subsequently, Ho and Lin (2003) redescribed this species based on a single female from Taiwan. Previously, Ho and Lin (2001) recorded one female and one male of *C. longipedis* Bassett-Smith, 1898 from Taiwan. However, when Venmathi Maran et al. (2009) redescribed the latter

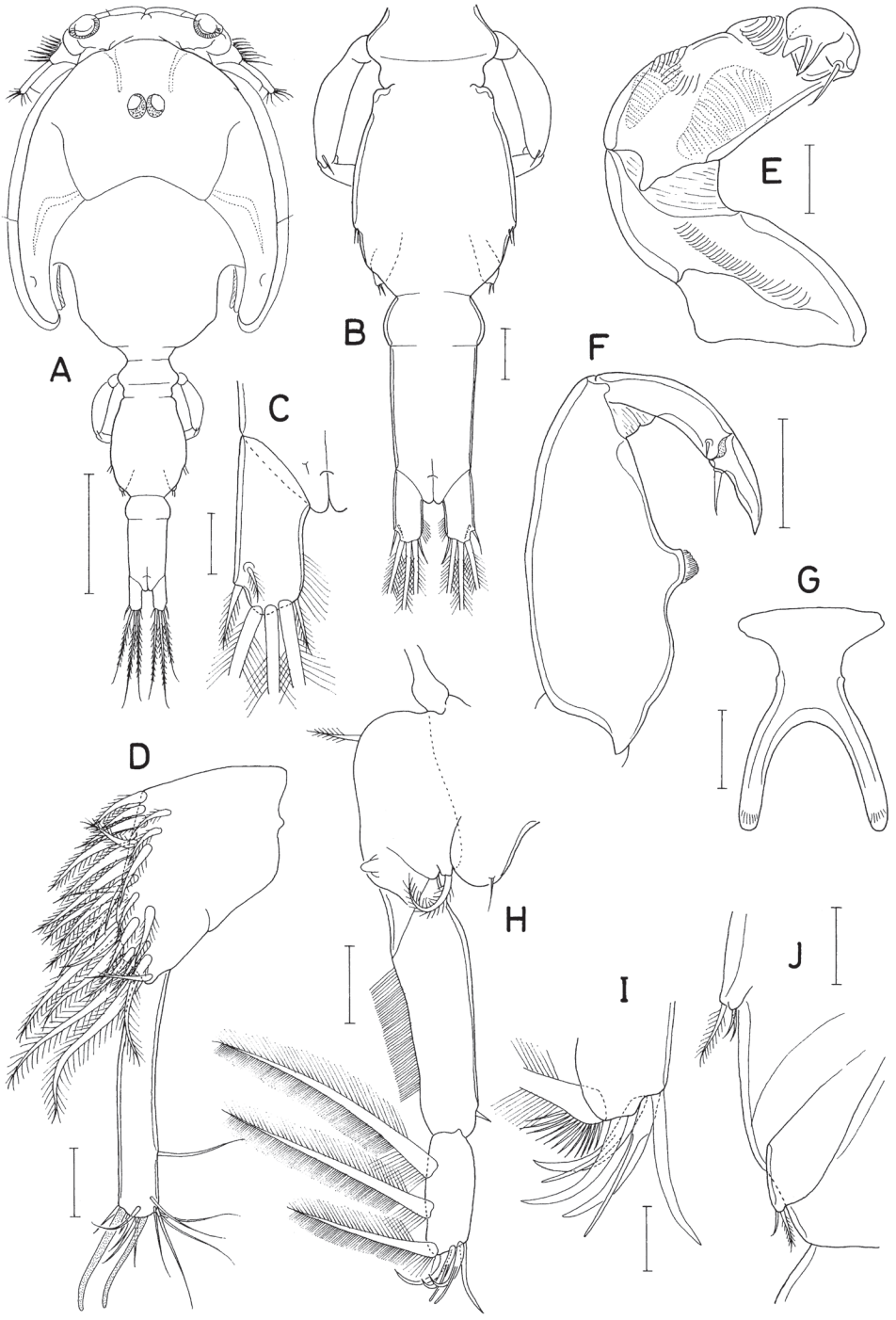

Figure 32. *Caligus amblygenitalis* Shiino, 1961, male **A** habitus, dorsal **B** urosome, dorsal **C** caudal ramus, ventral **D** antennule **E** antenna **F** maxilliped **G** sternal furca **H** leg 1 **I** distal region of leg 1 exopod **J** legs 5 and 6. Scale bars: 0.5 mm (**A**); 0.1 mm (**B, F**); 0.05 mm (**C–E, G, H, J**); 0.02 mm (**I**).

species based on females and males from Penang, Malaysia, they found that the female and the male of Ho and Lin (2001) were not conspecific. A comparison of our Korean material with the above records indicates that the male of Ho and Lin (2001) is not *C. longipedis* but *C. amblygenitalis*. Our female specimens collected by a light trap from Korea are identifiable as young adults, since they are ~ 3.0 mm long, compared to 4.14 mm long in the female of Ho and Lin (2003), and the female genital complex is immature. *Caligus amblygenitalis* is new to the Korean fauna. Both *C. amblygenitalis* and *C. longipedis* belong to the "*C. macarovi*-group" defined by Boxshall (2018).

Caligus fugu Yamaguti, 1936

Material examined. One ♀, Site 19, 04 Jun. 2020.

Remarks. This species had been placed in the genus *Pseudocaligus*, which is now synonymized with *Caligus* through a molecular analysis (Freeman et al. 2013). *Caligus fugu* is frequently found on the puffer fish *Takifugu niphobles* (Jordan & Snyder, 1901).

Caligus orientalis Gusev, 1951

Material examined. One ♀, 2 ♂♂, Site 21, 26 May 2017; 1 ♂, Site 25, 06 Jul. 2016; 1 ♂, Site 26, 06 Jul. 2016; 3 ♀♀, 3 ♂♂, Site 27, 09 Jul. 2016; 2 ♀♀, 6 ♂♂, Site 28, 07 Jul. 2016; 4 ♀♀, 1 ♂, Site 29, 09 Jul. 2016; 1 ♀, Site 30, 17 Oct. 2020.

Remarks. *Caligus orientalis* is a parasite of coastal marine and brackish-water fish in the East Asian waters. It has a wide host range and has been reported from over 20 fish species of different orders and families (Nagasawa 2004).

Caligus punctatus Shiino, 1955

Material examined. One ♂, Site 15, 04 Jul. 2020; 7 ♀♀, 12 ♂♂, Site 19, 04 Jun. 2020; 4 ♀♀, 7 ♂♂, Site 20, 06 Jun. 2020; 20 ♀♀, 5 ♂♂, Site 22, 31 May 2021.

Remarks. This caligid is common on the gobiid fishes living in brackish-waters in Korea. Kim (1993) studied post-embryonic developmental stages of this species.

Caligus triangularis Shiino, 1954

Material examined. Two ♀♀, 1 ♂, Site 10, 13 Oct. 2015.

Remarks. The genital complex of the female of this caligid is characteristically triangular. The only known host of this copepod was *Halichoeres poecilopterus* (Richardson,

1846) which has been treated as a junior synonym of *Parajulis poecilepterus* (Temminck & Schlegel, 1845).

Caligus undulatus Shen & Li, 1959

Fig. 33

Material examined. Four ♀♀, 1 ♂, Site 11, 16 Apr. 2014; 1 ♀, 1 ♂, Site 20, 05 Jun. 2020; 1 ♀, Site 26, 06 Jul. 2016; 1 ♀, 2 ♂♂, Site 31, 15 Nov. 2020.

Other material from fish host. 1 ♀ and 1 chalimus from the skin of the fish *Konosirus punctatus* (Temminck & Schlegel, 1846), at a market at Gonam, Hadong, south coast (34°59'47"N, 126°48'37"E), 25 Jul. 2012, leg. I.-H. Kim.

Supplementary description of female. Body (Fig. 33A) narrow. Body length 3.92 mm. Cephalothoracic shield distinctly longer than wide (1.76 × 1.36 mm); thoracic zone extending beyond posterior tips of lateral zones. Urosome longer than cephalothoracic shield. Genital complex nearly fusiform, ~ 1.4 × longer than wide (1.07 × 0.77 mm), incompletely articulated from fourth pedigerous somite, truncate posteriorly. Abdomen 0.61 × 0.26 mm, unsegmented, elongate, not articulated from genital complex, with wrinkled cuticle at proximal region. Caudal rami (Fig. 33B) slightly convergent, 2.50 × longer than wide (195 × 78 μm), armed with three large and three small setae; one of small setae positioned ventrally.

Sternal furca (Fig. 33C) narrow; tines gradually narrowed distally, with blunt apex. Distal exopodal segment of leg 1 (Fig. 33D) with three large, pinnate setae on inner margin and four distal armature elements comprising, from outer to inner, claw-like spine 1, smaller claw-like spine 2 bearing accessory process, transparent, aesthetasc-like seta, and long, naked seta. Leg 4 (Fig. 33E) consisting of protopod and two-segmented endopod; protopod with one small seta distally; proximal exopodal segment armed with one spine of 114 μm long; distal exopodal segment armed with four spines of 64, 62, 75, and 101 μm long, respectively, from proximal to distal.

Description. Male. Body (Fig. 33F) smaller than that of female, 3.30 mm long. Cephalic shield 1.75 × 1.24 mm. Genital complex longer than wide. Abdomen two-segmented; proximal and distal abdominal somites 310 × 250 μm and 360 × 185 μm, respectively. Caudal ramus 2.57 × longer than wide (185 × 72 μm).

Remarks. *Caligus undulatus* is distributed in tropical and warm waters of the world, and has been frequently found from plankton samples. Moon and Park (2019) also recorded its occurrence in plankton samples from Korea. Ohtsuka et al. (2020) recorded the fish *Sardinella zunasi* (Bleeker, 1854) as a host of *C. undulatus*, which was the first host record. In the present study, we report *Konosirus punctatus* as an additional host record. The fish hosts *S. zunasi* and *K. punctatus* live on East Asian coasts, sometimes entering bays or brackish waters. It is conceivable that *C. undulatus* and other caligids may detach from the hosts due to the salinity change when the hosts approach brackish waters.

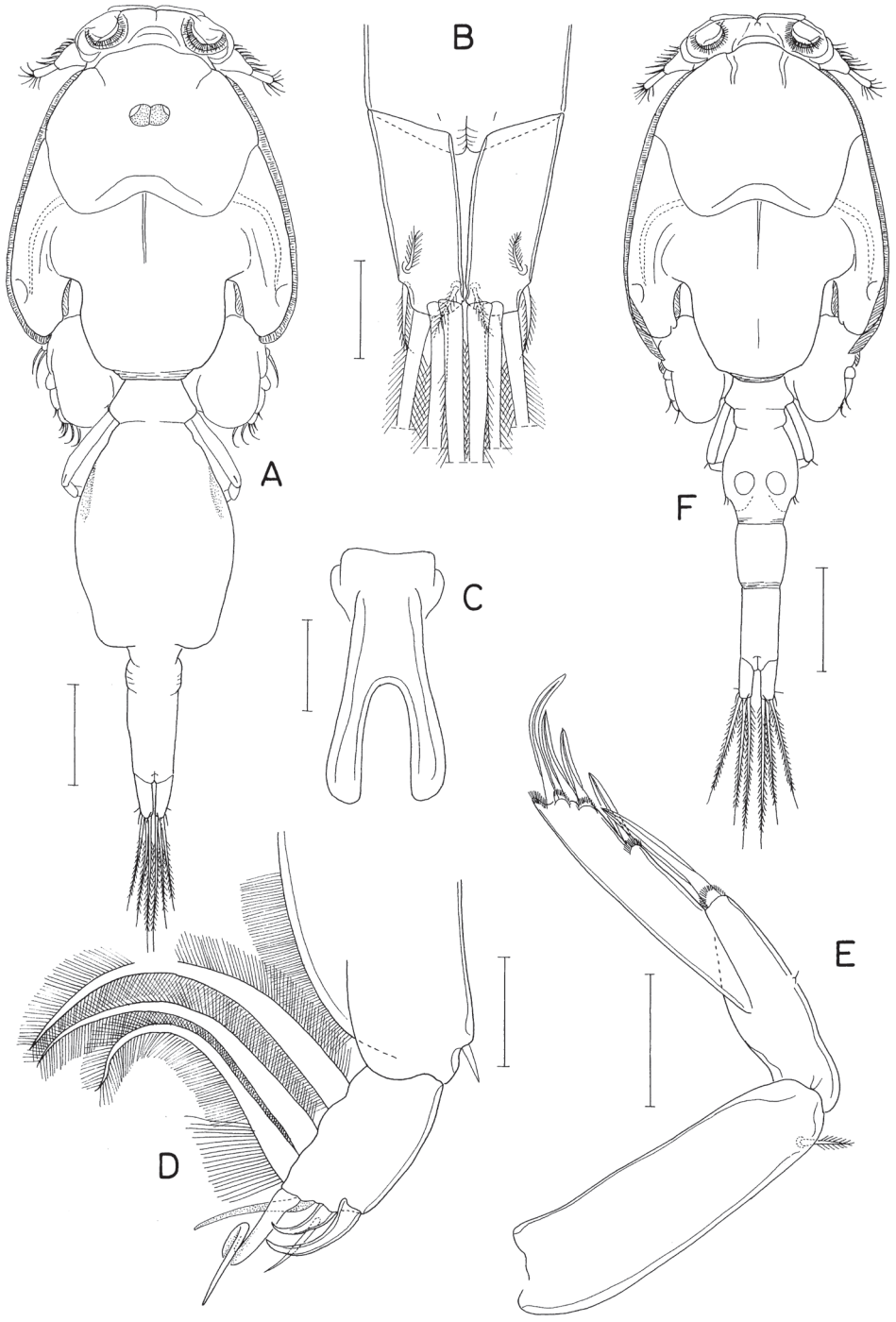

Figure 33. *Caligus undulatus* Shen & Li, 1959 Female **A** habitus, dorsal **B** caudal rami, dorsal **C** sternal furca **D** distal exopodal segment of leg 1 **E** leg 4. Male **F** habitus, dorsal. Scale bars: 0.5 mm (**A, F**); 0.1 mm (**B, C, F**); 0.05 mm (**D**).

A female specimen from Site 11 exhibited a shrunken genital complex with undulated lateral margins as observed in the type material of Shen and Li (1959). This form of the genital complex may occur immediately after oviposition.

Acknowledgements

We thank Dr. Jong Guk Kim of the Korea Institute of Ocean Science & Technology (KIOST) for his assistance in collecting samples. This research was supported by the National Marine Biodiversity Institute of Korea (2022M01100) and by the research program of KIOST (Contract No. PEA0016). We thank Prof. G. A. Boxshall and Prof. S. Ohtsuka for their critical comments on the manuscript.

References

Avdeev GV (1987) Two new copepod species (Sabelliphilidae, Poecilostomatoida) from bivalvian molluscs in the Peter the Great Bay of the Japan Sea. Zoologicheskoy Zhurnal 66(4): 608–613.

Bocquet C, Stock JH, Bernard F (1959) Copépodes parasites d'invertébrés des côtes de France. IX. Description d'une nouvelle espece remarquable de Lichomolgidae. *Heteranthessius scotti* n. sp. (Cyclopoida). Proceedings of the Koninklijke Nederlande Akademie van Wetenschappen series c 62(2): 111–118.

Bocquet C, Stock JH, Kleeton G (1963) Copépodes parasites d'invertébrés des côtes de la Manche. X. Cyclopoïdes Poecilostomes associés aux Annélides Polychètes, dans la région de Roscoff. Archives de Zoologie Expérimentale et Générale 102(notes et revue 1): 20–40.

Boxshall G (2018) The sea lice (Copepoda: Caligidae) of Moreton Bay (Queensland, Australia), with descriptions of thirteen new species. Zootaxa 4398(1): 1–172. https://doi.org/10.11646/zootaxa.4398.1.1

Boxshall GA, Halsey SH (2004) An Introduction to Copepod Diversity. The Ray Society, London, 966 pp.

Chan BKK, Shao K-T, Chang Y-W (2016) A simplified, economical, and robust light trap for capturing benthic and pelagic zooplankton. Journal of Experimental Marine Biology and Ecology 482: 25–32. https://doi.org/10.1016/j.jembe.2016.04.003

Chang CY (2012) First record of monstrilloid copepods in Korea: Description of a new species of the genus *Cymbasoma* (Monstrilloida, Monstrillidae). Animal Systematics, Evolution and Diversity 28(2): 126–132. https://doi.org/10.5635/ASED.2012.28.2.126

Chang CY (2014) Two new records of monstrilloid copepods (Crustacea) from Korea. Animal Systematics, Evolution and Diversity 30(3): 206–214. https://doi.org/10.5635/ASED.2014.30.3.206

Chang CY, Song SJ (1995) Marine harpacticoid copepods of genus *Eudactylopus* (Harpacticoida, Thalestridae) in Korea. Animal Systematics, Evolution and Diversity 11(3): 379–388.

Cho DH, Wi JH, Suh H-L (2018) A new species of *Eudactylopus* (Copepoda: Harpacticoida) from the south coast of Korea based on morphological and molecular evidence. Animal Systematics, Evolution and Diversity 34(3): 127–142. https://doi.org/10.5635/ASED.2018.34.3.127

Costanzo G, Brugnano C, Zagami G (2013) A new species of *Eupolymniphilus* (Copepoda: Cyclopoida: Sabelliphilidae) from an anchialine cave of the Mediterranean Sea with a key to the seven species of the genus. Vie et Milieu- Life and Environment 63(2): 75–80.

Do TT, Kajihara T (1984) Two poecilostomatoid copepods, *Anthessius graciliunguis* n. sp. and *Modiolicola bifidus* Tanaka, 1961 from the blue mussel, *Mytilus edulis galloprovincialis* Lamarck, in Japan. Fish Pathology 19(1): 5–15. https://doi.org/10.3147/jsfp.19.5

Eiselt VJ (1969) Revision von *Acontiophorus antennatus* Hansen 1923 und materialien zur variabilität von Acontiophorus armatus Brady 1880 (Cyclop. Siph., Copepoda, Crust.). Sitzungsberichten der Österreichischen Akademie der Wissenschaften. Mathematisch-Naturwissenschaftliche Klasse 177(8–10): 177–185.

Freeman MA, Anshary H, Ogawa K (2013) Multiple gene analyses of caligid copepods indicate that the reduction of a thoracic appendage in *Pseudocaligus* represents convergent evolution. Parasites & Vectors 6(1): 1–9. https://doi.org/10.1186/1756-3305-6-336

Hernandez FJ, Shaw RF (2003) Comparison of plankton net and light trap methodologies for sampling larval and juvenile fishes at offshore petroleum platforms and a coastal jetty off Louisiana. American Fisheries Society Symposium 36: 15–38.

Ho J-S, Kim I-H (1997) A new family of poecilostomatoid copepods (Polyankyliidae) from a tide pool on mud flat in Korea. Korean Journal of Biological Sciences 1: 429–434.

Ho J-S, Kim I-H (2003) New clausiid copepods (Poecilostomatoida) associated with polychaetes of Korea, with cladistic analysis of the family Clausiidae. Journal of Crustacean Biology 23(3): 568–581. https://doi.org/10.1651/C-2370

Ho J-S, Lin C-L (2001) Sea lice (Copepoda, Caligidae) parasitic on carangid fishes of Taiwan. Taiwan Shuichanxue Hui Kan 28(3): 177–201.

Ho J-S, Lin C-L (2003) Three species of *Caligus* (Copepoda: Caligidae) parasitic on fishes of the northeast coast of Taiwan. Taiwan Shuichanxue Hui Kan 30(1): 55–70.

Holmes JMC (1985) *Anchistrotos lucipetus* sp. nov. (Copepoda, Taeniacanthidae), a parasitic copepod From Lough Ine, South West Ireland. Crustaceana 48(1): 18–25. https://doi.org/10.1163/156854085X00684

Hong J-S, Kim I-H (2021) Copepods of the family Kelleriidae from tropical waters (Crustacea, Copepoda, Cyclopoida). Journal of Species Research 10(4): 364–386. https://doi.org/10.12651/JSR.2021.10.4.364

Humes AG (1986) *Myicola metisiensis* (Copepoda: Poecilostomatoida), a parasite of the bivalve *Mya arenaria* in eastern Canada, redefinition of the Myicolidae, and diagnosis of the Anthessiidae n. fam. Canadian Journal of Zoology 64(4): 1021–1033. https://doi.org/10.1139/z86-152

Jeon D, Lee W, Suh HY (2018) A new genus and two new species of monstrilloid copepods (Copepoda: Monstrillidae): integrating morphological, molecular phylogenetic, and ecological evidence. Journal of Crustacean Biology 38(1): 45–65. https://doi.org/10.1093/jcbiol/rux095

Jeon D, Lee W, Soh HY (2019) New species of *Caromiobenella* Jeon, Lee & Soh, 2018 (Crustacea, Copepoda, Monstrilloida) from Chuja Island, Korea. ZooKeys 814: 33–51. https://doi.org/10.3897/zookeys.814.29126

Karanovic T (2008) Marine interstitial Poecilostomatoida and Cyclopoida (Copepoda) of Australia. Crustaceana Monographs 9. Brill, Leiden, 331 pp. https://doi.org/10.1163/ej.9789004164598.i-332

Kim I-H (1993) Developmental stages of *Caligus punctatus* Shiino, 1955 (Copepoda: Caligidae). In: Boxshall GA, Defaye D (Eds) Pathogens of Wild and Farmed Fish: Sea Lice. Ellis Horwood, New York, etc., 16–29.

Kim I-H (1998) Illustrated Encyclopedia of Fauna & Flora of Korea. Vol. 38. Cirripedia, Symbiotic Copepoda, Pycnogonida. Ministry of Education, Korea, 1038 pp.

Kim I-H (2003) Copepodid stages of *Critomolgus anthopleurus* (Copepoda, Poecilostomatoida, Rhynchomolgidae). Journal of Crustacean Biology 23(3): 558–567. https://doi.org/10.1651/C-2375

Kim I-H (2004) Copepods associated with bivalves in Korea and their distribution. Zoological Studies 43(2): 187–192.

Kim I-H (2009) Poecilostome copepods (Crustacea: Cyclopoida) associated with marine invertebrates from tropical waters. Korean Journal of Systematic Zoology 7(Special Issue): 1–90.

Kim I-H (2010a) Invertebrate fauna of Korea, Vol. 21, No. 5. Symbiotic copepods. Flora and Fauna of Korea, National Institute of Biological Resources, Ministry of Environment, Korea, 222 pp.

Kim I-H (2010b) Siphonostomatoid Copepoda (Crustacea) associated with invertebrates from tropical waters. Korean Journal of Systematic Zoology 8(Special Issue): 1–176.

Kim I-H (2014) Six new species of Copepoda (Clausiidae, Pseudanthessiidae, Polyankyliidae) associated with polychaetes from Korea. Journal of Species Research 3(2): 95–122. https://doi.org/10.12651/JSR.2014.3.2.095

Kim I-H, Hong J-S (2014) Copepods (Crustacea, Copepoda, Cyclopoida) associated with marine invertebrates from Thailand. Animal Systematics, Evolution and Diversity 30(4): 274–318. https://doi.org/10.5635/ASED.2014.30.4.274

Kim I-H, Sato SI (2010) A review of copepods associated with bivalves in Japan, with description of two new species (Crustacea, Copepoda, Cyclopoida). Bulletin of the Tohoku University Museum 9: 1–22.

Kim I-H, Stock JH (1996) A new species of Clausidiidae (Copepoda, Poecilostomatoida) associated with the bivalve *Ruditapes philippinarum* in Korea. Cahiers de Biologie Marine 37(1): 1–6.

Lee J, Chang CY (2016) A new species of *Monstrilla* Dana, 1849 (Copepoda: Monstrilloida: Monstrillidae) from Korea, including a key to species from the north-west Pacific. Zootaxa 4174(1): 396–409. https://doi.org/10.11646/zootaxa.4174.1.24

Lee J, Kim D, Chang CY (2016) Two new species of the genus *Monstrillopsis* Sars, 1921 (Copepoda: Monstrilloida: Monstrillidae) from South Korea. Zootaxa 4174(1): 410–423. https://doi.org/10.11646/zootaxa.4174.1.25

López-González PJ, Conradi M (1995) *Heteranthessius hoi*, a new species (Copepoda: Pseudanthessiidae) from a sea-anemone in the Straits of Gibraltar, with remarks on the genus. Proceedings of the Biological Society of Washington 108(1): 107–116.

McLeod LE, Costello MJ (2017) Light traps for sampling marine biodiversity. Helgoland Marine Research 71(1): e2. https://doi.org/10.1186/s10152-017-0483-1

Moon SY, Kim I-H (2010) Three new species of *Hemicyclops* (Copepoda, Cyclopoida, Clausidiidae) from Korea. Korean Journal of Systematic Zoology 26(3): 279–293. https://doi.org/10.5635/KJSZ.2010.26.3.279

Moon SY, Park JS (2019) Occurrence of sea lice, *Caligus undulatus* Shen and Li, 1959 (Copepoda: Siphonostomatoida: Caligidae) in plankton samples collected from Korea. Journal of Species Research 8(4): 365–372. https://doi.org/10.12651/JSR.2019.8.4.36

Nagasawa K (2004) Sea lice, *Lepeophtheirus salmonis* and *Caligus orientalis* (Copepoda: Caligidae), of wild and farmed fish in sea and brackish waters of Japan and adjacent regions: a review. Zoological Studies 43(2): 173–178.

Nicholls AG (1944) Littoral Copepoda from South Australia (II) Calanoida, Cyclopoida, Notodelphyoida, Monstrilloida and Caligoida. Records of the South Australian Museum 8: 1–62.

Ohtsuka S, Nawata M, Nishida Y, Nitta M, Hirano K, Adachi K, Kondo Y, Venmathi Maran BA, Suárez-Morales E (2020) Discovery of the fish host of the 'planktonic' caligid *Caligus undulatus* Shen & Li, 1959 (Crustacea: Copepoda: Siphonostomatoida). Biodiversity Data Journal 8: e52271. https://doi.org/10.3897/BDJ.8.e52271

Øresland V (2007) Description of the IMR standard light trap and the vertical distribution of some decapod larvae (Homarus and Nephrops). Western Indian Ocean Journal of Marine Science 6(2): 225–231. https://doi.org/10.4314/wiojms.v6i2.48249

Pillai NK (1961) Copepods parasitic on South Indian fishes. Part. 1, Caligidae. Bulletin of the Research Institute. University of Kerala 8: 87–130.

Porter SS, Eckert GL, Byron CJ, Fosher JL (2008) Comparison of light traps and plankton tows for sampling brachyuran crab larvae in an Alaskan Fjord. Journal of Crustacean Biology 28(1): 175–179. https://doi.org/10.1651/06-2818R.1

Sars GO (1915) Copepoda Cyclopoida. Parts IX & X. Ascomyzontidae (concluded), Acontiophoridae, Myzopontiidae, Dyspontiidae, Artotrogidae, Cancerillidae. An account of the Crustacea of Norway with short descriptions and figures of all the species. Bergen Museum, Bergen 6: 105–140.

Sars GO (1918) Copepoda Cyclopoida. Parts XIII & XIV. Lichomolgidae (concluded), Oncaeidae, Corycaeidae, Ergasilidae, Clausiidae, Eunicicolidae, Supplement. An account of the Crustacea of Norway with short descriptions and figures of all the species. Bergen Museum, Bergen 6: 172–225.

Scott T (1903) On some new and rare Crustacea collected at various times in connection with the investigations of the Fisheries board for Scotland. Twenty-first Annual Report of the Fishery Board for Scotland 21(3): 109–135.

Shen CJ, Li HL (1959) Parasitic copepods from fishes of China, IV. Caligoida. Caligidae (3). Acta Zoological Sinica 11(1): 12–23.

Sigurdsson GM, Morse B, Rochette R (2014) Light traps as a tool to sample pelagic larvae of American lobster (*Homarus americanus*). Journal of Crustacean Biology 34(2): 182–188. https://doi.org/10.1163/1937240X-00002219

Stock JH (1954) Redescription de *Tococheres cylindraceus* Pelseneer, 1929, copépode commensal de Loripes lacteus. Beaufortia 4(38): 73–80.

Stock JH (1971) Découverte du genre Heteranthessius (Copepoda) on Méditerranée: *H. furcatus* n. sp. Bulletin de la Société Zoologique de France 95: 335–340.

Stock JH, Humes AG, Gooding RU (1964) Copepoda associated with West Indian invertebrates. IV. The genera *Octopicola*, *Pseudanthessius* and *Meomicola* (Cyclopoida, Lichomolgidae). Studies on the Fauna of Curaçao 18(77): 1–74.

Ueda H, Nagai H, Hibino M, Tanaka M (2006) Redescription of a symbiotic poecilostomatoid copepod *Anthessius graciliunguis* Do & Kajihara from plankton: The second record of the species and first record of the male. Plankton & Benthos Research 1(2): 102–108. https://doi.org/10.3800/pbr.1.102

Venmathi Maran BA, Seng, Ohtsuka S, Nagasawa K (2009) Records of *Caligus* (Crustacea: Copepoda: Caligidae) from marine fish cultured in floating cages in Malaysia with a redescription of the male of *Caligus longipedis* Bassett-Smith, 1898. Zoological Studies 48(6): 797–807.

WoRMS Editorial Board (2021) World Register of Marine Species. http://www.marinespecies.org [accessed 1 November 2021]

ZooKeys 1115: 73–79 (2022)
doi: 10.3897/zookeys.1115.81668
https://zookeys.pensoft.net

RESEARCH ARTICLE

A peer-reviewed open-access journal
ZooKeys
Launched to accelerate biodiversity research

First record of *Lepidiella* Enderlein, 1937 from the Oriental Region (Diptera, Psychodidae)

Santiago Jaume-Schinkel[1], Gunnar Mikalsen Kvifte[2]

1 *Zoologisches Forschungsmuseum Alexander Koenig, Leibniz-Institut zur Analyse des Biodiversitätswandels, Adenauerallee 160, D-53113 Bonn, Germany* **2** *Department of Biosciences and Aquaculture, Nord University, P.O. Box 2501, 7729 Steinkjer, Norway*

Corresponding author: Gunnar Mikalsen Kvifte (gunnar.mikalsen-kvifte@nord.no)

Academic editor: Kurt Jordaens | Received 3 February 2022 | Accepted 31 May 2022 | Published 29 July 2022

https://zoobank.org/24276D5B-8B19-4E24-BB77-C55B1D2BF6F7

Citation: Jaume-Schinkel S, Kvifte GM (2022) First record of *Lepidiella* Enderlein, 1937 from the Oriental Region (Diptera, Psychodidae). ZooKeys 1115: 73–79. https://doi.org/10.3897/zookeys.1115.81668

Abstract

We provide the first record of the genus *Lepidiella* Enderlein, 1937 from the Oriental Region with the description of *Lepidiella limicornis* **sp. nov.**, based on two male specimens collected in Thailand. Additionally, we provide a list of the world species of *Lepidiella* and discuss the diagnosis and taxonomic placement of the genus.

Keywords

Moth flies, new record, new species, Psychodinae, taxonomy

Introduction

The moth fly fauna of the Oriental Region is highly diverse and understudied, with the family Psychodidae including more than 420 described species (Lewis 1987; Ježek 2010; Curler and Priyadarsanan 2015; Ježek et al. 2015; Kvifte and Andersen 2016; Polseela et al. 2019). Regardless of the recent attention this family has received due to the medical importance of the subfamily Phlebotominae, there is still a large number of species that remain undescribed (Duckhouse and Duckhouse 2000; Curler 2009; Ježek 2010).

The genus *Lepidiella* Enderlein, 1937, formerly known as *Syntomoza* Enderlein, 1937 (see Quate, 1963; Collantes and Hodkinson 2003) has been thought to be restricted to the Neotropical Region. This genus has been recorded in Brazil, Bolivia, Colombia, Costa Rica, Mexico, Nicaragua, Panama, Peru, and the island of Santa Lucia in the Caribbean (Ibáñez-Bernal 2008; Bravo and Santos 2011; Araújo and Bravo 2013, 2019).

Here, we describe a new species of the genus *Lepidiella* and discuss its generic placement. Additionally, we record *Lepidiella* for the first time outside the Neotropical Region, and we update the generic diagnosis of this genus.

Materials and methods

The studied specimens are deposited at the Department of Natural History, University Museum of Bergen, Bergen, Norway (**ZMBN**). Specimens were collected with a hand net, stored in ethanol, and then mounted on permanent slides. In the material examined section, at the end of each record and between square brackets ([ ]), the holding institution is indicated. In the description of type labels, the contents of each label are enclosed in double quotation marks (“ ”), italics denote handwriting, and the individual lines of data are separated by a double forward-slash (//).

Measurements were made with an ocular micrometer in a microscope Leitz model Dialux 20, measures in millimeters (mm). Head width was taken at the widest part, approximately above the insertion of antennal scape, whereas the length was taken from the vertex to the lower margin of clypeus; wing length measured from the base of the wing at the start of the costal node to the apex of the wingtip, while the width was taken approximately at an imaginary vertical line crossing the radial and medial forks; palpal proportions consider the length of the first palpal segment as a unit (1.0).

Terminology

We follow the general terminology proposed by Cumming and Wood (2017). For the male genitalia, we follow the term of hypopods instead of cerci or surstyli proposed by Kvifte and Wagner (2017) as the origin of these caudal appendages seems to have combined origins of the proctiger and epandrium.

Results

Genus *Lepidiella* Enderlein, 1937

Lepidiella Enderlein 1937: 89. Type species: *Lepidiella lanuginosa* Enderlein 1937: 89–90, by monotypy and original designation.

Syntomoza Enderlein 1937: 88–89. Type species: S*yntomoza niveitarsis* Enderlein 1937: 89, by monotypy and original designation.

Kupara Rapp 1945: 310. Type species: *Kupara albipeda* Rapp 1945: 311, by monotypy and original designation (Bravo and Santos 2011; Collantes and Hodkinson 2003).

Diagnosis. Males and females with vertex dorsally expanded; males with or without corniculi, females without corniculi; males and females with 4 rows of facets on eye bridge, antennae with 14 barrel-shaped flagellomeres, flagellomeres 1–11 with a pair of simple digitate ascoids, flagellomeres 12–14 reduced in size and without ascoids; wing vein R_4 ending slightly before or at the wing apex; males with multiple apical tenacula on hypopods.

Species included. *Lepidiella albipeda* (Rapp, 1945), *L. amaliae* (Collantes & Martínez-Ortega, 1997), *L. cervi* (Satchell, 1955), *L. flabellata* Bravo & Santos, 2011, *L. hansoni* (Quate, 1996), *L. lanuginosa* Enderlein, 1937, *L. larryi* Ibáñez-Bernal, 2010, *L. limicornis* sp. nov., *L. maculosa* Araújo & Bravo, 2019, *L. matagalpensis* (Collantes & Martínez-Ortega, 1988), *L. monteveredica* (Quate, 1996), *L. niveitarsis* (Enderlein, 1937), *L. olgae* Bravo & Araújo, 2013, *L. pickeringi* (Quate, 1999), *L. robusta* Bravo & Santos, 2011, *L. spinosa* Bravo, 2005, *L. wagneri* Araújo & Bravo, 2019, *L. zumbadoi* (Quate, 1999).

Lepidiella limicornis sp. nov.

https://zoobank.org/067E7A52-E761-4849-B781-C52EAF35BACE
Figs 1–5

Examined material. ***Holotype***, ♂, slide mounted, . "*Lepidiella limicornis #m* // *HOLOTYPE* // Thailand: Chiang Mai, // Doi Pui Mong village, // waterfall/pond, // 18.8163°N, 98.8831°E // 9.IV.1991, (hand net) // J. Kjaerandsen leg. // **ZMBN #:**", [ZMBN], paratype, ♂, slide mounted, same label information [ZMBN].

Differential diagnosis. This species can be easily differentiated from all the species in *Lepidiella* by the combination of the following characters: eyes separated by 4 facet diameters, interocular suture as inverted U, second flagellomere asymmetrical, and hypopods with four tenacula.

Type locality. Thailand, Chiang Mai, Doi Pui Mong village (18.8163°N, 98.8831°E).

Description. Measurements in mm (n = 2). Wing length 1.81, width 0.68; head length 0.45, width 0.34; Antennal segments, scape: 0.19, pedicel: 0.07, flagellomere 1: 0.08, flagellomere 2: 0.08, flagellomeres 3–9: 0.06; Palpomeres 1: 0.08, 2: 0.12, 3: 0.12, 4: 0.16.

Male. ***Holotype. Head*** 2 × longer than wide, with a pair of 3-branched cornicula, eyes separated by approximately 4 facet diameters; eye bridge with four facet rows; interocular suture as an inverted U, extending towards middle of vertex, a little longer than eye bridge width. Antenna with scape about 4× longer than its width, about 3× length of pedicel, cylindrical, tapered at base, and broadening at apex; first flagellomere cylindrical, symmetrical, about ½ width of scape, second flagellomere asymmetrical with a protuberance on inner margin, subsequent flagellomeres symmetrical, cylindrical, about ½ width of first and second flagellomeres. Total number of flagellomeres unknown as apical flagellomeres are missing in examined specimens; maximum number of flagellomeres = 7. Palps extending to flagellomere 6, palpal proportions, 1.0:1.5:1.5:2.

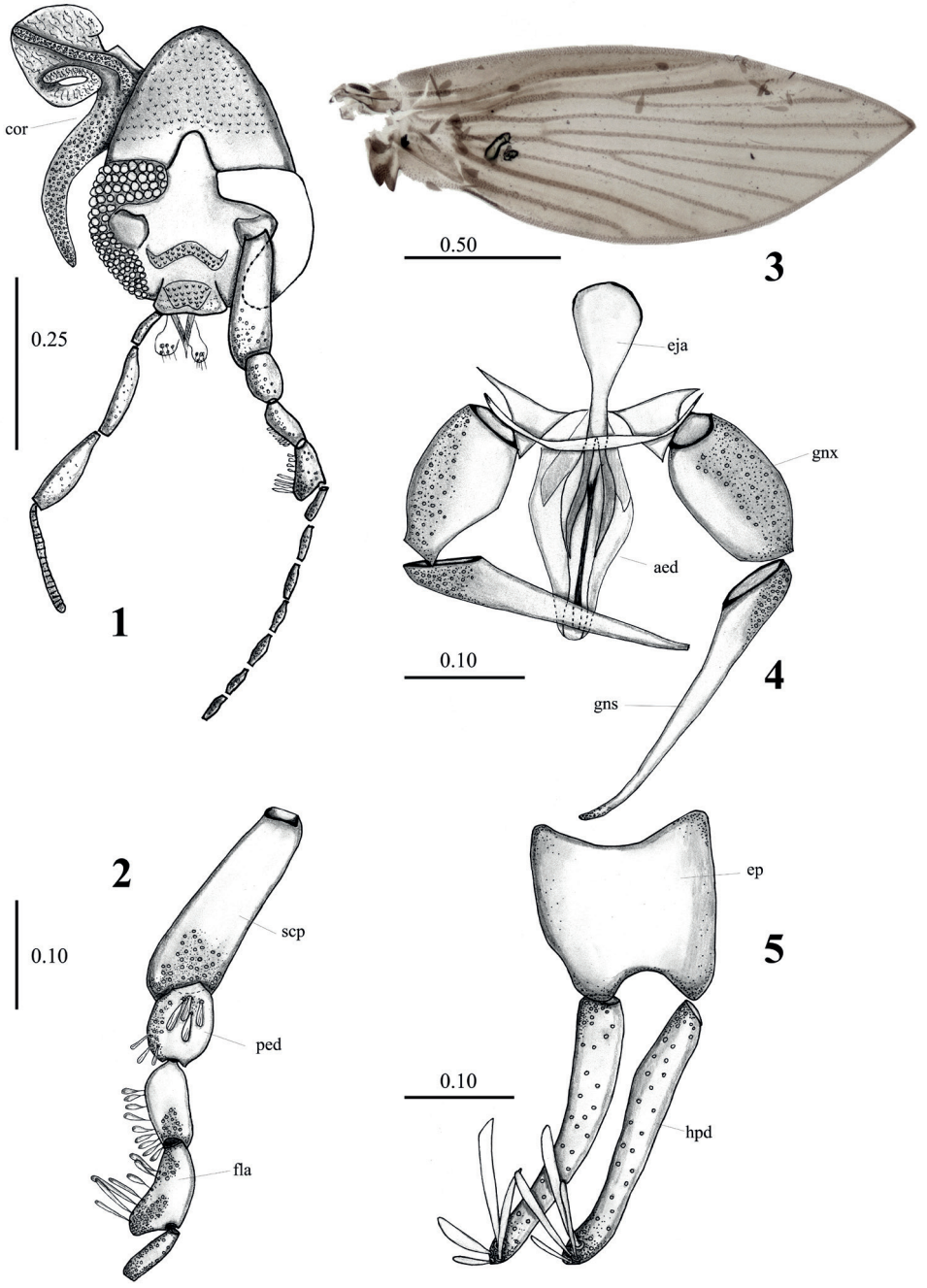

Figures 1–5. *Lepidiella limicornis* sp. nov., male holotype. **1** head **2** first antennal segments **3** wing **4** hypandrium, gonocoxites, gonostyli, aedeagus **5** epandrium and surstyli. Abbreviations: aed = aedeagus, cor = corniculi, eja = ejaculatory apodeme, ep = epandrium, fla = flagellomere, gns = gonostylus, gnx = gonocoxites, scp = scape, hpd = hypopod. Scale bars in millimeters.

Wing 2.7 × longer than wide, hyaline except costal cell which is brownish; Sc not reaching C but extending to junction of R_{2+3}+R_5; R_4 ending at wing apex, CuA reaching wing margin.

***Terminalia*.** Hypandrium narrow, with rounded margin, seems partially fused with gonocoxites; length of gonocoxites 0.60 length of gonostyli, about 2× longer than wide; gonostyli narrow, tapered towards apex, with alveoli in outer basal ⅓; gonocoxal apodemes triangular, medial extension connected to base of aedeagus; aedeagus symmetrical, bifurcated; paramere narrow, well sclerotized; ejaculatory apodeme dorsoventrally flattened, rounded at anterior margin and tapering towards aedeagus; epandrium about same length and width; basal margin concave around entire length, apical margin strongly concave at middle; hypopods about 1.75× length of gonocoxites, narrow with apical margin rounded; 4 apical tenacula on each; tenacula apex rounded, concave; epiproct triangular with apical margin rounded, covered in micropilosity.

Female. Unknown.

Etymology. From Latin *līmus* = oblique + *cornus* = horns, making references to the oblique shape of the fourth antennal segment (second flagellomere).

Distribution. Only known from the type locality.

Discussion

Quate (1996) recognized three diagnostic characters for the genus (as *Syntomoza*): corniculi present in males; males and females with vertex expanded dorsally; males and females with the apex of vein R_4 ending at the wing apex. Bravo (2005) later described a new species and transferred *Pericoma hansoni* (now *Lepidiella hansoni*) without corniculi. Bravo and Santos (2011) updated the diagnosis of the genus. Finally, Araújo and Bravo (2019) described a new species without the presence of corniculi and recognized six characters for the identification of males and females, specifically: vertex dorsally expanded; antenna with 14 barrel-shaped flagellomeres; flagellomeres 12–14 smaller, without ascoids; R4 ending at the wing apex; males with multiple tenacula on hypopods (as cercus); gonocoxal apodemes fused, forming a narrow and plate-like bridge, not extending anteriorly.

Of these six characters only five fit with the species described here: gonocoxal apodemes are not fused and are extended anteriorly. The diagnosis presented above reflects this.

Corniculi are present in many genera, including *Clytocerus* Eaton, 1904, *Jungiella* Vaillant, 1972, *Panimerus* Eaton, 1913, *Pangeogladiella* Ježek, 2001, *Mystropsychoda* Duckhouse, 1975, and *Neoarisemus* Botoseneanu & Vaillant, 1970. However, this species can be easily separated from *Mystropsychoda* by the presence of an eye bridge (absent in *Mystropsychoda*); from *Neoarisemus*, *Panimerus*, and *Jungiella* by barrel-shaped flagellomeres and wing venation with R_4 ending at the apex of the wing and R_5 endsing beyond apex (flagellomeres fusiform and R_4 before and R_5 at the apex in *Neoarisemus*, *Panimerus*, and *Jungiella*). Finally, *Lepidiella* can be differentiated from *Clytocerus* by

the absence of fusion of flagellomeres 1 and 2 (fused in *Clytocerus*), the absence of tuft of curved setae on basal flagellomeres (present in *Clytocerus*), and the setae alveoli of the frons being in a large continuous patch (*Clytocerus* having two separate patches).

The characters separating *Lepidiella* from *Clytocerus* are unique characters for *Clytocerus* and probably represent apomorphies. It may, therefore, be that *Lepidiella* represents either a plesiomorphic sister group to *Clytocerus* or even is the paraphyletic ancestoral taxon to it. As *Clytocerus* generally have fused gonocoxal apodemes, while *Lepidiella* as shown here is polymorphic for this character, we deem it more likely that *Lepidiella* is paraphyletic to *Clytocerus*. However, we refrain from synonymizing the two until more unambiguous characters, including molecular ones, are available.

Acknowledgements

We are grateful to Jostein Kjærandsen for collecting the type specimen of the new species and to Trond Andersen for making it available for us to study. Per Djursvoll and Steffen Roth kindly facilitated us working together for a month at the University Museum of Bergen. SJS extends his gratitude to Morgane A. Kerdoncuf for opening her flat to him during his stay in Bergen.

References

Araújo MX, Bravo F (2013) Two new species of moth flies (Diptera, Psychodidae) from the semi-arid region of Brazil. Zootaxa 3693(1): 85–90. https://doi.org/10.11646/zootaxa.3693.1.6

Araújo MX, Bravo F (2019) Two new species of Lepidiella Enderlein, 1937 (Diptera: Psychodidae) from the Neotropical Region with taxonomic comments about the species of the genus. Zootaxa 4551(4): 487–493. https://doi.org/10.11646/zootaxa.4551.4.9

Bravo F (2005) Primeiro registro de *Lepidiella* Enderlein (Diptera, Psychodidae, Psychodinae) no Brasil e descrição de uma espécie nova. Revista Brasileira de Zoologia 22(2): 490–493. https://doi.org/10.1590/S0101-81752005000200027

Bravo F, Santos CB (2011) Two new species of *Lepidiella* (Diptera: Psychodidae: Psychodinae) from the Atlantic Rainforest of southeastern Brazil. Zoologia 28(2): 264–268. https://doi.org/10.1590/S1984-46702011000200017

Collantes F, Hodkinson ID (2003) The genus *Syntomoza*, a homonymy in Hemiptera and Diptera. A proposal of new taxonomic status and check-list of related bibliography. Boletín de la Asociación Española de Entomología 27(1–4): 231–232.

Collantes F, Martínez-Ortega E (1997) Syntomoza amaliae, a new moth-fly (Diptera, Psychodidae) from Nicaragua. Studies on Neotropical Fauna and Environment 32: 239–243. https://doi.org/10.1080/01650521.1997.11432428

Cumming JM, Wood DM (2017) 3. Adult morphology and terminology. In: Kirk-Spriggs AH, Sinclair BJ (Eds) Manual of Afrotropical Diptera. Vol. 1. Introductory chapters and keys to Diptera families. Suricata 4. SANBI Graphics & Editing, Pretoria, 89–133.

Curler GR (2009) A revision of the genus *Gondwanoscurus* Ježek (Diptera: Psychodidae). Zootaxa 2169(1): 21–34. https://doi.org/10.11646/zootaxa.2169.1.2

Curler GR, Priyadarsanan DR (2015) Descriptions of Psychodidae (Diptera) from the Western Ghats of India. Acta Entomologica Musei Nationalis Pragae 55: 473–483.

Duckhouse DA, Duckhouse SR (2000) Insecta: Diptera, Psychodidae. In: Yule CM, Yong HS (Eds) Freshwater Invertebrates of the Malaysian Region. Malaysia Academy of Sciences, Kuala Lumpur, 750–762.

Enderlein G (1937) Klassifikation der Psychodiden (Dipt.). Deutsche Entomologische Zeitschrift 1936: 81–112. https://doi.org/10.1002/mmnd.48019360301

Ibáñez-Bernal S (2008) New records and descriptions of Mexican moth flies (Diptera: Psychodidae, Psychodinae). Transactions of the American Entomological Society 134(1): 87–131. https://doi.org/10.3157/0002-8320(2008)134[87:NRADOM]2.0.CO;2

Ježek J (2010) Further new taxa of non-biting moth flies (Diptera: Psychodidae: Psychodinae) from Malaysia. Acta Entomologica Musei Nationalis Pragae 50: 235–252.

Ježek J, Wahab RA, Ševčík J (2015) Two new species of *Sycorax* (Diptera: Psychodidae: Sycoracinae) from the Oriental region. Zootaxa 4057: 539–550. https://doi.org/10.11646/zootaxa.4057.4.4

Kvifte GM, Andersen T (2016) Two new species of *Nototelmatoscopus* (*Jozifekia*), with records of three other species from Thailand (Diptera: Psychodidae). Acta Entomologica Musei Nationalis Pragae 56: 827–835.

Kvifte GM, Wagner R (2017) Review of *Neurosystasis* Satchell, with two new species from Cuba and a discussion of cerci and surstyli in Psychodinae (Diptera: Psychodidae). Zootaxa 4306(1): 81–90. https://doi.org/10.11646/zootaxa.4306.1.4

Lewis DJ (1987) Phlebotomine sandflies (Diptera: Psychodidae) of the Oriental Region. Systematic Entomology 12(2): 163–180. https://doi.org/10.1111/j.1365-3113.1987.tb00194.x

Polseela R, Wagner R, Kvifte GM, Rulik B, Apiwathnasorn C (2019) Revision of Bruchomyiinae (Diptera, Psychodidae) of the Oriental Region, with description of a new genus and species and discussion of putative male/female antagonistic coevolution. Insect Systematics & Evolution 50(1): 67–82. https://doi.org/10.1163/1876312X-00002183

Quate LW (1963) Review of G. Enderlein's non-Holarctic genera of Psychodidae and description of new species (Diptera). Transactions of the Royal Entomological Society of London 115(6): 181–196. https://doi.org/10.1111/j.1365-2311.1963.tb00818.x

Quate LW (1996) Preliminary taxonomy of Costa Rican Psychodidae (Diptera), exclusive of Phlebotominae. Revista de Biología Tropical 44(Supplement 1): 1–81.

Quate LW (1999) Taxonomy of Neotropical Psychodidae (Diptera) 3. Psychodines of Barro Colorado Island and San Blas, Panama. In: Burger JF (Ed.) Contributions to the knowledge of Diptera: a collection of articles on Diptera commemorating the life and work of Graham B. Fairchild. Memoirs on Entomology, International 14: 1–648.

Rapp WF (1945) New Psychodidae from Barro Colorado Island. Journal of the New York Entomological Society 53: 309–311.

Satchell GH (1955) Two new subgenera of Psychodidae (Diptera) from Jamaica, with descriptions of five new species. Annals and Magazine of Natural History [Series 12] 8(86): 85–93. https://doi.org/10.1080/00222935508651831

ZooKeys 1115: 81–101 (2022)
doi: 10.3897/zookeys.1115.80146
https://zookeys.pensoft.net

RESEARCH ARTICLE

A peer-reviewed open-access journal
ZooKeys
Launched to accelerate biodiversity research

Updated taxonomic keys for European Hippoboscidae (Diptera), and expansion in Central Europe of the bird louse fly *Ornithomya comosa* (Austen, 1930) with the first record from Slovakia

Jozef Oboňa[1], Katarína Fogašová[1], Miroslav Fulín[2], Stanislav Greš[3], Peter Manko[1], Jakub Repaský[4], Jindřich Roháček[5], Oldřich Sychra[6], Martin Hromada[1,7]

1 *Laboratory and Museum of Evolutionary Ecology, Department of Ecology, Faculty of Humanities and Natural Sciences, University of Prešov, 17. novembra 1, SK – 081 16 Prešov, Slovakia* **2** *Puškinova 15, SK – 083 01 Sabinov, Slovakia* **3** *17. novembra 24, SK – 083 01 Sabinov, Slovakia* **4** *Ražňany 407, SK – 082 61 Ražňany, Slovakia* **5** *Department of Entomology, Silesian Museum, Nádražní okruh 31, CZ – 746 01 Opava, Czech Republic* **6** *Department of Biology and Wildlife Diseases, Faculty of Veterinary Hygiene and Ecology, University of Veterinary Sciences Brno, Palackého tř. 1946/1, CZ – 612 42 Brno, Czech Republic* **7** *Faculty of Biological Sciences, University of Zielona Góra, PL – 65-417 ZielonaGóra, Poland*

Corresponding author: Katarína Fogašová (katarinakanasova2@gmail.com)

Academic editor: Pierfilippo Cerretti | Received 5 January 2022 | Accepted 11 July 2022 | Published 29 July 2022

https://zoobank.org/D7AE9A4C-64D7-41D6-A3EF-07F09F2DCCFD

Citation: Oboňa J, Fogašová K, Fulín M, Greš S, Manko P, Repaský J, Roháček J, Sychra O, Hromada M (2022) Updated taxonomic keys for European Hippoboscidae (Diptera), and expansion in Central Europe of the bird louse fly *Ornithomya comosa* (Austen, 1930) with the first record from Slovakia. ZooKeys 1115: 81–101. https://doi.org/10.3897/zookeys.1115.80146

Abstract

The available keys for European Hippoboscidae are outdated and do not cover all species currently known from Europe. Therefore, identification keys to the eleven genera and 31 species of the European hippoboscids are provided here. *Ornithomya comosa* (Austen, 1930) (Diptera: Hippoboscidae) is recorded for the first time from the territory of Slovakia based on one female found on a sand martin, *Riparia riparia* (Linnaeus, 1758). The list of keds and louse flies recorded from the territory of Slovakia is increased to 20 species. New host records for Slovakia are presented.

Keywords

Birds, hippoboscid, new host records, new record, parasite, Slovakia, taxonomic keys

Introduction

Keds and louse flies (Diptera: Hippoboscidae) are among the most fascinating as well as disregarded group of blood-feeding ectoparasites, and they thrive on many animal species (Bezerra-Santos and Otranto 2020). This family is included in the superfamily Hippoboscoidea, along with the families Glossinidae (tse-tse flies), Streblidae, and Nycteribiidae (bat flies) (Petersen et al. 2007; Reeves and Lloyd 2019). Hippoboscidae are divided into the subfamilies Lipopteninae (tribe Lipoptenini parasitising exclusively mammals), Ornithomyinae (tribes Olfersiini and Ornithomyini composed of species that mostly parasitise birds) and Hippoboscinae (tribe Hippoboscini with all species in Europe affecting mammals) (Reeves and Lloyd 2019). Phylogenetic studies have indicated a monophyly among Hippoboscoidea members and that the ancestor of this superfamily was a free-living insect feeding on mammal blood (Nirmala et al. 2001; Dittmar et al. 2006; Petersen et al. 2007).

Worldwide, more than 213 hippoboscid species are known (e.g., Maa 1963; Dick 2006; Rahola et al. 2011), and 31 species of Hippoboscidae have been described from Europe (Pape et al. 2015; Nartshuk et al. 2019a; Oboňa et al. 2019b).

Ornithomya comosa (Austen, 1930) (Figs 1, 2), the most recent species found in Europe (see Nartshuk et al. 2019a) and originally described from India (Pusa, Bihar), was first collected from a grey-throated martin, *Riparia chinensis* (J. E. Gray, 1830) (Austen 1930). The host overview is presented in Table 1. According to Maa (1969a, b, 1977), *O. comosa* is distributed in India, Nepal (on *R. chinensis*; Maa (1969a) used the name *Riparia paludicola chinensis*), and Thailand and Malaysia (on a barn swallow, *Hirundo rustica* Linnaeus, 1758).

Subsequently, Doszhanov (1970, 2003) recorded this species from Kazakhstan, Kyrgyzstan and West Siberia of Russia (Novosibirsk), mostly from the host *Riparia riparia* (Linnaeus, 1758), rarely from *H. rustica* and *Delichon urbicum* (Linnaeus, 1758), and also from the Eurasian scops owl, *Otus scops* (Linnaeus, 1758) of the Strigiformes. Mogi (2014) reported this species from Japan (Honshu, Kyushu and Ryukyu islands on *R. riparia* and *H. rustica* hosts). Most recently, Nartshuk et al. (2019a) recorded *O. comosa* for the first time in Europe from western Russia (Kaliningrad Province, hosts *H. rustica* and *D. urbicum*). Further Russian records are from *Cecropis daurica* (Laxmann, 1769) from Primorskii krai in the Far East (Nartshuk et al. 2019b) and from *Riparia diluta* (Sharpe & Wyatt, 1893) from Tomsk in west Siberia (Matyukhin

Table 1. The overview of hosts of *Ornithomya comosa* (Austen, 1930).

Host species	Countries	References
Cecropis daurica	Russia	Nartshuk et al. (2019b)
Delichon urbicum	Kazakhstan, Kyrgyzstan, Russia	Doszhanov (1970); Nartshuk et al. (2019a)
Hirundo rustica	Japan, Kazakhstan, Kyrgyzstan, Malaysia, Russia, Thailand,	Maa (1969a); Doszhanov (1970); Mogi (2014); Nartshuk et al. (2019a)
Otus scops	Russia	Doszhanov (2003)
Riparia diluta	Russia	Matyukhin and Gashkov (2020)
Riparia chinensis	India, Nepal	Austen (1930); Maa (1969a)
Riparia riparia	Japan, Kazakhstan, Kyrgyzstan, Russia	Doszhanov (1970); Mogi (2014)

and Gashkov 2020). In this study *O. comosa* is recorded for the first time from Slovakia, demonstrating its further expansion in Central Europe.

A series of new records of louse flies and keds from Slovakia with several new host records is appended to supplement the recent review by Oboňa et al. (2019b). Because the available taxonomic keys for European Hippoboscidae are outdated, we present updated keys covering all species currently known from Europe.

Materials and methods

The key for European genera of Hippoboscidae follows the previous descriptions by Bequaert (1954), Theodor and Oldroyd (1964), and Hutson (1984). Keys for species of European Hippoboscidae follow Falcoz (1926), Povolný and Rosický (1955), Theodor and Oldroyd (1964), Maa (1966, 1969c), Hutson (1981, 1984), Ducháč and Bádr (1998), Farafonova (2001), Petersen et al. (2007), Iwasa and Choi (2013), Nartshuk et al. (2019b), and Salvetti et al. (2020).

In addition, new louse fly specimens from Slovakia were collected by hand on birds caught in mist nets, or keds by hand from humans. The majority of the samples come from the ornithological station "Vtáčí raj – Šalgovské rybníky" (Bird's Paradise

Figure 1. *Ornithomya comosa*, imago, dorsal view (left wing removed).

Figure 2. *Ornithomya comosa*, wing.

– Šalgov ponds) near the village Uzovský Šalgov (49°05'34.8"N, 21°04'00.4"E, 366 m a.s.l.). The birds were mist-netted in the standardised method (for more information, see Olekšák et al. 2007). Other samples, especially from humans, represent random and non-targeted sampling.

The collected hippoboscids were placed in microvials with 96% ethanol and subsequently identified in the laboratory using determination keys by Povolný and Rosický (1955) and Theodor and Oldroyd (1964). The focus on the local primary hosts follows Oboňa et al. (2019a, b, 2021). The newly recorded species *O. comosa* (Austen, 1930) was identified by Nartshuk et al. (2019b) using a key modified according Farafonova (2001). The material is deposited in the collection of the Laboratory and Museum of Evolutionary Ecology, Department of Ecology, University of Prešov (**LMEE PO**). The terminology follows Cumming and Wood (2017).

Results

Key for European genera of Hippoboscidae (updated)

1 Wings fully developed and functional (Figs 3–11) **2**

– Wings reduced, with strong veins (Figs 12–16) or absent (either by reduction or loss) **9**

2 Tarsal claws simple (Fig. 17), but with a pale basal lobe; humeral callus weak (Figs 21–24), postpronotum rounded, not produced anteriorly as conical lobes **3**

– Tarsal claw bifid and with a pale basal lobe (Fig. 18); humeral callus strong, postpronotum rounded, pair of conical lobes on either side of head (Figs 26–28), on birds **5**

3 Wing with one or two cross-veins; R_{4+5} well separated from C until apex; on mammals (Figs 4, 5) **4**

– Wings with three cross-veins enclosing cells posterior to radial veins; apical 1/2 of vein R_{4+5} running very close to C (Fig. 3); on birds..... ***Ornithoica***

4 Wing clear and hyaline, with only one cross-vein (Fig. 4); head broader than long; thorax markedly flattened (Figs 21–25); on mammals..... ***Lipoptena***

– Wing distinctly crenulated and tinted, with two cross-veins (Fig. 5); head not broader than long; thorax not so markedly flattened; on mammals..... ***Hippobosca***

5 Wing with three cross-veins posterior to radial veins (Figs 6, 7); scutellum with four or more strong marginal setae (Figs 32–37) **6**

– Wing with one or two cross-veins posterior to radius (Figs 8–11); scutellum at most with two strong marginal setae (Figs 31, 38) **7**

6 Vein R_{2+3} with apical 3/5 fused with C; wing membrane entirely bare (Fig. 6)..... ***Ornithophila***

– Vein R_{2+3} well separated from C except at apex; wing membrane usually with microtrichia (Fig. 7)..... ***Ornithomya***

7 Wing with only one cross-vein (Fig. 8) ..... ***Pseudolynchia***

– Wing with two cross-veins (Figs 9–11) **8**

8 Scutellum with two strong setae (Fig. 19) ..... ***Icosta***

– Scutellum with setulae (Fig. 31)..... ***Olfersia***

9 Wing long and narrow, at least 6 × as long as wide and twice as long as head and thorax (Fig. 12); female abdomen with strong spiniform setae in posterolateral area; male abdomen without spiniform setae..... ***Stenepteryx***

– Wing short and broad, at most 3 × as long as wide and ~ 1.5 × as long as head and thorax (Figs 13–16); tip of wing usually attenuated, C reaching to about 0.75 length of anterior wing margin; female abdomen only with short fine setae in posterolateral area..... ***Crataerina***

10 Wings either reduced to a veinless knob or broken off; haltere absent..... ***Melophagus***

– Wings absent, leaving a broad flat veined stump; haltere present .... ***Lipoptena***

Keys to species of European genera of Hippoboscidae (updated)

The genus *Crataerina* von Olfers, 1816

1 Wing shorter than hind femur; wing tip broadly rounded (Fig. 13)..... ***Crataerina obtusipennis* Austen, 1926**

– Wing longer than hind femur..... **2**

2 Wing more than twice as long as hind femur (Fig. 14); male abdomen with tergites 3 and 4 one-third as wide as abdomen and tergite 5 nearly as wide as abdomen; female abdomen with long and thick setae on posterior margin and with group of fine and long setae ventral to genital opening..... ***Crataerina melbae* (Rondani, 1879)**

– Wing < 2 × as long as hind femur; male abdominal tergites small or absent; all setae on posterior margin of female abdomen short and uniform in length..... **3**

3 Wing length 2 × as long as hind femur, extended beyond posterior end of abdomen; distal 1/2 of trailing edge of wing strongly concave (Fig. 15) .... ***Crataerina acutipennis*** **Austen, 1926**

– Wing length 1.3–1.5 × as long as hind femur, not extended beyond posterior end of abdomen; distal 1/2 of trailing edge of wing not strongly concave (Fig. 16)..... ***Crataerina pallida*** **(Olivier in Latreille, 1811)**

Host-parasite associations: Aves (Apodiformes, Passeriformes).

The genus *Hippobosca* Linnaeus, 1758

1 Vein R_{2+3} meets vein C at same place as R_1, shorter than distal section of R_{4+5} (measured from transverse vein r-m); front edge of thorax, with a transverse row of short thick setae; scutellum almost rectangular, with 2 dark and 3 light spots; wing length 7.0–8.0 mm..... ..... ***Hippobosca variegata*** **Megerle, 1803**

– Vein R_{2+3} end into vein C clearly separated from R_1, length is approximately equal to distal section of vein R_{4+5}; thorax without mentioned setae and characters; wing length shorter than 7.0–8.0 mm..... **2**

2 Dark brown specimens; veins of wings dark pigmented; scutellum white in middle, dark on sides; wing length 6.0–8.5 mm (Fig. 5)..... ..... ***Hippobosca equina*** **Linnaeus, 1758**

– Pale specimens; veins of wings light, only transverse veins and sections of longitudinal veins adjoining them are completely or partially dark; scutellum almost entirely white, sometimes with dark edge; wing length 5.0–6.0 mm ..... ***Hippobosca longipennis*** **Fabricius, 1805**

Host-parasite associations: Aves (Accipitriformes), Mammalia (Carnivora, Cetartiodactyla, Perissodactyla).

The genus *Icosta* Speiser, 1905

1 Large dark specimens; wing length 5.0–6.0 mm **2**

– Small pale specimens; wing length 3.5–4.0 mm..... **3**

2 Venter of hind femur bare; palp length more than twice width; microtrichia covering most of wing, but apical 1/2 of cell Cu+1A and entire 2A bare (Fig. 10); prescutum with setae reaching mesonotal suture; pale yellowish specimens; abdomen without tergite 3 (Fig. 39)..... ..... ***Icosta minor*** **(Bigot in Thomson, 1858)**

3 Venter of hind femur densely setose except near base; length of palp ~ 1.5 × width; wing with microtrichia covering most of its surface, including anterior 1/3 of cell 2A (Fig. 9); prescutum with short setae in several rows not reaching mesonotal suture, smaller and disordered short postalar setae in several rows

(Fig. 19); dark specimens; abdomen with distinct tergite 3 (Fig. 40) .... ***Icosta ardeae*** **(Macquart, 1835)**

– Enigmatic species, so far known from a single specimen; prescutum with one row of fine longer setae that reach mesonotal suture, setae in one row (Fig. 20) ..... ***Icosta massonati*** **(Falcoz, 1926)**

Host-parasite associations: Aves (Passeriformes, Pelecaniformes).

The genus *Lipoptena* Nitsch, 1818

1 Wing length 6.0 mm **2**

– Wing length 4.0 mm or less **3**

2 Body length 5.0–6.0 mm; scutellum with 6–8 setae; thorax mostly with 30–35 setae on each side, 9 postalar setae on each side (Fig. 21) .... ***Lipoptena cervi*** **(Linnaeus, 1758)**

– Body length 4.5–5.5 mm; scutellum with 8–10 setae; thorax mostly with 50–60 setae on each side, 6 postalar setae on each side (Fig. 22) .... ***Lipoptena couturieri*** **Séguy, 1935**

3 Wing length 4.0 mm; body length 2.8–3.2 mm; scutellum with 4–6 setae; thorax mostly with 8–12 strong setae on each side, 4 postalar setae on each side (Fig. 23) ..... ***Lipoptena fortisetosa*** **Maa, 1965**

– Wing length < 4.0 mm; scutellum with 6 setae; thorax mostly with 25 or more setae on each side, 3 or 4 postalar setae on each side **4**

4 Wing length 3.0–3.2 mm; body length 3.0–3.75 mm; body pale; thorax mostly with 30–35 setae on each side (Fig. 24) ..... ***Lipoptena capreoli*** **Rondani, 1878**

– Wing length < 3.0 mm body length 2.3–2.6 mm; body extremely dark; thorax mostly with 25–30 soft setae on each side (Fig. 25) .... ***Lipoptena arianae*** **Maa, 1969**

Host-parasite associations: Mammalia (Cetartiodactyla, Carnivora).

The genus *Melophagus* Latreille, 1802

1 Palps almost as long as head, in rest position completely covering proboscis (Fig. 29); parafrontalia almost touching in middle, mediovertex reduced; parafrontalia covered with numerous setae; tergal plates completely absent in male, in females only remnants of tergal plate 7 .... ***Melophagus ovinus*** **(Linnaeus, 1758)**

– Palps shorter than head, ~ 1/3 of head length, proboscis always protruding (Fig. 30); parafrontalia with few setae on inner margin; in males tergal plate 6 present, in females plates 6 and 7 present ..... ***Melophagus rupicaprinus*** **Rondani, 1879**

Host-parasite associations: Mammalia (Carnivora, Cetartiodactyla, Perissodactyla).

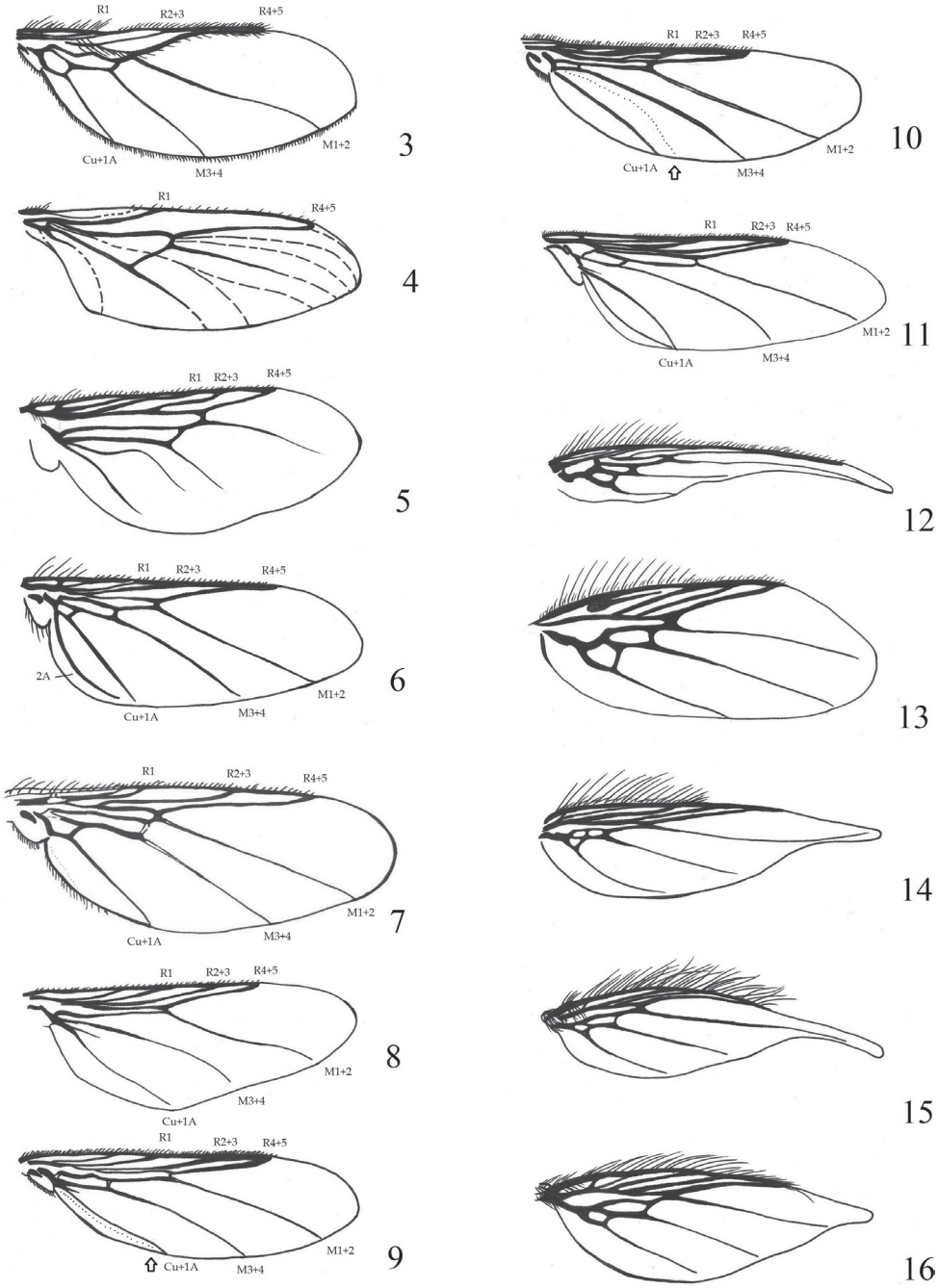

Figures 3–16. **3** *Ornithoica turdi*, wing **4** *Lipoptena cervi*, wing **5** *Hippobosca equina*, wing **6** *Ornithophila metallica*, wing **7** *Ornithomya avicularia*, wing **8** *Pseudolynchia canariensis*, wing **9** *Icosta ardeae*, wing (with the border of microtrichia) **10** *Icosta minor*, wing (with the border of microtrichia) **11** *Olfersia spinifera*, wing **12** *Stenepteryx hirundinis*, wing **13** *Crataerina obtusipennis*, wing **14** *Crataerina melbae*, wing **15** *Crataerina acutipennis*, wing **16** *Crataerina pallida*, wing.

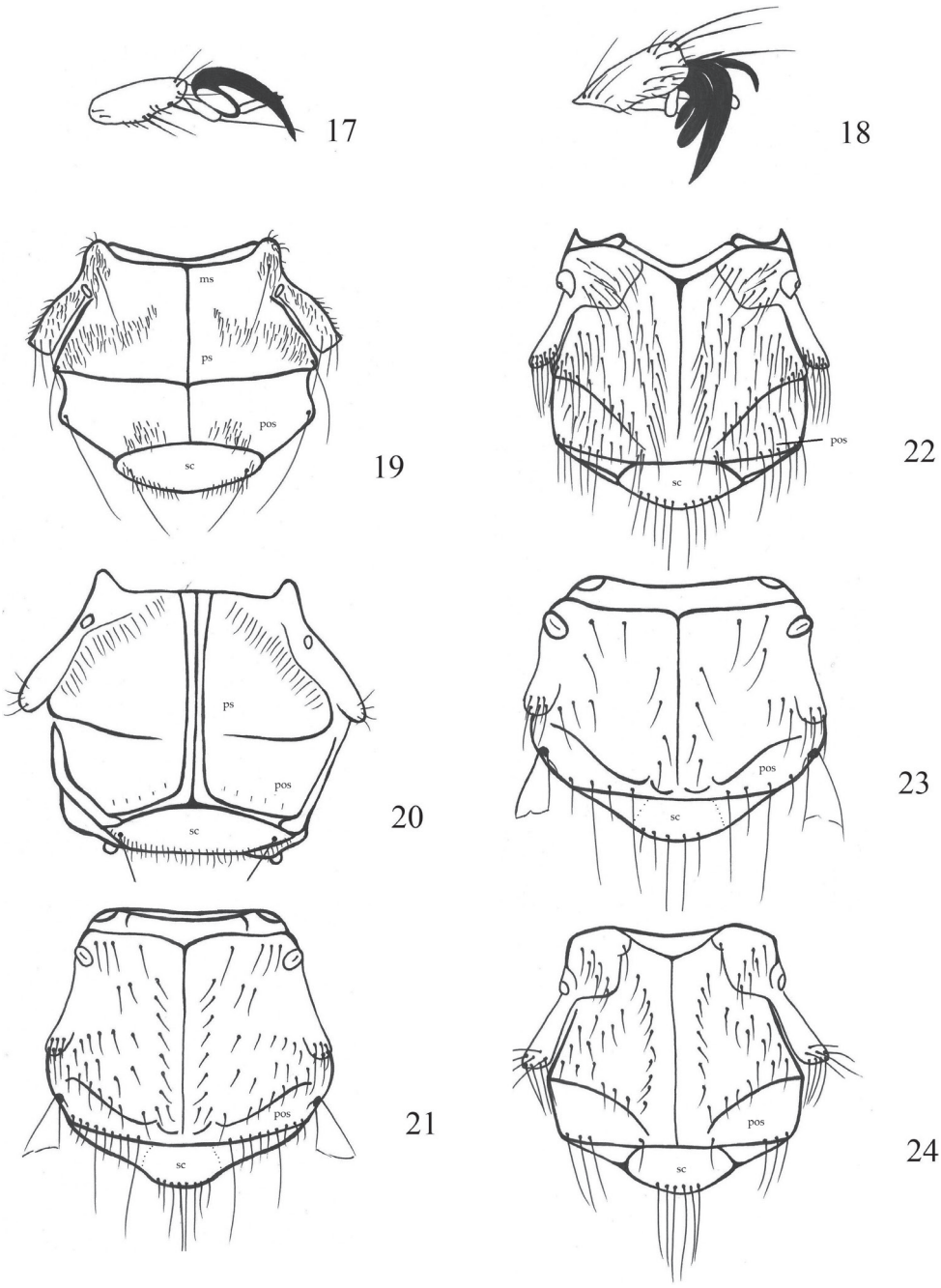

Figures 17–24. 17 *Lipoptena cervi*, tarsal claws **18** *Ornithomya avicularia*, tarsal claws **19** *Icosta ardeae*, thorax **20** *Icosta massonati*, thorax **21** *Lipoptena cervi*, thorax **22** *Lipoptena couturieri*, thorax **23** *Lipoptena fortisetosa*, thorax **24** *Lipoptena capreoli*, thorax. Abbreviations: ms – mesonotal suture, pos – postalar setae, ps – prescutum, sc – scutellum.

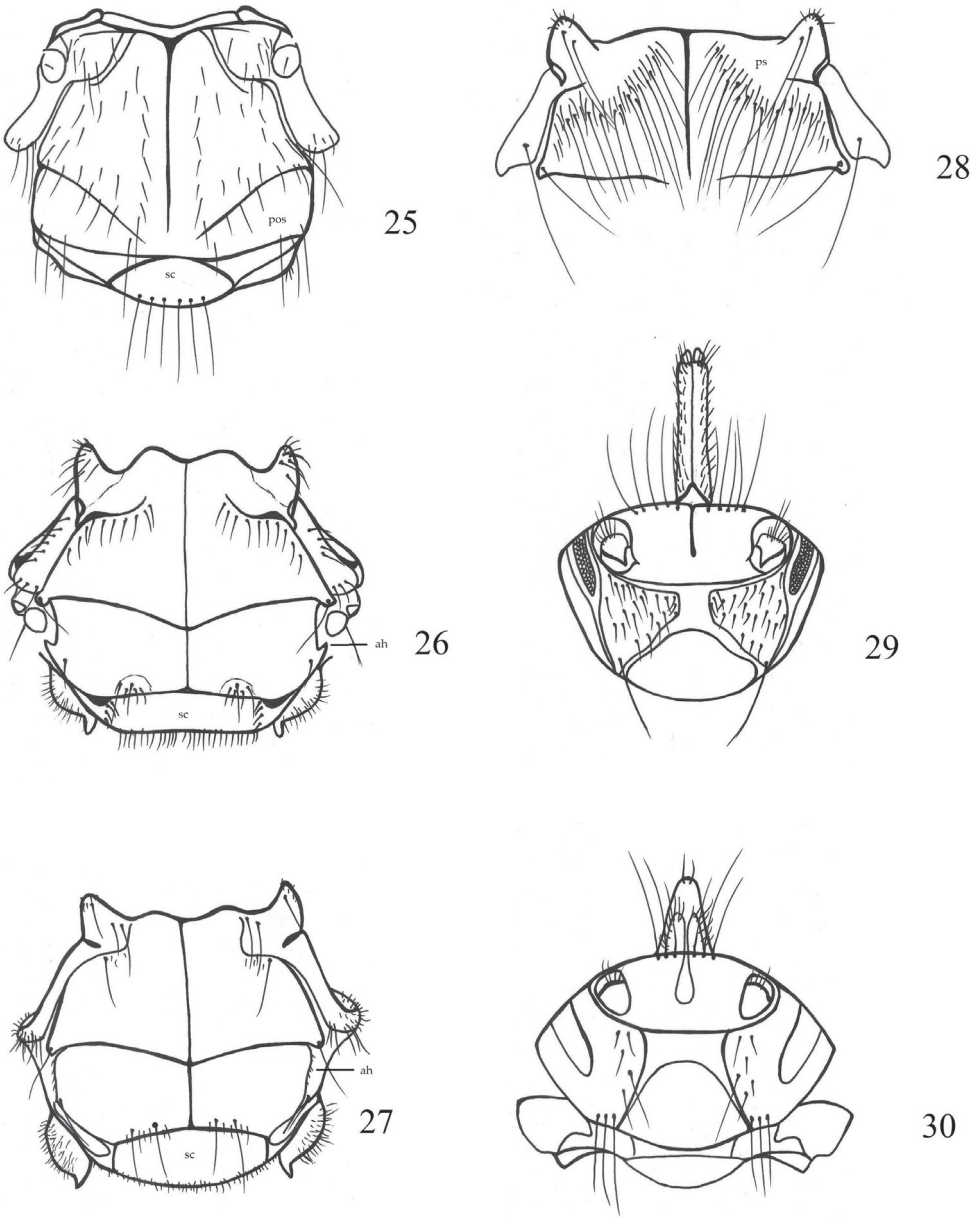

Figure 25–30. 25 *Lipoptena arianae*, thorax **26** *Olfersia spinifera*, thorax **27** *Olfersia fumipennis*, thorax **28** *Pseudolynchia canariensis*, frontal part of thorax **29** *Melophagus ovinus*, head with palps **30** *Melophagus rupicaprinus*, head with palps. Abbreviations: ah – alar horns, pos – postalar setae, ps – prescutum, sc – scutellum.

The genus *Olfersia* Wiedemann, 1830

1 Head on posterior margin with 3 distinct protrusions and deep indentations between postvertex and posterior orbit; postvertex protrudes noticeably

backwards over posterior orbites; tip of alar horns directed obliquely forward (Fig. 26); section of C between Sc and R_1 is shorter than section between R_1 and R_{2-3}. First basal cell is ca. as long as section of R_{4+5} distal to transverse vein r-m (Fig. 11); female pygidium separate and finger-shaped ..... ***Olfersia spinifera* (Leach, 1817)**

– Head protruding only a little over posterior orbit; tip of alar horns blunt and serrated (Fig. 27); sections of C between Sc and R_1 longer than section between R_1 and $R_{2+3.}$ First basal cell is significantly shorter than section of R_{4+5} distal to transverse vein r-m; female pygidium short and fused..... ***Olfersia fumipennis* (Sahlberg, 1886)**

Host-parasite associations: Aves (Accipitriformes, Gaviiformes, Charadriiformes, Pelecaniformes, Suliformes).

The genus Ornithoica *Rondani*, 1878 – one species only

***Ornithoica turdi* (Olivier in Latreille, 1812)**
Figs 3, 32

Host-parasite associations: Aves (Passeriformes).

The genus *Ornithomya* Latreille, 1802

1 C sector between R_1 and R_{2+3} not longer than sector between R_{2+3} and R_{4+5} ...**2**

– C sector between R_1 and R_{2+3} longer than between R_{2+3} and R_{4+5}.....**3**

2 Brown spots on ventral side of head do not reach jugular setae; scutellum with 4 setae (Fig. 33); wing in hind part with 4 longitudinal stripes of microtrichia; adult 1.9–2.5 mm ..... ***Ornithomya fringillina* Curtis, 1836**

– Triangular brown spots on ventral side of head are sharp (Fig. 41), narrowed and reach jugular setae, which are situated on sides of occipital foramen; scutellum usually with 6 or more setae (Fig. 34); wing in hind part with 3 longitudinal stripes of microtrichia; adult 2.1–2.6 mm ..... ***Ornithomya chloropus* Bergroth, 1901**

3 Wing dark and all surface evenly covered by microtrichia; scutellum with 10–12 setae (Fig. 35); all body covered by setae; adult 2.0–2.5 mm ..... ***Ornithomya comosa* (Austen, 1930)**

– Surface of wing covered by microtrichia no more than 2/3, base of wing without of microtrichia.....**4**

4 Wing with microtrichia only on apex and in cell m_1; scutellum with 8 setae (Fig. 36); abdomen on apex with numerous long setae; adult 3.0–3.5 mm ... ***Ornithomya avicularia* (Linnaeus, 1758)**

– Microtrichia covered nearly all wing except base or only cells r_3 and $m_{2,}$ long setae absent on apex of abdomen **5**

5 Wing dark with intensive microtrichia; thorax with 16–18 mesopleural setae on each side; scutellum with 6 setae (Fig. 37); abdomen similar as in following species; vibrissal spines almost missing..... ***Ornithomya biloba*** **Dufour, 1827**

– Wing light with extensive microtrichia, thorax with 6–10 mesopleural setae on each side; scutellum with 4 (6) setae; abdomen (Figs 43, 44); vibrissal spines present (Fig. 42) ..... ***Ornithomya rupes*** **Hutson, 1981**

Host-parasite associations: Aves (Accipitriformes, Anseriformes, Falconiformes, Passeriformes, Pelecaniformes, Strigiformes), Mammalia (Primates).

The genus *Ornithophila* Rondani, 1879

1 4.0–5.0 mm; scutellum dark, except for a narrow, light stripe at base; male tergal plates 3 and 4 as wide as scutellum..... ***Ornithophila metallica*** **(Schiner, 1864)**

– 5.0–7.0 mm; scutellum with a broad yellow band at base and a yellow triangle at apex; male tergal plates 3 and 4 as wide as a little more than 1/2 width of scutellum ..... ***Ornithophila gestroi*** **(Rondani, 1878)**

Host-parasite associations: Aves (Passeriformes).

The genus *Pseudolynchia* Bequaert, 1926

1 Hind scutellar margin in dorsal view straight or nearly straight (Fig. 38); interantennal area of frons as wide as or rarely slightly narrower than its distance to eye; prescutum with 20–30 long pale fine setae and before which with 2 or 3 series of shorter ones (Fig. 28); mid tarsus with group of peg-like modified spines under segment 1 at base..... ***Pseudolynchia canariensis*** **(Macquart in Webb & Berthelot, 1839)**

– Hind scutellar margin in dorsal view distinctly curved; interantennal area of frons always much narrower than its distance to eye; prescutum with 12–18 long, fairly robust and generally black setae and before which, with 1 or 2 series of shorter ones; mid tarsus with only pointed setae under segment 1 at base..... ***Pseudolynchia garzettae*** **(Rondani, 1879)**

Host-parasite associations: Aves (Accipitriformes).

The genus *Stenepteryx* Leach, 1817 – one species only

Stenepteryx hirundinis **(Linnaeus, 1758)**
Fig. 12

Host-parasite associations: Aves (Passeriformes: Hirundinidae).

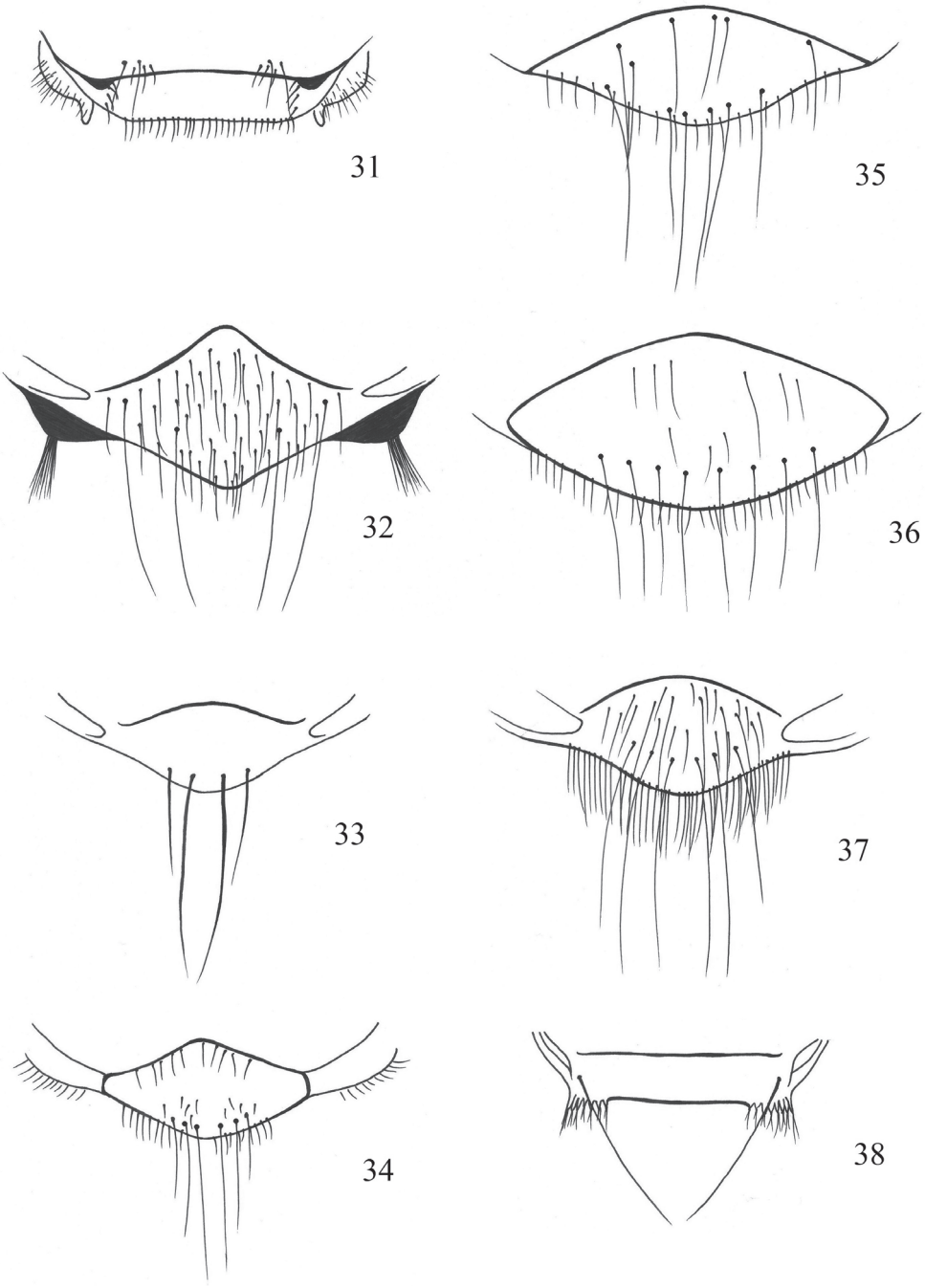

Figures 31–38. 31 *Olfersia fumipennis*, scutellum **32** *Ornithoica turdi*, scutellum **33** *Ornithomya fringillina*, scutellum **34** *Ornithomya chloropus*, scutellum **35** *Ornithomya comosa*, scutellum **36** *Ornithomya avicularia*, scutellum **37** *Ornithomya biloba*, scutellum **38** *Pseudolynchia canariensis*, scutellum.

Faunistics

New record for Slovakia

Ornithomya comosa (Austen, 1930)

Material examined. Uzovský Šalgov, around a pond, 49°05'34.8"N, 21°04'00.4"E, 366 m a.s.l., 14.7.2021, 1 ♀ (Fig. 1), from *R. riparia* [ring number – U69400] (LMEE PO).

Note. This is a dark louse fly (Fig. 1); all of its surfaces are unusually dark, wings are covered by microtrichia (Fig. 2). Scutellum with 10–12 long setae (6 subapical and 6 subbasal – see Fig. 35), and its body is covered by hairs.

Distribution. India (Pusa, Bihar), Japan (Honshu, Kyushu and Ryukyu islands), Kazakhstan, Kyrgyzstan, Malaysia, Nepal, Russia: western European Russia (Kaliningrad Prov.), West Siberia (Novosibirsk, Tomsk), Far East (Primorskii krai), and Thailand (Austen 1930; Maa 1969a, b, 1977; Doszhanov 1970, 2003; Mogi 2014; Nartshuk et al. 2019a, b, 2020; Matyukhin and Gashkov 2020).

Known hosts. see also in Table 1; Passeriformes: Hirundinidae (*C. daurica*, *D. urbicum*, *H. rustica*, *R. chinensis*, *R. diluta*, *R. riparia*) and Strigiformes: Strigidae (*O. scops*) (Austen 1930; Maa 1969a, b, 1977; Doszhanov 1970, 2003; Mogi 2014; Nartshuk et al. 2019a, b, 2020; Matyukhin and Gashkov 2020).

Additional records from Slovakia

Hippobosca equina Linnaeus, 1758

Material examined. Diviacka Nová Ves, margin of a *Quercus* forest, 48°45'12.3"N, 18°29'15.0"E, 320 m a.s.l., 1 ♀, 9.8.2021, from a human.

Note. Records from humans are accidental associations and the species do not complete development on this host.

Lipoptena cervi (Linnaeus, 1758)

Material examined. Lažany, 49°2'18.111"N, 21°5'22.029"E, 380 m a.s.l., 10.6.2021, 1 ♀, from a human.

Note. Similar to *H. equina*.

Lipoptena fortisetosa Maa, 1965

Material examined. Lažany, 49°2'18.111"N, 21°5'22.029"E, 380 m a.s.l., 10.6.2021, 2 ♀, from a human; Sabinov Bird Ringing Station, 49°06'02.7"N, 21°04'26.8"E, 370 m a.s.l., 5.7.2021, 1 ♀, from *Parus major* Linnaeus, 1758 [P132706], the same,

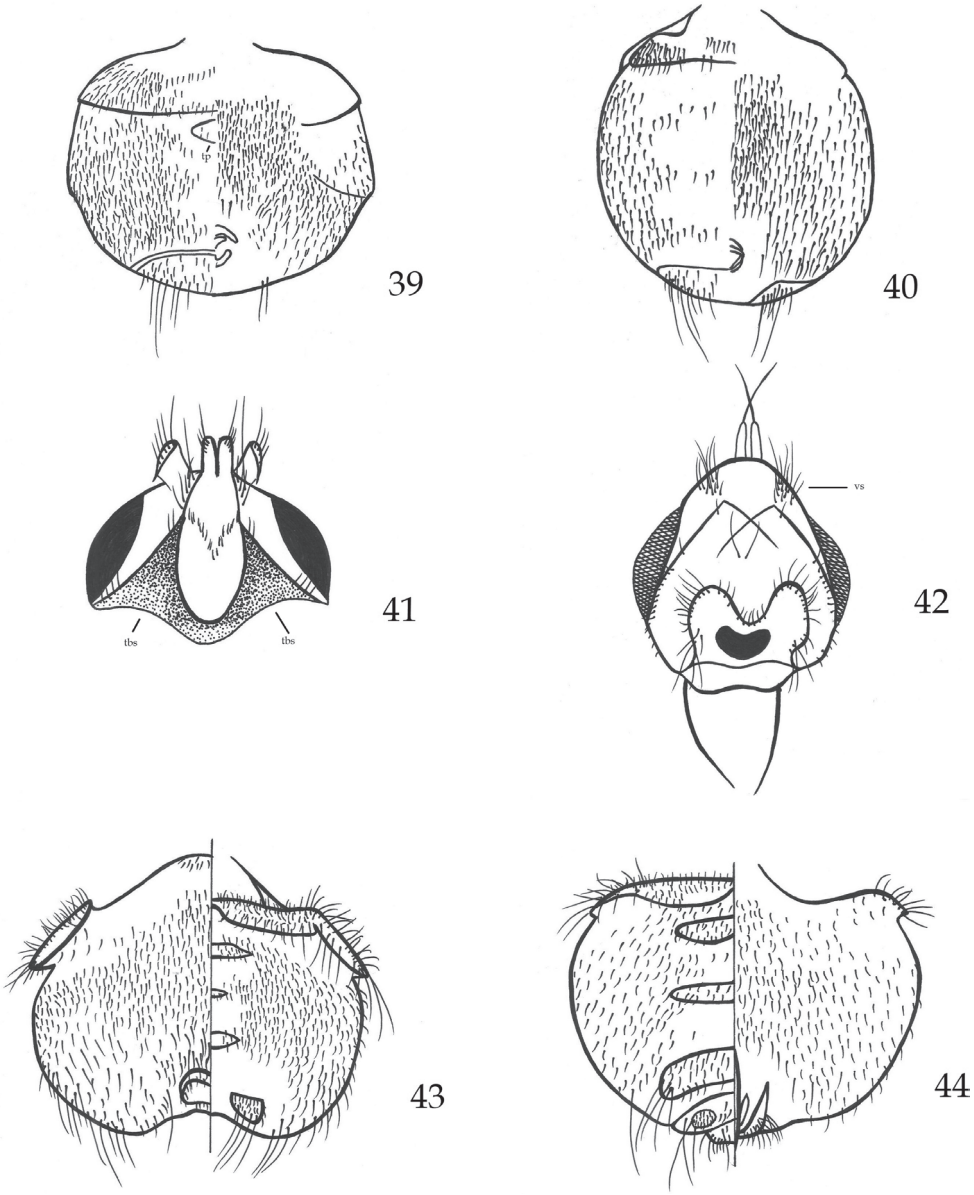

Figures 39–44. 39 *Icosta minor*, ♀ abdomen, dorsal and ventral view **40** *Icosta ardeae*, ♀ abdomen, dorsal and ventral view **41** *Ornithomya chloropus*, head, ventral view **42** *Ornithomya rupes*, head, ventral view **43** *Ornithomya rupes*, ♀ abdomen, dorsal and ventral view **44** *Ornithomya rupes*, ♂ abdomen, dorsal and ventral view. Abbreviations: tbs – triangle brown spot, tp – tergal plate, vs – vibrissal spines.

1 ♂, from a human, the same, 21.8.2021, 1 ♀, from a human, the same, 3.9.2021, 3 ♀, from a human; Pečovská Nová Ves, 49°07'04.2"N, 21°02'27.3"E, 26.7.2021, 1 ♀, from a human; Drienovec, 48°37'04.4"N, 20°55'29.9"E, 200 m a.s.l., 29.8.2021, 1 ♀, from a human; Prešov env. (near "pri Kríži"), 48°59'57.0"N, 21°13'03.7"E,

300 m a.s.l., 8.9.2021, 2 ♀, from a human; Vinné, 48°48'08.8"N, 21°58'22.7"E, 158 m a.s.l., 12.9.2021, 1 ♀, from a human.

Note. Records from humans and birds are accidental associations and the species do not complete development on this host.

Ornithomya avicularia (Linnaeus, 1758)

Material examined. Gbelce, 47°51'29.4"N, 18°30'17.9"E, 120 m a.s.l., 9.–10.7.2019. 7 ex. from *Panurus biarmicus* (Linnaeus, 1758), the same, 10.7.2019, 1 ex, from *Emberiza schoeniclus* (Linnaeus, 1758); Sabinov Bird Ringing Station, 49°06'02.7"N, 21°04'26.8"E, 370 m a.s.l., 5.7.2021, 1 ♀, from a human; Uzovský Šalgov, around a pond, 49°05'34.8"N, 21°04'00.4"E, 366 m a.s.l., 19.7.2021, 2 ♀, from *H. rustica*, [U62699, U62708], 20.7.2021, 1 ♀, from *H. rustica* [U62754], 23.7.2021, 1 ♀, from *Sturnus vulgaris* Linnaeus, 1758, 24.7.2021, 1 ♀, from *H. rustica*, [U62911], 28.7.2021, 1 ♂, 1 ♀, from a human, 30.7.2021, 3 ♀, from *H. rustica* [U74223, U62999, U74230], 10.8.2021, 1 ♀, from *H. rustica* [U74441].

Note. *Sturnus vulgaris* and *Emberiza schoeniclus* are here recorded as new hosts of *O. avicularia* in Slovakia.

Ornithomya biloba Dufour, 1827

Material examined. Uzovský Šalgov, around a pond, 49°05'34.8"N, 21°04'00.4"E, 366 m a.s.l., 15.7.2021, 1 ♂, 1 ♀, from *R. riparia*, 17.7.2021, 1 ♀, from *H. rustica* [U62640], 20.7.2021, 1 ♂, from *R. riparia* [U62741], 21.7.2021, 1 ♀, from *H. rustica* [U62777, S578974], 11.8.2021, 1 ♂, from *H. rustica*, 2.9.2021, 1 ♀, from *H. rustica* [U81448].

Ornithomya fringillina Curtis, 1836

Material examined. Uzovský Šalgov, around a pond, 49°05'34.8"N, 21°04'00.4"E, 366 m a.s.l., 23.7.2021, 1 ♀, from *H. rustica* [U62870]; Čerený Kláštor, 49°23'16.7"N, 20°23'49.8"E, 22.7.2021, 1 ♀, from *H. rustica* [U87187]; Drienovec, 48°37'04.4"N, 20°55'29.9"E, 200 m a.s.l., 31.8.2021, 1 ♀, from *Curruca curruca* (Linnaeus, 1758) [S564435].

Note. *Hirundo rustica* and *Curruca curruca* are here recorded as new hosts of *O. fringillina* in Slovakia.

Stenepteryx hirundinis (Linnaeus, 1758)

Material examined. Drienovec, 48°37'04.4"N, 20°55'29.9"E, 200 m a.s.l., 30.8.2021, 1 ♂, from *Delichon urbicum*.

Discussion

Updated keys to eleven European hippoboscid genera comprising 31 species are provided. We hope that they will contribute as a tool for determining European specimens of the most fascinating and neglected group of blood-feeding ectoparasites from the family Hippoboscidae (see Bezerra-Santos and Otranto 2020).

The recent checklist of louse flies of the family Hippoboscidae from Slovakia (see Oboňa et al. 2019b) includes 19 species; the present paper increases this list to 20 species. Four new host-parasite associations from Slovakia are also recorded (*O. avicularia* on the reed bunting and European starling, and *O. fringillina* on the barn swallow and the lesser whitethroat; see also Table 2).

Table 2. An overview of recorded host-parasites associations.

Parasites	Hosts
Hippobosca equina	Mammalia: Primates: *Homo sapiens**
Lipoptena cervi	Mammalia: Primates: *Homo sapiens**
Lipoptena fortisetosa	Mammalia: Primates: *Homo sapiens**; Aves: *Parus major**
Ornithomya avicularia	Aves: Passeriformes: *Emberiza schoeniclus*, *Hirundo rustica*, *Panurus biarmicus*, *Sturnus vulgaris*
Ornithomya biloba	Aves: Passeriformes: *Hirundo rustica*, *Riparia riparia*
Ornithomya comosa	Aves: Passeriformes: *Riparia riparia*
Ornithomya fringillina	Aves: Passeriformes: *Curruca curruca*, *Hirundo rustica*
Stenepteryx hirundinis	Aves: Passeriformes: *Delichon urbicum*

* Accidental association, parasite species do not complete development on this host.

Of a total of 20 Slovakian hippoboscid species, 12 are native. The remaining eight species (*Hippobosca longipennis* Fabricius, 1805, *H. variegata* Megerle, 1803, *Icosta minor* (Bigot, 1858), *Olfersia fumipennis* (Sahlberg, 1886), *Ornithoica turdi* (Latreille, 1812), *Ornithophila metallica* (Schiner, 1864), *Pseudolynchia canariensis* (Macquart, 1839), and the newly recorded *Ornithomyia comosa* (Austen, 1930) have been recorded from Slovakia based on very few records due to their hosts being usually occasional visitors (Oboňa et al. 2019b).

According to Nartshuk et al. (2019a), there are two possible explanations for the current distribution of *O. comosa*: *O. comosa* migrates with adult swallows from West Siberia or Kazakhstan to western Russia or *O. comosa* has always or for a long time been present in western Russia, but it has not been previously collected. For the European records of *O. comosa*, migrating swallows cannot bring *O. comosa* from Africa, as *O. comosa* does not occur there, but some *H. rustica* do, spending the winter in Asia, where *O. comosa* occurs. We also assume that records by Doszhanov (1970, 2003) from Kazakhstan and Kyrgyzstan could represent a bridge between the East Asian-Australasian Flyway and the African-Eurasian Flyway (see Boere and Stroud 2006). In this area, parasites can be transferred between hosts from East Asian countries (e.g., India, Nepal, Thailand, Malaya, Japan) to western Siberia, western Russia, and Europe. However, the question is whether *O. comosa* has already adapted to local conditions

and become a native species in Europe or will it continue to be only an occasionally introduced species.

The collection dates by Austen (1930) from India (February–April), King (1969) from Thailand (Bangkok) (ectoparasites collected during "winter"), and Mogi et al. (2002) from Japan (September–December) suggest that *O. comosa* is active mainly in autumn and winter (native populations). However, the findings from Kazakhstan by Doszhanov (1970) are from the period May–October, and the most recent records from the Kaliningrad region (Nartshuk et al. 2019a) correspond to the findings presented in this article, i.e., July and August. Therefore, we believe that the parasite does not have to come from the spring migration but, on the contrary, from the summer/autumn migration (possibly also from the Kaliningrad area). A similar phenomenon is recorded for the non-native species *Ornithoica turdi* (Olivier in Latreille, 1811) (e.g., records from Vienna from August, see Zittra et al. (2020)) transported by hosts from wintering grounds in Africa. The relatively late record after migration from the wintering grounds has two possible explanations. The first is that these parasites are able to live for more than two months (see Chalupský 1980). The second is that it could be a hatched fly, and therefore it may not be a casual traveller from Africa (*O. turdi*) or Asia (*O. comosa*), but that it is already breeding here (as a native species?). This is also indirectly confirmed by the negative findings from the spring migration.

Acknowledgements

We thank the subject editor and the anonymous reviewers for their valuable and constructive comments on the first version of the manuscript. The study was supported by the Slovak Research and Development Agency under the contract No. APVV-16-0411, by the grant VEGA 1/0876/21 (J. Oboňa, M. Hromada), by the Grant Agency of University of Prešov in Prešov under the contract No. GaPU 1/2022 (K. Fogašová), and by the Ministry of Culture of the Czech Republic through the institutional financing of long-term conceptual development of a research institution (the Silesian Museum, MK000100595) (J. Roháček).

References

Austen EE (1930) A new hippoboscid parasite (Diptera Pupipara) of the Indian sand-martin. Annals & Magazine of Natural History 10(5): 560–561. https://doi.org/10.1080/00222933008673165

Bequaert JC (1954) The Hippoboscidae or louse-flies (Diptera) of mammals and birds. Part II. Taxonomy, evolution and revision of American genera and species. Entomologica Americana 34: 1–232. [New Series]

Bezerra-Santos MA, Otranto D (2020) Keds, the enigmatic flies and their role as vectors of pathogens. Acta Tropica 209: 105521. https://doi.org/10.1016/j.actatropica.2020.105521

Boere GC, Stroud DA (2006) The flyway concept: what it is and what it isn't. Waterbirds around the world. In: Boere GC, Galbraith CA, Stroud DA (Eds) The Stationary Office, Edinburgh, Scotland, 40–47. [940 pp]

Chalupský J (1980) Hippoboscidae – Klošovití. In: Chvála M (Ed.) Krevsající mouchy a střečci. Fauna ČSSR, 22, Academia, Praha, 447–478. [In Czech]

Cumming JM, Wood DM (2017) Adult morphology and terminology. In: Kirk-Spriggs A, Sinclair BJ (Eds) Afrotropical Diptera. Vol. 1. South African National Biodiversity Institute, Pretoria, 89–133.

Dick CW (2006) Checklist of World Hippoboscidae (Diptera: Hippoboscoidea). Field Museum of Natural History, Chicago, 7 pp.

Dittmar K, Porter ML, Murray S, Whiting MF (2006) Molecular phylogenetic analysis of nycteribiid and streblid bat flies (Diptera: Brachycera, Calyptratae): implications for host associations and phylogeographic origins. Molecular Phylogenetics and Evolution 38(1): 155–170. https://doi.org/10.1016/j.ympev.2005.06.008

Doszhanov TN (1970) *Ornithomyia comosa* Austen (Diptera, Hippoboscidae), a new species for the USSR and the Palaearctic Region. Parazitologiia 4(1): 82–83. [In Russian]

Doszhanov TN (2003) Mukhi-krovososki (Diptera, Hippoboscidae) Palearktiki [Louse flies (Diptera, Hippoboscidae) of the Palaearctic Region]. Almaty, 277 pp. [In Russian]

Ducháč V, Bádr V (1998) Několik poznámek k druhu *Lipoptena fortisetosa* (Diptera: Hippoboscidae) [Several remarks of the species *Lipoptena fortisetosa* (Diptera: Hippoboscidae)]. Východočeský sborník přírodovědný práce a studie 6: 117–122. [In Slovak]

Falcoz L (1926) Diptères pupipares. Faune de France 14 - Diptères Pupipares. Fédération française des Sociétés de sciences naturelles (FFSSN), Paris, 53 pp.

Farafonova GV (2001) Fam. Hippoboscidae − louse flies. In: Lehr PA (Ed.) Key to the insects of Russian Far East. 6. Diptera and Syphonaptera. Pt 2. Dalnauka, Vladivostok, 252−258. [In Russian]

Hutson AM (1981) A new species of the Ornithomya biloba-group (Dipt., Hippoboscidae) from Crag Martin (*Ptyonoprogne rupestris*)(Aves, Hirundinidae). Mitteilungen der Schweizerischen Entomologischen Gesellschaft = Bulletin de la Société entomologique suisse 54: 157−162.

Hutson AM (1984) Keds, flat-flies and bat-flies. Diptera, Hippoboscidae and Nycteribiidae. Handbooks for the Identification of British Insects 10(7): 1–40.

Iwasa M, Choi CY (2013) Contribution to the knowledge of the Hippoboscidae (Diptera) from the Republic of Korea. Journal of Medical Entomology 50(2): 231–236. https://doi.org/10.1603/ME12179

King B (1969) Swallow banding in Bangkok, Thailand. Bird-banding 40(2): 95–104. https://doi.org/10.2307/4511553

Maa TC (1963) Genera and species of Hippoboscidae: Types, synonymy, habitats and natural groupings. Pacific Insects Monograph 6: 1–186. https://doi.org/10.1093/jmedent/1.1.4

Maa TC (1966) On the genus *Pseudolynchia* Bequaert. Pacific Insects Monograph 10: 125–138.

Maa TC (1969a) A revised checklist and concise host index of Hippoboscidae (Diptera). Pacific Insects Monograph 20: 261–299. https://doi.org/10.1093/jmedent/6.2.146

Maa TC (1969b) Notes on the Hippoboscidae (Diptera). II. Pacific Insects Monograph 20: 237–260. https://doi.org/10.1093/jmedent/6.2.146

Maa TC (1969c) Revision of *Icosta* (= *Lynchia* Auctt.) with erection of a related genus *Phthona* (Diptera: Hippoboscidae). Pacific Insects Monograph 20: 25–203.

Maa TC (1977) Family Hippoboscidae. A Catalog of the Diptera of the Oriental Region 3: 407–418.

Matyukhin AV, Gashkov SI (2020) First data on louse-fleas (Diptera, Hippoboscidae) of Tomsk. In: Ovtshinnikova OG, Shamshev IV (Eds) XI All-Russian Dipterological Symposium (with international participation), Voronezh, 24–29 August 2020: Materials. – St. Petersburg: Russian entomological society: LEMA Publishers, Voronezh, 132–135. [318 pp] https://doi.org/10.47640/978-5-00105-586-0_2020_132

Mogi M (2014) Family Hippoboscidae. In: Nakamura T, Saigusa T, Suwa M (Eds) Catalogue of the insects of Japan 8(2): 742–747.

Mogi M, Mano T, Sawada I (2002) Records of Hippoboscidae, Nycteribiidae and Streblidae (Diptera) from Japan. Medical Entomology and Zoology 53(Supplement 2): 141–165. https://doi.org/10.7601/mez.53.141

Nartshuk EP, Matyukhin AV, Shapoval AP (2019a) First record of the parasitic louse fly *Ornithomya comosa* (Diptera: Hippoboscidae) in Europe and western Russia. Zoosystematica Rossica 28(2): 356–359. https://doi.org/10.31610/zsr/2019.28.2.356

Nartshuk EP, Matyukhin AV, Shokhrin VP, Markovets MY (2019b) New records of ornithophilous louse-flies (Diptera: Hippoboscidae: Ornithomyinae) from the Russian Far East. Far Eastern Entomologist 384: 15–20. https://doi.org/10.25221/fee.384.4

Nartshuk EP, Matyukhin AV, Shapoval AP, Markovets MY, Tolstenkov OO (2020) Louse Flies (Diptera, Hippoboscidae) on the Courish Spit (Kaliningrad Province, Russia). Entomological Review 100(2): 231–238. https://doi.org/10.1134/S0013873820020128

Nirmala X, Hypša V, Žurovec M (2001) Molecular phylogeny of Calyptratae (Diptera: Brachycera): the evolution of 18S and 16S ribosomal rDNAs in higher dipterans and their use in phylogenetic inference. Insect Molecular Biology 10(5): 475–485. https://doi.org/10.1046/j.0962-1075.2001.00286.x

Oboňa J, Krišovský P, Hromada M (2019a) Short-term faunistic sampling of Louse flies (Diptera: Hippoboscidae) from Drienovec Bird Ringing Station, Slovakia. Biodiversity & Environment 11(2): 4–9.

Oboňa J, Sychra O, Greš S, Heřman P, Manko P, Roháček J, Šestáková A, Šlapák J, Hromada M (2019b) A revised annotated checklist of louse flies (Diptera, Hippoboscidae) from Slovakia. ZooKeys 862: 129–152. https://doi.org/10.3897/zookeys.862.25992

Oboňa J, Greš S, Krišovský P, Hromada M (2021) Faunistic records and new parasite-host associations of Louse flies (Diptera: Hippoboscidae) from Sabinov, Slovakia. Biodiversity & Environment 12(1): 74–79.

Olekšák M, Pjenčák P, Fulín M, Matis Š (2007) Bird nesting community of the Drienovec bird Ringing Station – CES programme. Tichodroma 19: 41–47.

Pape T, Beuk P, Pont A, Shatalkin A, Ozerov A, Woźnica A, Merz B, Bystrowski C, Raper C, Bergström C, Kehlmaier C, Clements D, Greathead D, Kameneva E, Nartshuk E, Petersen F, Weber G, Bächli G, Geller-Grimm F, Van de Weyer G, Tschorsnig H, de Jong H, van Zuijlen J, Vaňhara J, Roháček J, Ziegler J, Majer J, Hůrka K, Holston K, Rognes K, Greve-Jensen L, Munari L, de Meyer M, Pollet M, Speight M, Ebejer M, Martinez M,

Carles-Tolrá M, Földvári M, Chvála M, Barták M, Evenhuis N, Chandler P, Cerretti P, Meier R, Rozkosny R, Prescher S, Gaimari S, Zatwarnicki T, Zeegers T, Dikow T, Korneyev V, Richter V, Michelsen V, Tanasijtshuk V, Mathis W, Hubenov Z, de Jong Y (2015) Fauna Europaea: Diptera – Brachycera. Biodiversity Data Journal 3: e4187. https://doi.org/10.3897/BDJ.3.e4187

Petersen FT, Damgaard J, Meier R (2007) DNA taxonomy: How many DNA sequences are needed for solving a taxonomic problem? The case of two parapatric species of louse flies (Diptera: Hippoboscidae: Ornithomya Latreille, 1802). Arthropod Systematics & Phylogeny 65(2): 119–125.

Povolný D, Rosický B (1955) Faunisticko-bionomický nástin klošovitých (Hippoboscidae, Diptera) z území ČSR. Zoologické a entomologické listy 4: 5–20. [In Czech]

Rahola N, Goodman SM, Robert V (2011) The Hippoboscidae (Insecta: Diptera) from Madagascar, with new records from the "Parc National de Midongy Befotaka". Parasite 18(2): 127–140. https://doi.org/10.1051/parasite/2011182127

Reeves WK, Lloyd JE (2019) Louse flies, keds, and bat flies (Hippoboscoidea). Medical and Veterinary Entomology 421–438. https://doi.org/10.1016/B978-0-12-814043-7.00020-0

Salvetti M, Bianchi A, Marangi M, Barlaam A, Giacomelli S, Bertoletti I, Roy L, Giangaspero A (2020) Deer keds on wild ungulates in northern Italy, with a taxonomic key for the identification of *Lipoptena* spp. of Europe. Medical and Veterinary Entomology 34(1): 74–85. https://doi.org/10.1111/mve.12411

Theodor O, Oldroyd H (1964) Hippoboscidae. In: Lindner E (Ed.) Die Fliegen der Palaearktischen Region 12. Museum Wiesbaden Nafurwillenschaltliche Sammlung, Stuttgards, 1–70. [98 pp]

Zittra C, Schoener ER, Wagner R, Heddergott M, Duscher GG, Fuehrer HP (2020) Unnoticed arrival of two dipteran species in Austria: The synanthropic moth fly *Clogmia albipunctata* (Williston, 1893) and the parasitic bird louse fly *Ornithoica turdi* (Olivier in Latreille, 1811). Parasitology Research 119(2): 737–740. https://doi.org/10.1007/s00436-019-06563-9

ZooKeys 1115: 103–116 (2022)
doi: 10.3897/zookeys.1115.85249
https://zookeys.pensoft.net

RESEARCH ARTICLE

A peer-reviewed open-access journal
ZooKeys
Launched to accelerate biodiversity research

Complete mitochondrial genomes of two catfishes (Siluriformes, Bagridae) and their phylogenetic implications

Renyi Zhang[1*], Lei Deng[1*], Xiaomei Lv[1], Qian Tang[1]

1 *School of Life Sciences, Guizhou Normal University, 116 Baoshan Road, Guiyang, Guizhou, 550001, China*

Corresponding author: Renyi Zhang (zhangrenyi@gznu.edu.cn)

Academic editor: Tihomir Stefanov | Received 12 April 2022 | Accepted 12 July 2022 | Published 29 July 2022

https://zoobank.org/7A01B01B-92F7-469B-B2BE-81F1B9324D2F

Citation: Zhang R, Deng L, Lv X, Tang Q (2022) Complete mitochondrial genomes of two catfishes (Siluriformes, Bagridae) and their phylogenetic implications. ZooKeys 1115: 103–116. https://doi.org/10.3897/zookeys.1115.85249

Abstract

The mitochondrial genome (mitogenome) has been widely used as a molecular marker to investigate phylogenetic analysis and evolutionary history in fish. However, the study of mitogenomes is still scarce in the family Bagridae. In this study, the mitogenomes of *Tachysurus brachyrhabdion* and *T. gracilis* were sequenced, annotated, and analyzed. The mitogenomes were found to be 16,532 bp and 16,533 bp, respectively, and each contained 37 typical mitochondrial genes, which are 13 protein-coding genes (PCGs), 22 tRNA genes, two rRNA genes, and a control region. All PCGs begin with the codon ATG, except for the cytochrome c oxidase subunit 1 (*COI*) gene, while seven PCGs end with an incomplete termination codon. All tRNA genes can fold into their typical cloverleaf secondary structures, except for $tRNA^{Ser(AGY)}$, which lacks the dihydrouracil arm. The Ka/Ks ratios for all PCGs are far lower than one. Phylogenetic analyses based on Bayesian inference (BI) and maximum likelihood (ML) showed that the two clades in Bagridae excluded *Rita rita*. The monophyly of *Tachysurus* supports previous research and the traditional classification that *Leiocassis*, *Pseudobagrus*, *Pelteobagrus*, and *Tachysurus* belong to one genus (*Tachysurus*). These findings provide a phylogenetic basis for future phylogenetic and taxonomic studies of Bagridae.

Keywords

bagrid catfish, mitogenome, phylogenetic analysis, *Tachysurus brachyrhabdion*, *Tachysurus gracilis*

* These authors contributed equally to this work.

Introduction

The family Bagridae, commonly known as bagrid catfish, is widely distributed in Asia and Africa, with about 225 species in 19 genera (Fricke et al. 2022). It is one of the most diverse and complicated groups within Siluriformes. Regan (1911) first promoted bagrid fishes as a single-family and named Bagridae, including two subfamilies: Chrysichthyinae and Bagrinae. Based on osteological features, Jayaram (1968) divided Bagridae into five subfamilies: Ritinae, Chiysichthyinae, Bagrinae, Bagroidinae, and Auchenoglaninae. In 1992, Mo (1992) divided the traditional bagrid catfishes into three monophyletic groups: Caroteidae, Austroglanididae, and Bagridae; the latter Bagridae contained two subfamilies, Ritinae and Bagrinae. In the past two decades, molecular phylogenetic studies showed that Bagridae is monophyletic, with only *Rita* excluded (Sullivan et al. 2006; Vu et al. 2018). However, the phylogenetic relationships between different genera of Bagridae are not well understood, such as the monophyly or the validity of *Leiocassis*, *Pseudobagrus*, *Pelteobagrus*, and *Tachysurus*. Recently, *Leiocassis*, *Pseudobagrus*, *Pelteobagrus*, and *Tachysurus* were classified into *Tachysurus* according to morphological analysis (Cheng et al. 2021; Shao et al. 2021).

Tachysurus brachyrhabdion Cheng, Ishihara & Zhang, 2008 was firstly named *Pseudobagrus brachyrhabdion* in 2008 (Cheng et al. 2008). It is mainly distributed in the Yuanjiang and Xiangjiang rivers, including the southwest of Hunan Province and the northeast of Guizhou Province in China. *Tachysurus gracilis* Li, Chen & Chan, 2005 was firstly named *Pseudobagrus gracilis* in 2005 (Li et al. 2005). It inhabits in the freshwater drainages of southern China. They are essential economic species of freshwater fishes in local areas.

Mitochondria are eukaryotic organelles that play essential roles in oxidative phosphorylation and other biochemical functions. Similar to other vertebrates, fish mitochondrial DNA (mtDNA) is a circular double-stranded molecule, and it is independent of the nuclear genome (Xiao and Zhang 2000). Fish mtDNA is generally small (15–18 kb), containing 13 protein-coding genes (PCGs), 22 transfer RNA (tRNA) genes, two ribosomal RNA (rRNA) genes, and a non-coding region (D-loop) (Brown 2008; Zhang and Wang 2018; Zhang et al. 2021). The mitochondrial genome has been used to study fish species identification, genome evolution, and phylogenetic studies because of the advantages of its small size, multiple copies, maternal inheritance, rapid evolution rate, and lack of introns (Boore 1999; Xiao and Zhang 2000; Zhang and Wang 2018; Zhang et al. 2021).

In this study, the mitochondrial genomes of two catfishes (*T. brachyrhabdion* and *T. gracilis*) were sequenced, assembled, and compared to reveal their evolutionary relationship. These mitochondrial genomes will provide a phylogenetic basis for future phylogenetic and taxonomic studies of Bagridae.

Materials and methods

Sample collection and DNA extraction

Specimens of *T. brachyrhabdion* and *T. gracilis* were collected from Jiangkou County (27°46'12"N, 108°46'56"E) and Liping County (26°17'51"N, 109°7'25"E), Guizhou,

China, respectively. The samples were preserved in 95% ethanol and stored at -20 °C until DNA extraction. Specimens were recognized as *T. brachyrhabdion* and *T. gracilis* by traditional morphology. The voucher specimens were deposited in the fish specimen room, School of Life Science, Guizhou Normal University under the voucher numbers GZNUSLS201909001~006 and GZNUSLS201907029~030 for *T. brachyrhabdion* and GZNUSLS202005279 for *T. gracilis*. Specimens GZNUSLS201907029 and GZNUSLS202005279 were destroyed for the molecular analysis. Total genomic DNA was extracted from muscle tissues using a standard high salt method (Sambrook et al. 1989). The integrity of the genomic DNA was evaluated via 1% agarose gel electrophoresis, and the concentration and purity of DNA were measured using an Epoch 2 Microplate Spectrophotometer (Bio Tek Instruments, Inc, Vermont, USA).

PCR amplification and sequencing

The whole mitogenomes of *Tachysurus* species were amplified in overlapping PCR fragments using 13 primer pairs designed based on the mitogenome of *T. brevicaudatus* (GenBank accession number: NC_021393) by Primer Premier 5.0 software (Lalitha 2000) (Suppl. material 3). PCR amplification were performed as described previously (Zhang et al. 2021). The PCR products were fractionated by electrophoresis through 1% agarose gel electrophoresis. The lengths of fragments were determined by comparison with the DL2000 DNA marker (TaKaRa, Japan). The PCR products were sent to Sangon Biotech. Co., Ltd. (Shanghai, China) for sequencing.

Sequence analysis and gene annotation

After sequencing, the sequence fragments were edited and assembled using the SeqMan software of DNAStar (DNASTAR Inc., Madison, WI, USA) to obtain the complete mitogenome sequences. Assembled mitogenome sequences were annotated using the MitoAnnotator on the MitoFish homepage (Sato et al. 2018). tRNA genes and their secondary structures were predicted with MITOS (Bernt et al. 2013) and tRNAscan-SE 2.0 (Chan et al. 2021). The base composition, codon usage, and relative synonymous codon usage (RSCU) values were calculated using MEGA 6.0 (Tamura et al. 2013). Strand asymmetry was calculated using the following formulae: AT-skew = (A-T)/(A+T) and GC-skew = (G-C)/(G+C) (Perna and Kocher 1995). The ratio of non-synonymous substitutions (Ka), synonymous substitutions (Ks), and evolutionary rates (Ka/Ks) of each PCG was calculated using DnaSP v. 6.0 (Rozas et al. 2017).

Phylogenetic analysis

For phylogenetic analysis, sequences of 32 bagrid catfishes were downloaded from GenBank. Additionally, *Cyprinus carpio* (NC_001606.1), *Silurus asotus* (NC_015806.1), *Liobagrus andersoni* (NC_032035.1), and *L. styani* (NC_034647.1) were used as outgroups. The species used in the analysis are listed in Suppl. material 4. The shared 13 concatenated PCGs were extracted and recombined to construct a matrix using

PhyloSuite v.1.1.16 (Zhang et al. 2020). The 13 PCGs were aligned separately using MAFFT v.7.313 (Katoh and Standley 2013) and concatenated into a sequence matrix using PhyloSuite v.1.1.16 (Zhang et al. 2020). The optimal partitioning scheme and nucleotide sequence substitution model of each partition were estimated using PartitionFinder v.2.1.11 (Lanfear et al. 2017) with the Corrected Akaike information criterion (AICc) criteria and greedy algorithm. Bayesian inference (BI) analysis was performed using MrBayes v.3.2.6 (Ronquist et al. 2012) with the models determined by PartitionFinder (Lanfear et al. 2017). Two independent runs of four Markov Chain Monte Carlo (MCMC) chains (one cold chain and three heated chains) were performed for one million generations sampling every 100 generations. The first 25% of the generations was discarded as burnin, and the remaining trees were used to generate a majority rule consensus tree. Maximum likelihood (ML) analysis was carried out using IQ-TREE v.1.6.8 (Nguyen et al. 2015) with 10,000 bootstrap replicates using the ultrafast bootstrapping algorithm (Minh et al. 2013). The phylogenetic trees were visualized and edited using FigTree v1.4.2 (http://tree.bio.ed.ac.uk/software/figtree/).

Results

Genome structure, organization, and base composition

The entire mitogenome sequences of the two catfishes had lengths of 16,532 bp for *T. brachyrhabdion* and 16,533 bp for *T. gracilis* (GenBank accessions MW712739 and OM759888, respectively) (Fig. 1, Table 1). Both sequences contained 13 PCGs (*ND1-6*, *COI-III*, *ND4L*, *ATP6*, *ATP8*, and *Cytb*), 22 tRNA genes (one for each amino acid, two for Leucine and Serine), two rRNA genes (12S and 16S rRNA), and a non-coding region (D-loop) (Fig. 1, Table 1). Among these genes, one PCG and eight tRNA genes were encoded on the minority strand (L-strand), while another 28 genes were encoded on the majority strand (H-strand) (Fig. 1, Table 1).

The overall base composition for both species was very similar, 31.02% A, 27.05% T, 15.55% G, and 26.38% C for *T. brachyrhabdion* and 31.03% A, 27.14% T, 15.52% G, and 26.31% C for *T. gracilis* (Table 2). The third codon position of PCGs had the highest A+T content (65.75% for *T. brachyrhabdion* and 66.04% for *T. gracilis*), while the first codon position of PCGs had the lowest A+T content (49.00% for *T. brachyrhabdion* and 49.11% for *T. gracilis*) (Table 2). In addition, skew metrics of the mitogenomes showed positive AT-skew and negative GC-skew (Table 2), indicating that As and Cs were more abundant than Ts and Gs.

Protein-coding genes

The mitogenomes of *T. brachyrhabdion* and *T. gracilis* had one PCG (*ND6*) encoded on the L-strand and the remaining PCGs on the H-strand. Both mitogenomes had 11,405 bp coding for PCGs, accounting for 3627/3626 amino acids (Table 2, Suppl.

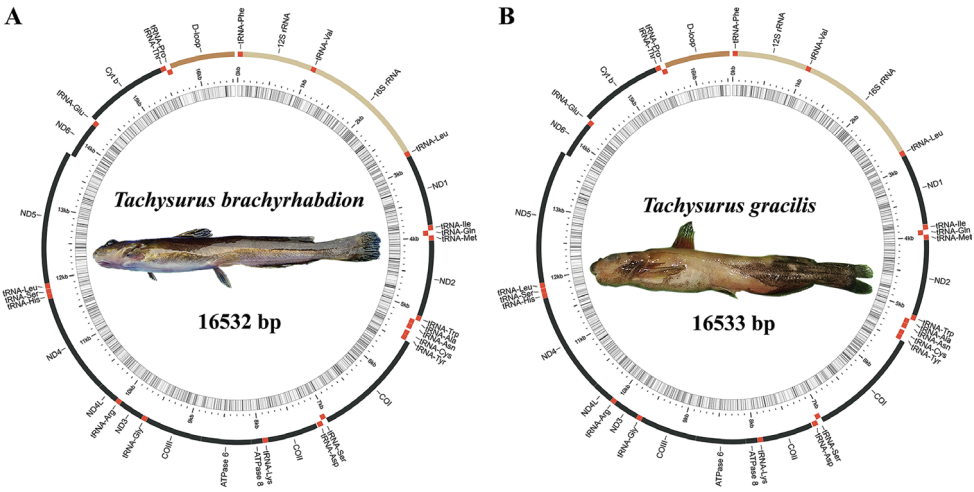

Figure 1. Circular map of the two catfishes mitochondrial genomes.

material 5). Both species had very similar codon usage, with the most commonly used amino acids being Leu (13.81%, 13.87%), Ser (9.98%, 10.04%), and Ile (8.88%, 8.80%) (Suppl. material 5). The RSCU values of the mitogenomes of the two species are summarized in Fig. 2. All PCGs start with ATG except for *COI*, which used GTG. For these protein-coding genes, the most common stop codon was TAA, although *ND1* used TAG and some used the incomplete stop codon T – or TA-.

To investigate the evolutionary patterns under different selective pressures among 13 PCGs in bagrid catfishes, the value of Ka/Ks was calculated for each PCG, respectively (Fig. 3). The gene (*ATP8*) exhibited the highest ratio of all the PCGs, whereas *COI* had the lowest ratio. However, the Ka/Ks ratios for all PCGs were far lower than one (Fig. 3).

Ribosomal, transfer RNA genes and control region

Both the *T. brachyrhabdion* and *T. gracilis* mitogenomes contained two rRNA genes: the large ribosomal RNA subunit (16S rRNA) and small ribosomal RNA subunit (12S rRNA). The 16S rRNA was located between $tRNA^{Val}$ and $tRNA^{Leu\ (UUR)}$, and the 12S rRNA was located between $tRNA^{Phe}$ and $tRNA^{Val}$. The 12S rRNA genes and the 16S rRNA genes of both mitogenomes were 953 bp and 1679 bp, respectively.

Twenty-one tRNA genes produced the typical cloverleaf secondary structure, while $tRNA^{Ser\ (AGY)}$ gene lacked the dihydrouracil (DHU) arm (Figs S1 and S2). The sizes of the tRNA genes ranged from 67 bp ($tRNA^{Cys}$ and $tRNA^{Ser\ (AGY)}$) to 75 bp ($tRNA^{Leu\ (UUR)}$) in both *T. brachyrhabdion* and *T. gracilis* (Table 1).

The putative control regions were located between $tRNA^{Pro}$ and $tRNA^{Phe}$ in the two bagrid catfishes. The control regions of *T. brachyrhabdion* and *T. gracilis* were 892 bp in size. The average A+T content of the CRs (62.33%–62.67%) was higher than that of the whole genomes, PCGs, rRNAs, or tRNAs (57.14%–58.24%) (Table2).

Table 1. Organization of mitochondrial genome of *T. brachyrhabdion* (TB) and *T. gracilis* (TG). H refers to the majority strand and L refers to the minority strand. Position numbers refer to positions on the majority strand.

Gene	Strand	Nucleotide number		Length (bp)	Intergenic nucleotide		Anticodon	Start/Stop codons	
		TB	TG		TB	TG		Start	Stop
tRNA^{Phe}	H	1–70	1–70	70	0	0	GAA		
12S rRNA	H	71–1023	71–1023	953	0	0			
tRNA^{Val}	H	1024–1095	1024–1095	72	0	0	TAC		
16S rRNA	H	1096–2774	1096–2774	1679	0	0			
tRNA$^{Leu\ (UUR)}$	H	2775–2849	2775–2849	75	0	0	TAA		
ND1	H	2850–3824	2850–3824	975	2	2		ATG	TAG
tRNA^{Ile}	H	3827–3898	3827–3898	72	-1	-1	GAT		
tRNA^{Gln}	L	3898–3968	3898–3968	71	-1	-1	TTG		
tRNA^{Met}	H	3968–4037	3968–4037	70	0	0	CAT		
ND2	H	4038–5082	4038–5082	1045	0	0		ATG	T
tRNA^{Trp}	H	5083–5153	5083–5153	71	2	2	TCA		
tRNA^{Ala}	L	5156–5224	5156–5224	69	1	1	TGC		
tRNA^{Asn}	L	5226–5298	5226–5298	73	32	32	GTT		
tRNA^{Cys}	L	5331–5397	5331–5397	67	0	0	GCA		
tRNA^{Tyr}	L	5398–5468	5398–5469	71/72	1	1	GTA		
COI	H	5470–7020	5471–7021	1551	0	0		GTG	TAA
tRNA$^{Ser\ (UCN)}$	L	7021–7091	7022–7092	71	4	4	TGA		
tRNA^{Asp}	H	7096–7168	7097–7169	73	14	14	GTC		
COII	H	7183–7873	7184–7874	691	0	0		ATG	T
tRNA^{Lys}	H	7874–7947	7875–7948	74	1	1	TTT		
ATPase 8	H	7949–8116	7950–8117	168	-10	-10		ATG	TAA
ATPase 6	H	8107–8789	8108–8790	683	0	0		ATG	TA
COIII	H	8790–9573	8791–9574	784	0	0		ATG	T
tRNA^{Gly}	H	9574–9647	9575–9648	74	0	0	TCC		
ND3	H	9648–9996	9649–9997	349	0	0		ATG	T
tRNA^{Arg}	H	9997–10067	9998–10068	71	0	0	TCG		
ND4L	H	10068–10364	10069–10365	297	-7	-7		ATG	TAA
ND4	H	10358–11738	10359–11739	1381	0	0		ATG	T
tRNA^{His}	H	11739–11808	11740–11809	70	0	0	GTG		
tRNA$^{Ser\ (AGY)}$	H	11809–11875	11810–11876	67	3	3	GCT		
tRNA$^{Leu\ (CUN)}$	H	11879–11951	11880–11952	73	0	0	TAG		
ND5	H	11952–13778	11953–13779	1827	-4	-4		ATG	TAA
ND6	L	13775–14290	13776–14291	516	0	0		ATG	TAA
tRNA^{Glu}	L	14291–14359	14292–14360	69	2	2	TTC		
Cytb	H	14362–15499	14363–15500	1138	0	0		ATG	T
tRNA^{Thr}	H	15500–15572	15501–15573	73	-2	-2	TGT		
tRNA^{Pro}	L	15571–15640	15572–15641	70	0	0	TGG		
D-loop	H	15641–16532	15642–16533 16533	892	0	0			

Phylogenetic analysis

To determine the phylogenetic relationship between *T. brachyrhabdion* and *T. gracilis* in the Characidae, we selected the concatenated nucleotide sequences of the combined mitochondrial gene set (13 PCGs) from 34 bagrid catfishes. As shown in Fig. 4, the phylogenetic analysis of the two tree models (BI and ML) using the combined mitochondrial gene set well supported the tree topologies and yielded identical results. Phylogenetic analysis reveals bagrid catfishes could be separated into two clades excluding *Rita rita* (Hamilton, 1822) with strong support (Fig. 4). Clade I included *Hemibagrus*, *Sperata*, and *Mystus* (BS = 100%, PP = 100%). Clade II was only composed of *Tachysurus* (BS = 100%, PP = 100%). Several monophyletic clades of *Tachysurus*,

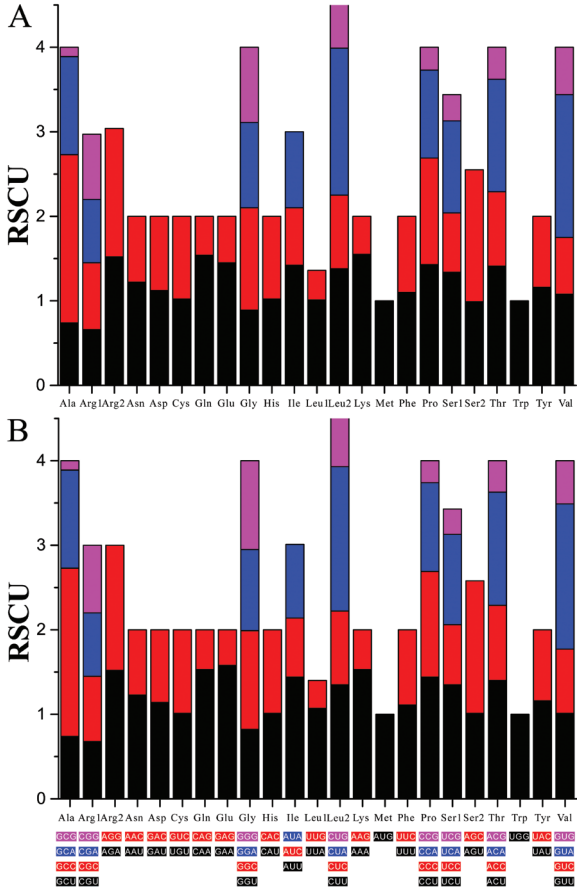

Figure 2. Relative synonymous codon usage (RSCU) in the mitogenomes of the *T. brachyrhabdion* **A** and *T. gracilis* **B**.

Table 2. Nucleotide composition of the mitochondrial genomes of *T. brachyrhabdion* (TB) and *T. gracilis* (TG).

	Length(bp)		A%		T%		G%		C%		A+T%		AT-skew		GC-skew	
	TB	TG	TB	TG	TB	TG	TB	TG	TB	TG	TB	TG	TB	TG	TB	TG
genome	16532	16533	31.02	31.03	27.05	27.14	15.55	15.52	26.38	26.31	58.07	58.17	0.0683	0.0669	-0.2585	-0.2580
PCGs	11405	11405	28.94	28.99	29.13	29.25	15.37	15.30	26.56	26.46	58.07	58.24	-0.0032	-0.0045	-0.2668	-0.2673
1st codon position	3806	3806	27.06	27.17	21.94	21.94	25.49	25.35	25.51	25.54	49.00	49.11	0.1046	0.1065	-0.0005	-0.0036
2nd codon position	3806	3806	18.61	18.63	40.87	40.95	13.55	13.53	26.97	26.89	59.47	59.58	-0.3743	-0.3746	-0.3312	-0.3307
3rd codon position	3806	3806	41.17	41.17	24.59	24.87	7.05	7.00	27.19	26.95	65.75	66.04	0.2522	0.2467	-0.5880	-0.5876
rRNA	2632	2632	34.77	34.65	22.38	22.34	19.64	19.72	23.21	23.29	57.14	56.99	0.2168	0.2160	-0.0833	-0.0830
tRNA	1566	1567	29.12	29.16	28.10	28.33	22.48	22.34	20.30	20.17	57.22	57.50	0.0179	0.0144	0.0507	0.0511
D-loop region	892	892	31.28	31.17	31.39	31.17	13.79	13.90	23.54	23.77	62.67	62.33	-0.0018	0.0000	-0.2613	-0.2619

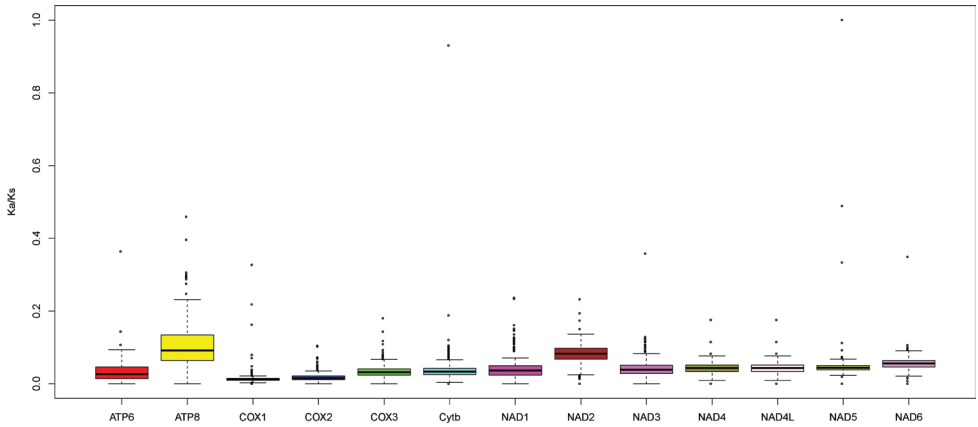

Figure 3. Ka/Ks of each PCG from 33 bagrid catfishes mitogenomes (*Rita rita* was excluded).

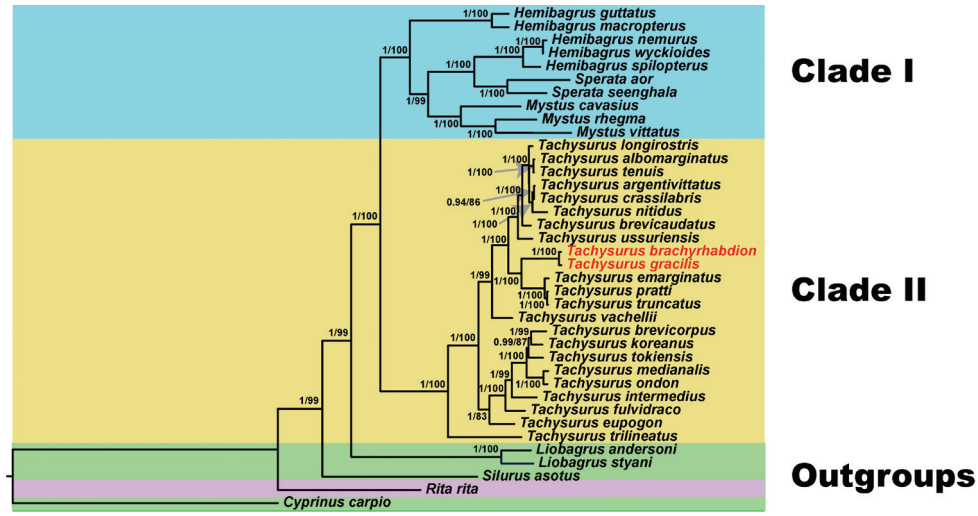

Figure 4. Phylogenetic tree obtained from BI and ML analysis based on the 13 PCGs dataset. The numbers at the nodes separated by "/" indicate the posterior probability (BI) and bootstrap value (ML).

Sperata, *Mystus*, and *Liobagrus* were strongly supported (Fig. 4). Nevertheless, the genus *Hemibagrus* was paraphyletic (Fig. 4). In addition, our phylogenetic trees showed that *T. brachyrhabdion* and *T. gracilis* clustered together forming a group.

Discussion

Over the past two to three decades, mitochondrial genes and genomes have been frequently used in fish studies (Xiao and Zhang 2000; Brown 2008; Zhang and Wang 2018). In this study, the complete mitochondrial genomes of *T. brachyrhabdion* and

T. gracilis were sequenced. The order and arrangement of the two mitogenomes were identical to that of other bagrid catfishes (Liang et al. 2014; Tian et al. 2016; Liu et al. 2019). The genomes had a total length of 16,532 bp and 16,533 bp, with A + T contents at 58.07% and 58.17%, respectively. These A+T biases were within the known range (56.37–59.80%) reported for mitochondrial genomes in closely related fishes (Tian et al. 2016; Liu et al. 2019).

Most of the PCGs of these two species had ATG as the start codon except *COI* that had GTG as the start codon. The *COI* gene usually uses GTG as the start codon in other fishes, such as *Lateolabrax*, *Sinocyclocheilus multipunctatus*, and *Microphysogobio elongatus* (Shan et al. 2016; Zhang and Wang 2018; Zhang et al. 2021). The PCGs of these two bagrid catfishes had an incomplete stop codon that was automatically filled by post-transcriptional polyadenylation (Ojala et al. 1981). This was a common character in metazoans mitogenomes (Shan et al. 2016; Jiang et al. 2019; Li et al. 2021). Twenty-one tRNA genes showed the typical cloverleaf secondary structure (Suppl. material 1, 2), while the tRNA-Ser^{AGY} gene lacked the dihydrouracil (DHU) arm as noted in other fish species (Zhang and Wang 2018; Zhang et al. 2021). The low Ka/Ks value for each PCG indicated that they were all under strong purifying selection. The DNA barcoding gene *COI* had the lowest evolutionary rate, consistent with the results observed from other fish groups (Sun et al. 2021; Yu et al. 2021).

Phylogenetic analysis revealed Bagridae was supported as a monophyletic group with *Rita rita* excluded (Fig. 4), which is consistent with previous phylogenetic studies (Sullivan et al. 2006; Vu et al. 2018). The phylogenetic tree suggested the classification of *R. rita* should be further revised and perfected. Clade I was composed of two monophyletic groups (*Sperata* and *Mystus*) and one paraphyletic group (*Hemibagrus*) (Fig. 4), which is consistent with the previous study of Liu et al. (2019). The traditional genera *Leiocassis*, *Pseudobagrus*, *Pelteobagrus*, and *Tachysurus* were not each monophyletic (Hardman 2005; Ku et al. 2007; Liu et al. 2019), but instead were grouped into *Tachysurus* as found in recent research (Cheng et al. 2021; Shao et al. 2021). Our results supported that the species in *Leiocassis*, *Pseudobagrus*, *Pelteobagrus*, and *Tachysurus* belong to the same genus, which by taxonomic priority should be *Tachysurus*. Thus, the current concept of *Tachysurus* includes the traditional genera *Leiocassis*, *Pseudobagrus*, *Pelteobagrus*, and *Tachysurus*. Due to limited sample size and molecular data, the phylogeny discussed in this research should be regarded as preliminary. The growing number of available mitogenomes will improve our understanding of the phylogeny and classification of bagrid catfish.

Conclusions

This study reported the complete mitochondrial genome sequences of two bagrid catfishes. The study showed that mitogenomes of Bagridae were conserved in structure, gene order, and nucleotide composition. Phylogenetic analysis confirmed that Bagridae is monophyletic group with *Rita rita* excluded and the traditional classification that *Leiocassis*, *Pseudobagrus*, *Pelteobagrus*, and *Tachysurus* belong to one genus.

Acknowledgements

This work was supported by the Joint Fund of the National Natural Science Foundation of China and the Karst Science Research Center of Guizhou Province (Grant No. U1812401), Guizhou Provincial Science and Technology Foundation (Qiankehejichu[2018]1113), Natural Science Foundation of Guizhou Educational Committee (QianjiaoheKY[2021]306) and the Undergraduate Research Training Program of Guizhou Normal University (DK2019A023).

References

Bernt M, Donath A, Juhling F, Externbrink F, Florentz C, Fritzsch G, Putz J, Middendorf M, Stadler PF (2013) MITOS: Improved de novo metazoan mitochondrial genome annotation. Molecular Phylogenetics and Evolution 69(2): 313–319. https://doi.org/10.1016/j.ympev.2012.08.023

Boore JL (1999) Animal mitochondrial genomes. Nucleic Acids Research 27(8): 1767–1780. https://doi.org/10.1093/nar/27.8.1767

Brown KH (2008) Fish mitochondrial genomics: Sequence, inheritance and functional variation. Journal of Fish Biology 72(2): 355–374. https://doi.org/10.1111/j.1095-8649.2007.01690.x

Chan PP, Lin BY, Mak AJ, Lowe TM (2021) tRNAscan-SE 2.0: Improved detection and functional classification of transfer RNA genes. Nucleic Acids Research 49(16): 9077–9096. https://doi.org/10.1093/nar/gkab688

Cheng JL, Ishihara H, Zhang E (2008) *Pseudobagrus brachyrhabdion*, a new catfish (Teleostei: Bagridae) from the middle Yangtze River drainage, South China. Ichthyological Research 55(2): 112–123. https://doi.org/10.1007/s10228-007-0020-3

Cheng JL, Shao WH, Lopez JA, Zhang E (2021) *Tachysurus lani*, a new catfish species (Teleostei: Bagridae) from the Pearl River basin, South China. Ichthyological Exploration of Freshwaters 30(4): 299–315. https://doi.org/10.23788/ief-1156

Fricke R, Eschmeyer WN, Van der Laan R (2022) Eschmeyer's catalog of fishes: genera, species, references. http://researcharchive.calacademy.org/research/ichthyology/catalog/fishcatmain.asp [Electronic version accessed 8 Mar. 2022]

Hardman M (2005) The phylogenetic relationships among non-diplomystid catfishes as inferred from mitochondrial cytochrome b sequences; the search for the ictalurid sister taxon (Otophysi: Siluriformes). Molecular Phylogenetics and Evolution 37(3): 700–720. https://doi.org/10.1016/j.ympev.2005.04.029

Jayaram KC (1968) Contributions to the study of bagrid fishes (Siluroidea: Bagridae). 3. A systematic account of the Japanese, Chinese, Malayan and Indonesian genera. Treubia 27(2–3): 287–386. https://doi.org/10.14203/treubia.v27i2-3.1560

Jiang L, Peng L, Tang M, You Z, Zhang M, West A, Ruan Q, Chen W, Merila J (2019) Complete mitochondrial genome sequence of the Himalayan Griffon, *Gyps himalayensis* (Accipitriformes: Accipitridae): Sequence, structure, and phylogenetic analyses. Ecology and Evolution 91(15): 8813–8828. https://doi.org/10.1002/ece3.5433

Katoh K, Standley DM (2013) MAFFT multiple sequence alignment software version 7: Improvements in performance and usability. Molecular Biology and Evolution 30(4): 772–780. https://doi.org/10.1093/molbev/mst010

Ku X, Peng Z, Diogo R, He S (2007) MtDNA phylogeny provides evidence of generic polyphyleticism for East Asian bagrid catfishes. Hydrobiologia 579(1): 147–159. https://doi.org/10.1007/s10750-006-0401-z

Lalitha S (2000) Primer Premier 5. Biotech Software & Internet Report 1(6): 270–272. https://doi.org/10.1089/152791600459894

Lanfear R, Frandsen PB, Wright AM, Senfeld T, Calcott B (2017) PartitionFinder 2: New methods for selecting partitioned models of evolution for molecular and morphological phylogenetic analyses. Molecular Biology and Evolution 34(3): 772–773. https://doi.org/10.1093/molbev/msw260

Li J, Chen XL, Chan B (2005) A new species of *Pseudobagrus* (Teleostei: Siluriformes: Bagridae) from southern China. Zootaxa 1067(1): 49–57. https://doi.org/10.11646/zootaxa.1067.1.3

Li R, Ying X, Deng W, Rong W, Li X (2021) Mitochondrial genomes of eight Scelieminae species (Orthoptera) and their phylogenetic implications within Tetrigoidea. PeerJ 9: e10523. https://doi.org/10.7717/peerj.10523

Liang HW, Meng Y, Li Z, Zhang Y, Zou GW (2014) Complete mitochondrial DNA genome of *Pseudobagrus brevicaudatus* (Siluriformes: Bagridae). Mitochondrial DNA 25(3): 169–170. https://doi.org/10.3109/19401736.2013.792060

Liu Y, Wu PD, Zhang DZ, Zhang HB, Tang BP, Liu QN, Dai LS (2019) Mitochondrial genome of the yellow catfish *Pelteobagrus fulvidraco* and insights into Bagridae phylogenetics. Genomics 111(6): 1258–1265. https://doi.org/10.1016/j.ygeno.2018.08.005

Minh BQ, Nguyen MA, von Haeseler A (2013) Ultrafast approximation for phylogenetic bootstrap. Molecular Biology and Evolution 30(5): 1188–1195. https://doi.org/10.1093/molbev/mst024

Mo TE (1992) Anatomy, relationships and systematics of the Bagridae (Teleostei: Siluroidei) with a hypothesis of siluroid phylogeny. Copeia 1992(4): 1132–1134. https://doi.org/10.2307/1446657

Nguyen LT, Schmidt HA, von Haeseler A, Minh BQ (2015) IQ-TREE: A fast and effective stochastic algorithm for estimating maximum-likelihood phylogenies. Molecular Biology and Evolution 32(1): 268–274. https://doi.org/10.1093/molbev/msu300

Ojala D, Montoya J, Attardi G (1981) tRNA punctuation model of RNA processing in human mitochondria. Nature 290(5806): 470–474. https://doi.org/10.1038/290470a0

Perna NT, Kocher TD (1995) Patterns of nucleotide composition at fourfold degenerate sites of animal mitochondrial genomes. Journal of Molecular Evolution 41(3): 353–358. https://doi.org/10.1007/BF01215182

Regan CT (1911) LXV. The classification of the Teleostean fishes of the order Ostariophysi. 2. Siluroidea. Annals & Magazine of Natural History 8(47): 553–577. https://doi.org/10.1080/00222931108693067

Ronquist F, Teslenko M, van der Mark P, Ayres DL, Darling A, Hohna S, Larget B, Liu L, Suchard MA, Huelsenbeck JP (2012) MrBayes 3.2: Efficient Bayesian phylogenetic inference and model choice across a large model space. Systematic Biology 61(3): 539–542. https://doi.org/10.1093/sysbio/sys029

Rozas J, Ferrer-Mata A, Sanchez-DelBarrio JC, Guirao-Rico S, Librado P, Ramos-Onsins SE, Sanchez-Gracia A (2017) DnaSP 6: DNA sequence polymorphism analysis of large data sets. Molecular Biology and Evolution 34(12): 3299–3302. https://doi.org/10.1093/molbev/msx248

Sambrook JE, Maniatis TE, Fritsch EF (1989) Molecular cloning: a laboratory manual. Cold spring harbor laboratory press.

Sato Y, Miya M, Fukunaga T, Sado T, Iwasaki W (2018) MitoFish and MiFish pipeline: A mitochondrial genome database of fish with an analysis pipeline for environmental DNA metabarcoding. Molecular Biology and Evolution 35(6): 1553–1555. https://doi.org/10.1093/molbev/msy074

Shan B, Song N, Han Z, Wang J, Gao T, Yokogawa K (2016) Complete mitochondrial genomes of three sea basses Lateolabrax (Perciformes, Lateolabracidae) species: Genome description and phylogenetic considerations. Biochemical Systematics and Ecology 67: 44–52. https://doi.org/10.1016/j.bse.2016.04.007

Shao WH, Cheng JL, Zhang E (2021) Eight in one: Hidden diversity of the bagrid catfish *Tachysurus albomarginatus* s.l. (Rendhal, 1928) widespread in lowlands of south China. Frontiers in Genetics 12: 713793. https://doi.org/10.3389/fgene.2021.713793

Sullivan JP, Lundberg JG, Hardman M (2006) A phylogenetic analysis of the major groups of catfishes (Teleostei: Siluriformes) using rag1 and rag2 nuclear gene sequences. Molecular Phylogenetics and Evolution 41(3): 636–662. https://doi.org/10.1016/j.ympev.2006.05.044

Sun CH, Liu HY, Xu N, Zhang XL, Zhang Q, Han BP (2021) Mitochondrial genome structures and phylogenetic analyses of two tropical characidae fishes. Frontiers in Genetics 12: e627402. https://doi.org/10.3389/fgene.2021.627402

Tamura K, Stecher G, Peterson D, Filipski A, Kumar S (2013) MEGA6: Molecular evolutionary genetics analysis version 6.0. Molecular Biology and Evolution 30(12): 2725–2729. https://doi.org/10.1093/molbev/mst197

Tian H, Que Y, Zhao N, Chen F, Zhu B, Huang D, Chang J, Liao X (2016) The complete mitochondrial genome of the spotted longbarbel catfish, *Hemibagrus guttatus* (Siluriformes, Bagridae). Mitochondrial DNA A: DNA Mapping. Sequencing, and Analysis 27(1): 467–468. https://doi.org/10.3109/19401736.2014.900670

Vu Q, Thi OT, Lan PTT, Linh TT, Thuy BD (2018) Molecular phylogeny of catfishes (Teleostei: Siluriformes) inferred from mitochondrial markers-implications for lower Mekong River basin. European Journal of Advanced Research in Biological and Life Sciences 6(3): 1–12.

Xiao WH, Zhang YP (2000) Genetics and evolution of mitochondrial DNA in fish. Shui Sheng Sheng Wu Hsueh Bao 24(4): 384–391. https://doi.org/1000-3207(2000)04-0384-08

Yu P, Zhou L, Yang WT, Miao LJ, Li Z, Zhang XJ, Wang Y, Gui JF (2021) Comparative mitogenome analyses uncover mitogenome features and phylogenetic implications of the subfamily Cobitinae. BMC Genomics 22(1): 50. https://doi.org/10.1186/s12864-020-07360-w

Zhang RY, Wang X (2018) Characterization and phylogenetic analysis of the complete mitogenome of a rare cavefish, *Sinocyclocheilus multipunctatus* (Cypriniformes: Cyprinidae). Genes & Genomics 40(10): 1033–1040. https://doi.org/10.1007/s13258-018-0711-3

Zhang D, Gao F, Jakovlic I, Zou H, Zhang J, Li WX, Wang GT (2020) PhyloSuite: An integrated and scalable desktop platform for streamlined molecular sequence data management

and evolutionary phylogenetics studies. Molecular Ecology Resources 20(1): 348–355. https://doi.org/10.1111/1755-0998.13096

Zhang RY, Tang Q, Deng L (2021) The complete mitochondrial genome of *Microphysogobio elongatus* (Teleostei, Cyprinidae) and its phylogenetic implications. ZooKeys 1061: 57–73. https://doi.org/10.3897/zookeys.1061.70176

Supplementary material 1

Figure S1. Predicted tRNA structures of *Tachysurus brachyrhabdion*

Authors: Renyi Zhang, Lei Deng1, Xiaomei Lv, Qian Tang

Data type: image

Link: https://doi.org/10.3897/zookeys.1115.85249.suppl1

Supplementary material 2

Figure S2. Predicted tRNA structures of *Tachysurus gracilis*

Authors: Renyi Zhang, Lei Deng1, Xiaomei Lv, Qian Tang

Data type: image

Link: https://doi.org/10.3897/zookeys.1115.85249.suppl2

Supplementary material 3

Table S1. Primers used for PCR

Authors: Renyi Zhang, Lei Deng1, Xiaomei Lv, Qian Tang

Data type:molecular data

Link: https://doi.org/10.3897/zookeys.1115.85249.suppl3

Supplementary material 4

Tables S2. Species, GenBank accession number and length of mitogenomes used in this study

Authors: Renyi Zhang, Lei Deng1, Xiaomei Lv, Qian Tang

Data type: molecular data

Link: https://doi.org/10.3897/zookeys.1115.85249.suppl4

Supplementary material 5

Table S3. Number of codons in *T. brachyrhabdion* (TB) and *T. gracilis* (TG) for mitochondrial PCGs

Authors: Renyi Zhang, Lei Deng1, Xiaomei Lv, Qian Tang

Data type: molecular data

Link: https://doi.org/10.3897/zookeys.1115.85249.suppl5

ZooKeys 1115: 117–150 (2022)
doi: 10.3897/zookeys.1115.83946
https://zookeys.pensoft.net

RESEARCH ARTICLE

A peer-reviewed open-access journal
ZooKeys
Launched to accelerate biodiversity research

Two new species of the dwarf centipede genus *Nannarrup* Foddai, Bonato, Pereira & Minelli, 2003 (Chilopoda, Geophilomorpha, Mecistocephalidae) from Japan

Sho Tsukamoto[1], Satoshi Shimano[2], Katsuyuki Eguchi[1,3]

1 *Systematic Zoology Laboratory, Graduate School of Science, Tokyo Metropolitan University, Minami-osawa 1-1 Hachioji-shi, Tokyo 192-0397, Japan* **2** *Science Research Center, Hosei University, Fujimi 2-17-1 Chiyoda-ku, Tokyo 102-8160, Japan* **3** *Department of International Health and Medical Anthropology, Institute of Tropical Medicine, Nagasaki University, Sakamoto 1-12-4, Nagasaki, Nagasaki 852-8523, Japan*

Corresponding author: Sho Tsukamoto (esutukamoto153@gmail.com)

Academic editor: Lucio Bonato | Received 17 March 2022 | Accepted 6 July 2022 | Published 1 August 2022

https://zoobank.org/AB895061-8444-4026-B593-37331E598259

Citation: Tsukamoto S, Shimano S, Eguchi K (2022) Two new species of the dwarf centipede genus *Nannarrup* Foddai, Bonato, Pereira & Minelli, 2003 (Chilopoda, Geophilomorpha, Mecistocephalidae) from Japan. ZooKeys 1115: 117–150. https://doi.org/10.3897/zookeys.1115.83946

Abstract

The genus *Nannarrup* Foddai, Bonato, Pereira & Minelli, 2003 is a monotypic genus established on the basis of the possibly introduced species *N. hoffmani* Foddai, Bonato, Pereira & Minelli, 2003, from New York, USA. In the present study, in a field survey conducted throughout Japan, *Nannarrup*-like specimens were collected from Honshu, Shikoku, and Kyushu. These specimens clearly showed the diagnostic characteristics of the genus but were morphologically distinct from *N. hoffmani*. Furthermore, morphological analysis and DNA barcoding revealed that these specimens could be assigned to two distinct undescribed species. On the basis of these results, *N. innuptus* Tsukamoto, **sp. nov.** and *N. oyamensis* Tsukamoto, **sp. nov.** are described. The three *Nannarrup* species can be distinguished from each other on the basis of the following combination of characteristics: presence or absence of a pair of smooth or weakly areolate areas along the posterior part of the paraclypeal sutures; the width-to-length ratio of the denticle on the trochanteroprefemur; the pigmentation of the denticle on the tarsungulum. Moreover, the field survey resulted in the collection of exclusively female specimens of *N. innuptus* Tsukamoto, **sp. nov.**, which shows the possibility of parthenogenesis of this species.

Keywords

Description, DNA barcoding, molecular phylogeny, morphology, sex ratio, taxonomy

Introduction

The geophilomorph family Mecistocephalidae Bollman, 1893, is a distinct monophyletic group, which is well characterized morphologically by a cephalic capsule and the forcipular segment that are obviously sclerotized and darker than the remaining trunk segments, the mandible with a series of pectinate lamellae only, trunk sternites with an internal apodeme, a mid-longitudinal sulcus, and the intraspecific invariance in the segment number, except in some species of the genus *Mecistocephalus* Newport, 1843 (Bonato et al. 2003, 2014; Uliana et al. 2007; Bonato 2011). The family is distributed mainly in tropical and subtropical regions and especially diversified at the species and higher phylogenetic levels in East Asia (Uliana et al. 2007; Bonato 2011). The family Mecistocephalidae comprises three subfamilies: Mecistocephalinae Bollman, 1893; Dicellophilinae Cook, 1896; and Arrupinae Chamberlin, 1912.

The subfamily Arrupinae comprises four valid genera: *Arrup* Chamberlin, 1912; *Agnostrup* Foddai, Bonato, Pereira & Minelli, 2003; *Partygarrupius* Verhoeff, 1939; *Nannarrup* Foddai, Bonato, Pereira & Minelli, 2003. Arrupinae has been reported mainly in East Asia and is diversified at the species level in Japan (Foddai et al. 2003; Uliana et al. 2007). To date, 21 species are reported in East Asia (18 spp.), Central Asia (1 sp.), California (1 sp.), New York (1 sp.), and 11 species are reported in Japan (Bonato et al. 2016).

The genus *Nannarrup* was established for a single species, *N. hoffmani* Foddai, Bonato, Pereira & Minelli, 2003. The genus has peculiar morphological characteristics (for details, see the section "Taxonomic account"), which likely evolved as a result of miniaturization. *Nannarrup hoffmani* was originally described on the basis of specimens from New York City, USA. Foddai et al. (2003) stated that the species has been definitely introduced from western America or East Asia. However, the native range of the species and the genus remain unknown.

In field surveys in Honshu, Shikoku and Kyushu, Japan (2017–2022), the authors of the present study (ST and KE) collected 88 mecistocephalid specimens, which clearly showed the diagnostic characteristics of the genus *Nannarrup*. However, these "*Nannarrup*-like" specimens can be distinguished from *N. hoffmani* by the shape of the denticle on the forcipular trochanteroprefemur. Therefore, the present study aimed to assign the Japanese "*Nannarrup*-like" specimens to the current classification of Arrupinae using an integrative approach of morphological analysis and DNA barcoding, using the mitochondrial *COI* and *16S* ribosomal RNA genes, and the nuclear *28S* ribosomal RNA genes.

Materials and methods

Taxon sampling

Eighty-eight "*Nannarrup*-like" specimens, including 13 juveniles (in which sex determination is not possible), were collected by hand from Honshu (Aomori, Akita, Iwate, Yamagata, Fukushima, Niigata, Tokyo, Kanagawa, Shizuoka, Wakayama, Hyogo,

Okayama, and Yamaguchi prefectures), Shikoku (Kochi and Ehime prefectures), and Kyushu (Fukuoka, Miyazaki, and Kagoshima prefectures). These specimens were included as ingroup in the present study. Each specimen was specified by its own specimen identification number in the form "TSYYYYMMDD-XX," where TS is an abbreviation of the first author's name, Tsukamoto Sho; YYYYMMDD designates the date on which the specimen was collected; XX is the identification number assigned to each specimen collected on a particular date (e.g., TS20171010-01).

Type specimens of *Nannarrup* were deposited at the Collection of Myriapoda, Department of Zoology, National Museum of Nature and Science, Tokyo (**NSMT**), and Museum of Nature and Human Activities, Hyogo (**MNHAH**). See the "Taxonomic account" section for the deposition site of each type specimen. All non-type voucher specimens of *Nannarrup* are retained by the first author. The collection sites of examined specimens are shown in Fig. 1 and Taxonomic account section. The altitude data provided by AW3D of JAXA (https://www.eorc.jaxa.jp/ALOS/jp/index_j.htm) and the coastal line provided by the digital nation land information (https://nlftp.mlit.go.jp/index.html) were used for generating Fig. 1.

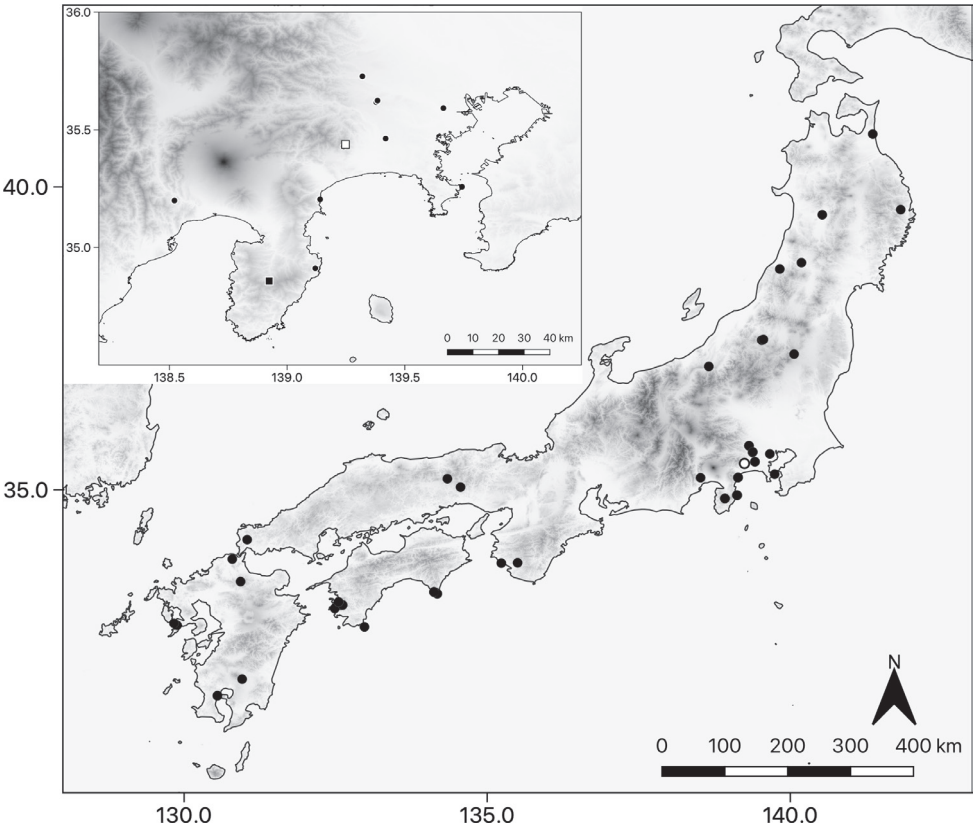

Figure 1. Map of collection sites of specimens examined in the present study. Black circle, *Nannarrup innuptus* sp. nov.; black square, the type locality of *N. innuptus* sp. nov.; white circle, *N. oyamensis* sp. nov.; white square, the type locality of *N. oyamensis* sp. nov.

Morphological analysis

Cephalic capsule, maxillae, mandibles, the forcipular segment and leg-bearing segments were made transparent using lactic acid or the Chelex-TE protocol to examine the anatomy and produce images (Satria et al. 2015). Cephalic capsule and maxillae of some specimens were mounted in Hoyer's medium (gum arabic, chloral hydrate, and glycerol) or Euparal. Multi-focused images of these body parts were produced using Helicon Focus Pro 6.7.1 (https://www.heliconsoft.com/helicon-focus-history-of-changes-win/) from a series of source images taken using a Canon EOS Kiss X9 digital camera attached to a Nikon AZ100 microscope and improved using Adobe Photoshop Elements 10. Body parts were then measured directly using an ocular micrometer attached to the microscope or by measuring on the basis of the images using ImageJ software (http://imageJ.nih.gov/ij/). The morphological terminology used in the present study is mainly derived from Bonato et al. (2010). Specimens with fully developed paired gonopods—that is, evidently bi-articulated in males and touching each other in females—were determined to be adults, and those with incompletely developed paired gonopods were determined to be subadults; specimens without gonopods were determined to be juveniles.

DNA sequencing

Genomic DNA was extracted from one or two legs, the head, or a body segment of each specimen by following the Chelex-TE-ProK protocol (Satria et al. 2015) with incubation for 24 h.

PCR amplification was performed in a MiniAmp Thermal Cycler (Thermo Fisher Scientific, Waltham, Massachusetts, USA) in a 10.5-μL reaction volume containing 5 μL 2× PCR buffer for KOD FX Neo, 2 μL of 2 mM dNTPs, 0.3 μL of 10 pmol/μL forward and reverse primers, 0.2 μL of 1.0 U/μL DNA polymerase KOD FX Neo (TOYOBO KFX-201X5), and 1.0 μL DNA template. The sequences of primers for the mitochondrial *COI* and *16S* and nuclear *28S* genes are shown in Table 1. Each PCR product was screened by electrophoresis on 2.0% agarose gel in 1× TAE.

Amplification conditions for mitochondrial *COI* were as follows: 98 °C for 2 min; 5 cycles of 98 °C for 10 s, 45 °C for 30 s, and 68 °C for 45 s; 40 cycles of 98 °C for 10 s, 48.5 °C for 30 s (annealing step), and 68 °C for 45 s; and 68 °C for 7 min. If the target fragment of *COI* was not appropriately amplified, the annealing temperature was changed from 48.5 °C to 50 °C, and PCR was performed again by omitting the first five cycles of annealing and the extension step.

Amplification conditions for mitochondrial *16S* were as follows: 98 °C for 2 min; 35 cycles of 98 °C for 10 s, 45 °C for 30 s (annealing step), and 68 °C for 45 s; and 68 °C for 7 min. If the target fragment of *16S* was not appropriately amplified, the annealing temperature was changed from 45 °C to 48 °C, and the number of annealing cycles was changed from 35 to 45.

Table 1. The list of primers used in the present study.

Genes	Primer name	Sequence (5' - 3')	Source
COI	LCO-CH	TTT CAA CAA AYC AYA AAG ACA TYG G	Tsukamoto et al. (2021)
	HCO-CH	TAA ACT TCT GGR TGR CCR AAR AAT CA	
16S rRNA	16Sa	CGC CTG TTT ATC AAA AAC AT	Xiong and Kocher (1991)
	16Sbi	CTC CGG TTT GAA CTC AGA TCA	
28S rRNA	28S D1F	GGG ACT ACC CCC TGA ATT TAA GCA T	Boyer and Giribet (2007)
	28S rD4b	CCT TGG TCC GTG TTT CAA GAC	Edgecombe and Giribet (2006)

Amplification conditions for nuclear *28S* were as follows: 98 °C for 2 min; 5 cycles of 98 °C for 10 s, 42 °C for 30 s, and 68 °C for 1 min; 30 cycles of 98 °C for 10 s, 50 °C for 30 s (annealing step), and 68 °C for 1 min; and 68 °C for 7 min. If the target fragment of *28S* was not appropriately amplified, the annealing temperature was changed from 50 °C to 48 °C, and the number of annealing cycles was changed from 30 to 40–45 cycles. Furthermore, PCR was performed again by omitting the first five cycles of annealing and the extension step.

The amplified products were incubated at 37 °C for 30 min and 80 °C for 20 min with IllustraTM ExoStar (GE Healthcare, Buckinghamshire, UK) to remove any excess primers and nucleotides. All nucleotide sequences were determined by direct sequencing using ABI PRISM BigDye Terminator Cycle Sequencing Kit ver. 3.1 (Thermo Fisher Scientific) or BrilliantDyeTM Terminator Cycle Sequencing Kit v. 3.1 (Nimagen, B.V., Nijmegen, Netherlands) with an ABI 3130xl automated sequencer (Thermo Fisher Scientific). The sequences were assembled using ChromasPro 1.7.6 (Technelysium Pty Ltd., Australia) and deposited in the databases DDBJ, EMBL, and GenBank under the accession numbers LC715482–LC715706 (Table 2).

Molecular phylogenetic analyses

The sequences obtained using the methods described above were used for phylogenetic analyses; the *COI*, *16S*, and *28S* sequences of the mecistocephalid species *Dicellophilus carniolensis* C.L. Koch, 1847; *Mecistocephalus guildingii* Newport, 1843; and *Mecistocephalus subgigas* (Silvestri, 1919), obtained from GenBank were used as outgroups (Table 2).

All sequences were aligned using MAFFT v. 7.475 (Katoh and Standley 2013). For *COI*, the alignment was performed using the default setting. For *16S* and *28S*, secondary structure alignment was performed using the X-INS-i option.

Maximum-likelihood (**ML**) trees were created on the basis of the sequence dataset for each gene using IQ-tree 1.6.12 (Nguyen et al. 2015). In the ML analysis for the *COI* dataset, TN + F was selected for the first codon position, TNe + G4 was selected for the second codon position, and F81 + F was selected for the third codon position as the optimal substitution model according to the Bayesian information criterion (BIC). In the ML analysis for the *16S* dataset, TIM3 + F + I + G4 was selected as the optimal substitution model according to BIC. In the ML analysis for the *28S* dataset,

Table 2. The list of specimens that were used in the phylogenetic analyses.

Species	Accession No.			Reference
	COI	16S	28S	
Nannarrup innuptus sp. nov.	LC715482–LC715554	LC715557–LC715629	LC715632–LC715704	the present study
Nannarrup oyamensis sp. nov.	LC715455–LC715556	LC715530–LC715631	LC715605–LC715706	the present study
Dicellophilus carniolensis (C.L. Koch, 1847)	KF569305	HM453225	HM453285	Murienne et al. (2010), Bonato et al. (2014)
Mecistocephalus guildingii Newport, 1843	AY288747	AY288728	HM453283	Edgecombe and Giribet (2004), Murienne et al. (2010)
Mecistocephalus subgigas (Silvestri, 1919)	AF370837	AF370862	HM453284	Giribet et al. (2001), Murienne et al. (2010)

TIM3e + G4 was selected as the optimal substitution model according to BIC. Ultrafast bootstrap analysis (**UFBoot**; Hoang et al. 2018) and SH-like approximate likelihood ratio test (**SH-aLRT**; Guindon et al. 2010) were performed with 1,000 replicates.

Calculation of genetic distances

Aligned datasets (*COI*, *16S*, and *28S*) used for phylogenetic analyses were also used to calculate the genetic distances. Pairwise p-distances and Kimura-two-parameter (K2P) distances were calculated for each of the three genes of "*Nannarrup*-like" specimens using MEGA X (Kumar et al. 2018) using the setting "pairwise deletion."

Results

Taxonomic position of "*Nannarrup*-like" specimens

All 88 "*Nannarrup*-like" specimens collected in Japan possessed the diagnostic characteristics of the subfamily Arrupinae (Bonato et al. 2003): body tapering backwards; leg-bearing trunk uniform in color, without dark patches; clypeus with 11–17 clypeal setae, placed in two lateral areas; internal margin of labral anterior ala reduced to a pointed end; posterior alae without longitudinal stripes; posterior margin of labral side-piece sinuous (and with short fringe, in contrast to "diagnosis" of Arrupinae in Bonato et al (2003)); cerrus absent.

Furthermore, these "*Nannarrup*-like" specimens possessed the diagnostic characteristics of the genus *Nannarrup* established by Foddai et al. (2003) on the basis of *N. hoffmani*: body length ca 10-mm long in adults, with 41 pairs of legs; frontal line absent; clypeus with two small plagulae; clypeal ratio ca 1:6–1:7; cephalic pleurites with a pair of short stili, without setae and a pair of spicula; side pieces of labrum subdivided into anterior and posterior alae; mandible with four well-developed pectinate lamellae; first maxillae separated from each other by a longitudinal line at the

coxosternite; second maxillae not separated from each other at the coxosternite, with metameric pores close to the posterior margin, without claw; forcipular telopodites not reaching the anterior margin of the head in the closed position; trochanteroprefemur with single distal denticle; forcipular femur without teeth; tarsungulum with basal, well-developed denticle; forcipular tergite without median sulcus; sternites with sulcus, which is not anteriorly furcate; last metasternite subtriangular; ventral surface of each coxopleurite with numerous pores; anal pores present.

These "*Nannarrup*-like" specimens (and even *N. hoffmani*) can be distinguished from the genus *Arrup*, which is speciose in the Japanese Archipelago (Uliana et al. 2007), by first maxillae separated from each other by a longitudinal line at the coxosternite. In addition, they can be distinguished from *Agnostrup* and *Partygarrupius*, that are also known from Japan, by two small clypeal plagulae (plagulae of *Agnostrup* and *Partygarrupius* covered one-half to most of their clypeus (Foddai et al. 2003; Uliana et al. 2007)). Therefore, these "*Nannarrup*-like" specimens were confidently assigned to *Nannarrup*.

Morphological comparison between Japanese *Nannarrup* and *N. hoffmani*

The Japanese *Nannarrup* specimens were distinguishable from *N. hoffmani* on the basis of two morphological characteristics: the width-to-length ratio of the denticle of the trochanteroprefemur, which was 1:0.53 in *N. hoffmani* (measured from fig. 14 in Foddai et al. (2003)) but 1:1.3–1.6 in the Japanese specimens; pigmentation of the denticle on the tarsungulum was less prominent than that of the denticle on the trochanteroprefemur in *N. hoffmani* but equivalent to that in the Japanese specimens (Foddai et al. 2003).

In two specimens from Kanagawa prefecture, in the Kanto Region of Japan (TS20210217-04 and TS20210725-02), "two additional smooth areas along the posterior part of the paraclypeal sutures" in the clypeus (sensu Foddai et al. (2003)) were not observed. However, this characteristic was observed in the remaining Japanese *Nannarrup* specimens.

Therefore, the Japanese *Nannarrup* specimens were divided into two morphospecies, namely *N.* sp. 1 and *N.* sp. 2 (see Table 3), both of which were morphologically distinct from *N. hoffmani*.

Table 3. Morphological comparison among three species of the genus *Nannarrup*.

Species	Clypeus	Forcipule	
	Two additional smooth areas along paraclypeal sutures	**The width to length ratio of the denticle on trochanteroprefemur**	**Pigmentation of the tooth on the tarsungulum**
Nannarrup innuptus sp. nov. (= *Nannarrup* sp. 1)	+	1: 1.3–1.6	equal to the denticle on trochanteroprefemur
Nannarrup oyamensis sp. nov. (= *Nannarrup* sp. 2)	-	1: 1.3	equal to the denticle on trochanteroprefemur
Nannarrup hoffmani Foddai, Bonato, Pereira & Minelli, 2003	+	1: 0.5	slighter than the denticle on trochanteroprefemur

Molecular phylogenetic analyses

The *COI*, *16S*, and *28S* sequences were successfully determined for 73 specimens of *Nannarrup* sp. 1 (except for two specimens from Tokyo, i.e., TS20171010-01 and TS20180627-01) and both specimens of *N*. sp. 2.

In the ML phylogenetic trees based on the *COI* dataset (Fig. 2), the clade comprising *N*. sp. 1 and *N*. sp. 2 was moderately supported (UFBoot = 81.2%, SH-aLRT = 94%). However, *N*. sp. 1 and *N*. sp. 2 were distinctly separated from each other, and each morphospecies was strongly supported in monophyly (UFBoot = 98.5%, SH-aLRT = 96%

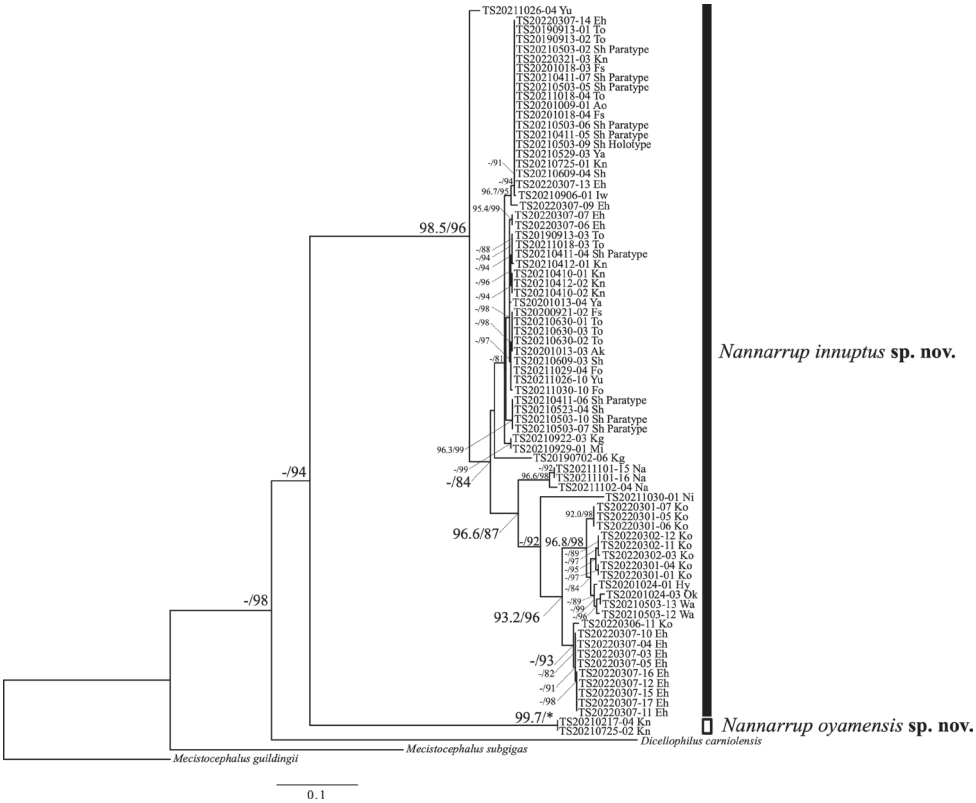

Figure 2. Maximum-likelihood tree of *Nannarrup* specimens and outgroups (*Mecistocephalus guildingii*, *M. subgigas*, and *Dicellophilus carniolensis*) based on the *COI* dataset. Nodal values are derived from Ultrafast bootstrap (UFBoot) and SH-like approximate likelihood ratio test (SH-aLRT). Asterisk (*) indicates values of 100% in UFBoot and SH-aLRT. A hyphen (-) indicates values <95% in UFBoot and <80% in SH-aLRT. Nodal values are not shown when both UFBoot and SH-aLRT values are <95% and <80%, respectively. The unit of evolutionary distance is the number of base substitutions per site. Ingroup specimens are shown as their specimen identification number. Abbreviations: Ao = Aomori pref.; Ak = Akita pref.; Iw = Iwate pref.; Ya = Yamagata pref.; Fs = Fukushima pref.; Ni = Niigata pref.; To = Tokyo pref.; Kn = Kanagawa pref.; Sh = Shizuoka pref.; Wa = Wakayama pref.; Hy = Hyogo pref.; Ok = Okayama pref.; Yu = Yamaguchi pref.; Ko = Kochi pref.; Eh = Ehime pref.; Fo = Fukuoka pref.; Mi = Miyazaki pref.; Kg = Kagoshima pref.

in *N*. sp. 1; UFBoot = 99.7%, SH-aLRT = 100% in *N*. sp. 2). The intraspecific phylogeographic structure of *N*. sp. 1 remains unclear because of low support values. It is noteworthy that one specimen, TS20210725-01, had been collected near the collection site of *N*. sp. 2, but this specimen was included in the *N*. sp. 1 clade (see also Fig. 1).

The ML phylogenetic trees based on the *16S* dataset (Fig. 3) showed that the clade comprising *N*. sp. 1 and *N*. sp. 2 was highly supported (UFBoot = 98.9%, SH-aLRT = 100%), and *N*. sp. 1 and *N*. sp. 2 were also distinctly separated from each other. Each morphospecies was also strongly supported in their monophyly, as observed in the phylogenetic trees based on the *COI* dataset (UFBoot = 92.4%, SH-aLRT = 97%

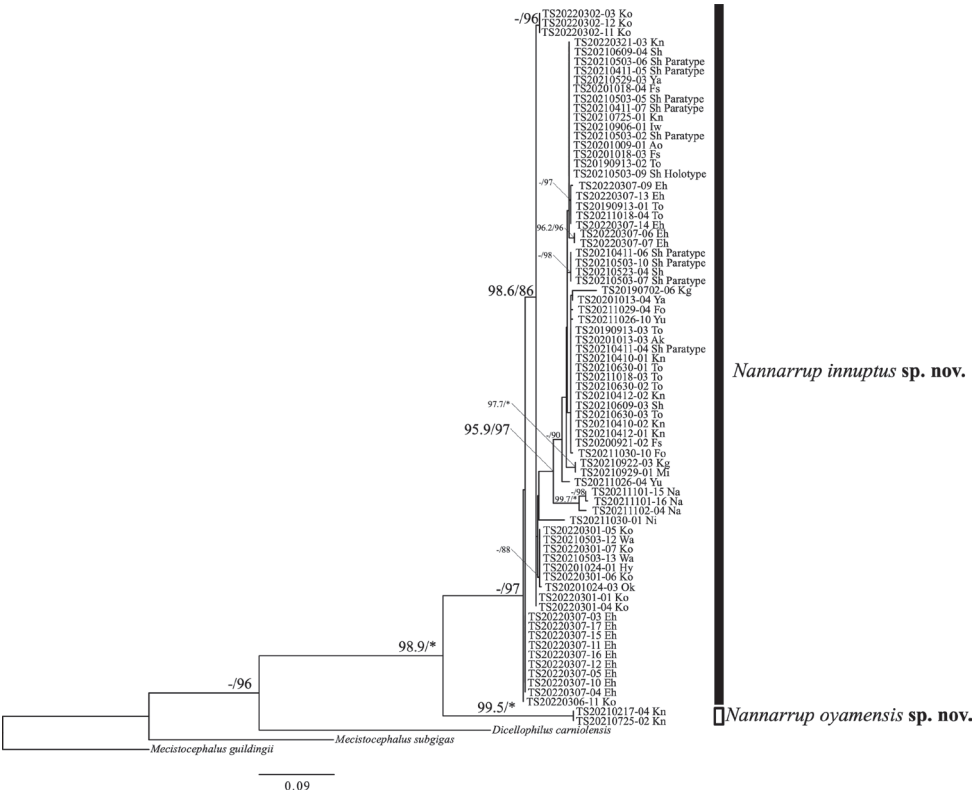

Figure 3. Maximum-likelihood tree of *Nannarrup* specimens and outgroups (*Mecistocephalus guildingii*, *M. subgigas,* and *Dicellophilus carniolensis*) based on the *16S* dataset. Nodal values are derived from Ultrafast bootstrap (UFBoot) and SH-like approximate likelihood ratio test (SH-aLRT). Asterisk (*) indicates values of 100% in UFBoot and SH-aLRT. A hyphen (-) shows < 95% in UFBoot and < 80% in SH-aLRT. Nodal values are not shown when both UFBoot and SH-aLRT values are < 95% and < 80%, respectively. The unit of evolutionary distance is the number of base substitutions per site. Ingroup specimens are shown as their specimen identification number. Abbreviations: Ao = Aomori pref.; Ak = Akita pref.; Iw = Iwate pref.; Ya = Yamagata pref.; Fs = Fukushima pref.; Ni = Niigata pref.; To = Tokyo pref.; Kn = Kanagawa pref.; Sh = Shizuoka pref.; Wa = Wakayama pref.; Hy = Hyogo pref.; Ok = Okayama pref.; Yu = Yamaguchi pref.; Ko = Kochi pref.; Eh = Ehime pref.; Fo = Fukuoka pref.; Mi = Miyazaki pref.; Kg = Kagoshima pref.

in *N*. sp. 1; UFBoot = 99.5%, SH-aLRT = 100% in *N*. sp. 2). The intraspecific phylogeographic structure of *N*. sp. 1 remains obscure because of low support values. TS20210725-01 is included in the *N*. sp. 1 clade as seen in the *COI* trees.

In the ML phylogenetic trees based on the *28S* dataset (Fig. 4), the clade comprising *N*. sp. 1 and *N*. sp. 2 was strongly supported (UFBoot = 98.3%, SH-aLRT = 99%). The monophyly of *N*. sp. 1 was not well supported (UFBoot = 62.6%, SH-aLRT = 49%), but the monophyly of *N*. sp. 2 was moderately supported (UFBoot = 91.7%, SH-aLRT = 97%).

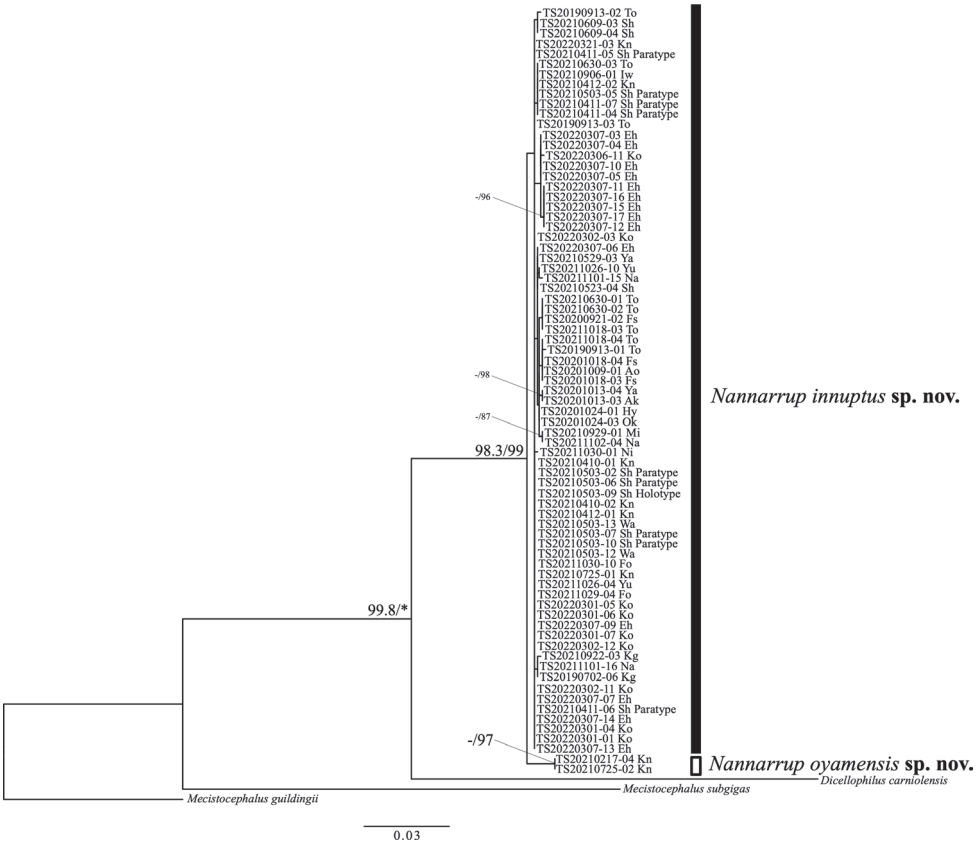

Figure 4. Maximum-likelihood tree of *Nannarrup* specimens and outgroups (*Mecistocephalus guildingii*, *M. subgigas*, and *Dicellophilus carniolensis*) based on the *28S* dataset. Nodal values are derived from Ultrafast bootstrap (UFBoot) and SH-like approximate likelihood ratio test (SH-aLRT). Asterisk (*) indicates values of 100% in UFBoot and SH-aLRT. A hyphen (-) shows < 95% in UFBoot and < 80% in SH-aLRT. Nodal values are not shown when both UFBoot and SH-aLRT values are < 95% and < 80%, respectively. The unit of evolutionary distance is the number of base substitutions per site. Ingroup specimens are shown as their specimen identification number. Abbreviations: Ao = Aomori pref.; Ak = Akita pref.; Iw = Iwate pref.; Ya = Yamagata pref.; Fs = Fukushima pref.; Ni = Niigata pref.; To = Tokyo pref.; Kn = Kanagawa pref.; Sh = Shizuoka pref.; Wa = Wakayama pref.; Hy = Hyogo pref.; Ok = Okayama pref.; Yu = Yamaguchi pref.; Ko = Kochi pref.; Eh = Ehime pref.; Fo = Fukuoka pref.; Mi = Miyazaki pref.; Kg = Kagoshima pref.

DNA barcoding of the Japanese *Nannarrup* specimens

According to the *COI* dataset of *Nannarrup*, the minimum divergence between *N.* sp. 1 and *N.* sp. 2 was 14.13% in p-distance and 15.73% in K2P distance (TS20211101-15 and TS20211101-16 from Nagasaki prefecture vs TS20210217-04 and TS20210725-02 from Kanagawa prefecture), whereas the maximum internal divergence within *N.* sp. 1 was 9.726% in p-distance and 10.58% in K2P distance (TS20211030-01 from Niigata prefecture vs TS20210412-01 from Kanagawa prefecture).

According to the *16S* dataset of *Nannarrup*, the minimum divergence between *N.* sp. 1 and *N.* sp. 2 was 14.92% in p-distance and 16.68% in K2P distance (TS20220306-11 from Kochi prefecture and TS20220307-03, TS20220307-04, TS20220307-05, TS20220307-11, TS20220307-12, TS20220307-15, TS20220307-16, TS20220307-17 from Ehime prefecture vs TS20210217-04 and TS20210725-02 from Kanagawa prefecture), whereas the maximum internal divergence within *N.* sp. 1 was 7.056% in p-distance and 7.443% in K2P distance (TS20211030-01 from Niigata prefecture vs TS20211102-04 from Nagasaki prefecture).

According to the *28S* dataset of *Nannarrup*, the minimum divergence between *N.* sp. 1 and *N.* sp. 2 was 1.207% in p-distance and 1.218% in K2P distance (TS20220301-01, TS20220301-04 TS20220302-03, TS20220302-11 from Kochi prefecture, TS20220307-07, TS20220307-13, TS20220307-14 from Ehime prefecture and TS20200411-06 from Shizuoka prefecture vs TS20210217-04 and TS20210725-02 from Kanagawa prefecture), whereas the maximum internal divergence within *N.* sp. 1 was 0.6757% in p-distance and 0.6796% in K2P distance (TS20220307-11, TS20220307-12, TS20220307-15, TS20220307-16, TS20220307-17 from Ehime prefecture vs TS20190913-01 from Tokyo prefecture).

Taxonomic account

Family Mecistocephalidae Bollmann, 1893

Genus *Nannarrup* Foddai, Bonato, Pereira & Minelli, 2003
New Japanese name: Himejimukade-zoku
Fig. 5

Nannarrup Foddai, Bonato, Pereira & Minelli, 2003: 1255–1256.

Type species. *Nannarrup hoffmani* Foddai, Bonato, Pereira & Minelli, 2003

Diagnosis. Partly modified from Foddai et al. (2003). Adult body length ca 10 mm (Fig. 5A). Cephalic plate only slightly longer than wide, with frontal line absent or replaced by areolation. Two small clypeal plagulae covering ca one-sixth of the clypeus. Bucca without setae. Stilus present, relatively short. Spiculum absent. Side-pieces of labrum only incompletely subdivided into anterior and posterior alae by fragmented line very poorly marked. Mandible provided with four well-developed pectinate lamellae. Coxosternite of

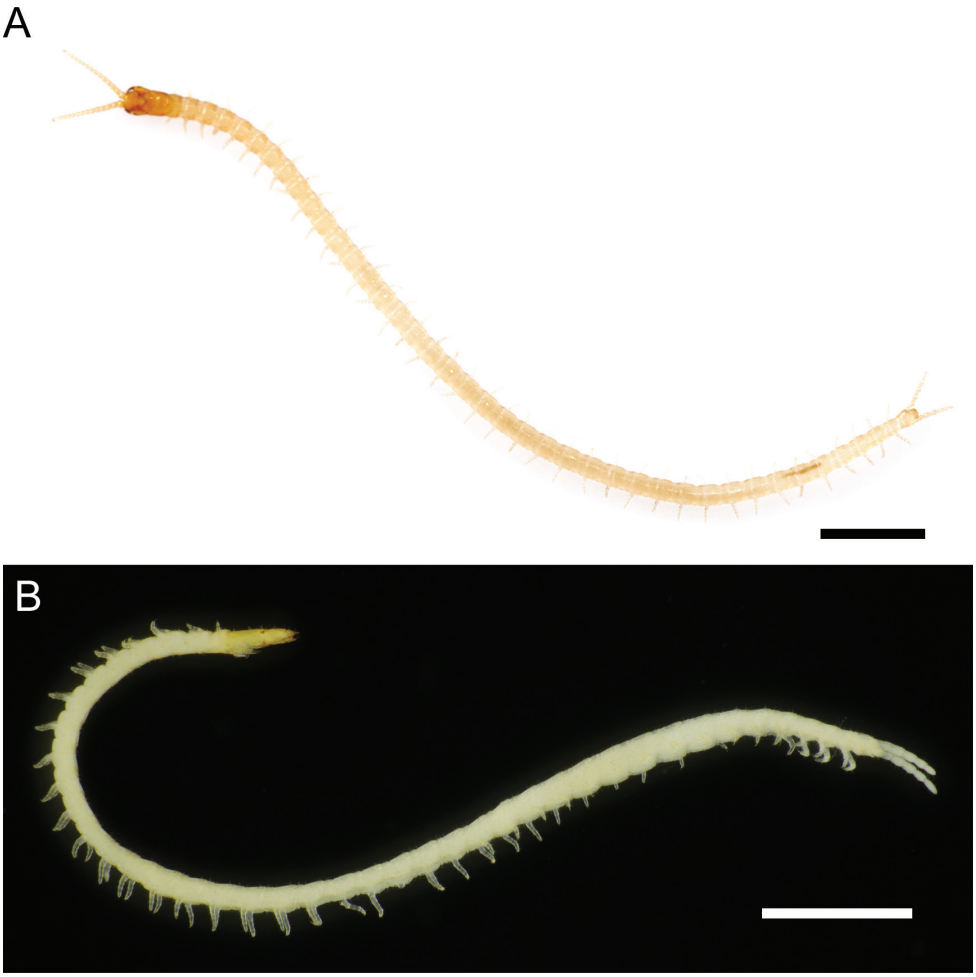

Figure 5. *Nannarrup innuptus* sp. nov., paratype (TS20210503-02) **A** habitus (provided by Dr Namiki Kikuchi) **B** "death pose" with head capsule detached. Scale bars: 1 mm.

first maxillae medially divided. Coxosternite of second maxillae undivided, without suture or membranous isthmus. Metameric pore close to posterior margin of coxosternum of second maxillae, not to lateral ones. Claw of second maxillae only represented by terminal spine. Forcipular telopodites far behind anterior margin of head in the closed position. Forcipular trochanteroprefemur with pigmented single distal denticle; femur without teeth; tarsungulum with basal, well-developed denticle. Forcipular tergite without median sulcus. Sternal sulcus not anteriorly furcate. Last metasternite subtriangular. Ventral surface of each coxopleuron with numerous pores. Anal pore present. Forty-one pairs of legs.

Remarks. The following characters included in the diagnosis sensu Foddai et al. (2003) are different among the three *Nannarrup* species: presence/absence of a pair of smooth or areolate areas along the posterior part of the paraclypeal sutures, pres-

ence/absence of a tubercle on the forcipular tibia, pigmentation of the denticle on the tarsungulum (Table 3). In total, 74 out of 88 collected specimens of *Nannarrup* (ca 84%) exhibited a leaning posture or even threw back their head when stored in ethanol (Fig. 5B). Although such a "death pose" has not been quantitatively investigated in Geophilomorpha, in the authors' experience, it is a unique phenomenon in *Nannarrup* that may be related to the internal morphological characteristics of the genus.

***Nannarrup innuptus* Tsukamoto, sp. nov.**

https://zoobank.org/D2906856-517E-45BE-B2A0-1FE9CBD4D779

New Japanese name: Kaguya-himejimukade

Figs 5–11

Type material. ***Holotype*.** 1 adult female, Yugashima, Izu-shi, Shizuoka prefecture, Japan (34°51.39'N, 138°55.40'E), 3 May 2021, coll. Mayu Susukida (labeled as TS20210503-09), deposited at the Collection of Myriapoda, Department of Zoology, **NSMT**.

***Paratype*.** 4 females, Yugashima, Izu-shi, Shizuoka prefecture, Japan (34°51.39'N, 138°55.39'E), 11 April 2021, leg. Katsuyuki Eguchi (labeled as TS20210411-04, TS20210411-05, TS20210411-06, TS20210411-07, respectively), deposited at the Collection of Myriapoda, Department of Zoology, **NSMT**. 5 females, Yugashima, Izu-shi, Shizuoka prefecture, Japan (34°51.39'N, 138°55.40'E), 3 May 2021, leg. Mayu Susukida (labeled as TS20210503-02, TS20210503-05, TS20210503-06, TS20210503-07, TS20210503-10, respectively), deposited at **MNHAH**.

Non-type specimens. 1 female, Minamiosawa, Hachioji-shi, Tokyo prefecture, Japan (35°37.02'N, 139°22.73'E), 27 June 2018, leg. Sho Tsukamoto (labeled as TS20180627-01). 1 female, Hirasawa, Akiruno-shi, Tokyo prefecture, Japan (35°43.64'N, 139°19.20'E), 10 October 2017, leg. Sho Tsukamoto (labeled as TS20171010-01). 3 females, Hirasawa, Akiruno-shi, Tokyo prefecture, Japan (35°43.64'N, 139°19.20'E), 13 September 2019, leg. Sho Tsukamoto (labeled as TS20190913-01, TS20190913-02, TS20190913-03, respectively). 1 female, Shiroyama, Kagoshima-shi, Kagoshima prefecture, Japan (31°35.88'N, 130°32.98'E), 2 July 2019, leg. Sho Tsukamoto (labeled as TS20190702-06). 1 female, Shibakusa, Hatori, Ten-ei-mura, Iwase-gun, Fukushima prefecture, Japan (37°14.37'N, 140°03.86'E), 21 September 2020, leg. Katsuyuki Eguchi (labeled as TS20200921-02). 1 female, Kubo, Hiranuma, Rokkasho-mura, Kamikita-gun, Aomori prefecture, Japan (40°52.37'N, 141°21.76'E), 9 October 2020, leg. Katsuyuki Eguchi (labeled as TS20201009-01). 1 female, Nakagawara, Nagano, Daisen-shi, Akita prefecture, Japan (39°32.41'N, 140°31.76'E), 13 October 2020, leg. Katsuyuki Eguchi (labeled as TS20201013-03). 1 female, Mukounadaka, Nadaka, Tozawa-mura, Mogami-gun, Yamagata prefecture, Japan (38°44.96'N, 140°11.15'E), 13 October 2020, leg. Katsuyuki Eguchi (labeled as TS20201013-04). 1 female, Nakagawa, Kaneyama-machi, Onuma-gun, Fukushima prefecture, Japan (37°28.25'N, 139°31.81'E), 18 October 2020, leg. Katsuyuki Eguchi

(labeled as TS20201018-03). 1 female, Sawanishi, Mizunuma, Kaneyama-machi, Onuma-gun, Fukushima prefecture, Japan (37°28.87'N, 139°33.48'E), 18 October 2020, leg. Katsuyuki Eguchi (labeled as TS20201018-04). 1 female, Tai, Yamasaki-cho, Shisou-shi, Hyogo prefecture, Japan (35°02.62'N, 134°33.68'E), 24 October 2020, leg. Katsuyuki Eguchi (labeled as TS20201024-01). 1 female, Kageishi, Nishiawakura-son, Aida-gun, Okayama prefecture, Japan (35°10.94'N, 134°20.64'E), 24 October 2020, leg. Katsuyuki Eguchi (labeled as TS20201024-03). 2 females and 2 juveniles (sex unknown), Teraodai, Ayase-shi, Kanagawa prefecture, Japan (35°27.76'N, 139°25.13'E), 10 April 2021, leg. Joe Kutsukake (labeled as TS20210410-01 and TS20210410-02 for females, TS20210410-03 and TS20210410-04 for juveniles, respectively). 2 females, Nebukawa, Odawara-shi, Kanagawa prefecture, Japan (35°12.00'N, 139°08.22'E), 12 April 2021, leg. Joe Kutsukake (labeled as TS20210412-01 and TS20210412-02, respectively). 3 juveniles (sex unknown), Nebukawa, Odawara-shi, Kanagawa prefecture, Japan (35°12.23'N, 139°08.43'E), 12 April 2021, leg. Joe Kutsukake (labeled as TS20210412-03, TS20210412-04 and TS20210412-05, respectively). 1 female, Shimada, Inami-cho, Hidaka-gun, Wakayama prefecture, Japan (33°47.36'N, 135°14.06'E), 3 of May 2021, leg. Katsuyuki Eguchi (labeled as TS20210503-12). 1 female, Kurisugawa, Nakahechi-cho, Tanabe-shi, Wakayama prefecture, Japan (33°47.69'N, 135°30.16'E), 3 of May 2021, leg. Katsuyuki Eguchi (labeled as TS20210503-13). 1 female, Futo, Ito-shi, Shizuoka prefecture, Japan (34°54.58'N, 139°07.72'E), 9 June 2021, leg. Joe Kutsukake (labeled as TS20210609-03). 1 female, Futo, Ito-shi, Shizuoka prefecture, Japan (34°54.66'N, 139°07.19'E), 9 June 2021, leg. Joe Kutsukake (labeled as TS20210609-04). 1 juvenile (sex unknown), Shishihara, Shimizu-ku, Shizuoka-shi, Shizuoka prefecture, Japan (35°11.94'N, 138°31.28'E), 23 of May 2021, leg. Katsuyuki Eguchi (labeled as TS20210523-04). 1 female, Nishiaraya, Tsuruoka-shi, Yamagata prefecture, Japan (38°38.64'N, 139°49.73'E), 29 May 2021, leg. Katsuyuki Eguchi (labeled as TS20210529-03). 3 females, Den-enchofu, Ota-ku, Tokyo prefecture, Japan (35°35.51'N, 139°39.86'E), 30 June 2021, leg. Joe Kutsukake (labeled as TS20210630-01, TS20210630-02 and TS20210630-03). 1 subadult female, Oyama, Isehara-shi, Kanagawa prefecture, Japan (35°25.74'N, 139°14.44'E), 25 July 2021, coll. Sho Tsukamoto (labeled as TS20210725-01; cephalic capsule lost). 1 female, Hikime, Miyako-shi, Iwate prefecture, Japan (39°37.49'N, 141°49.41'E), 6 September 2021, leg. Katsuyuki Eguchi (labeled as TS20210906-01). 3 juveniles (sex unknown), Hiyamizucho, Kagoshima-shi, Kagoshima prefecture, Japan (31°36.21'N, 130°33.02'E), 22 September 2021, leg. Joe Kutsukake (labeled as TS20210922-01, TS20210922-02 and TS20210922-03). 1 female, Natsuocho, Miyakonojo-shi, Miyazaki prefecture, Japan (31°52.49'N, 130°57.50'E), 29 September 2021, leg. Joe Kutsukake (labeled as TS20210929-01). 2 females and 1 juvenile (sex unknown), Minamiosawa, Hachioji-shi, Tokyo prefecture, Japan (35°37.43'N, 139°23.05'E), 18 October 2021, leg. Joe Kutsukake (labeled as TS20211018-03, TS20211018-04 for females and TS20211018-05 for the juvenile, respectively). 2 females and 1 juvenile (sex unknown), Era, Toyotacho, Shimonoseki-shi, Yamaguchi prefecture, Japan (34°10.56'N, 131°02.48'E), 26 October 2021, leg.

Sho Tsukamoto (labeled as TS20211026-04, TS20211026-10 for females and TS20211026-05 for the juvenile, respectively). 1 female, Hikosan, Soeda-machi, Tagawa-gun, Fukuoka prefecture, Japan (33°29.06'N, 130°55.94'E), 29 October 2021, leg. Sho Tsukamoto (labeled as TS20211029-04). 1 female, Tomaruhinoe, Tsunan-machi, Nakauonuma-gun, Niigata prefecture, Japan (37°02.16'N, 138°39.46'E), 30 October 2021, leg. Katsuyuki Eguchi (labeled as TS20211030-01). 1 female, Maeda, Yahatahigashi-ku, Kitakyushu-shi, Fukuoka prefecture, Japan (33°51.35'N, 130°47.72'E), 30 October 2021, leg. Sho Tsukamoto (labeled as TS20211030-10). 2 females and 2 specimens (the lower half of body lost, sex unknown), Nishiyama, Nagasaki-shi, Nagasaki prefecture, Japan (32°45.89'N, 129°53.00'E), 1 November 2021, leg. Sho Tsukamoto (labeled as TS20211101-15, TS20211101-16 for females and TS20211101-17, TS20211101-18 for sex-unknown specimens, respectively). 1 female, Nijigaoka, Nagasaki-shi, Nagasaki prefecture, Japan (32°47.73'N, 129°50.00'E), 2 November 2021, leg. Sho Tsukamoto (labeled as TS20211102-04). 1 female, Murotsu, Muroto-shi, Kochi prefecture, Japan (33°18.06'N, 134°09.31E), 1 March 2022, leg. Katsuyuki Eguchi (labeled as TS20220301-01). 1 female, Murotomisakicho, Muroto-shi, Kochi prefecture, Japan (33°16.87'N, 134°10.65E), 2 March 2022, leg. Joe Kutsukake (labeled as TS20220302-03). 1 female, Kamoi, Yokosuka-shi, Kanagawa prefecture, Japan (35°15.44'N, 139°44.61E), 21 March 2022, leg. Katsuyuki Eguchi (labeled as TS20220321-03). 1 female, Murotsu, Muroto-shi, Kochi prefecture, Japan (33°18.07'N, 134°09.31E), 1 March 2022, leg. Joe Kutsukake (labeled as TS20220301-04). 3 females, Makigawa, Tsushimacho, Uwajima-shi, Ehime prefecture, Japan (33°05.74'N, 132°35.58E), 7 March 2022, leg. Joe Kutsukake (labeled as TS20220307-03, TS20220307-04, TS20220307-05, respectively). 2 females, Sunokawa, Ainancho, Minamiuwa-gun, Ehime prefecture, Japan (33°02.50'N, 132°29.18E), 7 March 2022, leg. Joe Kutsukake (labeled as TS20220307-06, TS20220307-07, respectively). 1 female, Matsuo, Tosashimizu-shi, Kochi prefecture, Japan (32°44.16'N, 132°58.57E), 6 March 2022, leg. Joe Kutsukake (labeled as TS20220306-11). 2 females, Makigawa, Tsushimacho, Uwajima-shi, Ehime prefecture, Japan (33°05.87'N, 132°36.98E), 7 March 2022, leg. Joe Kutsukake (labeled as TS20220307-09, TS20220307-10, respectively). 2 females, Ryoke, Muroto-shi, Kochi prefecture, Japan (33°17.23'N, 134°10.59E), 2 March 2022, leg. Joe Kutsukake (labeled as TS20220302-11, TS20220302-12, respectively). 2 females and 1 specimen (the lower half of body lost, sex unknown), Motootsu, Muroto-shi, Kochi prefecture, Japan (33°18.81'N, 134°07.33E), 1 March 2022, leg. Joe Kutsukake (labeled as TS20220301-05, TS20220301-06 for females and TS20220301-07 for sex-unknown specimens, respectively). 7 females, Iwabuchi, Tsushimacho, Uwajima-shi, Ehime prefecture, Japan (33°08.81'N, 132°32.99E), 7 March 2022, leg. Joe Kutsukake (labeled as TS20220307-11, TS20220307-12, TS20220307-13, TS20220307-14, TS20220307-15, TS20220307-16, TS20220307-17, respectively).

Etymology. The species name is derived from unmarried in Latin. In the Japanese population, males of this species have not been discovered despite the wide collection range in Japan.

Diagnosis. Clypeus with a pair of smooth or weakly areolate areas along the posterior part of the paraclypeal sutures; forcipular trochantroprefemur with a large denticle (longer than wide); tarsungulum with a well-pigmented denticle; metasternite of ultimate leg-bearing segment wider than long.

Description. ***General features*** (Fig. 5A, B): Body 7.0–12.0 mm long (holotype 12.0 mm), gradually attenuated posteriorly, almost uniformly very pale yellow, with head and forcipular segment pale ocher.

Cephalic capsule (Fig. 6A–D): Cephalic plate ca 1.4–1.6× as long as wide; lateral margins more distinctly converging anteriorly than posteriorly; posterior margin straight; scutes approximately isometric and up to 15 μm wide; transverse suture absent but areolate line present in some individuals (Fig. 6A, C); setae up to ca 37.5 μm long. Clypeus ca 1.4–1.5× as wide as long, with lateral margins complete, almost uniformly areolate, with scutes ca 15 μm wide, clypeal areas absent; clypeus with 11–17 setae, 1+1 postantennal, 1–2+2 median, 3–6+3–5 prelabral; clypeal ratio ca 1: 6–1: 7; clypeal plagulae with additional smooth or weak areolation area along posterior part of paraclypeal sutures. Anterior and distolateral parts of pleurites areolate, without setae. Side-pieces of labrum medially in contact, only incompletely divided into anterior and posterior alae by weak chitinous line, without longitudinal stripes on posterior alae, with slightly visible short fringe on posterior margin of side-pieces; mid-piece as long as wide, converging anteriorly and posteriorly.

Antenna (Fig. 7A–D): Antenna with 14 articles, when stretched, ca 2.1–2.6× as long as head length. Intermediate articles slightly longer than wide. Article XIV ca 2.5× as long as wide, ca 1.9–2.4× as long as article XIII, and 1.8–2.4× as long as intermediate articles. Setae on articles VIII–XVI denser than articles I–VII. Setae gradually shorter from article VIII to XIV, up to 65 μm long on article I, up to 25 μm long on article VIII and < 15 μm long on article XIV. Article XIV with two types of sensilla; apical sensilla (arrows in Fig. 7C, D) ca 10 μm long, with wide flat ring at mid-length; club-like (arrowheads in Fig. 7C, D) sensilla ca 15 μm long, clustered in the distal part of the internal and the external sides of the article. Three longitudinal rows, each consists of ca 9 proprioceptive spine-like sensilla, at bases of antennal articles III–V, VII–IX, approximately dorsal, ventro-internal and ventro-external; the rows each consisting of 1–3 spine-like sensilla on articles I and VI, and 6 on the article II; 0–1 spine-like sensilla on articles X–XIV. A few pointed sensilla, up to 2.5 μm long, on both dorso-external and ventro-internal position, close to distal margin of articles II, V, IX and XIII.

Mandible (Fig. 8A): At least four pectinate lamellae present; first and second lamellae with ca 5 elongated teeth. Each tooth ca 2× as long as wide. Ventral surface hairy.

First maxillae (Fig. 8B): Coxosternite medially divided but slightly, without setae, faintly areolate. Coxal projections well developed and hyaline distally, with 1–2+1–2 setae and 3–4+3–4 small sensilla. Telopodite uni-articulated and hyaline distally, with one(two) seta(e). No lobes on either coxosternite or telopodites.

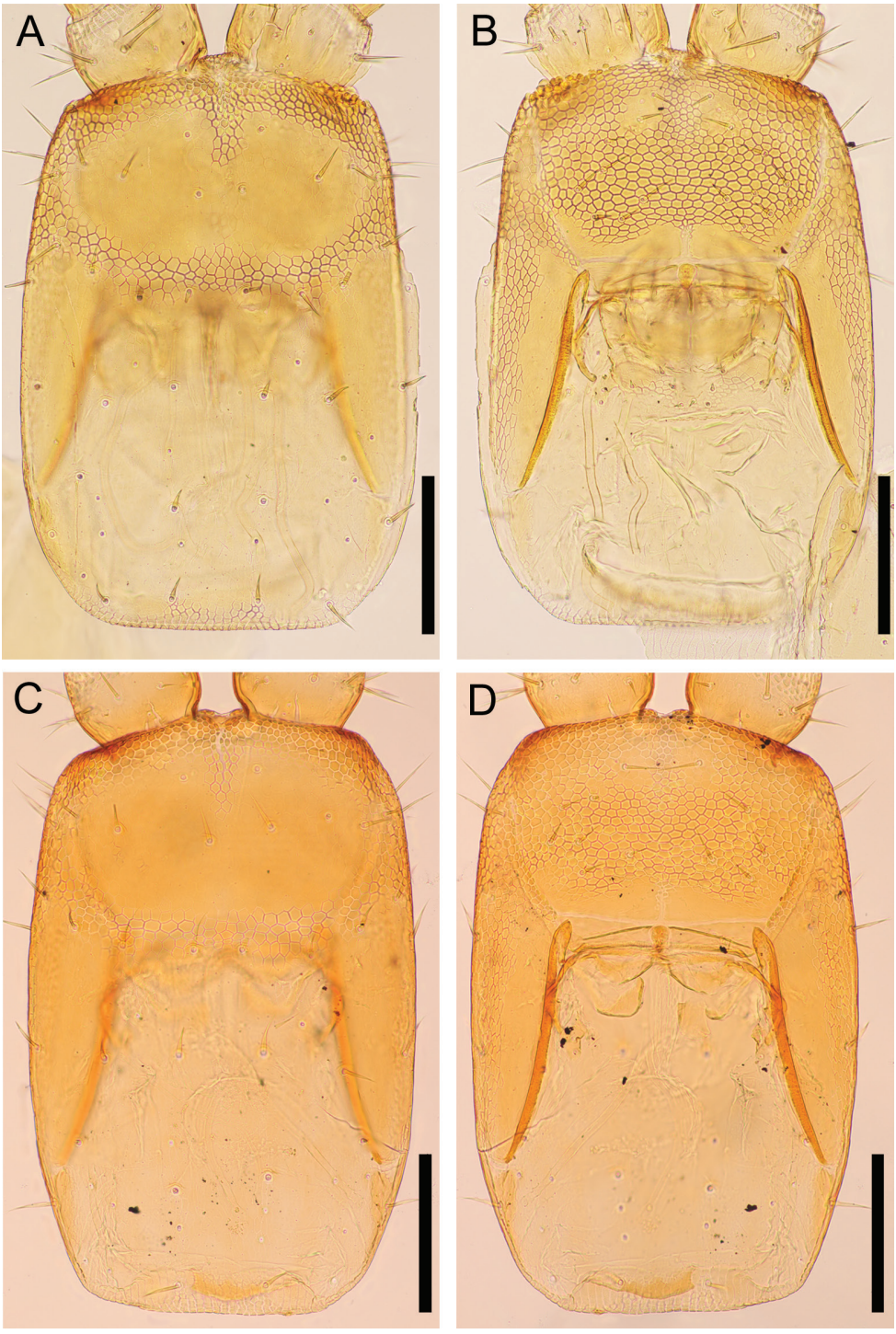

Figure 6. *Nannarrup innuptus* sp. nov. **A, B** holotype (TS20210503-09) **C, D** paratype (TS20210411-04). **A, B** cephalic plate, dorsal **C, D** clypeus and clypeal pleurite, ventral. Scale bars: 0.3 mm.

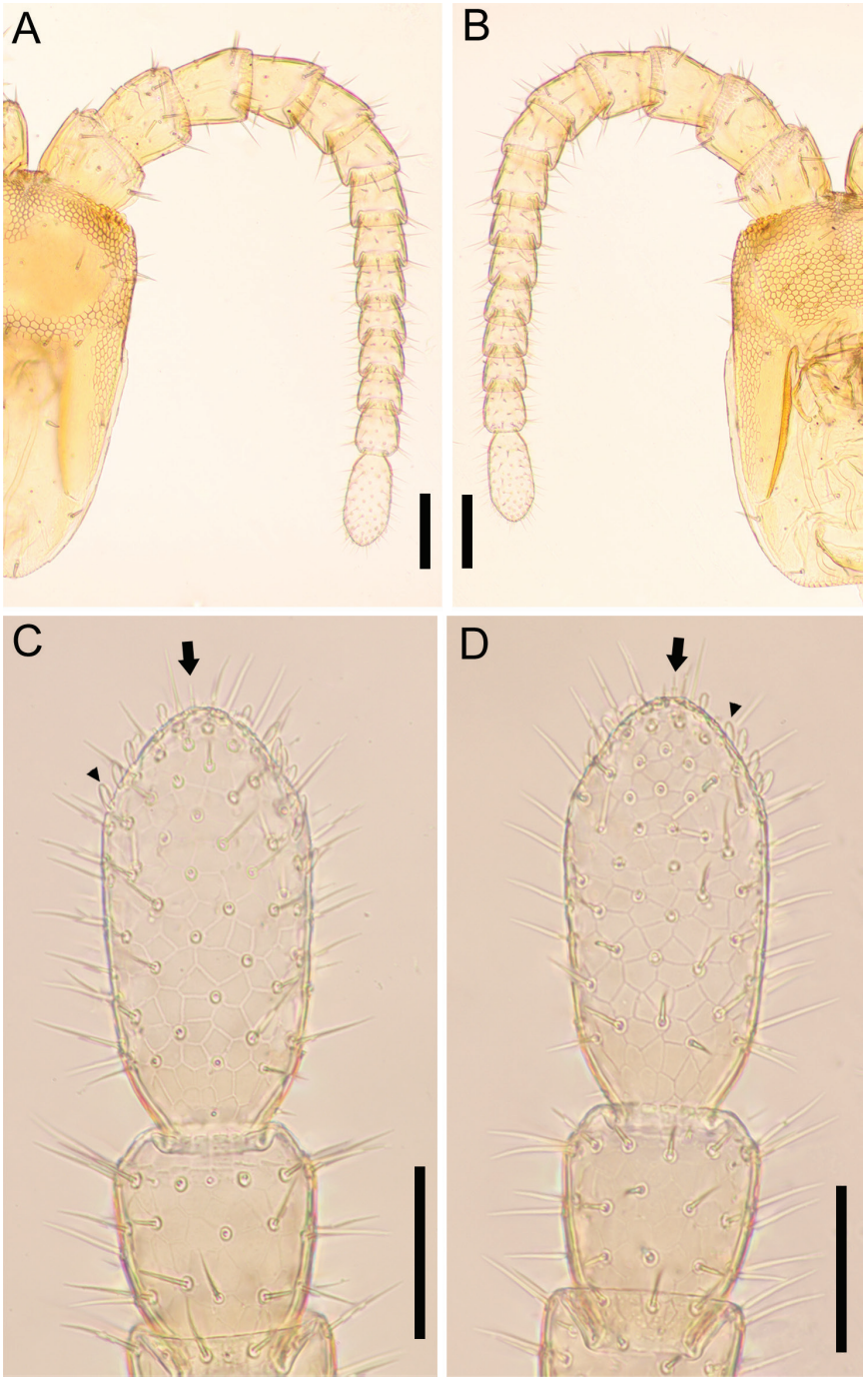

Figure 7. *Nannarrup innuptus* sp. nov., holotype (TS20210503-09) **A** right part of head and right antenna, dorsal **B** right part of head and right antenna, ventral **C** antennal article XIV, dorsal **D** antennal article XIV, ventral. Arrows indicate apical sensillum; arrowheads indicate club-like sensillum. Scale bars: 0.1 mm (**A, B**); 0.05 mm (**C, D**).

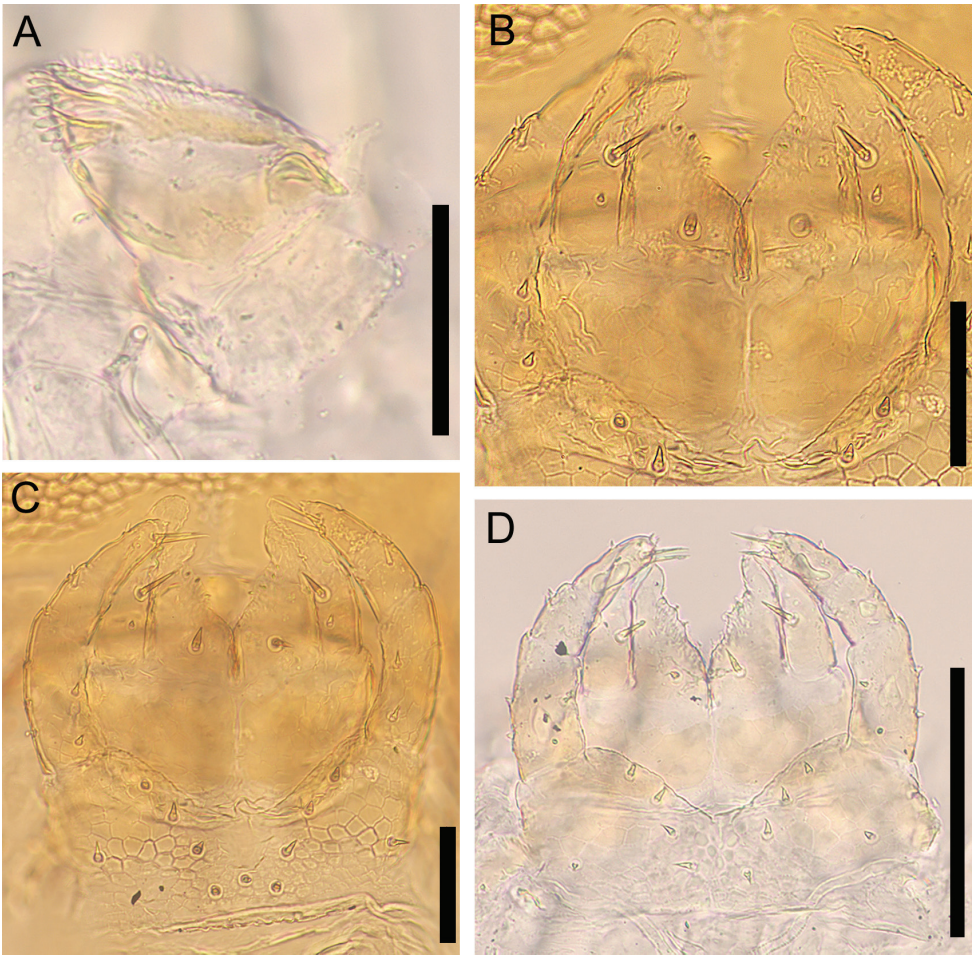

Figure 8. *Nannarrup innuptus* sp. nov. **A, D** paratype (TS20210411-05) **B, C** holotype (TS20210503-09). **A** right mandible, dorsal **B** first maxillae, ventral **C, D** second maxillae, ventral. Scale bars: 0.05 mm.

Second maxillae (Fig. 8C, D): Coxosternite medially undivided, without suture, with 2+2 setae along anterior margin, with 6–7 setae behind anterior margin, with 1–2+1–2 sensilla on posterior lateral margin in some individuals. with anterior margin slightly concave, with metameric pores on posterior part. Telopodites tri-articulate, reaching medial projections and telopodites of first maxillae in some individuals. Claw of telopodite virtually absent, represented by short spine only.

Forcipular segment (Fig. 9A–F): Tergite trapezoidal, ca 1.4–1.9× as wide as long, with lateral margins converging anteriorly, approximately as wide as cephalic plate and ca 0.7× as wide as following tergites; 1+1 setae of similar length arranged in an anterior row, and 3+3 setae of similar length arranged in a posterior row; one pair of longitudinal rows of three tiny setae located between middle and distal setae in posterior row. Mid-longitudinal sulcus of tergite not visible. Exposed part of coxosternite ca

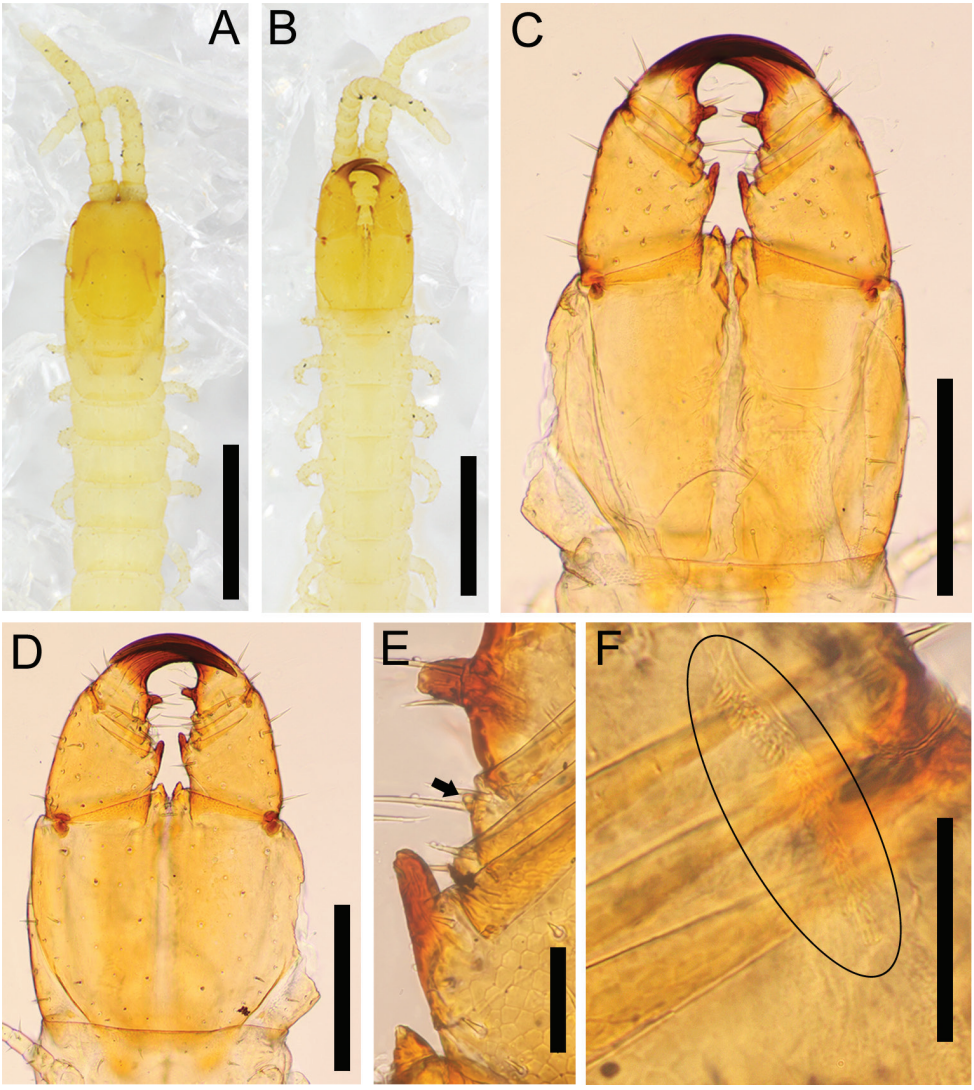

Figure 9. *Nannarrup innuptus* sp. nov. **A, B** paratype (TS20210411-05) **C, D** holotype (TS20210503-09) **E, F** paratype (TS20210411-04). **A** anterior part of body, dorsal **B** anterior part of body, ventral **C** forcipular segment, dorsal **D** forcipular segment, ventral **E** denticles on forcipule, dorsal **F** poison calyx, dorsal. Arrow indicates tubercle on tibia. Circle indicates poison calyx. Scale bars: 0.5 mm (**A, B**); 0.3 mm (**C, D**); 0.05 mm (**E, F**).

1.1× as wide as long; anterior margin with shallow medial concavity and with one pair of denticles; coxopleural sutures complete in entire ventrum, sinuous and diverging anteriorly; chitin-lines absent. Trochanteroprefemur ca 1.3–1.4× as long as wide; with a well-developed and strong pigmented denticle at distal internal margin, ca 1.3–1.6× as long as wide. Intermediate articles distinct, with a tubercle on tibia (arrowed in

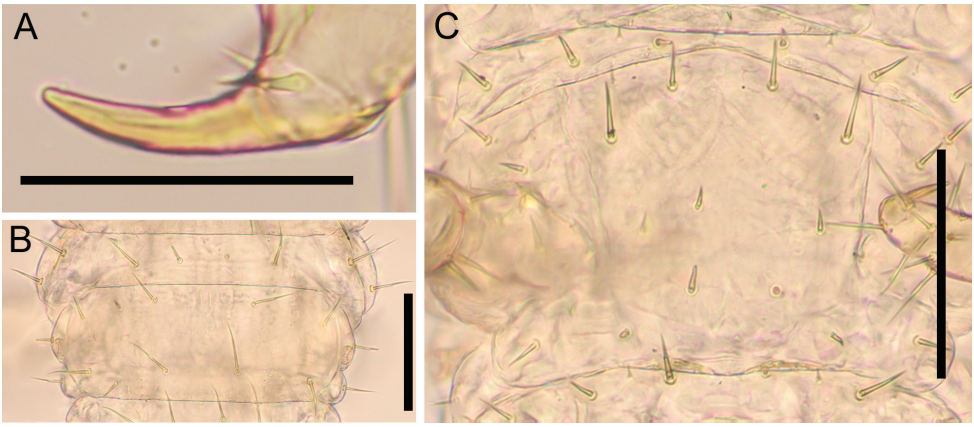

Figure 10. *Nannarrup innuptus* sp. nov. **A** holotype (TS20210503-09) **B, C** paratype (TS20210411-05) **A** pretarsus of left leg 2, anterolateral **B** tergite of leg-bearing segment 40, dorsal **C** sternite of leg-bearing segment 40, ventral. Scale bars: 0.05 mm (**A**); 0.1 mm (**B, C**).

Fig. 9E, some individuals not visible). Tarsungulum with well-pigmented basal denticle; both external and internal margins uniformly curved, except for moderate mesal basal bulge; ungulum not distinctly flattened. Elongated poison calyx (circle in Fig. 9F), ca 9× as long as wide, lodged inside intermediate forcipular articles.

Leg-bearing segments (Figs 9A, B, 10A–C): Forty-one pairs of legs present. Metatergite 1 slightly wider than subsequent one, with two paramedian sulci visible on tergites of anterior half of body, with pretergite. No paratergites. Walking legs shorter than width of trunk; legs of first pair much smaller than following ones; claws simple, uniformly bent, with 2 accessory spines; anterior spine reaching at most 10% of length of claw; posterior spine equal in length of the anterior spine. Metasternites slightly longer than wide. Sternal sulcus visible on a few anterior sternites, represented by very shallow mid-longitudinal thickening, anteriorly not furcate. No ventral glandular pores on each metasternite.

Ultimate leg-bearing segment (Fig. 11A–D): Pretergite not accompanied by pleurites but incomplete traces of sutures present at both sides. Metatergite subtrapezoidal, ca 1.1–1.3× as wide as long; lateral margins convex and converging posteriorly; posterior margin slightly curved. Coxopleuron ca 1.2–1.7× as long as metasternite; coxal organs of each coxopleuron opening through 5–10 independent pores, placed ventrally. Metasternite trapezoidal, ca 1.3–1.6× as wide as long, anteriorly ca 1.7–2.2× as wide as posteriorly; lateral margins slightly convex and converging backward; setae almost arranged symmetrically, dense on posterior margin. Telopodite ca 9–11× as long as wide, ca 1.9–2.1× as long and ca 1.5–1.6× as wide as penultimate telopodite, with six articles; tarsus 2 ca 3.6–4.2× as long as wide and ca 1.2–1.6× as long as tarsus 1; setae arranged uniformly, < 70 μm long; pretarsus represented by small tubercle.

Female postpedal segments (Fig. 11A, B): Two gonopods basally touching, subtriangular, without traces of articulation, covered with setae. Anal pore present.

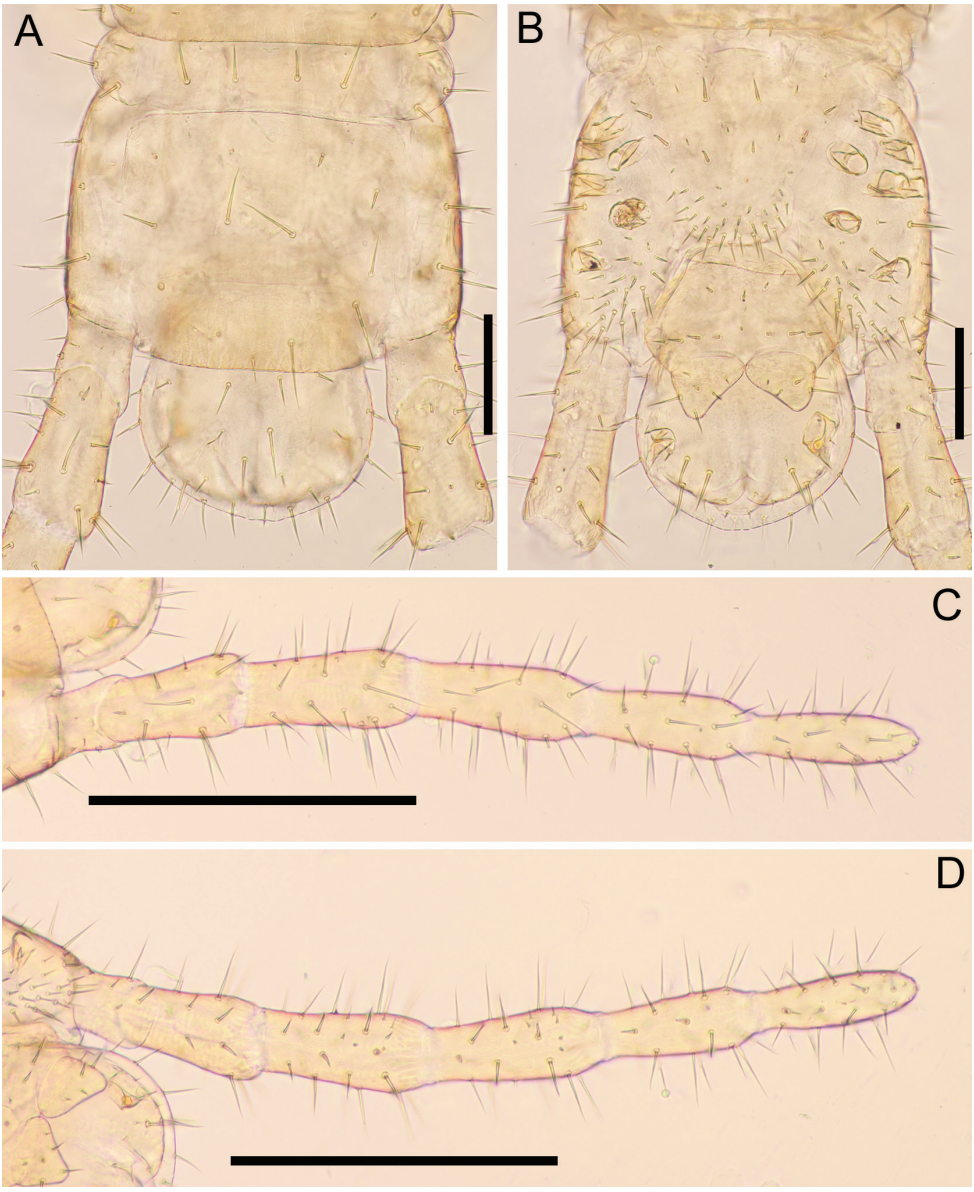

Figure 11. *Nannarrup innuptus* sp. nov., holotype (TS20210503-09) **A** ultimate leg-bearing segment and postpedal segment, dorsal **B** ultimate leg-bearing segment and postpedal segment, ventral **C** left ultimate leg, dorsal **D** left ultimate leg, ventral. Scale bars: 0.1 mm (**A, B**); 0.3 mm (**C, D**).

Male postpedal segments unknown (male unknown).

Distribution. Honshu, Shikoku and Kyushu.

Remarks. In pairwise comparisons, *N. innuptus* sp. nov. can be distinguished from *N. hoffmani* by the presence of a well-developed denticle on the trochanteroprefemur

(width: length = 1:1.3–1.6) and a well-pigmented denticle on the tarsungulum. In addition, *N. innuptus* sp. nov. is also distinguishable from *N. hoffmani* by the presence of a tubercle on the forcipular tibia, but this tubercle is not always visible. No male has been found so far.

***Nannarrup oyamensis* Tsukamoto, sp. nov.**
https://zoobank.org/1543ADD5-1C03-4471-9B6F-D473E4BB0F22
New Japanese name: Amefuri-himejimukade
Figs 12–17

Type material. ***Holotype*** 1 adult male, Hinata, Isehara-shi, Kanagawa prefecture, Japan (35°26.07'N, 139°14.75'E), 17 February 2021, coll. Sho Tsukamoto (labeled as TS20210217-04), deposited at the Collection of Myriapoda, Department of Zoology, **NSMT**. ***Paratype*** 1 subadult male, Hinata, Isehara-shi, Kanagawa prefecture, Japan (35°26.07'N, 139°14.75'E), 25 July 2021, coll. Sho Tsukamoto (labeled as TS20210725-02), deposited at **MNHAH**.

Etymology. The species name is derived from the name of Japanese mountain, namely Mt. Oyama. The word was further Latinized by adding the Latin masculine adjective suffix *-ensis*, to form *oyamensis*. The last "a" of Oyama and the first "e" of -ensis are merged into "e." Examined specimens were collected from Mt. Oyama, an object of the mountain worship.

Diagnosis. Clypeus without smooth or weakly areolate areas along the posterior part of the paraclypeal sutures; forcipular trochantroprefemur with a large denticle (longer than wide); tarsungulum with a well-pigmented denticle; metasternite of ultimate leg-bearing segment wider than long.

Description. ***General features*:** Body 8.6 mm long (holotype), gradually attenuate posterior, almost uniformly very pale yellow, with head and forcipular segment pale ocher.

Cephalic capsule (Fig. 12A, B): Cephalic plate ca 1.5× as long as wide, lateral margins more distinctly converging anteriorly than posteriorly, posterior margin straight; scutes approximately isometric and up to ca 15 μm wide; transverse suture absent; setae up to ca 50 μm long. Clypeus ca 1.5× as wide as long, with lateral margins complete, almost uniformly areolate, with scutes ca 10 μm wide, a pair of clypeal areas absent; 13 setae in holotype, 1+1 postantennal, 1+1 median, 5+4 prelabral; clypeal ratio ca 1: 7; clypeal plagulae without additional smooth area along posterior part of paraclypeal sutures; 17 pore-like organs on entire part of clypeus. Anterior and distolateral parts of pleurites areolate, without setae. Side-pieces of labrum medially in contact, only incompletely divided into anterior and posterior alae by weak chitinous line, without longitudinal stripes on posterior alae; with slightly visible short fringe on posterior margin of side-pieces; mid-piece as long as wide, converging anteriorly and posteriorly.

Antenna (Fig. 13A–D): Antenna with 14 articles, when stretched, ca 2.3× as long as head length. Intermediate articles slightly longer than wide. Article XIV ca 2.0× as long as wide, ca 1.9× as long as article XIII, and 1.9–2.1× as long as intermediate

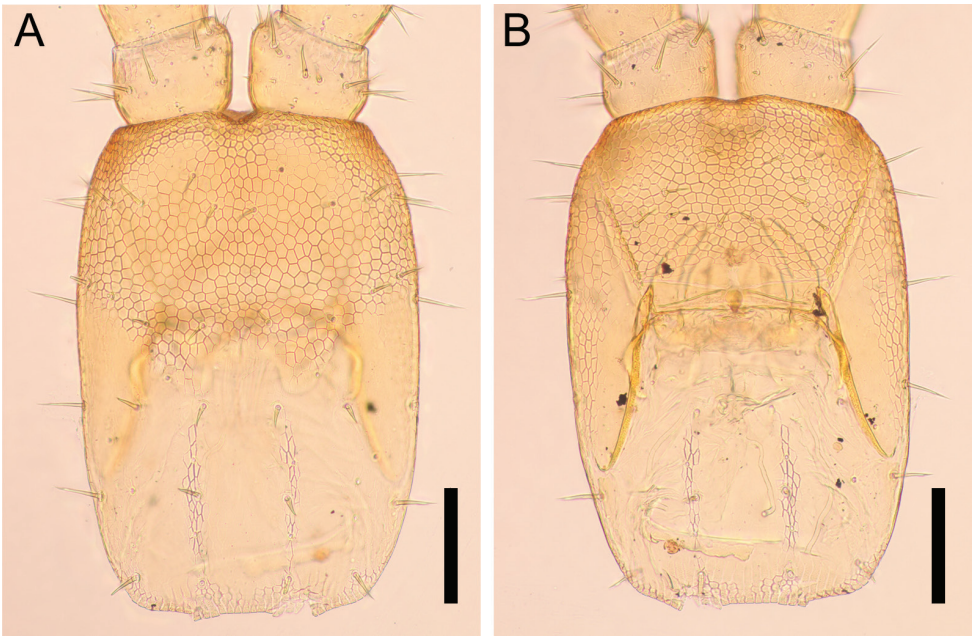

Figure 12. *Nannarrup oyamensis* sp. nov., holotype (TS20210217-04) **A** cephalic plate, dorsal **B** clypeus and clypeal pleurite, ventral. Scale bars: 0.1 mm.

articles. Setae on articles VIII–XVI denser than articles I–VII. Setae gradually shorter from article VIII to XIV, up to 50 μm long on article I, up to 33 μm long on article VIII and < 18 μm long on article XIV. Article XIV with two types of sensilla, apical sensilla (arrows in Fig. 13C, D) ca 5 μm long, with wide flat ring at mid-length; club-like sensilla (arrowheads in Fig. 13C, D) ca 10 μm long, clustered in the distal parts of the internal and external sides of the article. Three longitudinal rows consisted of ca 9 proprioceptive spine-like sensilla at bases of antennal articles II–V, VII–IX, approximately dorsal, ventro-internal and ventro-external; rows reduced to 1–3 spines on antennal articles I and VI, and 0–1 spine on antennal articles X–XIV. A few pointed sensilla, up to 2.5 μm long, on both dorso-external and ventro-internal position, close to distal margin of articles II, V, IX and XIII.

Mandible (Fig. 14A). At least four pectinate lamellae, with elongated teeth. Each tooth ca 2× as long as wide.

First maxillae (Fig. 14B): Coxosternite medially divided but slightly, without setae, faintly areolate. Coxal projections well developed and hyaline distally, provided with 1+1 setae and 3+4 small sensilla. Telopodite uni-articulated and hyaline distally, with one (two) seta(e). No lobes on either coxosternite or telopodites.

Second maxillae (Fig. 14B): Coxosternite medially undivided, without suture, with 2+3 setae along the anterior margin, with 4+4 setae located behind anterior margin, with anterior margin slightly concave, with metameric pores on posterior part. Telopodites tri-articulate overreaching medial projections and telopodites of first maxillae. Claw of telopodite virtually absent, represented by short spine only.

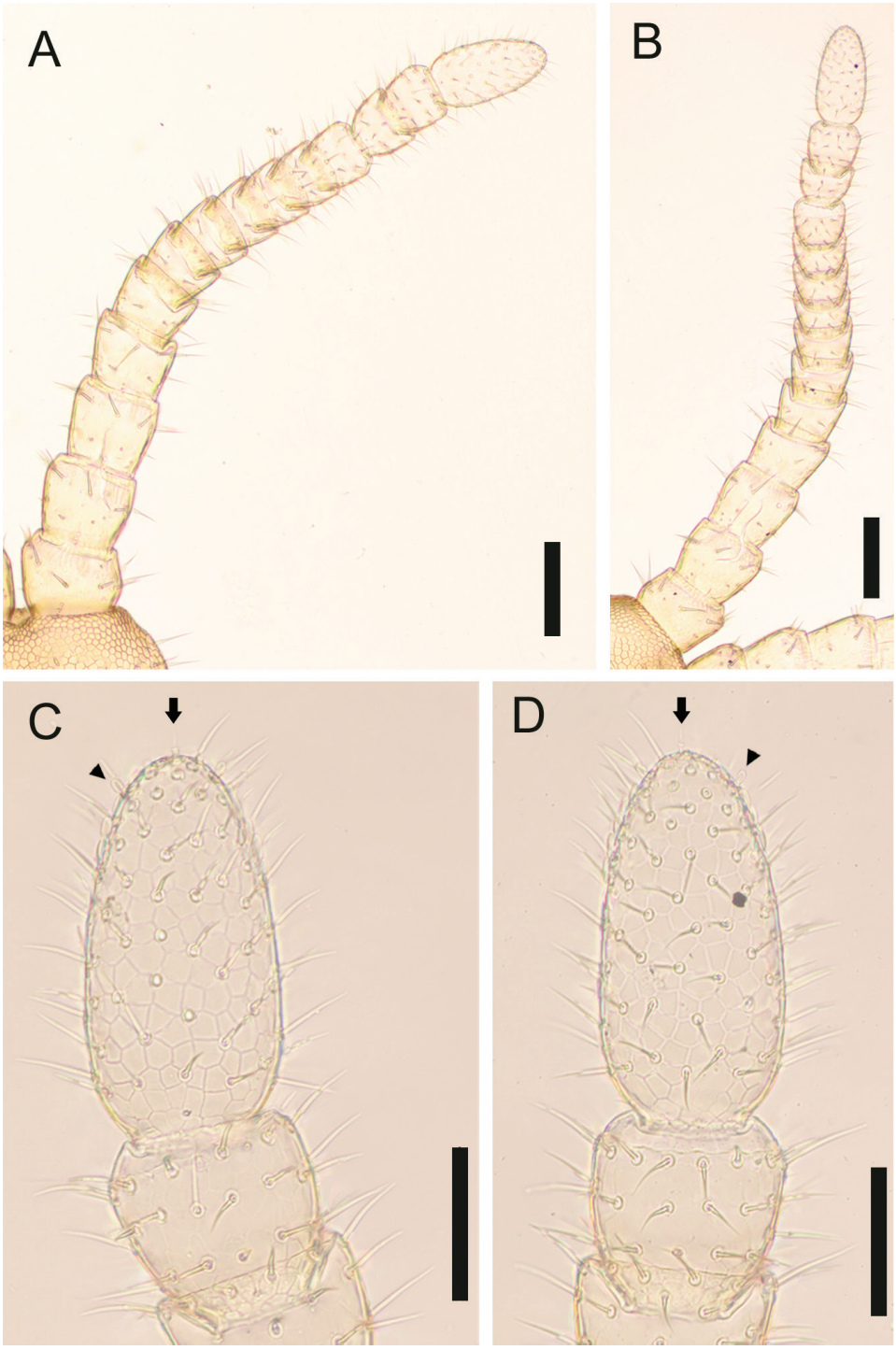

Figure 13. *Nannarrup oyamensis* sp. nov., holotype (TS20210217-04) **A** right antenna, dorsal **B** right antenna, ventral **C** antennal article XIV, dorsal **D** antennal article XIV, ventral. Arrows indicate apical sensillum; arrowheads indicate club-like sensillum. Scale bars: 0.1 mm (**A, B**); 0.05 mm (**C, D**).

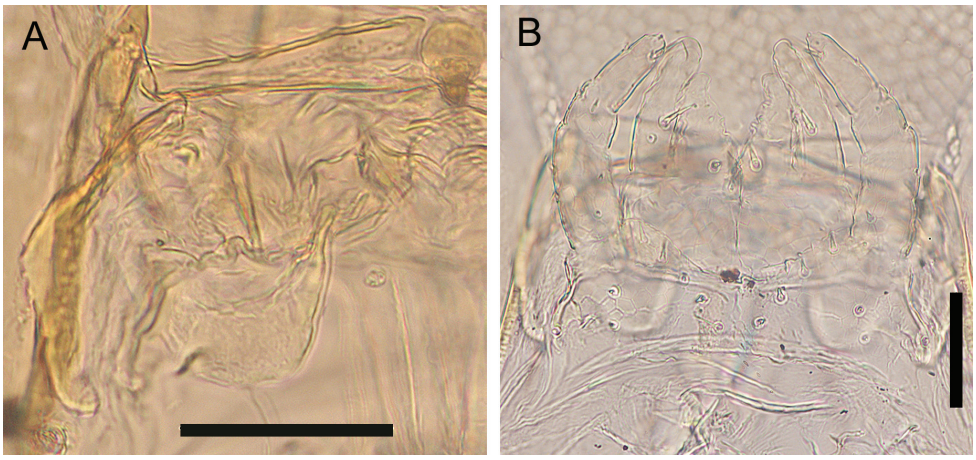

Figure 14. *Nannarrup oyamensis* sp. nov., holotype (TS20210217-04) **A** right mandible, ventral **B** maxillae complex, ventral. Scale bars: 0.05 mm.

Forcipular segment (Fig. 15A–D): Tergite trapezoidal, ca 1.9× as wide as long, with lateral margins converging anteriorly, approximately as wide as cephalic plate and ca 0.7× as wide as following tergite, 1+1 setae of similar length arranged in an anterior row, and 3+3 setae of similar length arranged in a posterior row, one pair of longitudinal rows of three tiny setae located between middle and distal setae in posterior row. Mid-longitudinal sulcus of tergite not visible. Exposed part of coxosternite ca 1.3× as wide as long; anterior margin with shallow medial concavity and with one pair of denticles; coxopleural sutures complete in entirely ventrum, sinuous and diverging anteriorly; chitin-lines absent. Basal distance between forcipules ca 0.1× of maximum width of coxosternite. Trochanteroprefemur ca 1.3× as long as wide; with a well-developed and strong pigmented denticle at distal internal margin, ca 1.3× as long as wide. Intermediate articles distinct, tubercle on tibia not visible. Tarsungulum with basal denticle well-pigmented; both external and internal margins uniformly curved, except for moderate mesal basal bulge; ungulum not distinctly flattened. Elongated poison calyx (circle in Fig. 15D), ca 6× as long as wide, lodged inside intermediate forcipular articles.

Leg-bearing segments (Fig. 16A–D): Forty-one pairs of legs present. Metatergite 1 slightly wider than subsequent one, with two paramedian sulci visible on tergites of anterior half of body, without pretergite. No paratergites. Walking legs shorter than width of trunk; legs of first pair much smaller than following ones; claws simple, uniformly bent, with two accessory spines; anterior spine reaching at most 10% of length of claw; posterior spine shorter than anterior spine. Metasternites slightly longer than wide. Sternal sulcus visible on a few anterior sternites, represented by very shallow mid-longitudinal thickening, anterior not furcate. No ventral glandular pores on each metasternite.

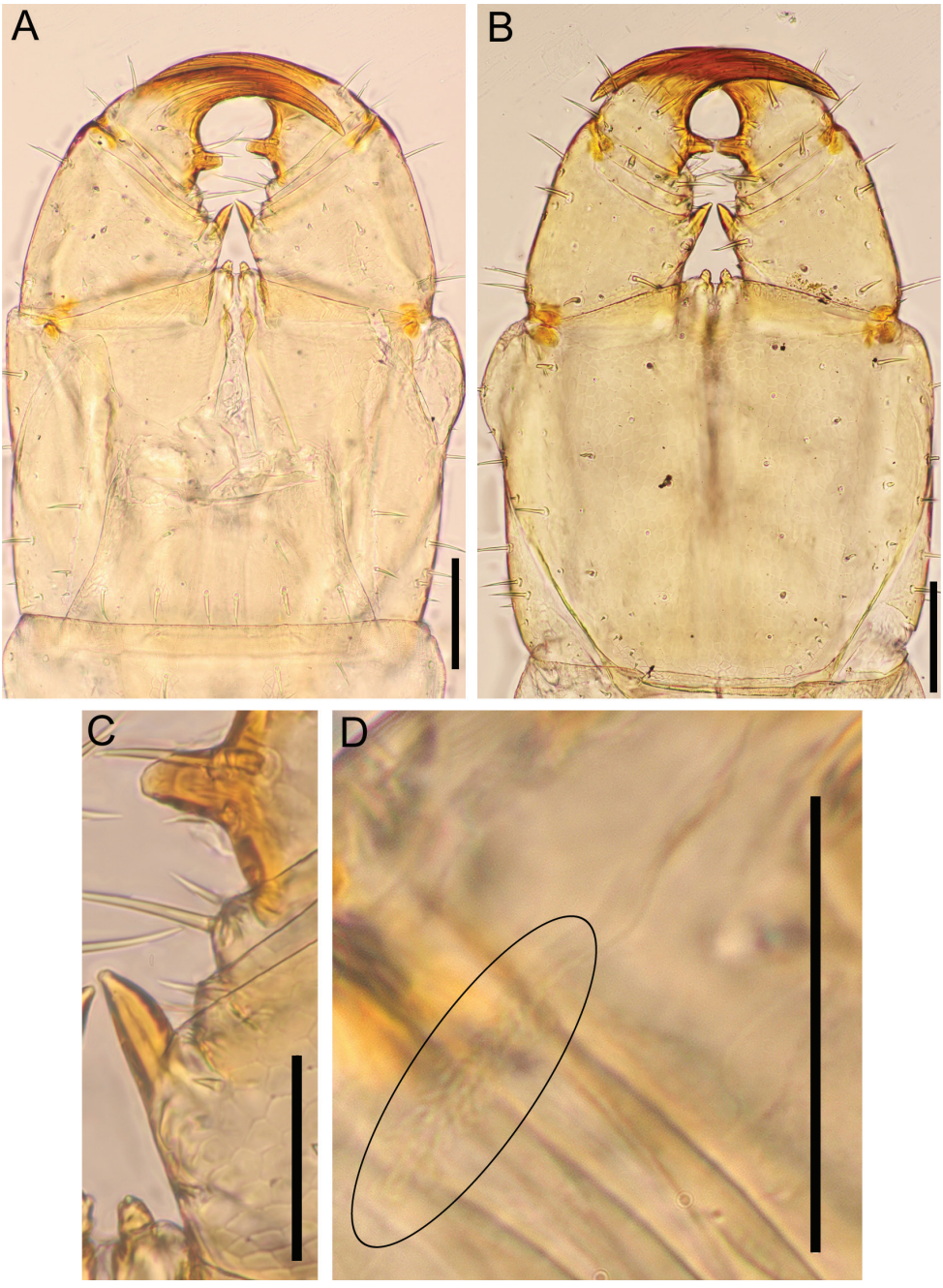

Figure 15. *Nannarrup oyamensis* sp. nov., holotype (TS20210217-04) **A** forcipular segment, dorsal **B** forcipular segment, ventral **C** denticles on right forcipule, dorsal **D** left poison calyx, dorsal. Circle indicates poison calyx. Scale bars: 0.1 mm (**A, B**); 0.05 mm (**C, D**).

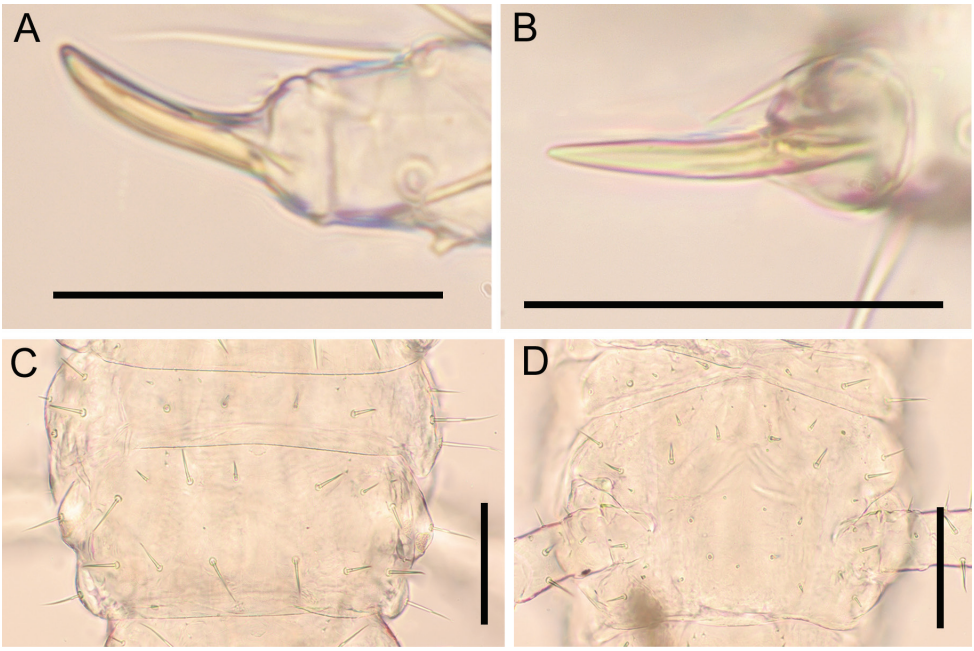

Figure 16. *Nannarrup oyamensis* sp. nov., holotype (TS20210217-04) **A** pretarsus of left leg 40, dorsal **B** pretarsus of left leg 40, ventral **C** tergite of leg-bearing segment 40, dorsal **D** sternite of leg-bearing segment 40, ventral. Scale bars: 0.05 mm (**A, B**); 0.1 mm (**C, D**).

Ultimate leg-bearing segment (Fig. 17A–D): Pretergite not accompanied by pleurites but incomplete traces of sutures present at both sides. Metatergite subtrapezoidal, almost as wide as long, lateral margins convex and converging posteriorly; posterior margin slightly curved. Coxopleuron ca 1.2× as long as metasternite; coxal organs of each coxopleuron opening through five or six independent pores, placed ventrally. Metasternite subtriangular, ca 1.6 as wide as long, anteriorly ca 3.5× as wide as posteriorly; lateral margins slightly convex and converging backward; setae almost arranged symmetrically, dense on posterior margin. Telopodite ca 11× as long as wide, ca 1.9× as long and ca 1.3× as wide as penultimate telopodite, with 6 articles; tarsus 2 ca 2.7× as long as wide and ca 1.5× as long as tarsus 1; setae arranged uniformly, < 50 μm long. Pretarsus represented by spines, up to 5 μm.

Male postpedal segments (Fig. 17A, B): Two gonopods, very widely separated from one another, conical in outline, uni-articulated without any sutures, covered with setae. Anal pore present.

Female postpedal segments unknown (female unknown).

Distribution. Only known from Mt. Oyama, located in Isehara-shi, Kanagawa prefecture.

Remarks. *Nannarrup oyamensis* sp. nov. is distinguishable from the two congeners by the absence of smooth or weakly areolate areas along the posterior part of the paraclypeal sutures. Specifically, *N. oyamensis* sp. nov. can be clearly distinguished from *N. hoffmani* by the presence of a well-developed denticle on the trochanteroprefemur (width:

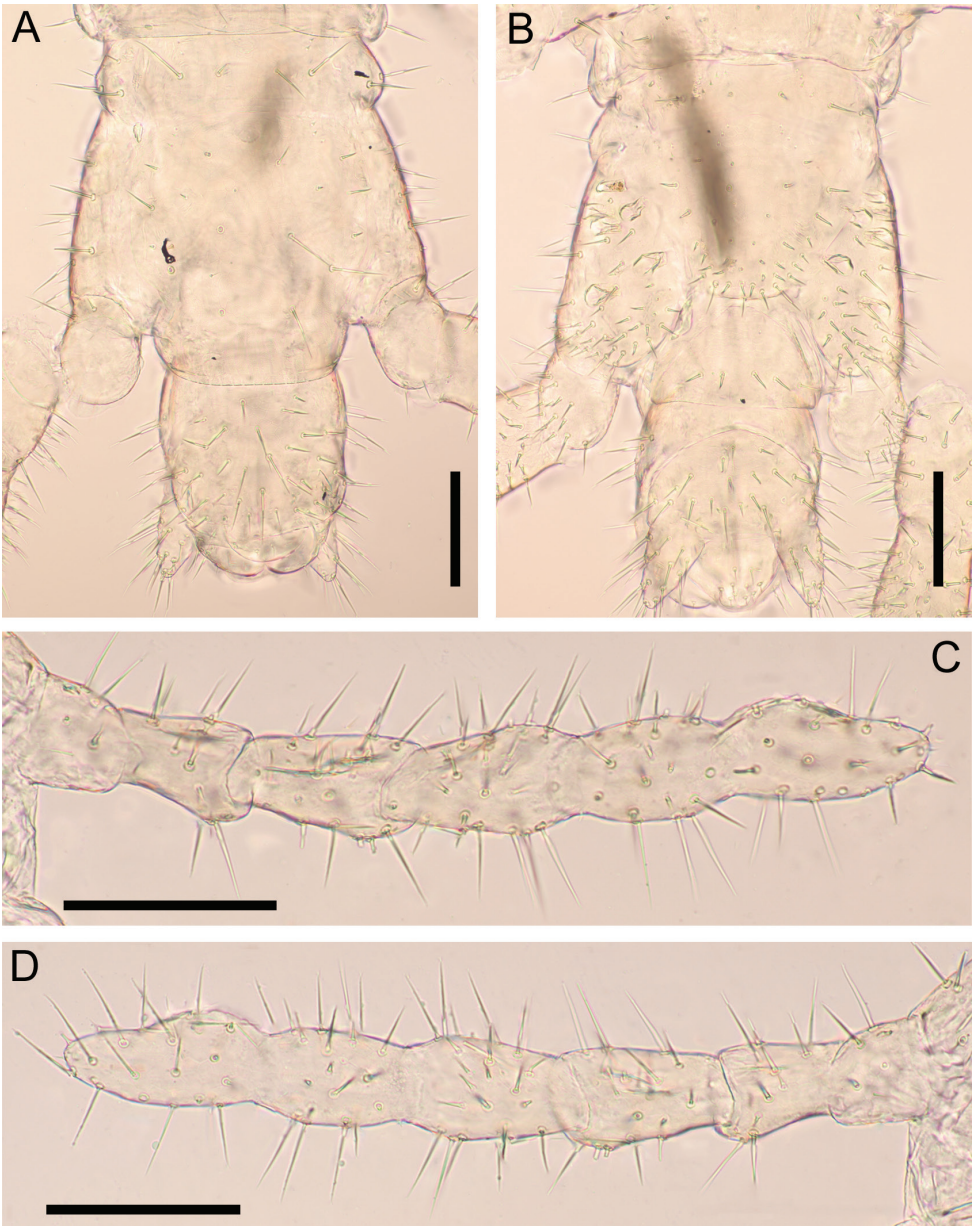

Figure 17. *Nannarrup oyamensis* sp. nov. **A, B** holotype (TS20210217-04) **C, D** paratype (TS20210725-02). **A** ultimate leg-bearing segment and male postpedal segment, dorsal **B** ultimate leg-bearing segment and male postpedal segment, ventral **C** right ultimate leg, dorsal **D** right ultimate leg, ventral. Scale bars: 0.1 mm.

length = 1:1.3) and the absence of smooth or weakly areolate areas along the posterior part of the paraclypeal sutures. Furthermore, *N. oyamensis* sp. nov. can be distinguished from *N. innuptus* sp. nov. by the absence of a pair of smooth or weakly areolate areas along the posterior part of the paraclypeal sutures (see Table 3 for a comparison of characteristics).

Discussion

Species recognition based on morphological analysis and DNA barcoding

All three morphospecies (including *N. hoffmani*) were determined to be similar to a certain extent. Nevertheless, each morphospecies was distinguished from the other two morphospecies on the basis of the following characteristics: presence or absence of a pair of smooth or weakly areolate areas along the posterior part of the paraclypeal sutures, the width-to-length ratio of the denticle of trochanteroprefemur, the pigmentation of the denticle on the tarsungulum. Table 3 shows the comparison among the three morphospecies regarding the key characters.

The maximum internal genetic divergence in the *COI*, *16S*, and *28S* sequences within each morphospecies was considerably smaller than the minimum divergence in the *COI*, *16S*, and *28S* sequences between each pair of the morphospecies, that is, the DNA barcoding gap was evident.

The presence of a DNA barcoding gap (especially in the nuclear *28S*) suggests that *N*. sp. 2 forms an independent gene pool that is reproductively isolated from *N*. sp. 1. Together, the morphological and molecular evidence suggests that the three morphospecies are distinct species and that *N*. sp. 1 and *N*. sp. 2 are two novel species; they are described under the section "Taxonomic account" as *Nannarrup innuptus* sp. nov. and *Nannarrup oyamensis* sp. nov., respectively.

Distribution of the genus *Nannarrup*

All examined *Nannarrup* specimens were collected from Honshu, Shikoku, and Kyushu, but the collectors (ST, KE, and collaborators) did not find *Nannarrup* in the Ryukyu Archipelago despite intensive and repetitive field surveys. Furthermore, Uliana et al. (2007) have also reported that there are no records of *Nannarrup* from the Ryukyus and Taiwan. The distribution range of *Nannarrup* is likely confined to the temperate zones of East Asia, namely Honshu, Shikoku, Kyushu, and surrounding islands. However, future field surveys in Hokkaido, and continental East Asia may lead to additional reports of *Nannarrup*.

Foddai et al. (2003) stated that *N. hoffmani* is not native to New York, the type locality of this species, but has been definitely introduced from western America or East Asia. In the present study, *N. hoffmani* was not collected in Japan. However, the existence of two congeners in Japan suggests that *Nannarrup* is native to East Asia. Additional field surveys to investigate the original distribution of *N. hoffmani* should be conducted mainly in East Asia.

According to the results of DNA barcoding based on *COI*, *16S*, and *28S* sequences, *N. innuptus* sp. nov. does not show a remarkable genetic structure that is consistent with the geography of Japan and physical distances among the collection sites in the present study. Nevertheless, considering this intraspecific genetic diversity, it is reasonable to assume that *N. innuptus* sp. nov. is not a species recently introduced by human activities but a native species in Japan. The reason for such a low genetic diversity and

no geographic structuring of diversity in mitochondrial genes remains unclear at present, but we propose the following two hypotheses to explain this finding: 1) the rate of evolution of mitochondrial genes is considerably lower than that in other centipedes, and 2) the establishment of *N. innuptus* sp. nov. as an independent species (either within the Japanese archipelago or following migration from the Asian continent) is geologically relatively recent. This question may be answered by examining sufficient specimens of other congeners (e.g., *N. oyamensis* sp. nov.) from East Asia including Japan and estimating the species divergence time by including other congeners and even genera belonging to Mecistocephalidae in Asia.

Likelihood of parthenogenesis in *Nannarrup innuptus* sp. nov.

Remarkably, all 71 adult and subadult specimens of *N. innuptus* sp. nov. examined in this study were females without exception. Furthermore, because different collectors (four) did the specimen collections, in different seasons (March–November), and in different habitats (forest, urban green space, and riverbed), the presence of any sampling bias that may have distorted the sex ratio is unlikely. Although there is no direct evidence, the abovementioned indirect evidence shows the possibility of parthenogenesis of *N. innuptus* sp. nov.

To date, a large part of the northern and eastern European population of *Geophilus proximus* C.L. Koch, 1847, the European population of *Tygarrup javanicus* Attems, 1929, and *Schendyla dentata* (Brölemann & Ribaut, 1911) have been discussed about their parthenogenesis (Sograff 1882; Barber and Jones 1999; Minelli 2011; Tuf et al. 2018). *Nannarrup innuptus* sp. nov. may be the second parthenogenetic species in the family Mecistocephalidae. In contrast, the Japanese congener, *N. oyamensis* sp. nov., exhibits sexual reproduction because two examined specimens were males, i.e., males of *N. oyamensis* sp. nov. should be common. In addition, the type series of *N. hoffmani* involved one juvenile male specimen (Foddai et al. 2003).

Acknowledgements

We are grateful to Ms Mayu Susukida (Tokyo Metropolitan University) and Mr Joe Kutsukake (Tokyo Metropolitan University) for collecting and providing *Nannarrup* specimens. We also would like to thank Dr Namiki Kikuchi (Tokyo Metropolitan University) for providing a high-quality photograph of the habitus of *Nannarrup innuptus* sp. nov., and Dr Keisuke Kawano (The Firefly Museum of Toyota Town) for guiding in the forests in Yamaguchi prefecture. We sincerely thank two reviewers for providing valuable comments which significantly improved this paper. We would like to thank Enago (www.enago.jp) for the English language review. This research was funded by the following foundations and societies: Asahi Glass Foundation [Leader: Katsuyuki Eguchi; FY2017–FY2020, and Leader: Satoshi Shimano; FY2020–FY2023] and Tokyo Metropolitan University Fund for TMU Strategic Research [Leader: Prof. Noriaki Murakami; FY2020–FY2022]. This research was also funded by JSPS KAKENHI Grant Numbers 17K07271, 18K06392 for SS.

References

Attems C (1929) Myriapoda. 1. Geophilomorpha. Das Tierreich 52. De Gruyter, Berlin, 388 pp. https://doi.org/10.1515/9783111430638

Barber AD, Jones RE (1999) Further notes on *Brachyschendyla dentata* Brolemann & Ribaut (Chilopoda: Geophilomorpha). Bulletin of the British Myriapod Group 15: 14–18.

Bollman CH (1893) Classification of the Syngnatha. In: Underwood LM (Ed.) The Myriapoda of North America by Charles Harvey Bollman. Bulletin of the United States National Museum, No. 46. Washington, Government Printing Office, 163–167. https://doi.org/10.5962/bhl.title.38711

Bonato L (2011) Order Geophilomorpha. In: Minelli A (Ed.) Treatise on Zoology – Anatomy, Taxonomy, Biology – The Myriapoda, Volume 1. Brill, Leiden – Boston, 407–443.

Bonato L, Foddai D, Minelli A (2003) Evolutionary trends and patterns in centipede segment number based on a cladistic analysis of Mecistocephalidae (Chilopoda: Geophilomorpha). Systematic Entomology 28(4): 539–579. https://doi.org/10.1046/j.1365-3113.2003.00217.x

Bonato L, Edgecombe GD, Lewis JGE, Minelli A, Pereira LA, Shelley RM, Zapparoli M (2010) A common terminology for the external anatomy of centipedes (Chilopoda). ZooKeys 69: 17–51. https://doi.org/10.3897/zookeys.69.737

Bonato L, Drago L, Murienne J (2014) Phylogeny of Geophilomorpha (Chilopoda) inferred from new morphological and molecular evidence. Cladistics 30(5): 485–507. https://doi.org/10.1111/cla.12060

Bonato L, Chagas Jr A, Edgecombe GD, Lewis JGE, Minelli A, Pereira LA, Shelley RM, Stoev P, Zapparoli M (2016) ChiloBase. Version 2.0. A World Catalogue of Centipedes (Chilopoda). http://chilobase.biologia.unipd.it [accessed 16 March 2022]

Boyer SL, Giribet G (2007) A new model Gondwanan taxon: Systematics and biogeography of the harvestman family Pettalidae (Arachnida, Opiliones, Cyphophthalmi), with a taxonomic revision of genera from Australia and New Zealand. Cladistics 23(4): 337–361. https://doi.org/10.1111/j.1096-0031.2007.00149.x

Brölemann HW, Ribaut H (1911) Diagnoses préliminaires d'espèces nouvelles de Schendylina [Myriap. Geophilomorpha]. Bulletin de la Société Entomologique de France 16(10): 219–222. https://doi.org/10.3406/bsef.1911.24916

Chamberlin RV (1912) The Chilopoda of California. III. Pomona College Journal of Entomology 4: 651–672.

Cook OF (1896) An arrangement of the Geophilidae a family of Chilopoda. Proceedings of the United States National Museum 18: 63–75. https://doi.org/10.5479/si.00963801.181039.63

Edgecombe GD, Giribet G (2004) Adding mitochondrial sequence data (16S rRNA and cytochrome c oxidase subunit I) to the phylogeny of centipedes (Myriapoda: Chilopoda): an analysis of morphology and four molecular loci. Journal of Zoological Systematics and Evolutionary Research 42: 89–134. https://doi.org/10.1111/j.1439-0469.2004.00245.x

Edgecombe GD, Giribet G (2006) A century later – a total evidence re-evaluation of the phylogeny of scutigeromorph centipedes (Myriapoda, Chilopoda). Invertebrate Systematics 20(5): 503–525. https://doi.org/10.1071/IS05044

Foddai D, Bonato L, Pereira LA, Minelli A (2003) Phylogeny and systematics of the Arrupinae (Chilopoda Geophilomorpha Mecistocephalidae) with the description of a new dwarfed species. Journal of Natural History 37(10): 1247–1267. https://doi.org/10.1080/00222930210121672

Giribet G, Edgecombe GD, Wheeler WC (2001) Arthropod phylogeny based on eight molecular loci and morphology. Nature 413, 157–161. https://doi.org/10.1038/35093097

Guindon S, Dufayard JF, Lefort V, Anisimova M, Hordijk W, Gascuel O (2010) New algorithms and methods to estimate maximum-likelihood phylogenies: Assessing the performance of PhyML 3.0. Systematic Biology 59(3): 307–321. https://doi.org/10.1093/sysbio/syq010

Hoang DT, Chernomor L, von Haeseler A, Minh BQ, Vinh LS (2018) UFBoot2: Improving the ultrafast bootstrap approximation. Molecular Biology and Evolution 35(2): 518–522. https://doi.org/10.1093/molbev/msx281

Katoh K, Standley DM (2013) MAFFT multiple sequence alignment software version 7: Improvements in performance and usability. Molecular Biology and Evolution 30(4): 772–780. https://doi.org/10.1093/molbev/mst010

Koch CL (1847) System der Myriapoden. In: Herrich-Schäffer L (Ed.) Kritische Revision der Insectenfauna Deutschlands, Volume 3. Pustet, Regensburg, 1–270. https://doi.org/10.5962/bhl.title.49866

Kumar S, Stecher G, Li M, Knyaz C, Tamura K (2018) MEGA X: Molecular evolutionary genetics analysis across computing platforms. Molecular Biology and Evolution 35(6): 1547–1549. https://doi.org/10.1093/molbev/msy096

Minelli A (2011) Chilopoda – Reproduction. In: Minelli A (Ed.) Treatise on Zoology – Anatomy, Taxonomy, Biology – The Myriapoda, Volume 1. Brill, Leiden – Boston, 279–294. https://doi.org/10.1163/9789004188266_014

Murienne J, Edgecombe GD, Giribet G (2010) Including secondary structure, fossils and molecular dating in the centipede tree of life. Molecular Phylogenetics and Evolution 57: 301–313. https://doi.org/10.1016/j.ympev.2010.06.022

Newport G (1843) On some new genera of the class Myriapoda. Proceedings of the Zoological Society of London 10(1842): 177–181. https://doi.org/10.1080/03745484309442474

Nguyen LT, Schmidt HA, von Haeseler A, Minh BQ (2015) IQ-TREE: A Fast and Effective Stochastic Algorithm for Estimating Maximum-Likelihood Phylogenies. Molecular Biology and Evolution 32(1): 268–274. https://doi.org/10.1093/molbev/msu300

Satria R, Kurushima H, Herwina H, Yamane S, Eguchi K (2015) The trap-jaw ant genus *Odontomachus* Latreille (Hymenoptera: Formicidae) from Sumatra, with a new species description. Zootaxa 4048(1): 1–36. https://doi.org/10.11646/zootaxa.4048.1.1

Silvestri F (1919) Contributions to a knowledge of the Chilopoda Geophilomorpha of India. Record of the Indian Museum, Calcutta 16: 45–107. https://doi.org/10.5962/bhl.part.25916

Sograff NJ (1882) Zur Embryologie der Chiiopoden. Zoologischer Anzeiger 5: 582–585.

Tsukamoto S, Nguyen AD, Eguchi K (2021) Confirmation of the phylogenetic position of the unique geophilomorph genus *Vinaphilus* Tran, Tran & Bonato, 2019 (Chilopoda: Geophilomorpha: Gonibregmatidae) by molecular phylogenetic analyses, with two new

species from the Central Highlands of Vietnam. Zoologischer Anzeiger 293: 74–88. https://doi.org/10.1016/j.jcz.2021.05.004

Tuf IH, Mock A, Dvořák L (2018) An exotic species spreads through Europe: *Tygarrup javanicus* (Chilopoda: Geophilomorpha: Mecistocephalidae) is reported from the Slovakia and the Czech Republic. Journal of Asia-Pacific Entomology 21(2): 560–562. https://doi.org/10.1016/j.aspen.2018.03.004

Uliana M, Bonato L, Minelli A (2007) The Mecistocephalidae of the Japanese and Taiwanese islands (Chilopoda: Geophilomorpha). Zootaxa 1396(1): 1–84. https://doi.org/10.11646/zootaxa.1396.1.1

Verhoeff KW (1939) Chilopoden der Insel Mauritius. Zoologische Jahrbücher, Abteilung für Systematik 72: 71–98.

Xiong B, Kocher TD (1991) Comparison of mitochondrial DNA sequences of seven morphospecies of black flies (Diptera: Simuliidae). Genome 34(2): 306–311. https://doi.org/10.1139/g91-050

ZooKeys 1115: 151–168 (2022)
doi: 10.3897/zookeys.1115.86477
https://zookeys.pensoft.net

RESEARCH ARTICLE

A peer-reviewed open-access journal
ZooKeys
Launched to accelerate biodiversity research

A new species of the ant *Platythyrea clypeata* species group (Hymenoptera, Formicidae, Ponerinae) from continental Asia

Weeyawat Jaitrong[1,2], Zhenghui Xu[3], Salinee Khachonpisitsak[4]

1 *Office of Natural Science Research, National Science Museum, 39 Moo 3, Khlong 5, Khlong Luang, Pathum Thani, 12120, Thailand* **2** *Biology Divisions, Faculty of Science and Technology, Rajamangala University of Technology Thanyaburi, Pathum Thani, 12120 Thailand* **3** *Key Laboratory of Forest Disaster Warning and Control in Yunnan Province, College of Biodiversity Conservation, Southwest Forestry University, Kunming, Yunnan Province 650224, China* **4** *Department of Biology, Faculty of Science, Burapha University, 169 Long-Hard Bangsaen Road, Sanesuk, Mueang, Chon Buri, 20131 Thailand*

Corresponding author: Salinee Khachonpisitsak (salineek@go.buu.ac.th)

Academic editor: Matthew Prebus | Received 12 May 2022 | Accepted 19 July 2022 | Published 1 August 2022

https://zoobank.org/E5B16FEC-B1B1-4244-9CE3-5E5108157039

Citation: Jaitrong W, Xu Z, Khachonpisitsak S (2022) A new species of the ant *Platythyrea clypeata* species group (Hymenoptera, Formicidae, Ponerinae) from continental Asia. ZooKeys 1115: 151–168. https://doi.org/10.3897/zookeys.1115.86477

Abstract

The *Platythyrea clypeata* species group is reviewed and three species, including one new species, *P. homasawini* **sp. nov.**, are recognized. This species group is distinguished from the *P. parallela* species group by the reddish-brown body, the elliptical shape of the propodeal spiracle, the elongate antennal scape, and the distinctly narrowed posteriad space between frontal carinae. *Platythyrea homasawini* **sp. nov.**, from Thailand and China, is described based on the worker caste. The type series of the new species was collected on the forest floor from dead wood in an advanced stage of decomposition. A key to the Oriental species of the genus *Platythyrea* based on the worker caste is provided.

Keywords

ant, distribution, new species, species group, Thailand

Introduction

The ant genus *Platythyrea* Roger, 1863 (Formicidae, Ponerinae) is a rarely collected group with recent reviews listing 39 species (Schmidt and Shattuck 2014; Antweb 2022). *Platythyrea* has small colonies usually with a few hundred workers or fewer (Villet et al. 1990; Villet 1991; Ito 1994, 2016; Djiéto-Lordon et al. 2001; Hartmann et al. 2005; Molet and Peeters 2006; Yéo et al. 2006). The genus is mainly and widely distributed within tropical and subtropical regions, with peak diversity in the Ethiopian region (17 spp.), followed by the Neotropical (9 spp.), Oriental (9 spp.), and Australian regions (6 spp.) (Schmidt and Shattuck 2014; Bolton 2022). At present, seven species have been recorded in Southeast Asia (*Platythyrea bidentata* Brown, 1975; *P. clypeata* Forel, 1911; *P. inermis* Forel, 1910; *P. parallela* (F. Smith, 1859); *P. quadridenta* Donisthorpe, 1941; *P. tricuspidata* Emery, 1900 and *P. janyai* Phengsi, Jaitrong, Ruangsittichai & Khachonpisitsak, 2018). Among them, five species are reported from Thailand, and they belong to two species groups (sensu Brown 1975): the *P. clypeata* group (*P. clypeata* and *P. janyai*) and *P. parallela* group (*P. parallela*, *P. quadridenta*, and *P. tricuspidata*) (Phengsi et al. 2018; Khachonpisitsak et al. 2020). Our recent examination of *Platythyrea* specimens from Thailand, Laos, Malaysia, and China has revealed the presence of a new species assigned to the *P. clypeata* group. The distribution data and diagnostic features for three species in this group are discussed. A key to the Oriental species of the genus *Platythyrea* based on the worker caste is updated from Phengsi et al. (2018).

Materials and methods

This study is mainly based on the material deposited in the Natural History Museum of the National Science Museum, Thailand (THNHM). The specimens were compared with high-resolution images of holotypes and paratypes of closely related species (*Platythyrea gracillima* Wheeler, 1922; *P. clypeata*; and *P. prizo* Kugler, 1977) available on Antweb (2022) and Antwiki (2022). The holotype and paratypes of *P. janyai* were also examined. The holotype and paratypes of *P. homasawini* sp. nov. are deposited in THNHM.

Most morphological observations were made with a ZEISS Discovery V12 stereoscope. Multi-focused montage images were produced using NIS-Elements-D from a series of source images taken by a Nikon Digital Sight-Ri1 camera attached to a Nikon AZ100M stereoscope. Specimens were measured for the following parts using a micrometer on a ZEISS Discovery V12 stereoscope. All measurements are given in millimeters and recorded to the second decimal place.

Standard measurements and indices used in the paper are as defined in Bolton (1975):

CI Cephalic index = HW/HL ×100.
DPW Dorsal petiole width: maximum width of petiole in dorsal view.
EI Eye index = EL/HW ×100.
EL Eye length: the maximum length of the eye.

HL Head length: straight-line length of head in perfect full-face view, measured from the mid-point of the anterior clypeal margin to the midpoint of the posterior margin. In species where one or both of these margins are concave, the measurement is taken from the mid-point of a transverse line that spans the apices of the projecting portions.

HW Head width: maximum width of head in full-face view, excluding the eyes.

ML Mesosoma length: the diagonal length of the mesosoma in lateral from the anterior margin of the pronotum to the posteroventral angle of the metapleuron, excluding the neck.

PH Petiole height: height of petiole measured in lateral view from the apex of the ventral (subpetiolar) process vertically to a line intersecting the dorsal most point of the node.

PL Petiole length: length of petiole measured in lateral view from the anterior articulation to the posterior articulation of petiole.

PW Pronotal width: maximum width of pronotum measured in dorsal view.

SL Scape length: straight-line length of the antennal scape, excluding the basal constriction or neck.

SI Scape index = SL/HW ×100.

TL Total length: total outstretched length of the individual, from the mandibular apex to the gastral apex.

Abbreviations of the type depositories are as follows:

BMNH The Natural History Museum, London, U.K.

MHNG Muséum d'Histoire Naturelle, Geneva, Switzerland.

THNHM Natural History Museum of the National Science Museum, Thailand.

Scanning electron microscope images of *Platythyrea* species were made at the Microscopic Center, Faculty of Science, Burapha University with a LEO 1450 VP scanning electron microscope on gold coated specimens.

Taxonomy

Platythyrea clypeata species group

The species group can be characterized by the following characteristics: 1) body reddish brown; 2) space between frontal carinae distinctly narrowed posteriad (compare Fig. 1B with Fig. 1A); 3) masticatory margin of mandible triangular with a large apical tooth, followed by 9 or 10 smaller teeth, with large and smaller teeth alternating; 4) propodeal spiracle opening elliptical; and 5) posterior margin of petiole convex without spines in dorsal view. Three species are recognized in continental Asia.

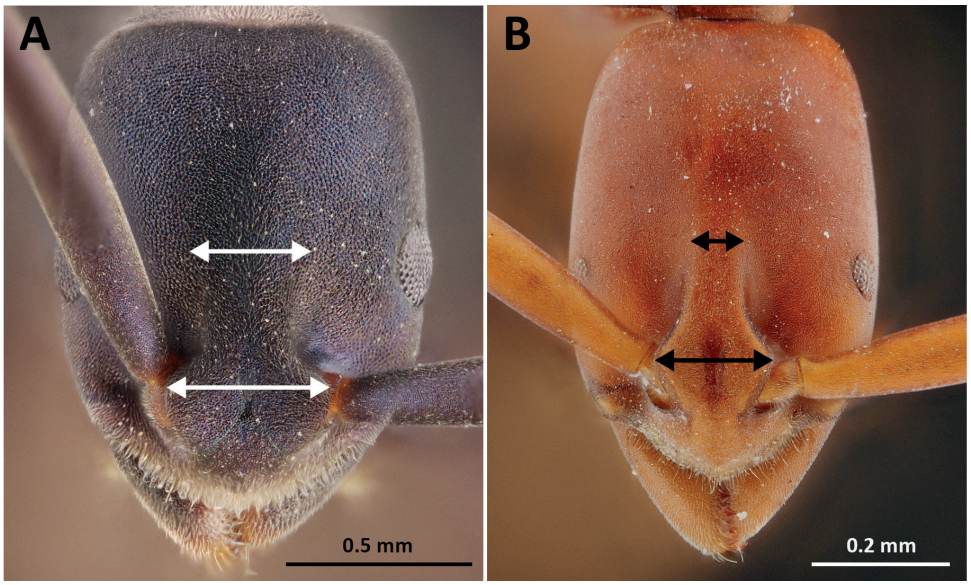

Figure 1. Frontal view focusing on the space between frontal carinae. **A** frontal carinae very widely spaced **B** frontal carinae relatively narrowly separated.

Platythyrea clypeata Forel, 1911

Figs 2, 5A1–A3

Platythyrea clypeata Forel, 1911: 378; Brown 1975: 50; Bolton 1995: 336; Schmidt and Shattuck 2014: 51; Khachonpisitsak et al. 2020: 153. Senior synonym of *P. thwaitesi*: Brown 1975: 8.

Platythyrea thwaitesi Donisthorpe, 1931: 496. Junior synonym of *P. clypeata*: Brown 1975: 8.

Type. ***Holotype*** of *P. clypeata*: alate queen from "Pays des Moïs", Cochinchinne française (Indochina), deposited in MHNG (AntWeb image examined, CASENT0907112). Holotype of *P. thwaitesi*: alate queen from Sri Lanka, deposited in BMNH (AntWeb image examined, CASENT0900568).

Non-type material examined. Laos • 10 workers (THNHM-I-24983) and 1 dealate queen (THNHM-I-24982), Laos, Vientiane, Pak Ngum District, Ban Phang Dang, ca 300 m alt., 14.VI.2010, W. Jaitrong leg., Colony no. WJT-LAO-143 (THNHM-I-24981) • 1 worker (THNHM-I-24984), Laos, Vientiane, Pak Ngum District, Ban Phang Dang, 14.VI.2010, Sk. Yamane leg., Colony no. LA10-SKY-128 • 1 worker (THNHM-I-24981) Laos, Vientiane, Pak Ngum District, Ban Phang Dang, ca 300 m alt., 12.VI.2010, W. Jaitrong leg. – Thailand • 9 workers (THNHM-I-02423 to THNHM-I-02431), eastern Thailand, Chachoengsao Province, Tha Takiab District, Khao Ang Reu Nai Wildlife Sanctuary, 27.IX.2002, W. Jaitrong leg., Colony no. WJT270902-01 • 3 workers (THNHM-I-02432 to THNHM-I-02434), same local-

ity, date and collector, Colony no. WJT270902-1 • 6 workers (THNHM-I-02435 to THNHM-I-02440), eastern Thailand, Sa Kaeo Province, Khao Ang Reu Nei Wildlife Sanctuary, 26.VI.2003, W. Jaitrong leg., Colony no. WJT03-TH-228; 22 workers (THNHM-I-02441 to THNHM-I-02452) and 1 male (THNHM-I-02453), eastern Thailand, Chanthaburi Province, Soi Dao District, 14.V.2008, W. Jaitrong leg., Colony no. WJT08-E065 • 14 workers (THNHM-I-24980, THNHM) and 1 dealate queen, central Thailand, Nakhon Nayok Prov., Muang Dist., Nang Rong Temple, in rotting wood, 29.VIII.2018, W. Jaitrong leg., Colony no. WJT290819-09.

Measurements and indices (*n* = 10). TL 5.74–6.20, HL 1.29–1.39, HW 0.86–0.89, SL 1.12–1.18, EL 0.10, PW 0.76–0.83, ML 1.85–2.05, PL 0.66–0.73, PH 0.46–0.53, DPW 0.40–0.43, CI 61–69, EI 11, SI 125–138.

Description of workers. ***Head*** in full-face view rectangular, clearly longer than broad, with sides weakly convex or almost parallel, posterior corners narrowly rounded, posterior margin feebly concave. Antennae relatively short, scapes extending beyond posterior corners of head by about 1/5 of their length. Clypeus roughly triangular, median portion distinctly convex, anterior margin bluntly angled. Mandibles triangular, masticatory margin with a large apical tooth, followed by about ten smaller teeth, large and small teeth alternating, basal margin without denticle. Eye very small and flat, located laterally at anterior to mid-length of head, with five ommatidia along longest axis. Frontal lobes close to each other and rounded. Space between frontal carinae distinctly narrowed posteriad.

Mesosoma elongate, in profile pronotum weakly convex, promesonotal suture distinct, dorsal outline of mesonotum and propodeum straight, metanotal groove absent, propodeal junction broadly rounded, declivity of propodeum obviously concave, propodeal spiracle opening elliptical. Legs long.

Petiole cylindrical in profile view and sessile; in profile view clearly longer than high, dorsal outline almost straight, anterodorsal corner broadly rounded, posterodorsal corner forming an acute angle, posterior margin weakly concave, ventral margin weakly concave with narrowly rounded anteroventral corner; in dorsal view the node roughly rectangular, longer than broad, slightly narrower posteriorly, posterior margin convex and with shallow median concavity.

Sculpture. Dorsum of head finely punctate, lateral face of head above eyes punctate, with dense foveae. Dorsum of mesosoma finely punctate similar to dorsum of head, lateral faces of pronotum, metapleuron and propodeum punctate, with sparse shallow foveae. Petiole finely micropunctate. Gastral tergites I and II finely reticulate. Antennal scapes finely micropunctate.

Pilosity. Pubescence very short and fine all over the body surface; standing hairs present on tip of gaster.

Coloration. Body color reddish brown to darkish brown; antennae, legs, and tip of gaster yellowish brown to reddish brown. Eyes grey. Pilosity white.

Description of dealate queen. See Phengsi et al. (2018).

Habitat. *Platythyrea clypeata* occurs in the lowlands (200–300 m alt.) and inhabits primary dry evergreen forest and disturbed forests. All colonies of this species were collected from dead wood on the forest floor in an advanced stage of decomposition.

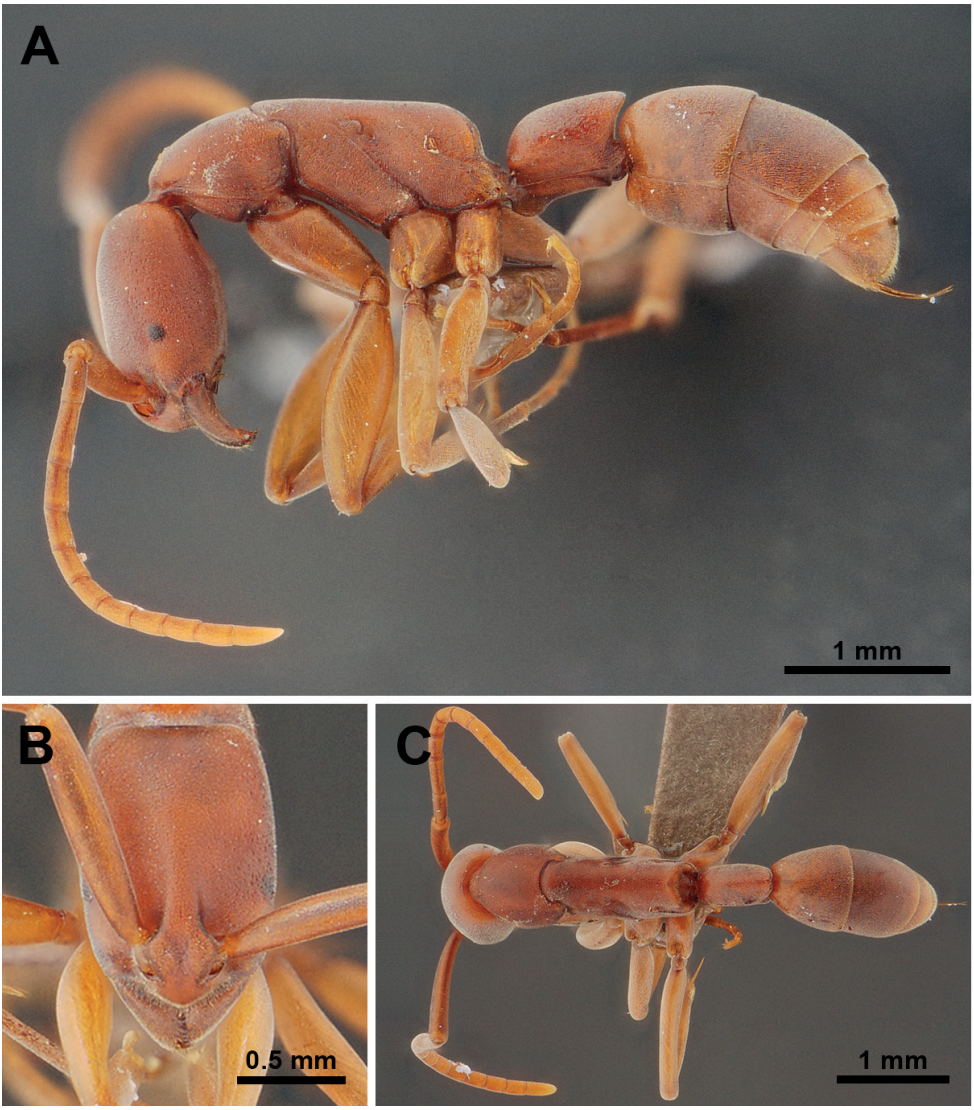

Figure 2. *Platythyrea clypeata* (non-type worker, WJT290819-09). **A** body in profile view **B** head in full-face view **C** body in dorsal view.

Distribution. Sri Lanka, Vietnam, Laos (Vientiane), and Thailand (Chachoengsao, Sa Kaeo, Chanthaburi, and Nakhon Nayok provinces) (Fig. 6).

Comparative notes. *Platythyrea clypeata* is similar to *P. gracillima*, *P. janyai*, and *P. prizo*. However, *P. clypeata* can be easily separated from *P. gracillima* by the following characteristics (characters of *P. gracillima* in parentheses unless otherwise stated): 1) body size smaller (TL = 5.74–6.20 in *P. clypeata*; TL = 9 mm in *P. gracillima*); 2) eye smaller and flat (0.1 mm long in *P. clypeata*; 0.3 mm long and convex in *P. gracillima*); 3) clypeus narrow and rather convex (clypeus broad and rather flat); 4) declivity of

propodeum concave (propodeal declivity flat); 5) seen from back propodeal declivity rounded above (propodeal declivity concave above); 6) petiole laterally swollen (petiole laterally compressed); 7) head finely punctate (head rather smooth).

Platythyrea clypeata can be distinguished from *P. prizo* by the following characteristics (characters of *P. prizo* in parentheses unless otherwise stated): 1) head shorter (CI = 61–69 in *P. clypeata*; CI = 70–72 in *P. prizo*); 2) eye flat and small (0.1 long mm in *P. clypeata*; eye very large, 0.31 long mm *P. prizo*); 3) eye without erect pubescence (eye covered with extremely fine short erect pubescence); 4) propodeum junction obtusely angulated (propodeum junction armed with a pair of short teeth or tubercles); 5) in profile, posterodorsal corner of petiole forming an acute angle (roundly convex).

Lastly, this species is separated from *P. janyai* (characters of *P. janyai* in parentheses unless otherwise stated) by 1) head relatively longer (CI 61–69 in *P. clypeata*; CI 72–74 in *P. janyai*); 2) eye clearly smaller (EL 0.10 mm long with 5 ommatidia on longest axis in *P. clypeata*; EL 0.20 mm long with 11 ommatidia on longest axis in *P. janyai*); 3) eye flat (eye convex); 4) head finely punctate with dense shallow foveae (dorsum and lateral face of head finely micropunctate without foveae); 5) in profile petiole slightly longer than high and in dorsal view its node slightly narrower posteriorly (clearly longer than high and in dorsal view node anteriorly as broad as posteriorly); 6) ventral outline of petiole feebly concave (weakly convex) (see Fig. 5 for comparison).

***Platythyrea homasawini* sp. nov.**
https://zoobank.org/B91E483E-24FB-454F-9F14-8EAC635F5631
Figs 3, 5B1–B3

Platythyrea clypeata: Xu and Zeng 2000: 214, figs 1–3.

Type. ***Holotype*** worker (THNHM-I-26225), northern Thailand, Chiang Mai Prov., Doi Saket Dist., Ban Mae Pong, 24.XI.2021, K. Homasawin leg., Colony No. WJT241121-01. ***Paratypes***: 29 workers (THNHM-I-26226 to THNHM-I-26250, THNHM-I-24977 to THNHM-I-24979, and THNHM-I-26445), same data as holotype.

Non-type material examined. China • 1 worker, Yunnan Prov., Menghai County, Meng'a Town, Papo Village, 1280 m, No. A97-2318, collected from secondary monsoon evergreen broadleaf forest, 10.IX.1997, Zhenghui Xu leg. – Thailand • 1 worker (THNHM-I-02463), northern Thailand, Chiang Mai Prov., Muang Dist., restored forest, 8.V.2002, S. Sonthichai leg. • 1 worker (THNHM-I-02454), western Thailand, Kanchanaburi Prov., Thong Pha Phum N.P., Natural Forest, 8.III.2005, W. Sakchooeong leg.

Measurements and indices. ***Holotype.*** TL 7.72, HL 1.60, HW 1.08, SL 1.72, EL 0.20, PW 0.96, ML 2.84, PL 1.08, PH 0.68, DPW 0.44, CI 68, EI 19, SI 159. ***Paratypes*** (n = 10). TL 7.72–7.80, HL 1.56–1.64, HW 1.08–1.12, SL 1.64–1.68, EL 0.16–0.20, PW 0.96–0.99, ML 2.80–2.84, PL 1.08–1.12, PH 0.60–0.64, DPW 0.40–0.44, CI 68–69, EI 15–19, SI 150–159.

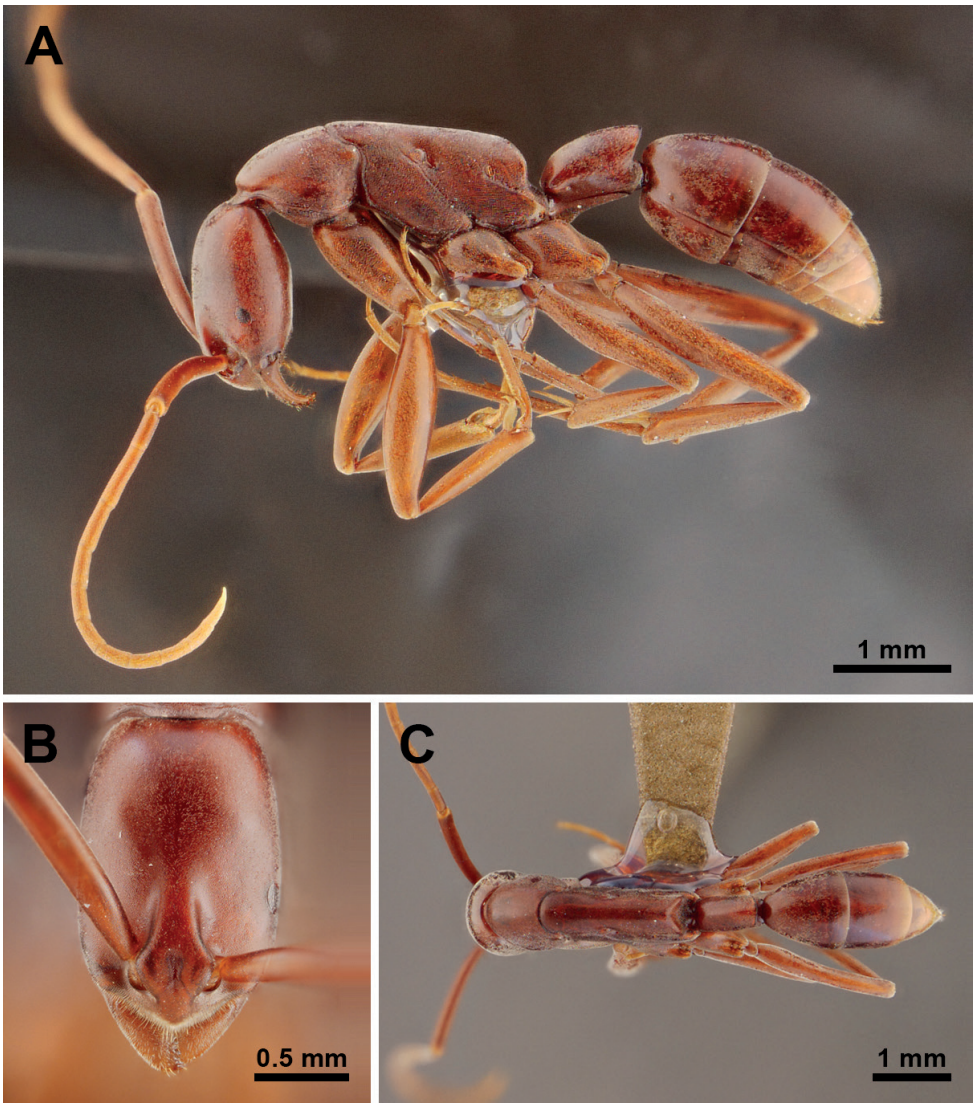

Figure 3. *Platythyrea homasawini* sp. nov. (holotype worker, THNHM-I-02463). **A** body in profile view **B** head in full-face view **C** body in dorsal view.

Description of workers (*holotype* and *paratypes*). *Head* in full-face view subrectangular, clearly longer than broad, weakly widening anteriorly, sides weakly convex, posterior margin almost straight, posterior corners narrowly rounded. Antennae relatively long, scapes extending beyond posterior corners of head by about 1/4 of their length. Clypeus roughly triangular, roundly convex medially, anterior margin bluntly angled. Mandibles triangular, masticatory margin with a large apical tooth, followed by eight smaller teeth, large and small teeth alternating, basal margin without denticle. Eyes flat, located at anterior 1/3 of head length, moderately large, each with 7 or 8

ommatidia along its longest axis. Frontal lobes close to each other and rounded. Space between frontal carinae distinctly narrowed posteriad.

Mesosoma elongate, in profile view pronotum weakly convex, promesonotal suture distinct, dorsal outline of mesonotum and propodeum straight, metanotal groove absent, propodeal junction broadly rounded, declivity of propodeum obviously concave; propodeal spiracle opening elliptical. Legs very long.

Petiole cylindrical and sessile, in profile view clearly longer than high, dorsal outline weakly convex, anterodorsal corner broadly rounded, posterodorsal corner extending into an acute angle, posterior margin oblique and straight, ventral margin almost straight with narrowly prominent anteroventral corner; in dorsal view the node of petiole rectangular, longer than broad, sides straight and parallel, posterior margin weakly convex.

Sculpture. Head entirely finely micropunctate. Dorsum of mesosoma finely micropunctate, mesopleuron, metapleuron and sides of propodeum punctate. Petiole finely micropunctate. Gaster superficially shagreened.

Pilosity. Whole body surface and appendages covered with very short thin pubescence. Standing hairs absent.

Coloration. Body color reddish brown; antennae, legs, and tip of gaster yellowish brown. Eyes grey. Pubescence white.

Distribution. China (Yunnan Province) and Thailand (Chiang Mai and Kanchanaburi provinces) (Fig. 6).

Etymology. The specific name is dedicated to Mr Kaisihanat Homasawin, who donated the type series.

Comparative notes. The new species is similar to *P. janyai* but it can be separated from *P. janyai* by the following characteristics (characters of *P. janyai* in parentheses unless otherwise stated): 1) head weakly widening anteriorly (head not widening anteriorly); 2) dorsal outline of petiole weakly convex (dorsal outline of petiole almost straight); 3) posterior margin of petiolar node without a concavity in the middle (posterior margin of petiolar node with a concavity in the middle): 4) body surface with thin pubescence (body surface with thick pubescence); 5) head longer (CI = 66 in *P. homasawini*, CI = 72 in *P. janyai*); 6) antennal scape relatively long, 1/3 of its length extending beyond posterolateral corner of head (clearly extending beyond posterolateral corner of head); 7) eye smaller and flat (EL = 0.17 mm in *P. homasawini*; EL = 0.20 mm and slightly convex in *P. janyai*); 8) seen from back propodeal declivity rounded above (propodeal declivity tapering above); 9) dorsal outline of petiole weakly convex (almost straight).

Platythyrea homasawini can be easily separated from *P. clypeata* by the following characteristics (characters of *P. clypeata* in parentheses unless otherwise stated): 1) head in full-face view, posterior margin weakly concave (posterior margin almost straight); 2) antennal scape relatively long, 1/3 of its length extending beyond posterolateral corner of head (antennal scape short, 1/4 of its length extending beyond posterolateral corner of head); 3) clypeus broad (clypeus narrow); 4) eye larger (EI = 15, with 7 ommatidia in *P. homasawini*; EI = 11, with 5 ommatidia in *P. clypeata*); 5) mesosoma relative

longer (WL = 2.64 in *P. homasawini*; WL=1.85–2.05 in *P. clypeata*); 6) mesopleuron not demarcated from mesonotum (mesopleuron clearly demarcated from mesonotum by shallow furrow); 7) in profile view, propodeal junction roundly convex (propodeal junction obtusely angulate); 8) in dorsal view, posterior margin of petiole clearly convex (posterior margin of petiole convex with shallow median concavity); 9) lateral face of head entirely micropunctate (lateral face of head areas behind, above and below eye punctate, with dense foveae); 10) gaster superficially shagreened (finely reticulate).

Platythyrea homasawini can be distinguished from *P. gracillima* by the following characteristics (characters of *P. gracillima* in parentheses unless otherwise stated): 1) clypeus roundly convex (rather flat in *P. gracillima*); 2) petiole laterally convex; 3) seen from above longer than high (petiole laterally compressed); 4) seen from above a little more than twice as long as broad); 5) mandible finely micropunctate (mandible finely and densely punctate); 6) head entirely finely micropunctate (rather smooth in *P. gracillima*).

Platythyrea janyai Phengsi, Jaitrong, Ruangsittichai & Khachonpisitsak, 2018

Figs 4, 5C1–C3

Platythyrea janyai Phengsi et al. 2018: 89, figs 1, 5B1–B3; Khachonpisitsak et al. 2020: 154.

Types. ***Holotype*** (THNHM-I-02392) and three ***paratypes*** (THNHM-I-02393 to THNHM-I-02395) workers, southern Thailand, Phatthalung Province, Si Banphot District, Riang Thong Waterfall, Khao Pu Khao Ya National Park, 28.IX.2007, W. Jaitrong leg., Colony no. WJT07-TH-2060 (THNHM-I-02392), deposited in THNHM (examined).

Non-type material examined. Malaysia • 1 worker, western Malaysia, Selangor, Ulu Gombak, 22.III.2013, F. Ito leg. (THNHM-I-02465) – Thailand • 2 workers, southern Thailand, Trang Province, Na Yong District, Khao Chong Botanical Garden, 7.XI.2014, W. Jaitrong leg., Colony No WJT071114-2 (THNHM-I-02421 to THNHM-I-02422) • 5 workers, same locality and collector, 26.XII.2018, Colony no. WJT261218-1 (THNHM).

Measurements and indices (n = 4). TL 6.63–6.96, HL 1.42–1.45, HW 1.06, SL 1.39–1.42, EL 0.20, ML 2.21–2.31, PL 0.73–0.79, PH 0.53, DPW 0.40, CI 72–74, EI 18, SI 131–134.

Description of workers (*holotype* and *paratypes*). ***Head*** in full-face view subrectangular, clearly longer than broad, sides weakly convex, posterior margin almost straight, posterior corners narrowly rounded. Antenna relatively long, scapes extending beyond posterior corners of head by about 1/4 of their length. Clypeus roughly triangular, median portion distinctly convex, anterior margin broadly convex. Mandibles triangular, masticatory margin with a large apical tooth, followed by 9 or 10 smaller teeth, large and small teeth alternating, basal margin without denticle. Eye slightly

convex, located anterior to mid-length of head, relatively large, with 11 ommatidia on the longest axis. Frontal lobes relatively close to each other, with roundly convex lateral margins. Space between frontal carinae distinctly narrowed posteriad.

Mesosoma elongate, in profile view pronotum weakly convex, promesonotal suture distinct, dorsal outline of mesonotum and propodeum almost straight, metanotal groove absent, propodeal junction narrowly rounded, declivity weakly convex in its upper half and obviously concave in the lower portion, propodeal spiracle opening elliptical. Legs very long.

Figure 4. *Platythyrea janyai* (holotype worker, THNHM-I-02392). **A** body in profile view **B** head in full-face view **C** body in dorsal view.

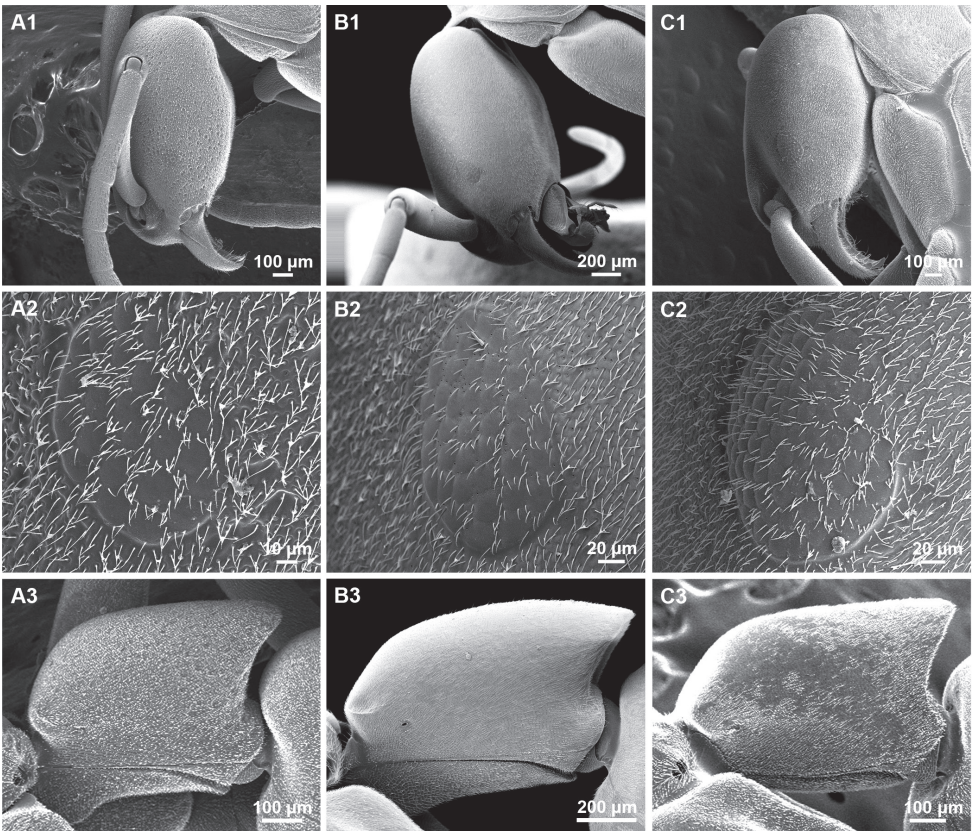

Figure 5. SEM images of *Platythyrea clypeata* (**A1–A3**) *P. homasawini* sp. nov. (**B1–B3**) and *P. janyai* (**C1–C3**). **A1, B1, C1** sculpture on lateral face of head **A2, B2, C2** ommatidia of eye **A3, B3, C3** petiole in profile view.

Petiole cylindrical and sessile, in profile view clearly longer than high, dorsal outline almost straight, anterodorsal corner broadly rounded, posterodorsal corner extending into an acute angle, posterior margin oblique and weakly concave, ventral margin almost straight with narrowly protruding anteroventral corner; in dorsal view node of petiole rectangular, longer than broad, slightly widening posteriorly, sides almost straight, posterior margin weakly convex with a concavity in the middle.

***Sculpture*.** Head, antennal scapes, mesosoma, petiole and gaster finely densely micropunctate.

***Pilosity*.** The whole body surface and appendages covered with short thick pubescence. Standing hairs absent.

***Coloration*.** Body color reddish brown; antennae, legs, and tip of gaster yellowish brown. Eyes grey. Pubescence white.

Distribution. Thailand (Phatthalung and Trang provinces) and Malaysia (Ulu Gombak National Park) (Fig. 6).

Comparative notes. *Platythyrea janyai* is similar to *P. clypeata*, *P. homasawini* and *P. gracillima*. However, *P. janyai* can be easily separated from *P. gracillima* by the

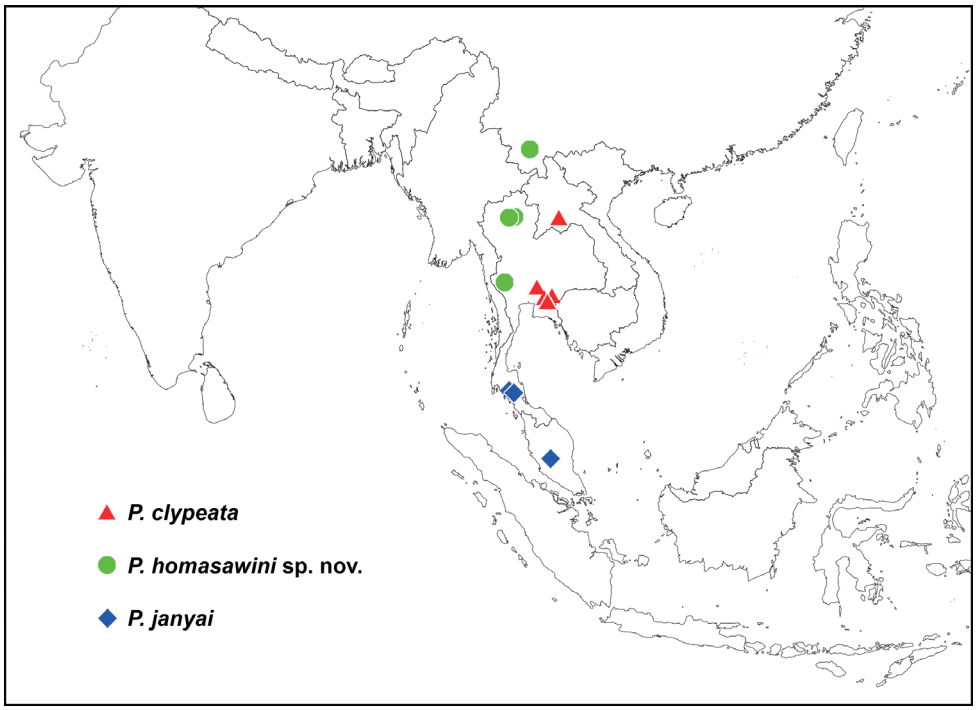

Figure 6. Distribution map of *Platythyrea clypeata* species group based on specimens in this study.

following characteristics (characters of *P. gracillima* in parentheses unless otherwise stated): 1) body size smaller (TL = 6.63 mm in *P. janyai*; 9 mm in *P. gracillima*); 2) eye relatively smaller (EL = 0.2 mm in *P. janyai*; 0.3 mm in *P. gracillima*); 3) seen from back, propodeal declivity tapering above (propodeal declivity weakly concave above); 4) petiole laterally convex, seen from above longer than broad (petiole laterally compressed, seen from above a little more than twice as long as broad). For differentiation of *P. janyai* and *P. clypeata*, see "Comparative notes" under *P. clypeata*, and of *P. janyai* and *P. homasawini*, see under *P. homasawini*.

Key to known Oriental species of genus *Platythyrea* based on the worker caste (modified from Phengsi et al. 2018)

1 Frontal carinae very widely spaced, not continuing beyond level of posterior margin of antennal insertions (Fig. 1A); propodeal spiracle opening circular...**2**

– Frontal carinae relatively narrowly separated, extending far beyond level of posterior margin of antennal insertions where space between them is very narrow (Fig. 1B); propodeal spiracle opening elliptical.....**8**

2 In dorsal view, posterior margin of petiole with 2 or 3 distinct spines, teeth or blunt angles (Fig. 7A, B **3**

– In dorsal view, posterior margin of petiole without distinct spines, teeth or sharp angles (Fig. 7C) **6**

3 In dorsal view, posterior margin of petiole clearly concave with distinct lateral blunt angles; in profile view, petiole almost as long as high **4**

– In dorsal view, posterior margin of petiole with 3 distinct spines (Fig. 7A); in profile view, petiole longer than high..... ..... ***P. tricuspidata*** **Emery, 1900**

4 In full-face view, head oval, almost as long as broad, posterior margin broadly convex (Fig. 8A); in profile view, posterodorsal corner of petiole nearly right angle (Fig. 7F) ..... ***P. sagei*** **Forel, 1900**

– In full-face view, head subrectangular, slightly longer than broad, posterior margin broadly almost straight or weakly concave (Fig. 8B); in profile view, posterodorsal corner of petiole bearing truncate spine (Fig. 7G) **5**

5 In profile view, lateral face of pronotum punctate, with dense foveae; lateral face of petiole wrinkled; in profile view, dorsal outline of petiole roundly convex (Fig. 7H)..... ***P. quadridenta*** **Donisthorpe, 1941**

– In profile view, lateral faces of pronotum and petiole rather smooth, without foveae; in profile view, dorsal outline of petiole almost straight or weakly convex (Fig. 7G)..... ***P. bidentata*** **Brown, 1975**

6 In full-face view, head elongate (CI < 77), posterior margin deeply concave.. ..... ***P. nicobarensis*** **Forel, 1905**

– In full-face view, head elongate (CI > 77), posterior margin shallowly concave..... **7**

7 In dorsal view, petiole clearly longer than broad (Fig. 7C); antennal scape relatively short, not reaching posterior corner of head..... ..... ***P. parallela*** **(Smith, 1859)**

– In dorsal view, petiole almost as long as broad (Fig. 7D); antennal scape relatively long, slightly extending beyond posterior corner of head .... ***P. inermis*** **Forel, 1910**

8 Lateral face of head and pronotum punctate, with dense foveae (Fig. 5A1); antennal scape relatively short (SI = 125–138); smaller species (TL 5.74–6.20; HW 0.86–0.89); eye with 5 or 6 ommatidia on longest axis..... ..... ***P. clypeata*** **Forel, 1911**

– Lateral face of head and pronotum finely micropunctate (Figs 5B1, 5C1); antennal scape relatively long (SI > 150); larger species (TL 7.59–7.80; HW 1.06–1.12)..... **9**

9 Head narrower posteriorly (Fig. 3B). Dorsal outline of petiole weakly convex, posterior margin of petiolar node without a concavity in the middle (Fig. 7E). Body surface with thin pubescence (Fig. 3A). Eyes with 7 or 8 ommatidia on longest axis (Fig. 5B2). ..... ***P. homasawini*** **sp. nov.**

– Head not narrower posteriorly (Fig. 4B). Dorsal outline of petiole almost straight, posterior margin of petiolar node with a concavity in the middle. Body surface with thick pubescence (Fig. 4A). Eyes with 9–11 ommatidia on longest axis (Fig. 5C2) ..... ***P. janyai*** **Phengsi et al., 2018**

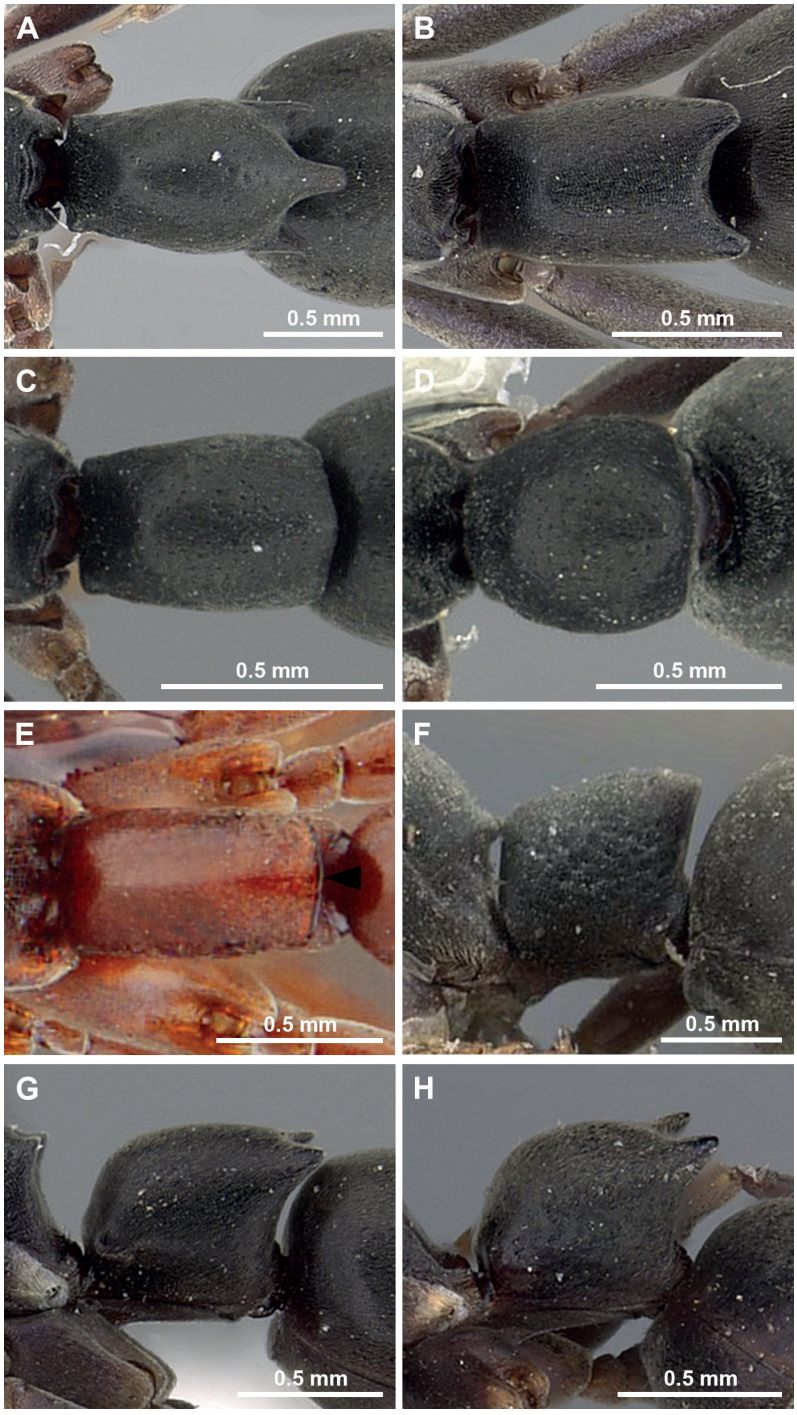

Figure 7. Petiole in dorsal view (**A–E**) and in profile view of *Platythyrea* (**F–H**). **A** *P. tricuspidata* (CASENT0281865) **B** *P. bidentata* (CASENT0281867) **C** *P. parallela* (CASENT0260477) **D** *P. inermis* (CASENT0260498) **E** *P. homasawini* sp. nov. **F** *P. sagei* (CASENT0907117) **G** *P. bidentata* (CASENT0281867) **H** *P. quadridenta* (CASENT0900569).

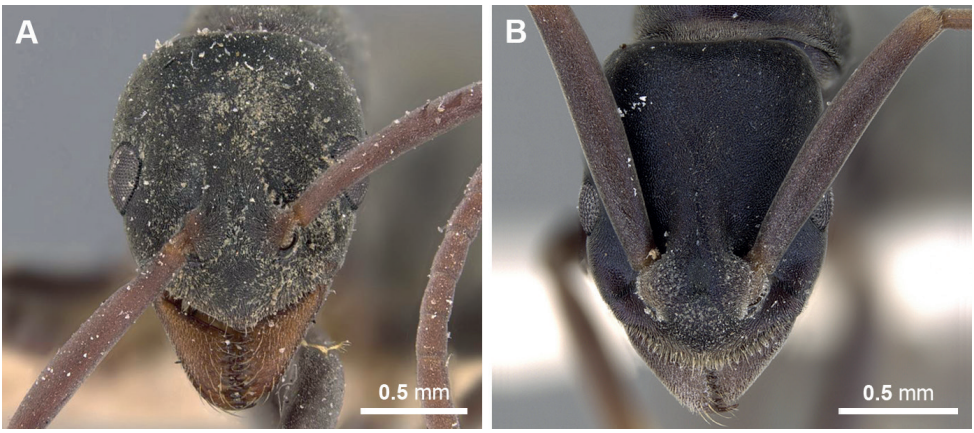

Figure 8. Head in full-face view of *Platythyrea*. **A** *P. sagei* (CASENT0907117) **B** *P. bidentata* (CASENT0281867).

Discussion

With this study, 40 valid species of the genus *Platythyrea* are now known around the world. Among them, six species are found in Thailand, and they belong to two species groups (sensu Brown, 1975): *P. clypeata* group (*P. clypeata*, *P. homasawini* sp. nov., and *P. janyai*) and *P. parallela* group (*P. parallela*, *P. quadridenta*, and *P. tricuspidata*).

The shape of the frontal lobe, mandibular shape and dentition, and shape of mesosoma and petiolar node were characters used by Brown (1975) to distinguish the two species groups mentioned here. These morphological characters were confirmed and used by several authors who described new species after Brown (1975) (Kugler 1977; Lattke 2003; De Andrade 2004; Aria et al. 2011; Phengsi et al. 2018). The present study follows the previous works and also proposed the peculiar shape of the propodeal spiracle, frontal carina condition, and shape of propodeal junction as more important characters to separate the two species groups.

The *P. clypeata* group can be distinguished from other congeners mainly by the following: body reddish brown; space between frontal carinae distinctly narrowed posteriad; propodeal spiracle opening elliptical, petiole longer than high, and posterior margin concave. The worker caste of *Platythyrea* species is generally monomorphic with little variation in size within species. Thus, worker body size can be used for separating large and small species. In this study, worker body size has been used to separate *P. homasawini* sp. nov., *P. janyai*, and *P. clypeata*.

Platythyrea clypeata is distinctly allopatric with *P. janyai* in geographic subregion in continental Asia (Phengsi et al. 2018). It has been recorded from Sri Lanka, Vietnam, Laos, and eastern Thailand (Brown 1975), whereas *P. janyai* occurs on the Malay Peninsula (South Thailand and West Malaysia). However, *P. clypeata* and *P. janyai* both were found in lowland (< 300 m a.s.l.). *Platythyrea clypeata* inhabits various habitats including plantations, secondary forests, and primary dry evergreen forests. *Platythyrea janyai* is confined to primary evergreen forests. *Platythyrea homasawini* sp. nov. is restricted to highland hill evergreen forests.

Acknowledgements

We thank Yudthana Samung from the Department of Medical Entomology, Faculty of Tropical Medicine, Mahidol University, Thailand for imaging assistance in this paper. This study was partly financially supported by Burapha University and Thailand Science Research and Innovation (TSRI) (grant no. FF 2.7/2565); Thailand Science Research and Innovation, the National Science Museum, Thailand; National Natural Science Foundation of China (no. 31860615); and Fauna Sinica Compiling Programs of the National Natural Science Foundation Committee of China (no. 31750002).

References

Antweb (2022) *Platythyrea* Roger, 1863. https://www.antweb.org/browse.do?subfamily=ponerinae&genus=platythyrea&rank=genus [accessed on 18 March 2022]

Antwiki (2022) Checklist of *Platythyrea* species. https://www.antwiki.org/wiki/Platythyrea [accessed on 18 March 2022]

Aria C, Perrihot V, Nel A (2011) Fossil ponerine in early Eocene amber in France. Zootaxa 2870: 53–62. https://doi.org/10.11646/zootaxa.2870.1.3

Bolton B (1975) A revision of the ant genus *Leptogenys* Roger (Hymenoptera: Formicidae) in the Ethiopian region with a review of the Malagasy species. Bulletin of the British Museum (Natural History). Entomology 31: 235–305. https://doi.org/10.5962/bhl.part.29487

Bolton B (1995) A New General Catalogue of the Ants of the World. Harvard University Press, Cambridge, 504 pp. https://doi.org/10.1086/419489

Bolton B (2022) An online catalog of the ants of the world. https://antcat.org [accessed on 17 March 2022]

Brown Jr WL (1975) Contributions toward a reclassification of the Formicidae. V. Ponerinae, tribes Platythyreini, Cerapachyini, Cylindromyrmecini, Acanthostichini and Aenictogitini. Search Agriculture. Entomology (Itaca) 5: 1–115.

De Andrade ML (2004) A new species of *Platythyrea* from Dominican amber and extant species from Honduras. Revue Suisse De Zoologie 111(3): 643–655. https://doi.org/10.5962/bhl.part.80258

Djiéto-Lordon C, Orivel J, Dejean A (2001) Consuming large prey on the spot: The case of the arboreal foraging ponerine ant *Platythyrea modesta* (Hymenoptera, Formicidae). Insectes Sociaux 48(4): 324–326. https://doi.org/10.1007/PL00001784

Forel A (1911) Fourmis nouvelles ou intéressantes. Bulletin de la Société Vaudoise des Sciences Naturelles 47: 331–400. https://doi.org/10.5281/zenodo.25597

Hartmann A, Wantia J, Heinze J (2005) Facultative sexual reproduction in the parthenogenetic ant *Platythyrea punctata*. Insectes Sociaux 52(2): 155–162. https://doi.org/10.1007/s00040-004-0786-5

Ito F (1994) Colony composition of two Malaysian ponerine ants, *Platythyrea tricuspidata* and *P. quadridenta*: sexual reproduction by workers and production of queens (Hymenoptera: Formicidae). Psyche 101: 209–218. https://doi.org/10.1155/1994/19319

Ito F (2016) Nesting and reproductive biology of *Platythyrea* sp. (parallela-group) in the Bogor Botanic Gardens, West Java, Indonesia (Hymenoptera: Formicidae). Asian Myrmecology 8: 111–117. https://doi.org/10.20362/am.008013

Khachonpisitsak S, Yamane S, Sriwichai P, Jaitrong W (2020) An updated checklist of the ants of Thailand (Hymenoptera, Formicidae). ZooKeys 998: 1–182. https://doi.org/10.3897/zookeys.998.54902

Kugler C (1977) A new species of *Platythyrea* (Hymenoptera; Formicidae) from Costa Rica. Psyche 83(2): 216–221. https://doi.org/10.1155/1976/18073

Lattke JE (2003) The genus *Platythyrea* Roger, 1863 in Dominican amber (Hymenoptera: Formicidae: Ponerinae). Entomotropica 18(2): 107–111.

Molet M, Peeters C (2006) Evolution of wingless reproductives in ants: Weakly specialized ergatoid queen instead of gamergates in *Platythyrea conradti*. Insectes Sociaux 53(2): 177–182. https://doi.org/10.1007/s00040-005-0856-3

Phengsi N, Jaitrong W, Ruangsittichai J, Khachonpisitsak S (2018) A sibling species of *Platythyrea clypeata* Forel, 1911 in Southeast Asia (Hymenoptera, Formicidae, Ponerinae). ZooKeys 729: 87–102. https://doi.org/10.3897/zookeys.729.21378

Schmidt CA, Shattuck SO (2014) The higher classification of the ant subfamily Ponerinae (Hymenoptera: Formicidae), with a review of Ponerine ecology and behavior. Zootaxa 3817: 1–242. https://doi.org/10.11646/zootaxa.3817.1.1

Villet MH (1991) Social differentiation and division of labour in the queenless ant *Platythyrea schultzei* Forel, 1910 (Hymenoptera: Formicidae). Tropical Zoology 4(1): 13–29. https://doi.org/10.1080/03946975.1991.10539472

Villet MH, Hart A, Crew RM (1990) Social organization of *Platythyrea lamellosa* (Roger) (Hymenoptera: Formicidae): I. Reproduction. South African Journal of Zoology 25(4): 250–253. https://doi.org/10.1080/02541858.1990.11448221

Xu ZH, Zeng G (2000) Discovery of the worker caste of *Platythyrea clypeata* Forel and a new species of *Probolomyrmex* Mayr in Yunnan, China. Entomologia Sinica 7: 213–217. https://doi.org/10.1111/j.1744-7917.2000.tb00410.x

Yéo K, Molet M, Peeters C (2006) When David and Goliath share a home: Compound nesting of *Pyramica* and *Platythyrea* ants. Insectes Sociaux 53(4): 35–438. https://doi.org/10.1007/s00040-005-0890-9

ZooKeys 1115: 169–186 (2022)
doi: 10.3897/zookeys.1115.75538
https://zookeys.pensoft.net

RESEARCH ARTICLE

A peer-reviewed open-access journal
ZooKeys
Launched to accelerate biodiversity research

Morphological, molecular, and life cycle study of a new species of *Oligogonotylus* Watson, 1976 (Digenea, Cryptogonimidae) from Colombia

Verónica Vélez-Sampedro[1,2], Mónica Uruburu[1], Carolina Lenis[1]

1 *Programa de Estudio y Control de Enfermedades Tropicales (PECET), Facultad de Medicina, Universidad de Antioquia, Calle 62 No. 52-59, CP 050010, Medellín, Antioquia, Colombia* **2** *Departamento de Ciencias Biológicas, Universidad EAFIT, Carrera 49 No. 7 sur 50, Medellín, Antioquia, Colombia*

Corresponding author: Verónica Vélez-Sampedro (vvelezs@eafit.edu.co)

Academic editor: David Gibson | Received 21 September 2021 | Accepted 4 April 2022 | Published 1 August 2022

http://zoobank.org/AD5D01DF-CCF7-4E31-B4BC-468467494B6D

Citation: Vélez-Sampedro V, Uruburu M, Lenis C (2022) Morphological, molecular, and life cycle study of a new species of *Oligogonotylus* Watson, 1976 (Digenea, Cryptogonimidae) from Colombia. ZooKeys 1115: 169–186. https://doi.org/10.3897/zookeys.1115.75538

Abstract

The present study describes *Oligogonotylus andinus* **sp. nov.** and its life cycle from a rural fish farm in Sopetrán, Antioquia, Colombia. The endemic species of snail *Aroapyrgus colombiensis* and the fishes *Poecilia caucana* and *Andinoacara latifrons* are identified as the first intermediate host, the second intermediate host and the definitive host, respectively. The new species was defined through an integrative approach, combining the traditional morphology of its developmental stages with molecular analyses of the markers ITS2 from ribosomal DNA and COI from mitochondrial DNA. This new species can be distinguished from its congeners by genetic divergence, the position of the vitelline fields, and the number of gonotyls. This work represents the first report of a species of this genus in South America.

Keywords

Blue mojarra, Cauca molly, *Oligogonotylus*, South America, taxonomy, Trematoda

Introduction

The genus *Oligogonotylus* Watson, 1976 (Digenea: Cryptogonimidae) includes two species, both occurring in Middle America (Choudhury et al. 2016, 2017). These infect the gastrointestinal tract of freshwater cichlid and characid fishes and have a distinctive

morphological characteristic of a longitudinal row of gonotyls; these small sucker-like structures are present in a number of flukes in this family. The type species, *Oligogonotylus manteri* Watson, 1976, is distributed between southeastern Mexico and Costa Rica (Watson 1976; Pérez-Ponce de León et al. 2007; Sandlund et al. 2010). A second species, *O. mayae* Razo-Mendivil, Rosas-Valdez & Pérez-Ponce de León, 2008, is restricted to the Ría Celestun, Estero Progreso at Corchito, and the Ría Lagartos, Yucatán, Mexico (Razo-Mendivil et al. 2008). Both species utilize three hosts in their life cycle; the operculate micromollusk *Pyrgophorus coronatus* Pfeiffer, 1840 (Cochliopidae) as the first intermediate host (Ditrich et al. 1997; Jiménez-García and Vidal-Martínez 2005; May-Tec et al. 2020), several species of fishes as second intermediate hosts, and the native cichlid fish *Mayaheros urophthalmus* (Günther, 1862) as intermediate and the main definitive host among other 11 species of cichlids (Scholz et al. 1994, 1995; Pérez-Ponce de León et al. 2007; Sosa-Medina et al. 2015; May-Tec et al. 2020). In the present study, we describe a new species of *Oligogonotylus* and its life cycle from a rural fish farm in Colombia using an integrative approach combining ecological, molecular, and morphological data.

Methods

Sampling

We conducted fieldwork in La Miranda village, municipality of Sopetrán, Antioquia, Colombia (6°30'42"N, 75°45'22"W; Fig. 1) in March 2019 and February 2020. The sampling was performed in two fishponds supplied by La Mirandita brook in the Middle Cauca river basin. The ponds are approximately 5 m deep, 14 m long, 13 m wide for the first and 15 m wide for the second, with a total volume of 910 m^3 and 1050 m^3, respectively. Snails *Aroapyrgus colombiensis* Malek & Little, 1971 (n = 451), and fishes of the species *Andinoacara latifrons* (Steindachner, 1878) (n = 22), *Colossoma macropomum* (Cuvier, 1816) (n = 6), *Oreochromis aureus* (Steindachner, 1864) (n = 6), *O. mossambicus* (Peters, 1852) (n = 9), and *Poecilia caucana* (Steindachner, 1880) (n = 105) were collected from the ponds. All animals were transported live to the Laboratory of Helminthology, Programa de Estudio y Control de Enfermedades Tropicales, Facultad de Medicina, Universidad de Antioquia (Medellín, Colombia) and were placed in aquaria prepared with dechlorinated water, artificial aeration, an approximate temperature of 22–24 °C and a controlled photoperiod of 12 h of light and 12 h of darkness.

Collection of the cercariae, metacercariae and adults

The search for the parasite specimens was based on standard techniques, cercarial emission in snails (Vergara and Velásquez 2009; Anucherngchai et al. 2016) and organ dissection of fishes to search for parasite infections under a stereo-dissecting microscope. To induce the cercarial emission, the snails were separated and examined individually under a microscope in 1.5 mL Eppendorf tubes with 0.1 mL of distilled water and stimulated under a cold light source for 4 h. To determine the prevalence

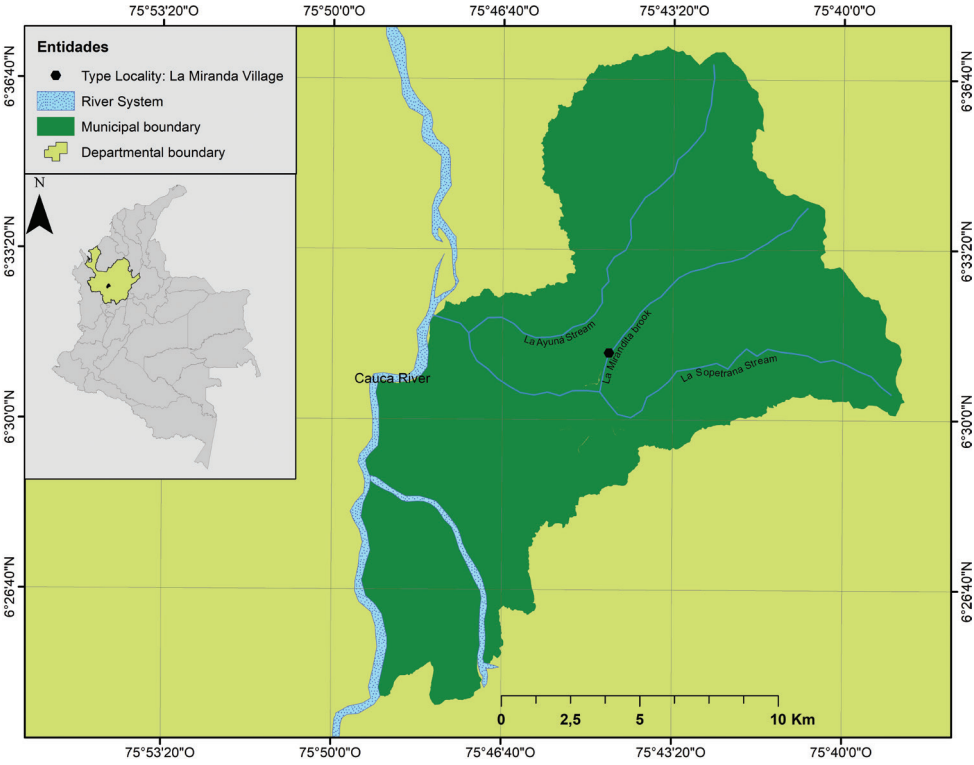

Figure 1. Type locality of the new species of *Oligogonotylus* from La Miranda village, Sopetrán, Antioquia, Colombia. Map made in ArcGIS 18.1.

of infection, non-emitting snails were analysed in triplicate for 21 d. The collected fishes were sacrificed with an overdose of isoeugenol according to Erikson (2011). The muscle of *P. caucana* was examined for the presence of metacercariae, and the digestive tract of *A. latifrons*, *C. macropomum*, *O. aureus*, *O. mossambicus*, and *P. caucana* were examined for the presence of juvenile and adult parasites. The trematodes were rinsed in saline solution, counted, and preserved in 1% glutaraldehyde (cercariae), alcohol-formalin-acetic acid (AFA), and 70% ethanol for morphological identification, or fixed directly in 96% molecular-grade ethanol. The ecological parameters of infections (prevalence, mean intensity and abundance of infection, and intensity range) were calculated according to Bush et al. (1997).

Morphological analyses

Cercariae were studied as temporary mounts stained with methylene blue. Metacercariae and adults were dehydrated in an alcohol series, stained with Meyer's carmine or Borax carmine, cleared in methyl salicylate, and mounted on permanent slides in Canada balsam. A Nikon Alphaphot YS-2 with a Nikon 1.25× drawing tube was used to illustrate the parasites. A Leica DM500 (ICC50 W) microscope was used to analyse

and photograph the stained specimens. Morphometric data are given as the mean and range in micrometers (μm). Line drawings and photographic images were prepared using Inkscape 0.92. Type specimens were deposited in the Colección Colombiana de Helmintos, CCH.116, Universidad de Antioquia, Medellín, Colombia.

DNA extraction, PCR, and sequencing

The DNA was extracted from individual specimens following the protocol of the genELUTE Mammalian genomic DNA miniprep kit. For barcoding, the nuclear ribosomal second internal transcribed spacer region (ITS2) was amplified using the primer pair: ITS-F 5'-CGGTGGATCACTCGGCTCGT-3' and ITSR 5'-CCTGGT-TAGTTTCTTTTCCTCCGC-3' (Iwagami et al. 2000), and the partial cytochrome c oxidase subunit 1 mitochondrial gene (COI) was amplified using the primer pair: JB3 5'-TTTTTTGGGCATCCTGAGGTTTAT-3', and JB4 5'-TAAAGAAAGAACAT-AATGAAAATG-3' (Bowles et al. 1993). All amplification reactions were as follows: 5 min at 95 °C, followed by 35 cycles each of denaturing (94 °C, 30 s), annealing (50 °C, 45 s), and extension (72 °C, 1 min) for ITS2; annealing (53 °C, 45 s), and extension (72 °C, 1 min) for COI, and 5 min at 95 °C, followed by 35 cycles each for denaturing (94 °C, 30 s). The final extension was done at 72 °C for 5 min. PCR products were purified and sequenced by the Sanger method at Macrogen Inc., Seoul, Korea. The accession numbers in GenBank are given for each barcoded specimen.

Phylogenetic tree construction

The ITS2 and partial COI sequences of individual *Oligogonotylus* (ITS2: $n = 4$ adults, $n = 1$ metacercaria, $n = 1$ cercaria; COI: $n = 6$ adults) were edited and assembled in GENEIOUS 2022.0.1 (http://www.geneious.com; Kearse et al. 2012). All sequences were aligned with MUSCLE (Edgar 2004) including sequences of ITS2 and COI of other *Oligogonotylus* species and representative species of other genera of opisthorchids available in GenBank. The best-fitted nucleotide substitution models based on the Bayesian information criterion were estimated in JMODELTEST (Darriba et al. 2012). The genetic divergence (p-value) was calculated for each data set using MEGA X (Kumar et al. 2018) and the resulting alignments were analysed using IQ-TREE 2.1.3 (Nguyen et al. 2015) where all phylogenetic trees were constructed using the maximum-likelihood method. The ITS2 phylogenetic tree was based on the symmetrical model with gamma distribution (SYM+G); the COI phylogenetic tree was based on the general time-reversible model with gamma distribution (GTR+G); and COI–ITS2 concatenated tree was based on the general time-reversible model with proportion of invariable sites and gamma distribution (GTR+I+G). Downloaded sequences of some species of the same family (Cryptogonimidae) and another close family (Heterophyidae) were used in all cases as outgroup taxa to ensure the phylogenetic position of the new species. Trees were drawn to scale, and branch-support values were obtained with the ultrafast bootstrap approximation (UFBoot) (Hoang et al. 2018) implemented in IQ-TREE 2.1.3 (Nguyen et al. 2015) based on 1000 bootstrap replicates.

Results

We report a new species of *Oligogonotylus* from Colombia based on new morphological, molecular, and ecological evidence from a total of 1,306 worms. This taxon has a three-host life cycle, with the snail *A. colombiensis* as the first intermediate host, *P. caucana* as the second intermediate host, and *A. latifrons* as the definitive host (Fig. 2).

Taxonomy

Family Cryptogonimidae Ward, 1917
Genus *Oligogonotylus* Watson, 1976

***Oligogonotylus andinus* sp. nov.**
http://zoobank.org/265EF8A3-982C-4EEA-AA61-3EF1737E6B49

Diagnosis. Adult with longitudinal row of three or four sucker-like gonotyls. Vitelline follicles extending between level of pharynx and anterior margin of ovary and occupying 25–38% of body length.

Cercaria description (Figs 2A, 3A). Pleurolophocercous type. Cercaria elongate, 149 (114–190) long by 82 (72–100) wide. Oral sucker 35 (18–46) long by 30 (24–34) wide, with three or four anterior rows of hook-like spines. Eyespots anterior to penetration glands. Pharynx located between eyespots. Esophagus and ceca undifferentiated. Penetration glands in middle body; seven pairs lead to exterior in four ducts running parallel to oral sucker in two bundles on each side. Rudimentary ventral sucker in middle body. Cystogenic glands on lateral margins of body. Excretory vesicle bilobed delimited anteriorly by primordial ventral sucker and posteriorly by insertion of tail. Tail longer than body with lateral fin, 294 (274–316) long by 22 (18–26) wide.

Metacercaria description (Figs 2B, 3B, C). Encysted form spherical with thin cyst wall of variable thickness occupying entire cyst cavity (Fig. 3B). Cyst 281 (247–327) long by 193 (136–223) wide. Unencysted forms covered with numerous, simple, single-pointed tegumental spines which are smaller and less dense posteriorly. Oral sucker (Os) large, subterminal, 79 (58–98) long by 67 (50–84) wide. Ventral sucker (Vs) just pre-equatorial to equatorial, 53 (34–70) long by 49 (34–66) wide, smaller than oral sucker; Os/Vs (ratio) 1:0.7 (1:0.6–1:0.8) long by 1:0.7 (1:0.6–1:0.9) wide. Pharynx large, 43 (36–48) long by 38 (30–46) wide. Esophagus short; ceca wide, reaching middle hindbody. Remnants of eyespots at pharyngeal level. Genital primordium indistinct, posterior to ventral sucker. Excretory vesicle large, Y-shaped, with large lateral branches reaching anteriorly to level of ventral sucker and with short posterior duct opening at excretory pore.

Adult description (Figs 3D, 4A–F). Body oval to elongate-oval, widest at ovarian level, 517 (271–821, $n = 21$) long by 248 (167–335, $n = 21$) wide. Anterior and posterior ends of body rounded. Tegument spinose, with spines becoming shorter and less dense in posterior region. Remnants of eyespots diffuse and scattered at pharyngeal level.

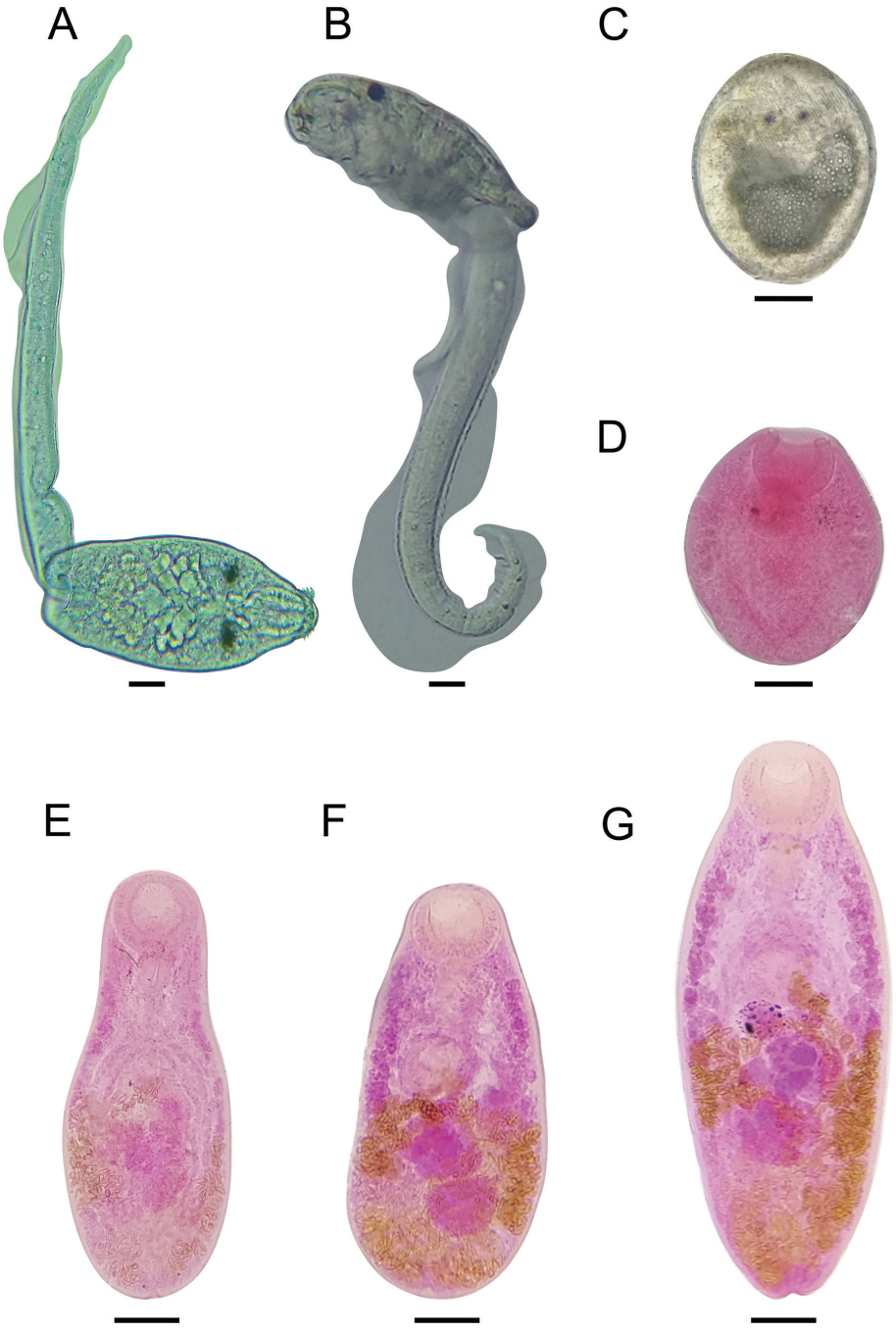

Figure 2. Micrographs of different stages of *Oligogonotylus andinus* sp. nov. **A, B** cercariae emerged from *Aroapyrgus colombiensis*, as temporary mounts **C** encysted metacercaria from *Poecilia caucana*, as a temporary mount **D** unencysted metacercaria isolated from *P. caucana*, as a permanent slide **E, F** paratype specimens, as temporary mounts **G** holotype adult specimen, isolated from *A. latifrons*, as a permanent slide. Scale bars: 20 μm (**A, B**); 20 μm (**C, D**); 100 μm (**E–G**).

Oral sucker rounded, subterminal, without circumoral crown of spines, 106 (84–128, *n* = 21) long by 110 (66–144, *n* = 21) wide. Prepharynx short or inconspicuous, 18 (12–28, *n* = 9) long by 24 (16–28, *n* = 6) wide, with small extramural glands. Pharynx large, 59 (30–86, *n* = 18) long by 50 (26–70, *n* = 18) wide. Esophagus 40 (10–70, *n* = 13) long. Intestinal bifurcation immediately anterior to ventral sucker. Ceca reach just into post-testicular zone; distance from cecal extremities to posterior end of body 86 (60–114, *n* = 10). Longitudinal row of 4 (3–4, *n* = 17) sucker-like gonotyls located between mid-level of pharynx and anterior margin of ventral sucker, increasing in size from anterior to posterior. Ventral sucker rounded, pre-equatorial, 79 (56–100, *n* = 21) long by 78 (52–104, *n* = 21) wide, enclosed in ventrogenital sac, smaller than oral sucker; Os/Vs (ratio) 1:0.74 (1:0.61–1:0.88, *n* = 21) long by 1:0.72 (1:0.60–1:0.83, *n* = 21) wide; Os–Vs distance 112 (40–178, *n* = 15). Genital pore close to anterior margin of ventral sucker. Testes two, rounded to oval, in tandem, intercecal, in mid hindbody: anterior testis 72 (20–120, *n* = 20) long by 82 (50–112, *n* = 20)

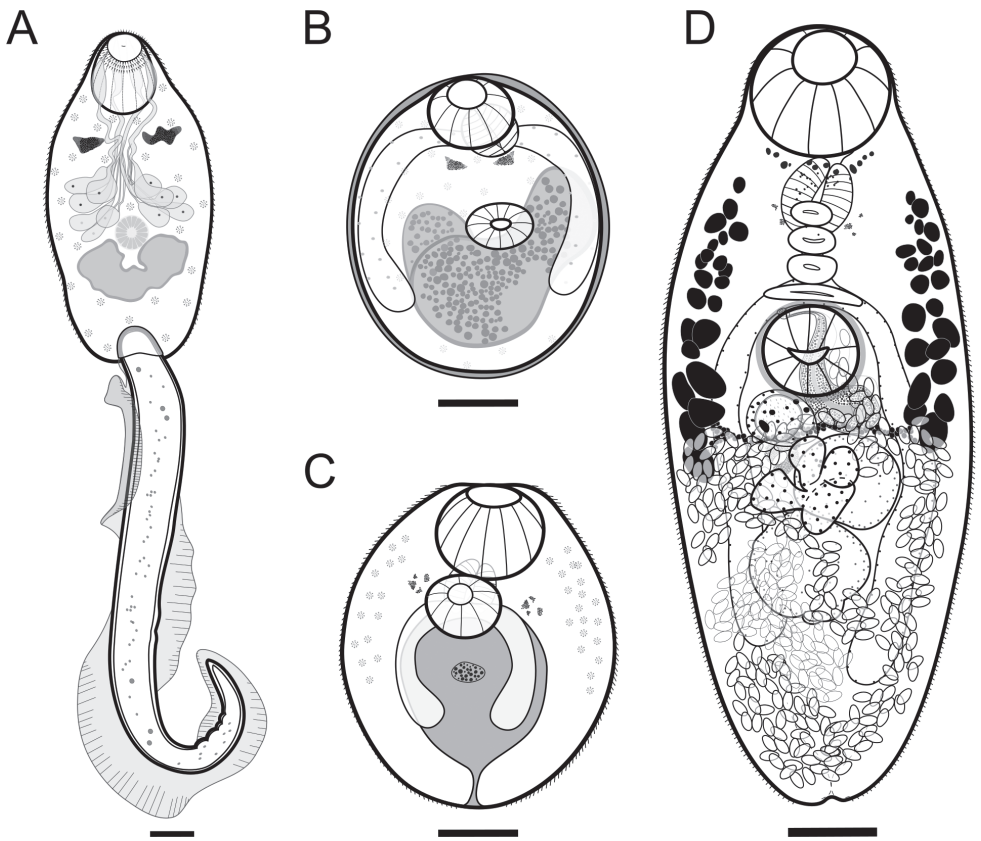

Figure 3. Developmental stages of *Oligogonotylus andinus* sp. nov. **A** pleurolophocercous cercaria emerged from *Aroapyrgus colombiensis* **B** encysted metacercaria isolated from the muscle of *Poecilia caucana* **C** unencysted metacercaria isolated from *P. caucana* **D** holotype, adult isolated from the large intestine of the trans-Andean cichlid *Andinoacara latifrons*. Scale bars: 20 μm (**A**); 20 μm (**B, C**); 100 μm (**D**).

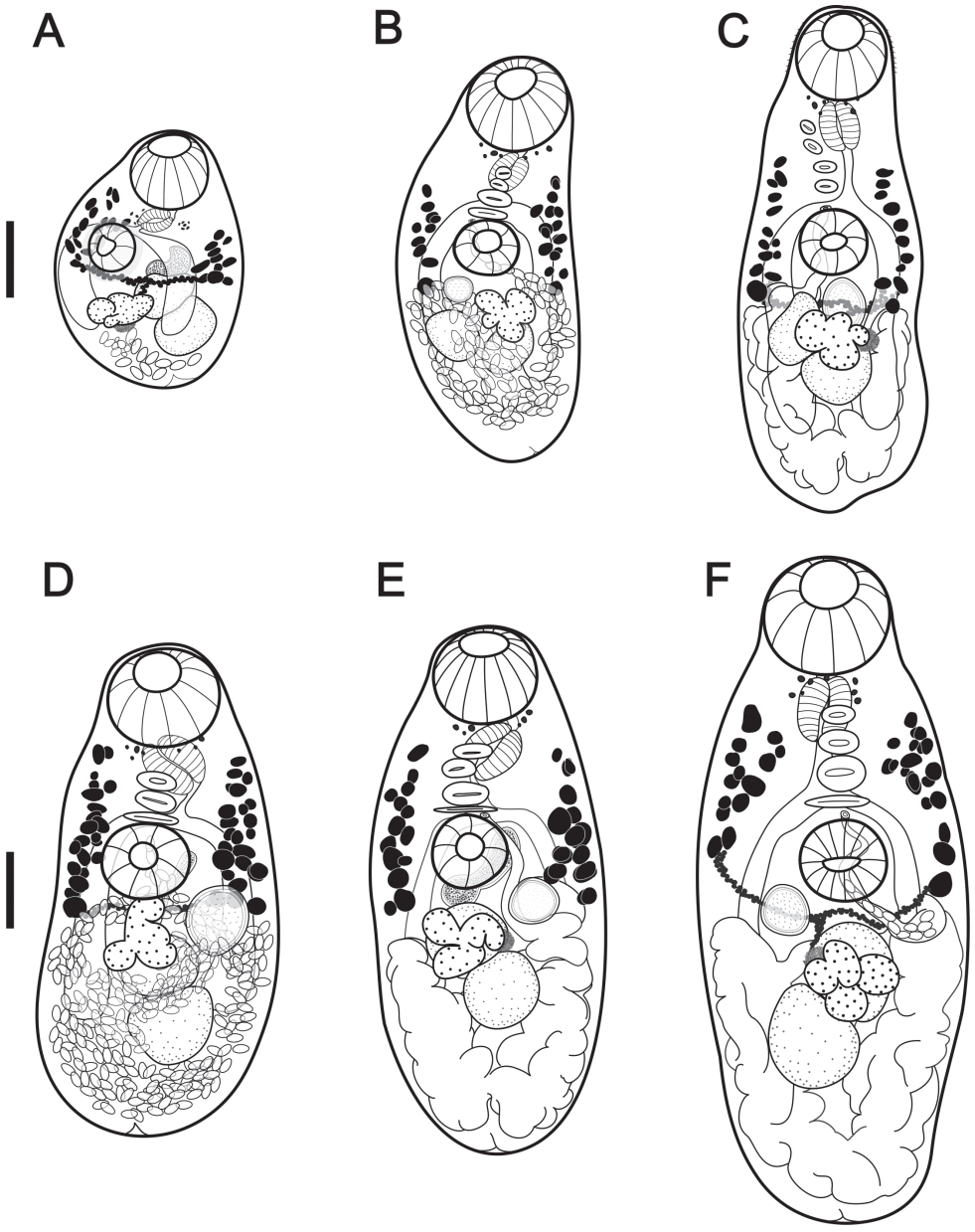

Figure 4. Paratypes of *Oligogonotylus andinus* sp. nov.; adults at different degrees of maturity **A** specimen in partly lateral orientation with the first eggs in utero; gonotyls were not observed **B, D–F** specimens with the seminal receptacle visible (left on **B** and **F**, right on **E** and **D**) and four gonotyls **A, C, D, F** specimens with the vitelline duct visible **A, D, E** specimens with the seminal vesicle dorsal to the ventral sucker. Scale bars: 100 μm (**A–F**).

wide; posterior testis 80 (50–140, *n* = 21) long by 81 (46–140, *n* = 21) wide. Seminal vesicle tubulosaccular, undivided, mostly posterolateral to ventral sucker, 95 (30–128, *n* = 10) long by 82 (48–120, *n* = 11) wide. Cirrus sac and cirrus absent. Ovary lobed, median, post-equatorial, intercecal, between ventral sucker and posterior testis, partially overlaps anterior testis, 74 (38–108, *n* = 17) long by 90 (30–120, *n* = 17) wide. Seminal receptacle median, ovoid, dorsal, anterolateral to ovary, and ventral to vitelline duct, 65 (40–94, *n* = 11) long by 59 (40–82, *n* = 11) wide. Ootype posterolateral to ovary (on right side in type specimen and three paratypes, on left side in three other paratypes). Vitelline follicles small, irregular in shape to oval; arranged in lateral fields partly overlapping ceca or extracecal. Vitelline fields not confluent, extending from mid of pharynx to anterior region of ovary, occupying 32% (0.25–0.38, *n* = 15) of body length. Uterus in hindbody with several loops, passes medially between ovary and ventral sucker and forward to genital pore. Eggs small, 21 (18–24, *n* = 57) long by 10 (10–12, *n* = 57) wide. Excretory pore terminal. Excretory vesicle Y-shaped.

Taxonomic summary. Type specimens. *Holotype*: permanent slide; CCH.116: 170. ***Paratypes*:** permanent slides; CCH.116: 171 to 178.

Type locality. Colombia – Antioquia • Sopetrán, La Mirandita village; 6°30'42.0"N, 75°45'22.6"W; fishponds at 750 m a.s.l., February 2020, V. Vélez-Sampedro and C. Lenis leg.

Type hosts. *Andinoacara latifrons* (Steindachner, 1878) (Actinopterygii: Cichlidae).

Other hosts. Cercariae in *Aroapyrgus colombiensis* Malek & Little, 1971 (Gastropoda, Cochliopidae); metacercariae in *Poecilia caucana* (Steindachner, 1880) (Actinopterygii, Poeciliidae).

Prevalence [N (%)]. Cercariae 451 (2.0%); metacercariae 105 (38.1%); juveniles/adults 22 (100%).

Intensity [mean (range)]. Cercariae 8.6 (2–19); metacercariae 8.3 (5–14); juveniles/adults 41.1 (5–108).

Abundance [mean]. Cercariae (0.2); metacercariae (3.1); juveniles/adults (39.3).

Site in hosts. Cercariae in hepatopancreas; encysted metacercariae in muscle; adults in medial region of large intestine.

Etymology. The specific epithet (*andinus*) refers to the geographic distribution of the hosts, which are endemic to the Andes.

Key to *Oligogonotylus* species

1 Vitelline fields restricted to hindbody or barely extending forebody **2**

– Vitelline fields extended into forebody; between mid-region of pharynx and anterior margin of ovary; 3 or 4 gonotyls ..... ***O. andinus* sp. nov.**

2 Vitelline fields between posterior margin of ventral sucker and posterior margin of posterior testis; 5–8 gonotyls..... ***O. manteri* Watson, 1976**

– Vitelline fields between anterior margin of posterior testis and region of esophagus and pharynx; 6–8 gonotyls..... ***O. mayae* Razo-Mendivil et al., 2008**

Molecular phylogenetic analyses

For the analysis of the ITS2 rDNA gene region, a total of four sequences from Colombia were obtained (GenBank MW621150, MW621151, MW621152, and MW621153). The final alignment includes 18 sequences from GenBank and consists of 22 sequences of 220 bp in total. The phylogenetic tree reconstructed by ML based on the SYM+G model (-lnL = 1232.8754) shows two clades within *Oligogonotylus* (Fig. 5). Clade I includes five sequences of O. *manteri* from Mexico, Belize, and Guatemala. Clade II includes four sequences of O. *mayae* from Yucatán. Between these clades are the four sequences that represent the new species from Colombia forming a polytomy. The sequences of the cercaria (n = 1), metacercaria (n = 1, not included in the trees), and adults (n = 4, one not included in the trees) are identical, indicating that they belong to the same species. The bootstrap values are strong to include *O. andinus* sp. nov. in this genus and in the family Cryptogonimidae. The intraspecific genetic distances range from 0% (*O. andinus* sp. nov. and *O. manteri*) to 0.45% (*O. mayae*). The interspecific genetic distances (*p*-distances) are 0.45–0.46% for *O. andinus* sp. nov. versus *O. manteri*, 0.91–1.39% for *O. andinus* sp. nov. versus *O. mayae*, and 1.36–1.82% for *O. manteri* versus *O. mayae*.

For the analysis of the COI mtDNA gene region, five sequences from Colombia were obtained (GenBank MW658570, MW658572, MW658573, MW658574, and MW658575). The final alignment includes 22 sequences from GenBank and consists of 27 sequences of 330 bp in total. The phylogenetic tree reconstructed by ML based on the GTR+G model (-lnL = 2541.9707) shows two major monophyletic clades within *Oligogonotylus* (Fig. 6). Clade I includes five sequences of *O. manteri* from Mexico, Belize, and Guatemala. Clade II includes five sequences representing the new species, all adult specimens. Clade III includes eight sequences of *O. mayae* from Yucatán that form a polytomy. The bootstrap values are strong (>85%) in each case supporting the position of the new species in *Oligogonotylus* and the family Cryptogonimidae. This topology identifies O. *andinus* sp. nov. and O. *manteri* as sister taxa with bootstrap support of 77%. The intraspecific genetic distances are 0% for *O. andinus* sp. nov., 0.28–3.66% for *O. manteri*, and 0.28–0.85% for *O. mayae*. The interspecific genetic distances (*p*-distances) are 10.27–11.28% for *O. andinus* sp. nov. versus *O. manteri*, 8.46–9.06% for *O. andinus* sp. nov. versus *O. mayae*, and 9.30–10.42% for *O. manteri* versus *O. mayae*.

The extended analysis of concatenated COI and ITS2 sequences includes four sequences from Colombia. The final alignment includes 18 sequences from GenBank and consists of 22 sequences of 330 bp in total. The phylogenetic tree reconstructed by ML based on the GTR+I+G model (-lnL = 7111.7722) shows three major clades (Fig. 7) within *Oligogonotylus*. Clade I includes five sequences of *O. manteri* from Mexico, Belize, and Guatemala; clade II includes the four sequences of *O. andinus* sp. nov.; and clade III includes four sequences of *O. mayae* from Yucatán. The three clades are monophyletic within a monophyletic genus, supporting the results of the COI topology for the new species and also giving more resolution to the phylogenetic

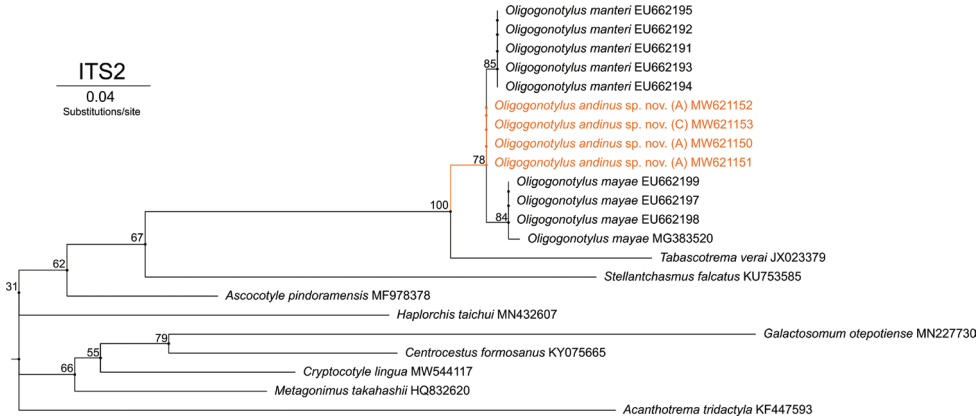

Figure 5. Phylogenetic relationships of ITS2 sequences of *Oligogonotylus andinus* sp. nov., *Oligogonotylus manteri*, and *Oligogonotylus mayae*. Phylogenetic tree reconstructed using the maximum-likelihood method based on the symmetrical model with gamma distribution (SYM+G). Numbers on the branches correspond to the ultrafast bootstrap approximation support values. Each terminal is identified by the alphanumeric accession number of GenBank. Terminals in orange correspond to the sequences obtained in this report. Diagram made with IQ-TREE 2.1.3.

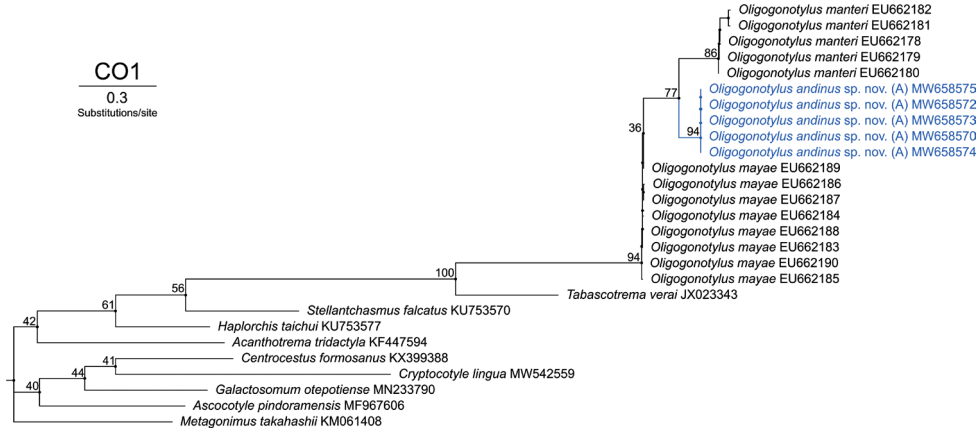

Figure 6. Phylogenetic relationships of COI sequences of *Oligogonotylus andinus* sp. nov., *Oligogonotylus manteri*, and *Oligogonotylus mayae*. Phylogenetic tree reconstructed using the maximum-likelihood method based on the general time reversible with gamma distribution model (GTR+G). Numbers on the branches correspond to the ultrafast bootstrap approximation support values. Each terminal is identified by the alphanumeric accession number of GenBank. Terminals in blue correspond to the sequences obtained in this report. Diagram made with IQ-TREE 2.1.3.

relationships within the genus. The bootstrap values are strong (>90%) for clades I, II, and III, and this topology also identifies O. *andinus* sp. nov. and O. *manteri* as sister taxa. However, the bootstrap support is low (57%). The intraspecific genetic distances are 0% for O. andinus sp. nov., 0–2.18% for *O. manteri*, and 0.18–0.73%

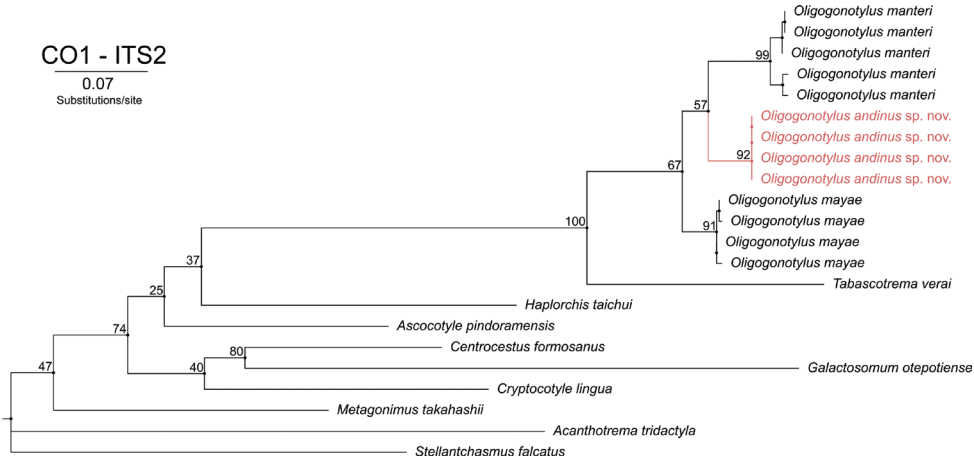

Figure 7. Phylogenetic relationships of COI and ITS2 concatenated sequences of *Oligogonotylus andinus* sp. nov., *Oligogonotylus manteri*, and *Oligogonotylus mayae*. Phylogenetic tree reconstructed using the maximum-likelihood method based on the general time reversible with proportion of invariable sites and gamma distribution model (GTR+I+G) model. Numbers on the branches correspond to the ultrafast bootstrap approximation support values. Terminals in red correspond to the sequences obtained in this report. Diagram made with Garli IQ-TREE 2.1.3.

for *O. mayae*. The interspecific genetic distances (*p*-distances) are 6.36–6.96% for *O. andinus* sp. nov. versus *O. manteri*, 5.64–6.04% for *O. andinus* sp. nov. versus *O. mayae*, and 6.55–7.09% for *O. manteri* versus *O. mayae*.

The interspecific distances obtained from both the internal transcribed spacer (ITS2) and the mitochondrial gene (COI) together with the concatenated sequences provide clear support to the distinction of the new species. Our phylogenetic analysis using mitochondrial data shows that consistent with the wide distribution, the Middle American species have intraspecific mitochondrial variation —0.28–3.66% (*p*-distance)—over a wide latitudinal gradient from Costa Rica to Mexico. The intraspecific distance for the new species is null, consistent with all samples coming from a single Colombian population.

Remarks

Oligogonotylus andinus sp. nov. represents the first species described in the Colombian cichlid *A. latifrons* and the third for the genus *Oligogonotylus*, with *O. manteri* and *O. mayae* as being parasites of Middle American cichlids. Morphological data from cercariae and metacercariae of *O. andinus* are compatible with those previously reported for *O. manteri* (see Scholz et al. 1994). The cercaria of the new species also corresponds to the pleurolophocercous type for having a lateral fin on the tail (Schell 1970; Yamaguti 1975; Scholz et al. 1994; Bray et al. 2008) and differs from that of *O. manteri* in having the tegument without hair-like

sensory structures (Fig. 3A); hair-like sensory structures were reported on the body margins in *O. manteri*.

As adults, *O. andinus* sp. nov. is easily distinguishable from the other species in this group based on differences in the distribution of the vitelline fields as well as the number of gonotyls. The new species has vitelline fields between the mid-level of the pharynx and the anterior margin of the ovary and three or four gonotyls. *Oligogonotylus manteri* has vitelline fields between the posterior margin of the ventral sucker and the posterior-end of the posterior testis and has five to eight gonotyls (Watson 1976), whereas *O. mayae* has vitelline fields from a level between the pharynx and the esophagus and the anterior margin of the posterior testis and six to eight gonotyls (Razo-Mendivil et al. 2008).

The analysis of the morphology of the reproductive system of *O. andinus* sp. nov. at different stages of maturity (Figs 3D, 4A–F) reveals that the seminal receptacle is ventral to the vitelline duct; the ootype complex overlaps the lateral region of the ovary dorsally (on right side in the type specimen and three paratypes but on left side in three other paratypes, on the same side of the seminal receptacle); and the distal region of the uterus and the seminal vesicle reach the anterior margin of the ventral sucker and converge at the genital pore. These features are not detailed in the description of *O. manteri*. In *O. mayae*, as in the new species, the seminal vesicle is tubulo-saccular and posterolateral to the ventral sucker.

Morphology-based taxonomic conclusions are supported by the analysis of molecular data from the ITS2, COI and COI–ITS2 barcoding. Our analyses show that the specimens from Colombia represent a new species. The polytomy formed by the sequences of the new species in the phylogenetic tree of ITS2 is due to the low rate of mutation that this molecular marker has. In conjunction, the phylogenetic trees of COI and the concatenated sequences of COI and ITS2 show that all isolates from Sopetrán represent a reciprocally monophyletic assemblage, distinct from isolates of *O. manteri* and *O. mayae*, which are shown in both topologies to be sister taxa.

Discussion

In the present study, *O. andinus* sp. nov. is described and associated with three endemic Andean hosts from Sopetrán, Antioquia, Colombia. Initially, molecular analyses of cercariae which had emerged from *A. colombiensis* enabled identification to the generic level. Subsequently, the location of the focus in the fishponds facilitated the life cycle study using five species of fishes present in the fish farm; two are endemic species (*P. caucana* and *A. latifrons*), and three are exotic cultured species (*O. aureus*, *C. macropomum*, and *O. mossambicus*). Of these, the two endemic fishes act as intermediate and definitive hosts of the parasite, respectively. The high prevalence of *O. andinus* in *P. caucana* (38.1%) and *A. latifrons* (100%) are a result of at least three factors: (a) the confinement of the snails and fishes in small semi-closed ponds, which increases the rate of parasite-host encounters; (b) the establishment of a large

population of *P. caucana* in the fishpond, with few predators (*A. latifrons* and birds such as kingfishers); and (c) a voracious diet of *A. latifrons* that included snails, poecilids, and insects (judging from the stomach content; present study). Despite their close confinement, the farmed fish were negative for the new species because their diets are based on plants and fish feed.

Previous studies have shown that both *O. manteri* and *O. mayae* use the cochliopid snail *P. coronatus* (misidentified as *Benthonella gaza*), and that *O. manteri* also uses the cochliopid snail *Aroapyrgus alleei* Morrison, 1946 as the first intermediate host and the cichlid fish *M. urophthalmus* either as the second intermediate or the main definitive host among other 11 species of cichlids (Scholz et al. 1994; Jiménez-García and Vidal-Martínez 2005; Pérez-Ponce de León et al. 2007; May-Tec et al. 2020; Velázquez-Urrieta and Pérez-Ponce de León 2021). *Oligogonotylus andinus* sp. nov. is related to hosts whose history has been shaped by the Andes Mountains and whose life cycle occurs in lentic systems. A cochliopid snail (*A. colombiensis*) is the first intermediate host, a poecilid fish (*P. caucana*) is the second intermediate host, and a trans-Andean cichlid fish (*A. latifrons*) is the definitive host; thus, the present work extends the *Oligogonotylus*–Cochliopidae–Cichlidae association. Therefore, species of *Oligogonotylus* are still considered as members of the core helminth fauna of cichlids (Pérez-Ponce De León and Choudhury 2005), but also as members of the core helminth fauna of cochliopids (May-Tec et al. 2020; Velázquez-Urrieta and Pérez-Ponce de León 2021; present study).

Aroapyrgus colombiensis is distributed in the Magdalena–Cauca basin and inhabits small lotic systems with abundant stretches of slow water and decomposing dead leaves (Linares et al. 2018). It has been reported as a host for *Paragonimus caliensis* Little, 1968 in Valle del Cauca (Malek and Little 1971) and Antioquia (Lenis et al. 2018). *Poecilia caucana*, which is commonly called Pipón, Piponcita, or Cauca Molly, is distributed in the hydrographic slopes of the Pacific and the Caribbean, especially in the Magdalena–Cauca basin (Castellanos-Morales et al. 2011; Martínez et al. 2016; Mojica et al. 2018; Ruiz-Guerra and Echeverry-Galvis 2019). Normally it inhabits rivers and brooks (Roman-Valencia 1990), but small streams also lead it to lagoons and natural or artificial ponds where it is reported in Magangué, Bolívar, Los Palmitos, Sucre (Navarro et al. 2019), and Sopetrán (present study). *Andinoacara latifrons* is colloquially named Blue mojarra and it is grouped in two lineages in Colombia, (1) the upper Magdalena and Catatumbo clade, and (2) the upper Cauca and upper Magdalena clade (De la Ossa-Guerra et al. 2020), where our host population belongs. It inhabits muddy waters, clean-water streams, and lentic environments. It feeds on worms, insects, plant materials, fish remains, debris, and other live prey, such as crustaceans (Maldonado-Ocampo et al. 2006; Olaya-Nieto et al. 2016), making it susceptible to infection by trematodes.

This is the first study of the helminth fauna associated with *A. colombiensis* and *A. latifrons* and extends the known geographic distribution of *Oligogonotylus* spp. from Middle America to South America (Choudhury et al. 2016, 2017) where *O. andinus* sp. nov. was found at 750 m above sea level. Further field-based studies must include an increased sampling size to determine whether major intraspecific distances exist or

if there are other populations in the Cauca river basin, and to reveal the ecogeographic limits of *Oligogonotylus* spp. in Colombia, particularly in areas with a likely suitable habitat where the species has yet to be found. Future taxonomic and ecological host-parasite research must lead to an understanding of fish parasite diversity and the risk of the transmission of zoonotic diseases, considering the dependence on fish as a food resource in rural areas of Colombia.

Acknowledgements

We acknowledge Carlos Muskus (PECET), Iván Darío Vélez (PECET), and Javier Correa Álvarez (EAFIT) for their support in conducting this research. We also thank Enderson Murillo Ramos (UBMC-PECET), Juan Manuel Martínez Cerón (EAFIT), and Jorge Luis Escobar (UdeA) for their assistance, recommendations, and contributions regarding the methodology used; we highly appreciate it. Special thanks go to Gildardo Méndez (Yayo) and his family for allowing us to carry out this research in their fish farm. This work is funded by the Helminthology Unit-PECET and the Ministry of Science, Technology and Innovation-MINCIENCIAS (grant 80740-571-2020). The authors declare that they have no competing interests exist.

References

Anucherngchai S, Tejangkura T, Chontananarth T (2016) Epidemiological situation and molecular identification of cercarial stage in freshwater snails in Chao-Phraya Basin, Central Thailand. Asian Pacific Journal of Tropical Biomedicine 6(6): 539–545. https://doi.org/10.1016/j.apjtb.2016.01.015

Bowles J, Hope M, Tiu WU, Liu X, McManus DP (1993) Nuclear and mitochondrial genetic markers highly conserved between Chinese and Philippine *Schistosoma japonicum*. Acta Tropica 55(4): 217–229. https://doi.org/10.1016/0001-706X(93)90079-Q

Bray RA, Gibson DI, Jones A [Eds] (2008) Keys to the Trematoda, Volume 3. CAB International and Natural History Museum, London, 824 pp. https://doi.org/10.1079/9780851995885.0000

Bush AO, Lafferty K, Lotz J, Shostak W (1997) Parasitology meets ecology on its own terms: Margolis et al. revisited. The Journal of Parasitology 83(4): 575–583. https://doi.org/10.2307/3284227

Castellanos-Morales CA, Marino-Zamudio LL, Guerrero-V L, Maldonado-Ocampo JA (2011) Peces del departamento de Santander, Colombia. Revista de la Academia Colombiana de Ciencias Exactas, Físicas y Naturales 35: 189–212.

Choudhury A, Aguirre-Macedo ML, Curran SS, Ostrowski de Núñez M, Overstreet RM, Pérez-Ponce de León G, Portes Santos C (2016) Trematode diversity in freshwater fishes of the globe II: 'New World.'. Systematic Parasitology 93(3): 271–282. https://doi.org/10.1007/s11230-016-9632-1

Choudhury A, García-Varela M, Pérez-Ponce De León G (2017) Parasites of freshwater fishes and the Great American Biotic Interchange: A bridge too far? Journal of Helminthology 91(2): 174–196. https://doi.org/10.1017/S0022149X16000407

Darriba D, Taboada G, Doallo R, Posada D (2012) jModelTest 2: More models, new heuristics and parallel computing. Nature Methods 9(8): 772–772. https://doi.org/10.1038/nmeth.2109

De la Ossa-Guerra LE, Santos MH, Artoni RF (2020) Genetic diversity of the cichlid *Andinoacara latifrons* (Steindachner, 1878) as a conservation strategy in different Colombian basins. Frontiers in Genetics 11: 1–9. https://doi.org/10.3389/fgene.2020.00815

Ditrich O, Scholz T, Aguirre-Macedo L, Vargas-Vázquez J (1997) Larval stages of trematodes from freshwater molluscs of the Yucatan Peninsula, Mexico. Folia Parasitologica 44: 109–127.

Edgar R (2004) MUSCLE: Multiple sequence alignment with high accuracy and high throughput. Nucleic Acids Research 32(5): 1792–1797. https://doi.org/10.1093/nar/gkh340

Erikson U (2011) Assessment of different stunning methods and recovery of farmed Atlantic salmon (*Salmo salar*): isoeugenol, nitrogen and three levels of carbon dioxide. Animal Welfare, the UFAW Journal 20: 365–375.

Hoang DT, Chernomor O, Von Haeseler A, Minh BQ, Vinh LS (2018) UFBoot2: Improving the ultrafast bootstrap approximation. Molecular Biology and Evolution 35(2): 518–522. https://doi.org/10.1093/molbev/msx281

Iwagami M, Ho LY, Su K, Lai PF, Fukushima M, Nakano M, Blair D, Kawashima K, Agatsuma T (2000) Molecular phylogeographic studies on *Paragonimus westermani* in Asia. Journal of Helminthology 74(4): 315–322. https://doi.org/10.1017/S0022149X00000469

Jiménez-García MI, Vidal-Martínez VM (2005) Temporal variation in the infection dynamics and maturation cycle of *Oligogonotylus manteri* (Digenea) in the cichlid fish, "*Cichlasoma*" *urophthalmus*, from Yucatán, México. The Journal of Parasitology 91(5): 1008–1014. https://doi.org/10.1645/GE-380R2.1

Kearse M, Moir R, Wilson A, Stones-Havas S, Cheung M, Sturrock S, Buxton S, Cooper A, Markowitz S, Duran C, Thierer T, Ashton B, Meintjes P, Drummond A (2012) Geneious Basic: An integrated and extendable desktop software platform for the organization and analysis of sequence data. Bioinformatics (Oxford, England) 28(12): 1647–1649. https://doi.org/10.1093/bioinformatics/bts199

Kumar S, Stecher G, Li M, Knyaz C, Tamura K (2018) MX (2018) MEGA X: Molecular Evolutionary Genetics Analysis across computing platforms. Molecular Biology and Evolution 35(6): 1547–1549. https://doi.org/10.1093/molbev/msy096

Lenis C, Galiano A, Vélez I, Vélez ID, Muskus C, Marcilla A (2018) Morphological and molecular characterization of *Paragonimus caliensis* Little, 1968 (Trematoda: Paragonimidae) from Medellin and Pichinde, Colombia. Acta Tropica 183: 95–102. https://doi.org/10.1016/j.actatropica.2018.03.024

Linares EL, Lasso CA, Vera-Ardila LM, Morales-Betancourt AM (2018) XVII. Moluscos dulceacuícolas de Colombia. Serie Editorial Recursos Hidrobiológicos y Pesqueros Continentales de Colombia. Instituto de Investigación de Recursos Biológicos Alexander von Humboldt. Bogotá, 326 pp. https://doi.org/10.21068/a2018n03

Maldonado-Ocampo JA, Ortega-Lara A, Usma Oviedo JS Germán, Galvis V, Villa-Navarro FA, Vásquez Gamboa L, Prada-Pedreros S, Ardila Rodríguez C (2006) Peces de Los Andes de Colombia. Instituto de Investigación de Recursos Biológicos Alexander von Humboldt, Bogotá, 346 pp.

Malek EA, Little MD (1971) *Aroapyrgus colombiensis* n. sp. (Gastropoda: Hydrobiidae), snail intermediate host of *Paragonimus caliensis* in Colombia. Nautilus 85: 20–26. https://doi.org/10.1038/scientificamerican01221846-76b

Martínez JD, Cadena CD, Torres M (2016) Critical thermal limits of *Poecilia caucana* (Steindachner, 1880) (Cyprinodontiformes: Poeciliidae). Neotropical Ichthyology 14(1): 1–7. https://doi.org/10.1590/1982-0224-20150171

May-Tec AL, Herrera-Castillo NA, Vidal-Martínez VM, Aguirre-Macedo ML (2020) Following the infection dynamics of the tropical trematode *Oligogonotylus mayae* in its intermediate and definitive hosts for 13 years. Journal of Helminthology 94: e208. https://doi.org/10.1017/S0022149X20000875

Mojica JI, Martínez-González CC, Acosta-Vela AG, Larrate-River E, González-Daza W, Ávila-Rojas FL, Martínez-Aguirre E, Forero-Cano JD (2018) Lista de los peces de la cuenca del río Mira, vertiente Pacífico, Colombia. Biota Colombiana 18(2): 191–199. https://doi.org/10.21068/c2017.v18n02a12

Navarro B, Tovar H, Caraballo P (2019) Composición y distribución de la ictiofauna asociada a jagüeyes, en la región Caribe colombiana. Intropica 14: 120–126. https://doi.org/10.21676/23897864.3277

Nguyen LT, Schmidt HA, Von Haeseler A, Minh BQ (2015) IQ-TREE: A fast and effective stochastic algorithm for estimating maximum-likelihood phylogenies. Molecular Biology and Evolution 32(1): 268–274. https://doi.org/10.1093/molbev/msu300

Olaya-Nieto CW, Camargo-Herrera L, Díaz-Sajonero V, Segura-Guevara FF (2016) Feeding habits of Cocobolo *Andinoacara pulcher* in the cienaga Grande de Lorica, Colombia. Revista Mvz Cordoba 21: 5189–5197. https://doi.org/10.21897/rmvz.29

Pérez-Ponce De León G, Choudhury A (2005) Biogeography of helminth parasites of freshwater fishes in Mexico: The search for patterns and processes. Journal of Biogeography 32(4): 645–659. https://doi.org/10.1111/j.1365-2699.2005.01218.x

Pérez-Ponce de León G, Luis G-P, Mendoza-Garfias B (2007) Trematode parasites (Platyhelminthes) of wildlife vertebrates in Mexico. Zootaxa 1534(1): 1–247. https://doi.org/10.11646/zootaxa.1534.1.1

Razo-Mendivil U, Rosas-Valdez R, Pérez-Ponce de León G (2008) A new cryptogonimid (Digenea) from the Mayan cichlid, *Cichlasoma urophthalmus* (Osteichthyes: Cichlidae), in several localities of the Yucatan Peninsula, Mexico. The Journal of Parasitology 94(6): 1371–1378. https://doi.org/10.1645/GE-1546.1

Roman-Valencia C (1990) Lista y distribución de peces en la cuenca medio del río Atrato, Chocó, Colombia. Caldasia 16: 201–208.

Ruiz-Guerra C, Echeverry-Galvis MÁ (2019) Prey consumed by wading birds in mangrove swamps of the Caribbean coast of Colombia. Journal of Natural History 53(29–30): 1823–1836. https://doi.org/10.1080/00222933.2019.1667037

Sandlund OT, Daverdin RH, Choudhury A, Brooks DR, Diserud OH (2010) A survey of freshwater fishes and their macroparasites in the Guanacaste Conservation Area (ACG), Costa Rica. NINA Report 935: 1–45. http://hdl.handle.net/11606/639

Schell S (1970) How to Know the Trematodes. Wm. C. Brown Company Publishers, Dubuque, Iowa, 355 pp.

Scholz T, Lavadores JIP, Vargas VJ, Mendoza FEF, Rodriguez CR, Vivas RC (1994) Life cycle of *Oligogonotylus manteri* (Digenea: Cryptogonimidae), a parasite of cichlid fishes in southern Mexico. Journal of the Helminthological Society of Washington 61: 190–199. http://bionames.org/bionames-archive/issn/1049-233X/61/190.pdf

Scholz T, Vargas-Vázquez J, Moravec F, Vivas-Rodríguez C, Franco-Mendoza E (1995) Cenotes (sinkholes) of the Yucatan Peninsula, Mexico, as a habitat of adult trematodes of fish. Folia Parasitologica 42: 37–47.

Sosa-Medina T, Vidal-Martínez VM, Aguirre-Macedo ML (2015) Metazoan parasites of fishes from the Celestun coastal lagoon, Yucatan, Mexico. Zootaxa 4007(4): 529–544. https://doi.org/10.11646/zootaxa.4007.4.4

Velázquez-Urrieta Y, Pérez-Ponce de León G (2021) Morphological and molecular assessment of the diversity of trematode communities in freshwater gastropods and bivalves in Los Tuxtlas tropical rainforest. Journal of Helminthology 95: E44. https://doi.org/10.1017/S0022149X21000407

Vergara D, Velásquez LE (2009) Larval stages of digenea from *Melanoides tuberculata* (Gastropoda: Thiaridae) in Medellín, Colombia. Acta Biologica Colombiana 14: 135–142.

Watson DE (1976) Digenea of fishes from Lake Nicaragua. Investigations of the Ichthyofauna of Nicaraguan Lakes 15: 251–260. https://digitalcommons.unl.edu/ichthynicar/15

Yamaguti S (1975) A Synoptical Review of the Life Histories of Digenetic Trematodes of Vertebrates, with Special Reference to the Morphology of Their Larval Forms. Keigaku Publishing Co., Tokyo, 575 pp.

ZooKeys 1115: 187–198 (2022)
doi: 10.3897/zookeys.1115.84527
https://zookeys.pensoft.net

RESEARCH ARTICLE

A peer-reviewed open-access journal
ZooKeys
Launched to accelerate biodiversity research

Taxonomic review of the subgenus *Tatsipolia* Benedek, Behounek, Floriani & Saldaitis of the genus *Dasypolia* Guenée with descriptions of two new species from southern Xizang, China (Insecta, Lepidoptera, Noctuidae)

Enyong Chen[1], Zhaohui Pan[1], Anton V. Volynkin[2], Aidas Saldaitis[3], Balázs Benedek[4]

1 *Key Laboratory of Forest Ecology in Tibet Plateau (Institute of Plateau Ecology, Tibet Agricultural and Animal Husbandry University), Ministry of Education, Linzhi 860000, China* **2** *Altai State University, Lenina Avenue, 61, RF-656049, Barnaul, Russia* **3** *Nature Research Centre, Akademijos str., 2, LT-08412, Vilnius-21, Lithuania* **4** *H-2045 Törökbálint, Árpád u. 53, Hungary*

Corresponding authors: Zhaohui Pan (panzhaohui2005@163.com), Anton V. Volynkin (monstruncusarctia@gmail.com)

Academic editor: Donald Lafontaine | Received 29 March 2022 | Accepted 20 June 2022 | Published 3 August 2022

https://zoobank.org/6368C676-ABAC-40A1-8147-342D9569C40D

Citation: Chen E, Pan Z, Volynkin AV, Saldaitis A, Benedek B (2022) Taxonomic review of the subgenus *Tatsipolia* Benedek, Behounek, Floriani & Saldaitis of the genus *Dasypolia* Guenée with descriptions of two new species from southern Xizang, China (Insecta, Lepidoptera, Noctuidae). ZooKeys 1115: 187–198. https://doi.org/10.3897/zookeys.1115.84527

Abstract

The subgenus *Tatsipolia* Benedek, Behounek, Floriani & Saldaitis, 2011 of the genus *Dasypolia* Guenée, 1852 is reviewed. Two new species, *D.* (*T.*) *sejilaensis* **sp. nov.** and *D.* (*T.*) *cerritula* **sp. nov.** are described from the Linzhi (Nyingchi) Prefecture in southern Xizang, China. The adults and the male and female genitalia of all species in the subgenus are illustrated. Additionally, *Dasypolia* (*Auropolia*) *carlotta* Floriani, Benedek, Behounek & Saldaitis, 2011 is reported from Xizang for the first time.

Keywords

Antitypina, new record, Noctuinae, Owlet moth, systematics, taxonomy, Xylenini

Introduction

Dasypolia Guenée, 1852 is a large noctuid genus distributed in the Palearctic region and reaching its greatest diversity in high mountain areas of Asia. The genus belongs to the subtribe Antitypina of the tribe Xylenini of the subfamily Noctuinae (Lafontaine and Schmidt 2010; Zahiri et al. 2011; Keegan et al. 2021). Many species of *Dasypolia* were described during the last two decades (Nupponen and Fibiger 2006; Ronkay et al. 2010; Benedek et al. 2011, 2014; Volynkin 2012; Benedek and Saldaitis 2014; Ronkay et al. 2014). However, it is likely that additional undescribed species will be found.

The subgenus *Tatsipolia* Benedek, Behounek, Floriani & Saldaitis, 2011 was erected to solely include *D. ruficilia* Benedek, Behounek, Floriani & Saldaitis, 2011 (Benedek et al. 2011). Subsequently, another species of the genus, *D. vignai* L. Ronkay & Zilli, 1993 was assigned to *Tatsipolia* after the discovery of the male of the species (Benedek and Saldaitis 2014). During entomological studies in the southern Xizang Province of China short series of two unknown small *Dasypolia* specimens was collected by the senior and the second authors of the present paper. After comparing the male genitalia structures of these specimens with other species in the genus, they proved to belong to the subgenus *Tatsipolia* and express significant distinctive characters. The species are described herein as new to science.

Materials and methods

Abbreviations for private and institutional collections used herein: **AFM** = collection of Alessandro Floriani (Milan, Italy); **HNHM** = Hungarian Natural History Museum (Budapest, Hungary); **TAAHU** = Tibet Agricultural and Animal Husbandry University (Linzhi, China); **ZSM** = Bavarian State Collection of Zoology (Zoologische Staatssammlung München, Munich, Germany). Other abbreviations used: **HT** = holotype; **PT** = paratype. In the type labels citations, different labels are separated by a slash ("/") whereas the different lines of the same label are separated by an upright slash ("|").

The male and female genitalia terminology follows Kononenko (2010).

Results

Noctuidae Latreille, 1809
Noctuinae Latreille, 1809
Xylenini Guenée, 1837
Antitypina Forbes & Franclemont, 1954
Genus *Dasypolia* Guenée, 1852

Subgenus *Tatsipolia* Benedek, Behounek, Floriani & Saldaitis, 2011

Dasypolia (*Tatsipolia*) Benedek et al. 2011: 108. Type species: *Dasypolia* (*Tatsipolia*) *ruficilia* Benedek, Behounek, Floriani & Saldaitis, 2011, by original designation.

Diagnosis. Members of the subgenus are small moths (forewing length is 11-13 mm) externally similar to taxa of the subgenus *Cteipolia*. However, despite the external similarity, the subgenus is characterised by the following diagnostic features in the male genitalia: (1) The uncus is short but wide, triangular, dorso-ventrally flattened; (2) The harpe is reduced, tubercle- or spine-like; (3) The digitus is robust, thorn-like; (4) The juxta bears a medial process posteriorly; and (5) The phallus is relatively short but broad, with vesica bearing one or two clusters of spine-like cornuti. In the female genitalia, the broad ostium bursae and the sideways curved ductus and corpus bursae are characteristic for the subgenus.

Distribution. Species of the subgenus are known only from south-western China (Sichuan and southern Xizang).

Species content of *Dasypolia* (*Tatsipolia*).

D. (*T.*) *sejilaensis* sp. nov.
D. (*T.*) *cerritula* sp. nov.
D. (*T.*) *vignai* L. Ronkay & Zilli, 1993.
D. (*T.*) *ruficilia* Benedek, Behounek, Floriani & Saldaitis, 2011.

***Dasypolia* (*Tatsipolia*) *sejilaensis* sp. nov.**

https://zoobank.org/9AD848DE-FFAF-4D00-B6E2-CB8F8A2DACBE
Figs 1–3, 9, 10, 15

Type material. ***Holotype*** (Figs 1, 9): male, "STS-40065 | Sejila Mountain, Linzhi City, | Xizang, China, | N:29°37'5" | E:94°39'38" | 5-X-2020 | h [Altitude] 4500 m (coll. Pan Zhaohui | and Chen Enyong)" gen. prep. in glycerol by Enyong Chen (TAAHU). ***Paratypes*:** 5 males, 1 female, Sejila Mountain, Linzhi City, Xizang, China, 29°37'2"N, 94°38'30"E, 4-X-2020, h [Altitude] 4500 m (coll. Pan Zhaohui | and Chen Enyong), unique numbers: STS-32784, STS-32786, STS-32789–32792, gen. preps. in glycerol by Enyong Chen (TAAHU).

Diagnosis. The new species is externally reminiscent of *D. vignai* but is distinguished by the straight costal margin of the forewing, the more elongate forewing apex, the more diffuse forewing pattern in males, and the longer discal spot of the hindwing. Additionally, compared to *D. vignai*, the reniform stigma of *D. sejilaensis* sp. nov. is positioned closer to the forewing costa, and the pale suffusion on the transverse lines and stigmata are grey whereas they are brown in the congener. The male genital capsule of the new species differs clearly from *D. vignai* in the broader valva with a broader and less down curved cucullus, the shorter but considerably thicker, up-curved digitus (it is down curved in *D. vignai*), the broader sacculus and the less prominent, triangular ventral lobe of the valva (whereas it is more rounded in *D. vignai*). Additionally, the uncus, the penicular lobe and the juxta of *D. sejilaensis* sp. nov. are wider than in *D. vignai*. The phallus of the new species is shorter and broader than in *D. vignai* (in proportion to the genital capsule). The vesicae of the two species are similar but the cornuti are more or less equal in size in *D. sejilaensis* sp. nov. whereas the distal cornuti of *D. vignai* are markedly longer and thicker than the proximal ones. In the female

genitalia, *D. sejilaensis* sp. nov. differs from *D. vignai* in the longer apophyses anteriores (in proportion to the ovipositor), the narrower, more asymmetrically sclerotised and sideways curved ductus bursae (it is nearly straight in *D. vignai*), and the straight posterior section of the corpus bursae which is sideways curved in *D. vignai*. The detailed comparison with *D. cerritula* sp. nov. is provided below in the diagnosis of the latter species.

Description. External morphology of adults (Figs 1–3). Forewing length 11–12 mm in males (11.5 mm in the holotype) and 13 mm in female. Antenna serrulate in male and filiform in female. Head and thorax covered with long hair-like scales, dark brown with admixture of pale grey. Forewing elongate, narrow, with almost parallel costal and anal margins and convex outer margin. Forewing ground colour dark brown, with intense pale grey suffusion along transverse lines and in subterminal area in female; costal margin with diffuse ochreous-brown or grey spots of various sizes. Forewing pattern diffuse, blackish-brown, more distinct in female. Subbasal line short, indistinct. Antemedial line sinuous, double. Orbicular stigma elliptical, filled with ochreous scales in male and pale grey scales in female. Reniform stigma narrow, filled with pale grey scales in female. Postmedial line medially curved, serrulate in female. Subterminal line interrupted into row of indistinct dash-like spots of various sizes between veins. Terminal line interrupted into blackish spots between veins. Outer margin edged with rusty-brown scales. Forewing cilia long, dark brown. Hindwing creamy with greyish-brown suffusion subterminally and terminally and along costal and anal margins. Discal spot large, falcate. Hindwing cilia long, creamy with admixture of brownish-grey scales. Abdomen covered with long hair-like scales, uniform brown. **Male genitalia** (Figs 9, 10). Tegumen short with large trapezoid penicular lobes. Vinculum longer than tegumen, robust, U-shaped. Valva lobular with heavily sclerotised costa and weakly sclerotised, short, broadly triangular and apically rounded ventral lobe. Digitus robust, directed distally, with up curved and distally tapered distal section. Cucullus short, trapezoid, densely covered with hair-like setae. Sacculus short but broad, elliptical. Clasper slightly curved and dilated distally, with very short, tubercle-like harpe. Uncus short but broad, triangular with rounded apex, dorso-ventrally flattened, weakly sclerotised. Juxta broad, shield-like, bearing broad, triangular and apically pointed, heavily sclerotised medial process posteriorly. Anellus weakly granulose. Phallus broad with rounded coecum, somewhat dilated distally. Main chamber of vesica somewhat shorter than phallus, tapered distally, directed ventro-distally, weakly granulose, with short semiglobular dorsal subbasal diverticulum and lengthwise cluster of 6–7 small but robust spike-like cornuti dorso-medially. **Female genitalia** (Fig. 15). Anterior section of corpus bursae membranous, dilated, teardrop-shaped. Posterior section of corpus bursae equal in width to anterior section of ductus bursae, membranous, tubular. Appendix bursae short and narrow, conical, positioned postero-laterally on right side at junction with ductus bursae. Ductus bursae short, its anterior section heavily sclerotised, dorso-ventrally flattened, strongly curved sideways to the right. Posterior section of ductus bursae funnel-like, bearing short, band-shaped antevaginal plate. Ostium bursae broad. Ovipositor short, broad, conical. Apophyses long and thin, apophysis anterioris slightly shorter than apophysis posterioris. Papilla analis setose.

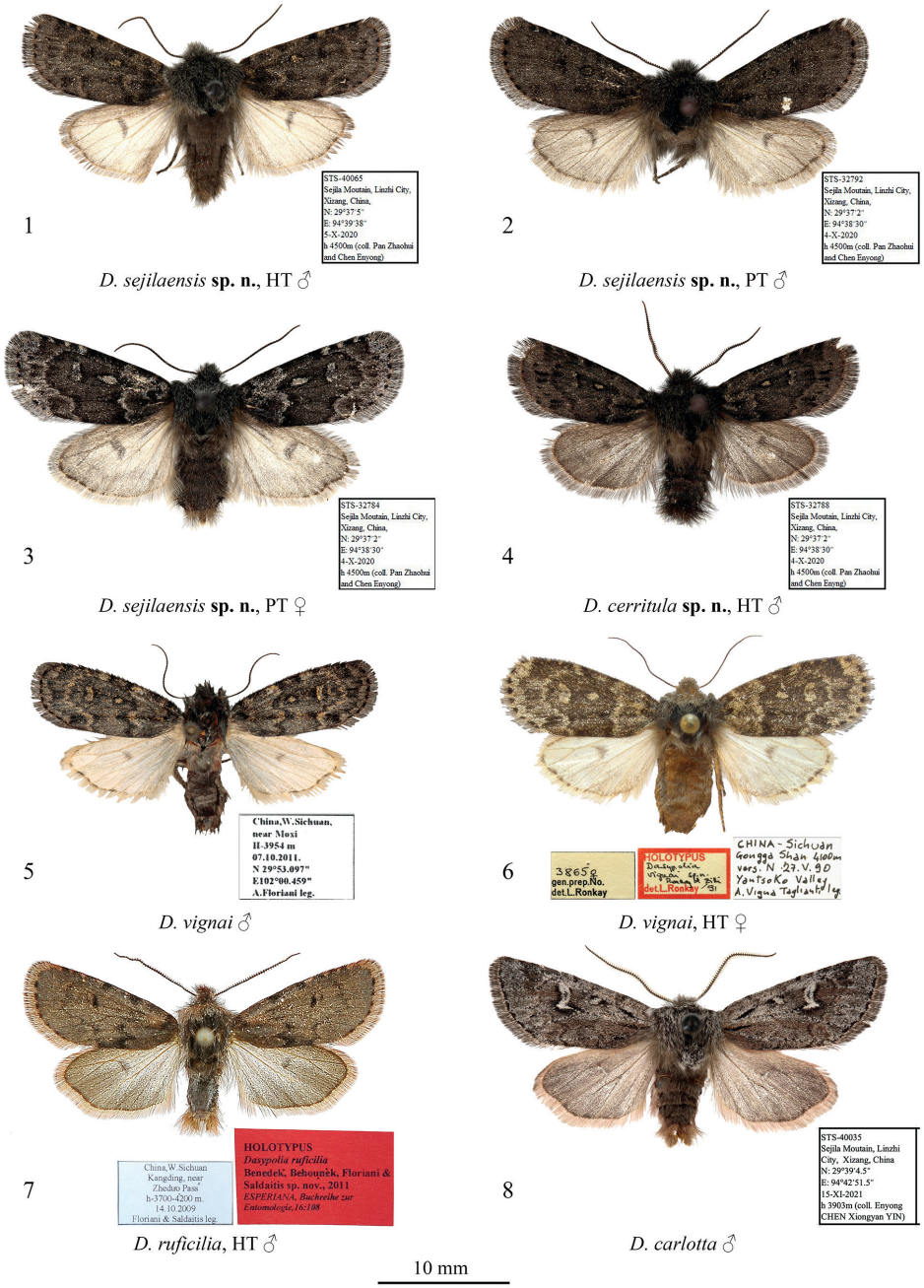

D. sejilaensis **sp. n.**, HT ♂ — *D. sejilaensis* **sp. n.**, PT ♂

D. sejilaensis **sp. n.**, PT ♀ — *D. cerritula* **sp. n.**, HT ♂

D. vignai ♂ — *D. vignai*, HT ♀

D. ruficilia, HT ♂ — *D. carlotta* ♂

Figures 1–8. *Dasypolia* (*Tatsipolia* and *Auropolia*) spp., adults. Depositories of the specimens: **1–4** and **8** in TAAHU **5** in AFM **6** in HNHM (photo by B. Tóth) **7** in ZSM.

Distribution. The new species is known only from Sejila Mountain in southern Xizang Province of China.

Etymology. The specific epithet refers to the type locality.

***Dasypolia* (*Tatsipolia*) *cerritula* sp. nov.**
https://zoobank.org/CC24CD6D-E613-4517-8E36-9FD1FCE81CE3
Figs 4, 11

Type material. ***Holotype*** (Figs 4, 11): male, "STS-32788 | Sejila Mountain, Linzhi City, | Xizang, China, | N:29°37'2" | E:94°38'30" | 4-X-2020 | h [Altitude] 4500 m (coll. Pan Zhaohui | and Chen Enyong)" gen. prep. in glycerol by Enyong Chen (TAAHU).

Diagnosis. The new species is very similar to the sympatric *D. sejilaensis* sp. nov. but differs in the greyish-brown hindwing with a smaller and rounded discal spot whereas the hindwing of *D. sejilaensis* sp. nov. is creamy with intense greyish suffusion outwardly and along the costal and the anal margins, and the discal spot is large and falcate. The abdomen of *D. cerritula* sp. nov. is covered with black hair-like scales medially and distally whereas it is monotonous brown in *D. sejilaensis* sp. nov. Compared to *D. sejilaensis* sp. nov., the male genital capsule of *D. cerritula* sp. nov. has a narrower uncus, a larger penicular lobe with a more elongated posterior corner, and a shorter valva with a markedly broader cucullus densely covered with more robust setae. Additionally, the digitus of *D. cerritula* sp. nov. is shorter and narrower than in *D. sejilaensis* sp. nov., the ventral lobe of the valva is conspicuously narrower and shorter, the harpe is absent (it is present in *D. sejilaensis* sp. nov.), and the juxta is narrower and bears a somewhat shorter and basally broader posterior medial process. The phalli of the two species display no remarkable differences. The vesica of *D. cerritula* sp. nov. is similar to that of *D. sejilaensis* sp. nov. but differs in the presence of an additional small cluster of small spine-like cornuti ventrally, and the dorsal cluster consisting of markedly larger cornuti.

Description. External morphology of adult (Fig. 4). Forewing length 11.5 mm in holotype male. Male antenna serrulate. Head and thorax covered with long hair-like scales, dark brown with admixture of pale grey. Forewing elongate, narrow, with almost parallel costal and anal margins and convex outer margin. Forewing ground colour dark brown with black suffusion in medial area; costal margin with diffuse pale brown spots of various sizes. Forewing pattern diffuse, blackish-brown. Subbasal line short, indistinct. Subbasal lengthwise dash narrow, diffuse. Antemedial line sinuous, with pale brown suffusion inwardly. Orbicular stigma elliptical, filled with pale brown scales. Reniform stigma narrow, filled with pale brown scales. Postmedial line medially curved, slightly dentate posteriorly. Subterminal line interrupted into row of blackish cuneal spots of various sizes between veins. Terminal line indistinct, interrupted into small diffuse blackish spots between veins. Outer margin edged with rusty-brown scales. Forewing cilia long, dark brown. Hindwing brown with somewhat paler subbasal and medial areas. Discal spot small, rounded, diffuse. Outer margin edged with rusty-brown scales. Hindwing cilia long, creamy with admixture of brownish-grey scales. Abdomen covered with long hair-like scales, brown with strong admixture of black scales medially and posteriorly.

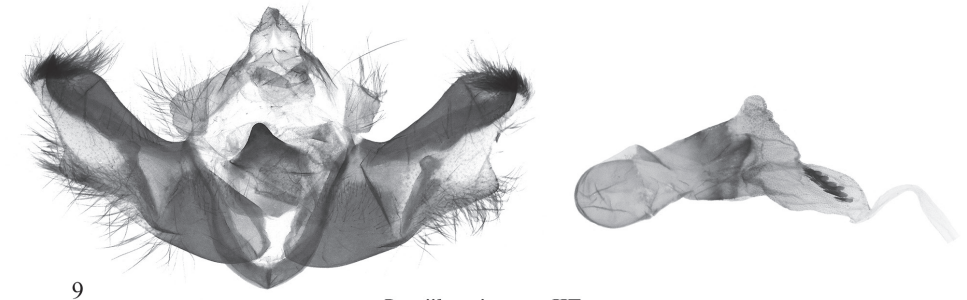

9

***D. sejilaensis* sp. n., HT**
China, Xizang, Linzhi City, Sejila Mt., gen. prep. by Enyong Chen

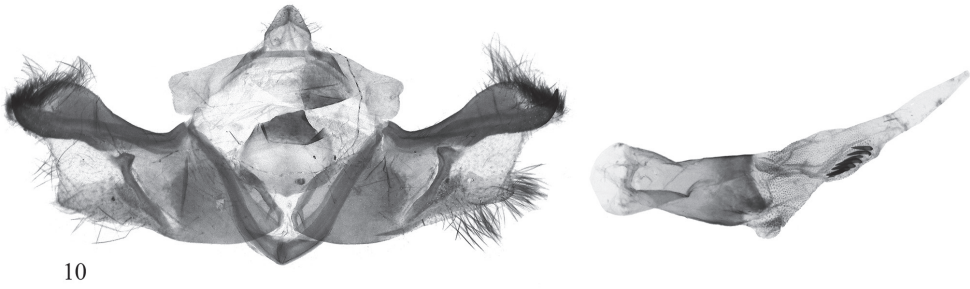

10

***D. sejilaensis* sp. n., PT**
China, Xizang, Linzhi City, Sejila Mt., gen. prep. by Enyong Chen

11

***D. cerritula* sp. n., HT**
China, Xizang, Linzhi City, Sejila Mt., gen. prep. by Enyong Chen

Figures 9–11. *Dasypolia* (*Tatsipolia*) spp., male genitalia. The specimens dissected are deposited in TAAHU.

Male genitalia (Fig. 11). Tegumen short, penicular lobe large, trapezoid with elongate posterior corner. Vinculum longer than tegumen, robust, U-shaped. Valva lobular with heavily sclerotised costa and short, triangular, moderately sclerotised ventral lobe. Digitus heavily sclerotised, directed ventro-distally, with up curved and apically pointed distal section. Cucullus broad, rounded, densely covered with robust spine-like setae.

Sacculus short but broad, elliptical. Clasper slightly curved and dilated distally, without harpe. Uncus short but broad, arrowhead-shaped with rounded apex, dorso-ventrally flattened, weakly sclerotised. Juxta broad, rectangular with rounded corners, bearing broad, triangular and apically pointed, heavily sclerotised medial process posteriorly. Anellus weakly granulose. Phallus broad with rounded coecum, somewhat dilated distally. Main chamber of vesica somewhat shorter than phallus, tapered distally, directed ventro-distally, weakly granulose, with short semiglobular dorsal subbasal diverticulum and two lengthwise clusters of cornuti medially: dorsal one consisting of five robust, slightly curved spike-like cornuti, and ventral one consisting of four smaller spine-like cornuti.

Female unknown.

Distribution. The new species is known only from Sejila Mountain in southern Xizang Province of China.

Etymology. In Latin, 'cerritulus' means 'weird.' The specific epithet refers to the unusual cucullus densely covered with robust, spine-like setae.

Dasypolia (*Tatsipolia*) *vignai* L. Ronkay & Zilli, 1992

Figs 5, 6, 12, 16

Dasypolia (*Sinipolia*) *vignai* Ronkay & Zilli, 1992: 500, fig. 12 (female genitalia), pl. O: fig. 11 (adult) (Type locality: "China – Sichuan, Gongga Shan 4100 m ... Yantsoko Valley").

Type material examined. ***Holotype*** (Figs 6, 16): female, "China – Sichuan | Gongga Shan 4100 m | vers. N 27.V.[19]90 | Yantso Ko Valley, A. Vigna Taglianti leg." | "Holotypus | *Dasypolia* | *vignai* sp. nov. | Ronkay & Zilli | det. L. Ronkay/91" / "3865♀ | gen. prep. No. | det.L.Ronkay" (HNHM).

Additional material examined. 1 male, China, W Sichuan, near Moxi, H-3954 m, 07.X.2011, 29°53.097'N, 102°00.459'E, A. Floriani leg., gen. prep. No.: JB2170 (prepared by Babics) (AFM).

Diagnosis. The forewing length is 12 mm in both sexes. The species is externally similar to *D. sejilaensis* sp. nov. and *D. cerritula* sp. nov. but is distinguished by the slightly convex costal margin of the forewing, the shorter and more rounded forewing apex, the more distinct forewing pattern in males, and the shorter discal spot of the hindwing. Additionally, compared to the congeners, the reniform stigma *D. vignai* is positioned more inwardly from the forewing costa. The male genitalia of *D. vignai* differ clearly from other species of the subgenus *Tatsipolia* in the narrow cucullus, the long, down curved and apically pointed digitus, and the large and rounded ventral lobe of the valva. The detailed comparison with *D. sejilaensis* sp. nov. is provided above in the diagnosis of the latter species.

Distribution. The species is known from two localities in Sichuan Province, southwestern China.

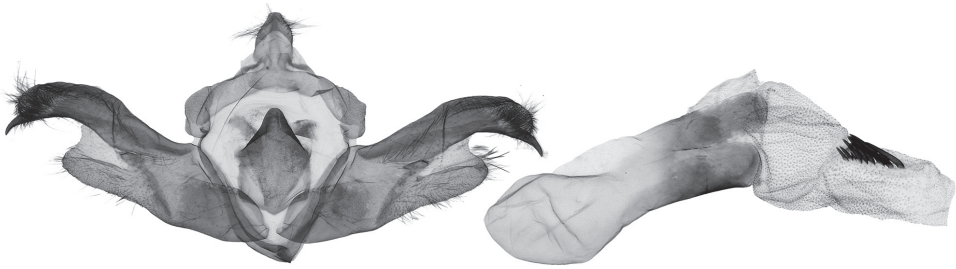

12

D. vignai
China, Sichuan, near Moxi, slide BJ2170 Babics

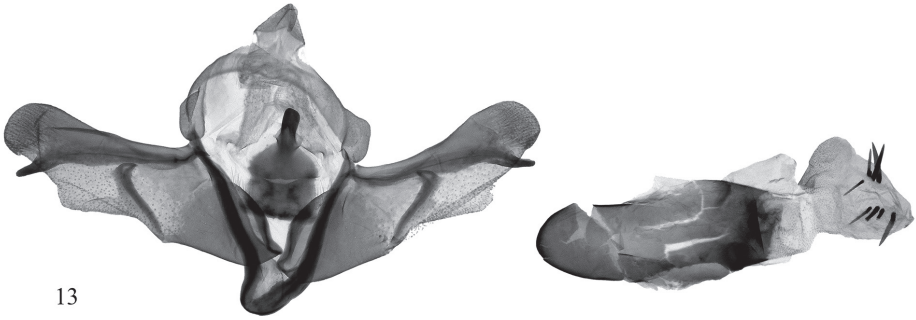

13

***D. ruficilia*, HT**
China, Sichuan, near Moxi, slide BG7015 Behounek

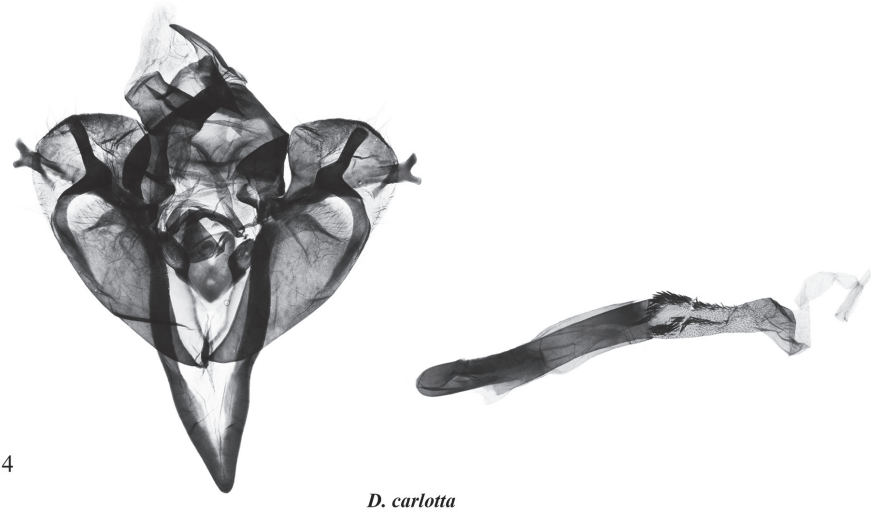

14

D. carlotta
China, Xizang, Linzhi City, Sejila Mt., gen. prep. by Enyong Chen

Figures 12–14. *Dasypolia* (*Tatsipolia* and *Auropolia*) spp., male genitalia. Depositories of the specimens dissected: **12** in AFM **13** in ZSM **14** in TAAHU.

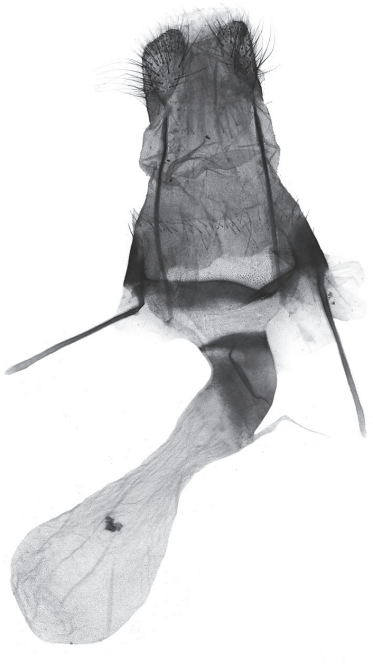

15

***D. sejilaensis* sp. n., PT**
China, Xizang, Linzhi City, Sejila Mt., gen. prep. by Enyong Chen

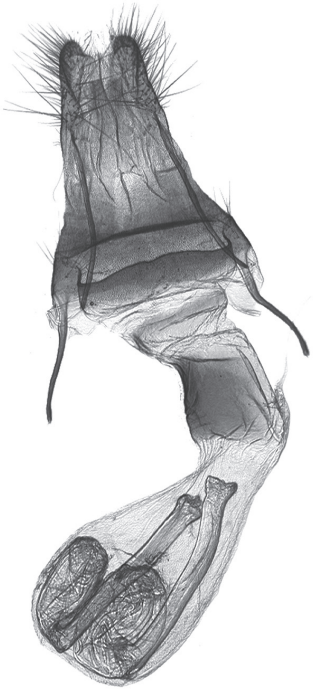

16

***D. vignai*, HT**
China, Sichuan, Gongga Shan, slide RL3865 Ronkay

Figures 15–16. *Dasypolia* (*Tatsipolia*) spp., female genitalia. Depositories of the specimens dissected: **15** in TAAHU **16** in HNHM (photo by B. Tóth).

Dasypolia (*Tatsipolia*) *ruficilia* Benedek, Behounek, Floriani & Saldaitis, 2011

Figs 7, 13

Dasypolia (*Tatsipolia*) *ruficilia* Benedek, Behounek, Floriani & Saldaitis, 2011: 108, fig. 2 (male genitalia), pl. 15: fig. 4 (adult) (Type locality: "China, W. Sichuan, Kangding, near Zheduo Pass, 3700–4200 m").

Type material examined. ***Holotype*** (Figs 7, 13): male, "China, W.Sichuan | Kangding, near | Zheduo Pass | h-3700–4200 m | 14.10.2009 | Floriani & Saldaitis leg." / red label "Holotypus | *Dasypolia ruficilia* | Benedek, Behounek, Floriani & | Saldaitis sp. nov., 2011 | *Esperiana*, Buchreihe zur | Entomologie, 16: 108," gen. prep. No.: BG7015 (prepared by Behounek) (ZSM).

Diagnosis. The forewing length is 12 mm in the holotype male. The species externally differs from other members of the subgenus *Tatsipolia* in the monotonous pale brown forewing colouration and reddish-brown forewing cilia. The male genital capsule is characterised by the broad, trapezoid and weakly setose cucullus and the nearly straight digitus. The phallus of *D. ruficilia* is distally tapered whereas it is distally somewhat dilated in other species in the subgenus. The vesica of *D. ruficilia* bears two short

lengthwise clusters consisting of four long and thin spine-like cornuti each, whereas the clusters of other *Dasypolia* (*Tatsipolia*) species consist of more robust cornuti.

The female is unknown.

Distribution. The species is known only from its type locality in the western Sichuan Province of China (Benedek et al. 2011).

Subgenus *Auropolia* Hreblay & L. Ronkay, 1999

Dasypolia (*Auropolia*) *carlotta* Floriani, Benedek, Behounek & Saldaitis, 2011

Figs 8, 14

Dasypolia (*Auropolia*) *carlotta* Floriani, Benedek, Behounek & Saldaitis in Benedek et al. 2011: 111, fig. 6 (male and female genitalia), pl. 14: figs 7–9 (adults) (Type locality: "China, W. Sichuan, Kangding, near Zheduo Pass, 3700–4200 m").

Material examined. 1 male, Sejila Mountain, Linzhi City, Xizang, China, 29°39'4.5"N, 94°42'51.5"E, 15-XI-2021, [Altitude] h 4160 (coll. Enyong Chen, Xiongyan Yin), unique number: STS-40035, gen. prep. in glycerol by Enyong Chen (TAAHU).

Distribution. The species is known from south-western China: western Sichuan (Benedek et al. 2011), north-western Yunnan (Benedek and Saldaitis 2014) and southern Xizang (new record).

Acknowledgements

The work of Enyong Chen and Zhao-Hui Pan was supported by the Second Tibetan Plateau Scientific Expedition and Research Program (Grant No. 2019QZKK05010602) and Tutor innovation project of Forestry Subject of Tibet agricultural and Animal Husbandry University (Species diversity and conservation of Geometridae (Lepidoptera) in southeastern Tibet). Anton Volynkin, Aidas Saldaitis and Balázs Benedek had no foundation. We express our sincere thanks to National Forest Ecosystem Observation & Research Station of Nyingchi Tibet, Key Laboratory of Forest Ecology in Tibet Plateau, Key Laboratory of Alpine Vegetation Ecological Security in Tibet, and South-East Tibetan plateau Station for integrated observation and research of alpine environment in Linzhi. We are also indebted to Dr Balázs Tóth (HNHM, Budapest, Hungary) for pictures of the holotype of *D. vignai* provided.

References

Benedek B, Saldaitis A (2014) New *Dasypolia* species from China, part II (Lepidoptera, Noctuidae). Esperiana 19: 103–119.

Benedek B, Behounek G, Floriani A, Saldaitis A (2011) New *Dasypolia* species (Lepidoptera, Noctuidae) from China, Sichuan, part I (plates 14–17). Esperiana 16: 107–125.

Benedek B, Saldaitis A, Babics J (2014) On the taxonomy of the genus *Dasypolia* (Lepidoptera, Noctuidae, Xylenini). Entomofauna (Supplement 17): 17–28.

Keegan KL, Rota J, Zahiri R, Zilli A, Wahlberg N, Schmidt BC, Lafontaine JD, Goldstein PZ, Wagner DL (2021) Toward a stable global Noctuidae (Lepidoptera) taxonomy. Insect Systematics and Diversity 5(3): 1–24. https://doi.org/10.1093/isd/ixab005

Kononenko VS (2010) Noctuidae Sibiricae. Vol. 2. Micronoctuidae, Noctuidae: Rivulinae—Agaristinae (Lepidoptera). Entomological Press, Sorø, 475 pp.

Lafontaine JD, Schmidt BC (2010) Annotated check list of the Noctuoidea (Insecta, Lepidoptera) of North America north of Mexico. ZooKeys 40: 1–239. https://doi.org/10.3897/zookeys.40.414

Nupponen K, Fibiger M (2006) Additions and corrections to the list of Bombyces, Sphinges and Noctuidae of the Southern Ural Mountains. Part I. (Lepidoptera: Lasiocampidae, Lemoniidae, Sphingidae, Notodontidae, Noctuidae, Pantheidae, Lymantriidae, Nolidae, Arctiidae) (plates 22–26). Esperiana 12: 167–195.

Ronkay L, Zilli A (1993) New high montane *Dasypolia* species from Sichuan and Sikkim with remarks on the dasypolioid generic complex. Esperiana 3: 497–506.

Ronkay G, Ronkay L, Gyulai P, Hacker H (2010) New Xylenini (Lepidoptera, Noctuidae, Xyleninae) species and genera from the wide sense Himalayan region. Esperiana 15: 245–358.

Ronkay G, Ronkay L, Gyulai P (2014) New Xyleninae and Psaphidinae species from Asia, with special reference to the Central and Inner Asiatic *Dasypolia* Guenée, 1852 (Lepidoptera, Noctuidae). Fibigeriana (Supplement 2): 141–169.

Volynkin AV (2012) A review of the genus *Dasypolia* Guenée, 1852 from the Russian part of the Altai Mountain Country, with descriptions of two new species (Lepidoptera, Noctuidae). Zootaxa 3478(1): 416–428. https://doi.org/10.11646/zootaxa.3478.1.37

Zahiri R, Kitching IJ, Lafontaine JD, Mutanen M, Kaila L, Holloway JD, Wahlberg N (2011) A new molecular phylogeny offers hope for a stable family level classification of the Noctuoidea (Lepidoptera). Zoologica Scripta 4(2): 158–173. https://doi.org/10.1111/j.1463-6409.2010.00459.x